

DIGITAL ACCESS TO SCHOLARSHIP AT HARVARD

Modeling sporadic Alzheimer's disease using induced pluripotent stem cells

The Harvard community has made this article openly available. Please share how this access benefits you. Your story matters.

Citation	No citation.
Accessed	February 17, 2015 1:22:36 AM EST
Citable Link	http://nrs.harvard.edu/urn-3:HUL.InstRepos:13094355
Terms of Use	This article was downloaded from Harvard University's DASH repository, and is made available under the terms and conditions applicable to Other Posted Material, as set forth at http://nrs.harvard.edu/urn-3:HUL.InstRepos:dash.current.terms-of-use#LAA

(Article begins on next page)

HARVARD UNIVERSITY
Graduate School of Arts and Sciences

DISSERTATION ACCEPTANCE CERTIFICATE

The undersigned, appointed by the

Division of Medical Sciences

in the subject of Biological Chemistry and Molecular Pharmacology

have examined a dissertation entitled

Modeling sporadic Alzheimer's disease using induced pluripotent stem cells

presented by Heather Ward McLaughlin

candidate for the degree of Doctor of Philosophy and hereby certify that it is worthy of acceptance.

Signature: _____

Typed Name: Dr. George Church

Signature: _____

Typed Name: Dr. Kevin Eggan

Signature: _____

Typed Name: Dr. Stephen Helfand

_____

Dr. Susan Dymecki, Program Head

Date: June 03, 2014

_____

Dr. David Lopes Cardozo, Director of Graduate Studies

Modeling Sporadic Alzheimer's Disease Using Induced Pluripotent Stem Cells

A dissertation presented

by

Heather Ward McLaughlin

to

The Division of Medical Sciences

in partial fulfillment of the requirements

for the degree of

Doctor of Philosophy

in the subject of

Biological Chemistry and Molecular Pharmacology

Harvard University

Cambridge, Massachusetts

June 2014

© 2014 Heather Ward McLaughlin

All rights reserved.

Dissertation Advisor: Professor Bruce Yankner **Heather Ward McLaughlin**

Modeling sporadic Alzheimer's disease using induced pluripotent stem cells

Abstract

Despite being the leading cause of neurodegeneration and dementia in the aging brain, the cause of Alzheimer's disease (AD) remains unknown in most patients. The terminal pathological hallmarks of abnormal protein aggregation and neuronal cell death are well-known from the post-mortem brain tissue of Alzheimer's disease patients, but research into the earliest stages of disease development is hindered by limited model systems. In this thesis, an *in vitro* human neuronal system was derived from induced pluripotent stem (iPS) cell lines reprogrammed from dermal fibroblasts of AD patients and age-matched controls. This allows us to investigate the cellular mechanisms of AD neurodegeneration in the human neurons of sporadic AD (SAD) patients, whose development of the disease cannot be explained by our current understanding of AD. We show that neural progenitors and neurons derived from SAD patients show an unexpected expression profile of enhanced neuronal gene expression resulting in premature differentiation in the SAD neuronal cells. This difference is accompanied by the decreased binding of the repressor element 1-silencing transcription/neuron-restrictive silencer factor (REST/NRSF) transcriptional inhibitor of neuronal differentiation in the SAD neuronal cells. The SAD neuronal cells also have increased production of amyloid-β and higher levels of tau protein, the main components of the plaques and tangles in the AD brain.

Table of Contents

Appendix I: Supplementary Tables

(available online at http://eresearch.lib.harvard.edu/V)

Supplementary Table 1: Differentially Expressed Fibroblast Genes ($q \leq 0.15$)

Supplementary Table 2: No Significant Differentially Expressed iPS Genes (shown are genes with $p \leq 0.05$)

Supplementary Table 3: Differentially Expressed Neural Progenitor Genes ($q \leq 0.15$)

Supplementary Table 4: Neural Progenitors Enrichment Analysis (MetaCore)

Supplementary Table 5: Overconnected Interactions for NPs (MetaCore)

Supplementary Table 6: Upstream Regulators of NP Gene Expression Profile (Ingenuity Pathway Analysis)

Supplementary Table 7: Differentially Expressed Neural Progenitor Additional Clones Genes ($q \leq 0.15$)

Supplementary Table 8: Overconnected Interactions for NP Additional Clones (MetaCore)

Supplementary Table 9: Upstream Regulators of NP Additional Clones Gene Expression Profile (Ingenuity Pathway Analysis)

Supplementary Table 10: Differentially Expressed Neuron Genes ($q \leq 0.035$)

Supplementary Table 11: Neurons Enrichment Analysis (MetaCore)

Supplementary Table 12: Overconnected Interactions for Neurons (MetaCore)

Supplementary Table 13: Upstream Regulators of Neuronal Gene Expression Profile (Ingenuity Pathways Analysis)

Acknowledgements

There are a number of people to whom I am deeply indebted for their support and generosity of time and ideas during the course of my graduate school career. First, I would like to express my sincere gratitude to my mentor, Dr. Bruce Yankner, for his enthusiastic support, guidance, and scientific insight. His door was always open to discuss an exciting new result or troubleshoot an unsuccessful experiment. I deeply appreciate the opportunity to work on this project and learn both the intellectual and practical approaches to scientific research from him.

Secondly, I would like to thank the members of the Yankner lab for their ideas, technical expertise, and commiseration when the project has encountered complications. Specifically, I'd like to acknowledge Amy Ryan for her mentoring during my rotation and being my first introduction to scientific research at Harvard Medical School, Haeyoung Kim for his advice on both scientific technique and career as we worked in the tissue culture room, and Joseph Zullo for his vision into the bigger picture for my project as well as making working late into the night much less isolated. I am deeply in debt to Tao Lu and Ying Pan for taking care of my cells when I was unable to as well as providing more technical and scientific guidance than I could ever begin to enumerate. Additionally, fellow graduate student Kelly Dakin showed me the ropes for being a Harvard graduate student, all while being the best of lunch mates to discuss lab and life. Monlan Yuan is an exceptional lab manager who worked tirelessly to quickly solve any problem. Also, the lab administrators during my time here in the Yankner lab were invaluable for their ability to keep all of us organized: Ruth Capella, Will Anderson, and Allison Harwick. Most importantly, I want to extend my gratitude to Nick Bishop for starting this project and generating all the iPS cell lines, as well as training me to take over for him. Without his early work, this project would not have started so successfully.

I am also deeply indebted to a number of collaborators and people who provided technical support. Dr. Li-Huei Tsai and the members of her lab were invaluable in both collaborating to perform electrophysiology on my iPS-derived cells and general discussion about the greater meaning and implications of my results. Technical aid was kindly provided by Michelle Ocaña in the use of MetaCore software and John Sullivan for FACS analysis. Dr. Yoshiho Ikeuchi from Dr. Azad Bonni's laboratory went above and beyond to help me set up glial co-culture and utilize the Banker method. More specific technical and experimental contributions are recognized at the close of each chapter.

I would also like to thank the members of my dissertation advisory and defense committees. In my advisory committee, Dr. Azad Bonni, Dr. Michael Wolfe, and Dr. Alex Meissner provided much needed feedback and encouragement throughout the development of my project. Their periodic insight into my project as well as refocusing on the most important direction for the research improved this project in innumerable ways. I would also like to express my gratitude to my defense committee of Dr. George Church, Dr. Kevin Eggan, Dr.Stephen Helfand, and Dr. Michael Wolfe, whose close reading of my thesis and subsequent inquiries and ideas were inspiring.

Finally, I would like to thank my family and friends who have enriched this journey in so many ways and reminded me of why the research that I do is important and worthwhile. In particular, my parents for their constant support and ready hospitality when I needed to escape home to Vermont. I also have the deepest gratitude to my teammates on both the Cambridge Running Club and Harvard University Cycling Association who have shown me that it is possible to both have a wonderful social life, a rewarding career, and maintain your fitness levels as long as you do it all at the same time: on a long run or ride with some of the smartest and

kindest people that I have ever met. Most of all, I would like to thank my fiancé, Cameron, who has endured the last two years of living separately across the country as I completed this project. His unwavering support and readiness to sacrifice our vacations, weekends, and nights alongside me as I looked after finicky cells made this project possible.

Chapter 1: Introduction

Alzheimer's disease (AD) is the most common form of dementia, highly prevalent with increasing age. It is characterized by a progressive and incurable loss of cognitive abilities, especially related to memory and learning. Approximately 5.3 million people in the United States are currently afflicted with AD and numbers are expected to rise as the average lifespan increases (Hebert et al 2003, Thies et al 2013). Despite its prevalence, the cause of Alzheimer's disease remains unknown in the vast majority of patients and there is no treatment available that delays or halts the progression of AD. It is definitively diagnosed post-mortem by the presence of extraneuronal aggregates of Aβ, a proteolysis product of the amyloid precurser protein (APP), and intraneuronal neurofibrillary tangles (NFTs) of hyperphosphorylated tau protein. However, it is unclear if these pathologies are a cause or a consequence of the neurodegeneration.

Research into the mechanisms of cellular degeneration in AD is hindered by the lack of a model system that reproduces the cellular behavior of human neurons. This thesis characterizes an innovative model using induced pluripotent stem cells for studying AD pathogenesis in human neurons. We discovered novel differences in neuronal activity between cells derived from sporadic AD and normal patients, leading to new possible insights into the cause of Alzheimer's disease and future directions for therapeutics.

A. Pathology of Alzheimer's disease

Alzheimer's disease is characterized by the abnormal accumulation of proteins in the brain accompanied by excessive cell death. APP is an intramembrane protein with a long extracellular N-terminus and a smaller intracellular C-terminus. The Aβ fragment is produced by a series of proteolysis events, catalyzed by a family of proteases called secretases. First, the β-secretase (BACE) cleaves the N-terminus from APP, leaving a 99-residue membrane-bound

remnant (Cole & Vassar 2008). Next, the γ-secretase, presenilin 1 or 2 (PSEN1, PSEN2), cleaves APP twice within the membrane, producing the APP intracellular domain (AICD) and Aβ (Wolfe 2009). There are two major forms of Aβ, depending on the PSEN1 cleavage site: Aβ40 or Aβ42. The longer Aβ42 is thought to be more pathogenic since it is the major species detected in the brains of AD patients (Iwatsubo et al 1994) and is required for Aβ deposition *in vivo* (McGowan et al 2005).

Tau is a microtubule-binding protein that localizes to axons in the adult nervous system (Hanger et al 2009). When phosphorylated at multiple residues, tau releases from the axonal microtubules and binds to itself, forming large intracellular aggregates (Buee et al 2000, Cho & Johnson 2003, Grundke-Iqbal et al 1986). These neurofibrillary tangles (NFTs) of hyperphosphorylated tau are prevalent during AD and the severity of these tangles is the most highly correlated disease pathology with cognitive decline (Arriagada et al 1992).

Alzheimer's disease is also characterized by excessive cell and synapse loss in localized regions of the brain (Duyckaerts et al 2009). Layer II of entorhinal cortex loses up to 90% of cells (Gomez-Isla et al 1996), while other areas disrupted by cell death include the CA1 region of the hippocampus and parts of the parietal and temporal cortices (Duyckaerts et al 2009). This neuronal loss actually begins quite early during AD pathogenesis, with a 64% loss of neurons in Layer II of the entorhinal cortex seen in patients with mild cognitive impairment (MCI), the early stage of AD (Kordower et al 2001). The cells of this layer are predominantly glutamatergic, consisting mainly of large stellate pyramidal cells that form the perforant pathway that connects to the dentate gyrus and is crucial in memory formation (Hyman et al 1984, Kirkby & Higgins 1998). Although cell loss is severe in these regions during AD, the mechanism of cell death and cause of increased susceptibility in certain brain regions remains unclear.

B. Causes of Alzheimer's disease

The cause of AD in the vast majority of patients remains unknown. Most cases of AD are associated with increasing age and have no known dominant genetic basis and are termed sporadic Alzheimer's disease (SAD). Although the definitive instigator of disease development in these patients is unknown, there are genetic susceptibility factors, including the *APOE4* isoform which has the largest effect on the development of SAD (Corder et al 1993). There are also a number of single nucleotide polymorphisms (SNPs) associated with changed susceptibility to the development of AD that have been identified through genome-wide association studies, but the functional consequences of these differences are still being investigated (Lambert et al 2013).

In addition to the more common SAD, there is also a relatively rare early onset form of AD that is inherited in an autosomal dominant manner called familial Alzheimer's disease (FAD). FAD is caused by mutations in *APP* or its γ-secretases: *PSEN2* or the most prevalent *PSEN1* (Ertekin-Taner 2007). Less than 1% of AD cases are caused by these familial mutations (Ertekin-Taner 2010), yet much of current cellular AD research uses mutations in these genes to model AD.

The presence of these familial mutations that affect Aβ processing led to the development of the amyloid cascade hypothesis to explain the development of Alzheimer's disease. Mutations in PSEN1 and PSEN2 cause an increase in the production of Aβ42, the more aggregation-prone form of Aβ (Oddo et al 2003, Wolfe 2002). Thus the amyloid cascade hypothesis supposes that the aberrant proteolysis and accumulation of Aβ42 is causative for the formation of neurofibrillary tangles and Alzheimer's disease neurodegeneration (Tanzi & Bertram 2005). However, the dynamics of actual Aβ42 production and solubility varies considerable between the

different mutations causing familial Alzheimer's disease and sporadic Alzheimer's disease in the human brain (Hellstrom-Lindahl et al 2009), indicating that the pathogenesis of AD may be more complicated than just the aberrant production of Aβ42.

C. The study of Alzheimer's disease

The earliest stages in the development of Alzheimer's disease are very difficult to investigate since the disease is only diagnosed once extensive damage has already occurred. Animal models of AD are based on the familial mutations which account for only a small proportion of cases in humans and may not recapitulate the disease progression seen in humans with Alzheimer's disease. Most animal models overexpress mutant forms of *APP*, *PSEN1*, and/or *MAPT*, the gene for the tau protein. Although *MAPT* mutations do not cause AD in humans, they do cause another neurodegenerative disorder, frontotemporal lobe dementia (FTD) (Spillantini et al 1998), and are prone to hyperphosphorylation and aggregation *in vivo*. A widely used AD murine model is the 'triple-transgenic,' which recapitulates the plaques and tangles seen in human AD and contains mutations in *APP*, *PSEN1*, and *MAPT* (Oddo et al 2003). However, this artificial combination of mutations is quite severe and could be damaging to the brain in mechanisms entirely distinct from late-onset, sporadic AD. Focusing primarily on the causes of familial neurodegeneration in a mouse system may miss important mechanisms that contribute to sporadic neurodegeneration in humans.

Due to the presence of Alzheimer's disease in the brain, previous studies of human neurons came from post-mortem brain samples, since biopsy of the affected tissue while the patient is still living is not possible. The analysis of these samples is often complicated by high levels of cell loss and inflammation from advanced AD and limited identified samples with preclinical symptoms. By the time of diagnosis and death, the most susceptible brain cells are

already lost. Furthermore, during the time following death and before sample collection, the tissue can be altered including increased pH, changes in protein oxidation, and changes in protein expression (Chandana et al 2009). Therefore, a different approach is needed to study the earliest stages of disease development in the vast majority of Alzheimer's disease patients.

D. Induced pluripotent stem cells and Alzheimer's disease

The technology of induced pluripotent stem cells (iPSCs) allows somatic cells from patients, such as skin fibroblasts, to be converted into a pluripotent stem cell capable of forming many different types of differentiated cells (Takahashi et al 2007). The iPSCs can be differentiated into neurons, thus allowing the neuronal activities to be compared in the cells with the genetic background of patients that have actually developed sporadic AD and unaffected, age-matched individuals. This allows us to study human neurons derived from patients that develop sporadic Alzheimer's disease without the complications of post-mortem degradation and advanced disease state.

At the commencement of this study, Alzheimer's disease had yet to be studied using iPSCs or similar technology, however in the last three years several papers have been published using this or similar model systems. In Israel et al (2012), iPSCs were derived from two patients with sporadic Alzheimer's disease, two patients with familial Alzheimer's disease with a duplication of *APP*, and two non-demented controls age-matched to the sporadic AD patients. They found increased Aβ40 production, phosphorylated-tau ratio, and active GSK3β in the FAD patients and one of the sporadic patients in purified neurons, but not the other SAD patient. GSK3β is a kinase that has been shown to phosphorylate tau and induce Aβ production (Takashima 2006). Qiang et al (2011) was recently retracted due to falsification of the figures related to AD pathology, however in the remainder of the study, skin fibroblasts from three

unaffected control individuals, three sporadic AD patients, and three familial AD patients (a PSEN2 N141I and two PSEN1 A246E mutations) were transdifferentiated directly into a neuronal culture. Kondo et al (2013) derived iPSCs from three control patients, two familial patients with different mutations in APP and two sporadic AD patients. They found increased accumulation of intracellular Aβ in one of the APP mutants and one of the sporadic patients which caused oxidative stress. They observed no difference in soluble Aβ40 or Aβ42 production in the sporadic AD neurons.

Other recent studies have focused entirely on familial Alzheimer's disease. This approach is attractive due to having a known genetic defect that causes AD but thus far incomplete elucidation of the cellular effects from these mutations. In Yagi et al (2011), the iPSCs from two patients with presenilin mutations (PSEN1 A246E and PSEN2 N141I) were derived and showed increased Aβ42 secretion when differentiated into neurons. Similar results were seen in Sproul et al (2014) which found increased Aβ42 ratio in neural progenitors derived from three patients with mutations in PSEN1 (M146L and A246E). Finally, Muratore et al (2014) generated iPS cells from two patients harboring a V717I mutation in APP which had increased β- and γ-secretase cleavage of APP resulting in elevated APPsβ and Aβ (both Aβ42 and Aβ38) as well as increased levels of total and phosphorylated tau.

Together, these studies show that it is possible to model Alzheimer's disease *in vitro* using cells derived from patients, and that changes in Aβ processing are seen in all familial AD lines, but not all sporadic patient-derived neurons. No study has shown a conserved phenotype in cells derived from sporadic Alzheimer's disease patients. This is possibly due to the low number of sporadic patients included or it could be due to the fact that sporadic lines do not share a common pathway in the development of AD. However, this thesis refutes the second

possibility since we found a novel conserved phenotype in neuronal cells derived from a set of seven sporadic Alzheimer's disease patients in which the SAD cells show a premature tendency towards neuronal differentiation. Therefore, for the first time, a conserved phenotype has been found in cells derived from iPS cells derived from patients without a known genetic cause for Alzheimer's disease.

Chapter 2: From Fibroblasts to Induced Pluripotent Stem Cells

Abstract

Dermal fibroblasts from seven patients who developed Alzheimer's disease (six sporadic patients and one *PSEN1* familial patient) and six age-matched controls were acquired from the Coriell Cell Repository. They were reprogrammed into induced pluripotent stem cells using retroviral transgene induction of *OCT4*, *SOX2, KLF4*, and *cMYC*. The iPS cells derived from each individual express the pluripotency markers SOX2, NANOG, TRA-1-81, and OCT3/4 and differentiated into all three germ layers *in vitro* and *in vivo*. Most lines maintain normal karyotypes and all show inactivation of the viral transgenes. Microarray analysis of the fibroblasts, but not the iPS cells, reveals a unique gene expression profile in the sporadic Alzheimer's disease lines.

Introduction

Skin biopsies from patients with Alzheimer's disease and age-matched controls (often non-consanguineous relatives that do not have AD) were performed in the 1980s and the resulting fibroblast cell lines were banked in the Coriell Cell Repository. The sporadic AD patient lines selected had a relatively early age of onset with 75% developing Alzheimer's disease before the age of 75 (see later in the chapter), while the prevalence of AD in the general population before age 75 is less than 3% (Qiu et al 2009). By enriching for the presence of individuals who developed AD earlier and thus may have increased susceptibility, we hope to identify more robust changes in the behavior of cells derived from these individuals. We also have one patient with an early-onset, familial form of AD due to a putative mutation in *PSEN1* (Sherrington et al 1995, St George-Hyslop et al 1987). Although it will be difficult to draw conclusions whether familial AD and sporadic AD have the same cellular processes and gene

expression from only one FAD line, it will be interesting to see if it more closely aligns with the SAD or NL individuals.

One important variable that affects the onset of sporadic Alzheimer's disease is the *APOE* genotype. There are three different alleles of *APOE: APOE3* is the most common allele with an allele frequency of 79% in the general population, while *APOE2* accounts of 7% of the allele frequency and *APOE4* accounts for 14% (www.alzgene.org) (Bertram et al 2007). The resulting proteins vary at two amino acids at positions 112 and 158, with *APOE2* coding for cysteine/cysteine, *APOE3* coding for cysteine/arginine, and *APOE4* coding for arginine/arginine (Weisgraber et al 1981). The *APOE4* genotype is the most important genetic contributor to sporadic Alzheimer's disease, increasing the risk of developing AD from 20% to 90%, dependent on the number of *APOE4* alleles, while the *APOE2* allele has a minor protective effect (Corder et al 1993).

The mechanism by which *APOE4* increases the likelihood of developing AD and lowers the age of onset remains unclear. *APOE* is an apolipoprotein predominately expressed by astrocytes and microglia in the central nervous system and released into the extracellular space in lipoprotein particles (Holtzman et al 2012). There it may play a role in both sequestering or clearing soluble Aβ as well as its more traditional role mediating cholesterol transport through binding to its receptors on neurons. The different isoforms vary in their ability to clear Aβ in the brains of mice, with APOE2 being the most efficient and APOE4 being the least effective (Castellano et al 2011). More recent evidence supports a competition for clearance model in which both Aβ and APOE bind the same receptors, and APOE prevents Aβ from being cleared (Verghese et al 2013).

Modulation of Aβ clearance is not the only way that APOE may mediate the development of AD. The functional significance of the APOE receptor interactions in the central nervous system is still being determined, but it has been implicated in synaptogenesis, synaptic plasticity, neuroprotection, and neurogenesis (Holtzman et al 2012). The different *APOE* isoforms also affect the affinity of receptor binding and the rate at which bound receptors are recycled back to the surface of the cell, suggesting more possible mechanisms by which the *APOE* isoform could affect the onset of AD (Chen et al 2010, Ruiz et al 2005). Although it is clear that the *APOE* isoform is the strongest genetic risk factor for the development of sporadic AD, the mechanism by which it increases the likelihood of developing AD and lowers the age of onset remains unclear. Thus by including lines with a variety of *APOE* genotypes, we hope to elucidate whether differences in cellular processes and gene expression are dependent on *APOE* or whether *APOE4* may enhance any molecular tendencies of sporadic AD cells.

Reprogramming of fibroblasts into iPS cells will change many characteristics of the cells. The process of transcription factor-induced reprogramming should ideally return the fibroblast cells to an undifferentiated state, functionally indistinguishable from the embryonic stem (ES) cells that arise during the earliest stages of development. In order to be considered pluripotent, the iPS cells must be capable of differentiating into cells from all three germ layers of early development: the ectoderm, endoderm, and mesoderm. These germ layers arise during gastrulation, a folding of the blastula which creates three different layers of differentiating cells: the ectoderm, which gives rise to the epidermis and nervous system, the endoderm, which differentiates into the respiratory and digestive system, and the mesoderm, which becomes muscle, cartilage, bone, and connective tissue. In order to evaluate the pluripotency of the iPS

cells, we differentiate the cells both *in vivo* and *in vitro* to show tissue and expression markers from all three germ layers.

Reprogramming should also return the transcriptional profile and epigenetic state of the differentiated cell to one resembling an ES cell. However, gene expression studies show that iPSCs have a profile unique from ES cells, possibly due to differential binding by the reprogramming factors (Chin et al 2009). Whole genome profiles of DNA methylation show significant variability of epigenomic reconfiguration in different iPS lines (Lister et al 2011). Although reprogramming induces a robust reset of the DNA methylation patterns in most areas of the genome to the embryonic state, there are regions of the genome where aberrant methylation either retains memory of the differentiated state or shows iPSC-specific methylation patterns. Therefore, although iPS cells are in many ways functionally identical to ES cells, differences in epigenetics may remain through the reprogramming process and affect downstream differentiation.

Another factor that may affect the differentiation capabilities of iPS cells is insufficient inactivation of the reprogramming factors. Following complete reprogramming to an ESC-like state, the retroviral vectors should be silenced (Hotta & Ellis 2008). However, transgene inactivation can be variable between iPS lines and prevent later differentiation (Toivonen et al 2013). Therefore, it is important to evaluate transgene expression levels to show that there is no difference between the SAD and NL experimental groups that may affect differentiation into neurons.

Materials and Methods

APOE Genotyping: APOE genotyping was based on the protocol of Hixson and Vernier (1990). DNA was extracted from fibroblasts using a silica-based spin column DNA purification kit

(DNAeasy Blood and Tissue kit, Qiagen). *APOE* was amplified using polymerase chain reaction (PCR) with 10 μM F6 and F4 primers (5'-ACAGAATTCGCCCCGGCCTGGTACAC-3', 5'-TAAGCTTGGCACGGCTGTCCAAGGA-3'), 10 mM dNTPs, 200 ng of DNA template, 1 unit *Taq* polymerase (Qiagen), and the suggested buffer, water, and Q solution to 50 μL. The PCR reaction was denatured at 95ºC for 5 min, and then subjected to 30 cycles of amplification (60ºC for 1 minute, 70ºC for 2 minutes, and 95ºC for 1 minute) before a final extension of 70ºC for 3 minutes. After amplification, 5 units of Hha1 restriction enzyme (New England Biolabs) diluted to 1uL in NEBuffer 4 (New England Biolabs), was added to each reaction chamber and incubated overnight at 37ºC. The next day, the restriction enzyme was inactivated at 65ºC for 20 minutes. The resulting digestion products were run on a 3% agarose gel.

Genotyping of PSEN1 L286V: DNA from neural progenitors was harvested and isolated using Gentra Puregene Core kit A (Qiagen). The *PSEN1* gene was amplified to a 262 basepair product from exon 8 using 10 uM each primer (5'-CACCCATTTACAAGTTTAGC-3', 5'-GATGAGAACAAGTACCATGAA-3'), 1 unit *Taq* polymerase, 10 mM dNTPS, 200 ng DNA template, and the suggested buffer, water and Q solution to 50 μL. The PCR reaction was denatured at 94ºC for 5 min, and then subjected to 35 cycles of amplification (30 seconds at 94ºC, 45 seconds at 55ºC, and 1 minute at 72ºC) before a final extension of 72ºC for 7 minutes. The PCR product was purified using Purelink PCR Purification Kit (Life Technologies). DNA sequencing was performed by the Biopolymers Facility at Harvard Medical School using the same primers from the PCR reaction. Both forward and reverse reactions were performed to confirm results. For restriction digest, 0.4 μg purified *PSEN1* PCR product was incubated with 7 units PvuII restriction enzyme (New England Biolabs) in NEBuffer 2 (New England Biolabs)

and water to 50 µL. The reaction was incubated for 3 hours at 37ºC and the products were immediately run on a 1.2% agarose gel.

Microarray Data Analysis and Statistics: Gene expression in fibroblasts and iPS cells were measured using Affymetrix U133 Plus 2.0 arrays by the Molecular Biology Core Facility at Dana Farber (Boston, MA). Expression data was background adjusted and quantile normalized according the Robust Multichip Average (RMA) approach (Bolstad et al 2003, Irizarry et al 2003a, Irizarry et al 2003b) using the RMAExpress Software (v1.10.0-alpha-4, released March 2, 2014). Annotated probes (using Affymetrix Release 34, November 24, 2013) were preprocessed in GenePattern (Broad Institute) using the PreprocessDataset module (v5, released 12/2/2013) with default floor and ceiling values (Kuehn et al 2008). Variation filtering was set to the default fold change of 3 and delta of 100. The resulting data was $\log_2$ transformed and significant gene expression differences between normal and SAD lines were calculated using Comparative Marker Selection (v10, released 12/4/2013) in GenePattern (Gould et al 2006). Asymptotic p-values were used to calculate q-value and the significance threshold of 0.15 was used (Storey & Tibshirani 2003). Analyses of the significant gene lists were performed using MetaCore (Thomson Reuters), Ingenuity Pathway Analysis (Ingenuity), and DAVID algorithms (Huang da et al 2009a, Huang da et al 2009b). Heat maps and Pearson correlations were produced using dChip (build date August 7, 2009) (Li & Wong 2001).

iPS Cell Reprogramming and Culture: iPS cells were generated based on the described protocol (Park et al 2008a) with some modifications. In brief, pMIG-hKLF4 (Addgene 17227), pMIG-hSOX2 (Addgene 17226), MSCV hc-MYC (Addgene 18119), pMIG-hOCT4 (Addgene 17225), and pMXs-GFP as a positive control were each transfected into Plat-GP (Cell Biolabs) cells using Fugene 6 reagent (Promega) along with pMD2.G (Addgene 12259) encoding the VSV-G

envelop. All four of the reprogramming factors are linked to GFP with an IRES element. The media was changed daily until harvest and 0.45 μm filtration at day 4. The viruses were ultracentrifuged at 112,000 x *g* for 90 minutes at 4º and resuspended in PBS overnight at 4º. The concentration of the viruses was measured through titration in 293FT cells (Life Technologies) by expression of the IRES-GFP. $5x10^4$ fibroblast cells from each SAD, control, and FAD individual were infected with the reprogramming factor viruses at a multiplicity of infection (MOI) of 5 with 4 ug polybrene. After three days, viral transgene induction was verified through expression of IRES-GFP. After four days, the infected fibroblasts were plated on mouse embryonic fibroblasts (iMEFs) inactivated by 10 μg/mL mitomycin C (Sigma-Aldrich) and grown in fibroblast media (DMEM with 10% FBS, 2 mM L-glutamine, 50 U/mL penicillin, and 50 mg/mL streptomycin) on 0.1% gelatin.

After 48 hours, the media was changed to hESC media (DMEM/F-12 with 20% knockout serum, 10 ng/mL bFGF (R&D Systems), 1 mM L-glutamine, 100 μM non-essential amino acids, 100 μM 2-mercaptoethanol, 50 U/mL penicillin, and 50 mg/mL streptomycin (all Life Technologies unless noted). Media was changed daily until iPS colonies formed after 21-30 days. Each colony was isolated and grown on iMEFs according to the described protocol (Lerou et al 2008) unless otherwise specified. The hESC media for the iPS cell was changed daily and colonies were split every 6-8 days using either manual passaging or collagenase IV enzymatic passage.

Immunofluorescence and Antibodies: iPS cells grown on iMEFs adhered to glass coverslips were washed with Hank's Balanced Salt Solution (HBSS) and fixed for 30 minutes with 4% paraformaldehyde (PFA) at room temperature. The coverslips were washed three times with PBS before permeablization with 0.2% Triton X-100 for 20 minutes at room temperature. The

coverslips were blocked in 0.02% Triton X-100 and 5% goat serum in PBS for 30 minutes at room temperature. The primary antibody was diluted in blocking buffer at the below specified concentrations and incubated with the cells for 1 hour at room temperature. The coverslips were washed three times with PBS for 5 minutes each before treatment with secondary antibody diluted 1:200 in blocking buffer (Goat anti-mouse IgG H&L DyLight 488 and Goat anti-rabbit IgG H&L DyLight 594 (Abcam)). The coverslips were incubated 1 hour at room temperature in the dark before washing three times for 5 minutes each with PBS. Excess salt was washed off with distilled water before inverting the coverslip on a glass slide with Prolong Gold with DAPI (Life Technologies). The slides were left overnight at room temperature in the dark to dry before image acquisition on an Olympus Fluoview confocal microscope.

Target	**Host**	**Source**	**Catalogue #**	**Dilution**
Oct3/4	Rabbit	Santa Cruz	sc-9081	1:100
Tra-1-81	Mouse	Millipore	MAB4381	1:250
Nanog	Rabbit	Santa Cruz	sc-33759	1:250
Sox2	Rabbit	Millipore	AB5603	1:250
Sox2	Mouse	Millipore	MAB4343	1:100

Alkaline Phosphatase Assay: The level of alkaline phosphatase activity was evaluated in iPSCs using the Alkaline Phosphatase Detection Kit (Millipore) according to the manufacturer's guidelines. Images of the staining marking phosphatase activity were acquired on a brightfield microscope attached to a CCD camera.

Karyotype Analysis: Cytogenetic analysis was performed by Cell Line Genetics (Madison, WI) on twenty G-banded metaphase cells.

Transgene Inactivation Analysis: cDNA for the both the endogenous and transgene version of each reprogramming factor was derived from iPS cells using TRIzol-harvested RNA ran through an extended one-step RT-PCR cycle in an iQ5 (Bio-Rad) (reverse transcription at 50º for 30 minutes, denatured at 95ºC for 12 min, and then subjected to 60 cycles of amplification (20 seconds at 95ºC, 30 seconds at 55ºC, and 30 seconds at 68ºC) before a final extension of 65ºC for 10 minutes). The primers used were as described and listed below (Park et al 2008b). The cDNA product was run on a 2% agarose gel and the correct product band was extracted using QIAquick Gel Extraction kit (Qiagen) according to the manufacturer's guidelines. The extracted product was concentrated through ethanol precipitation and final concentration measured using a NanoDrop 1000 Spectrophotometer. The resulting purified DNA was titrated and used to create a qRT-PCR standard curve using QuantiTect SYBR Green RT-PCR kit (Qiagen). The concentration of mRNA for each reprogramming factor in the iPS lines (one per individual) was calculated through comparison to its specific standard curve following qRT-PCR in an iQ5 (Bio-Rad) using QuantiTect SYBR Green RT-PCR kit (Qiagen) and a standard cycle of reverse transcription at 50º for 30 minutes, denaturation at 95ºC for 12 min, and then 30 cycles of amplification (20 seconds at 95ºC, 30 seconds at 55ºC, and 30 seconds at 68ºC) before a final extension of 65ºC for 10 minutes. GFP expression was measured using the below primers and the same qRT-PCR protocol.

Primer Target	Forward Sequence	Reverse Sequence
OCT4-Transgene	CCTCACTTCACTGCACTGTA	CCTTGAGGTACCAGAGATCT
OCT4-Endogenous	CCTCACTTCACTGCACTGTA	CAGGTTTTCTTTCCCTAGCT
SOX2-Transgene	CCCAGCAGACTTCACATGT	CCTTGAGGTACCAGAGATCT
SOX2-Endogenous	CCCAGCAGACTTCACATGT	CCTCCCATTTCCCTCGTTTT
KLF4-Transgene	GATGAACTGACCAGGCACTA	CCTTGAGGTACCAGAGATCT
KLF4-Endogenous	GATGAACTGACCAGGCACTA	GTGGGTCATATCCACTGTCT
cMYC-Transgene	TGCCTCAAATTGGACTTTGG	CGCTCGAGGTTAACGAATT
cMYC-Endogenous	TGCCTCAAATTGGACTTTGG	GATTGAAATTCTGTGTAACTGC

Primer Target	Forward Sequence	Reverse Sequence
GFP	AAGCTGACCCTGAAGTTCATCTGC	CTTGTAGTTGCCGTCGTCCTTGAA

In Vitro Formation of Three Germ Layers: iPS cells growing on Matrigel hESC-qualified matrix (BD Biosciences) in mTESR1 media (Stemcell Technologies) were washed with phosphate buffered saline (PBS) and dissociated with collagenase for 10 minutes at 37º. After partial dissociation, the colonies were harvested using a cell scraper and pelleted at 200 x *g* for 5 minutes. The colonies were resuspended in Aggrewell media (Stemcell Technologies) and transferred to ultra-low attachment plates (Corning) to form embryoid bodies. The media was changed every 3 days until day 7, when the embryoid bodies were transferred to 0.1% gelatin-coated plates in culture media (DMEM with 10% fetal bovine serum (FBS), 2 mM L-glutamine, and 1% penicillin/streptomycin (Life Technologies)). The media was changed every 3 days until day 7, at which point RNA was TRIzol-harvested. Reverse-transcription PCR (RT-PCR) for genes representative of the three germ layers was performed on the isolated RNA by the Harvard Stem Cell Institute's iPSC Core Facility (Cambridge, MA).

Teratoma Formation: iPS cells growing on 10 cm plates coated with Matrigel hESC-qualified matrix (BD Biosciences) in mTESR1 media (Stemcell Technologies) were detached using collagenase and washed with PBS with 0.5% bovine serum albumin (BSA). The pellet was resuspended in 30 µL PBS with 0.5% BSA. The Genome Modification Facility (Harvard University, Cambridge, MA) performed teratoma analysis by injecting 10 µL of iPS cells, containing more than $1x10^6$ cells, into the kidney subcapsules of NOD-SCID mice (three per line). Teratomas appeared after 6-10 weeks and were dissected and fixed in 4% paraformaldehyde (PFA) for 24 hours before being stored in 70% ethanol at 4ºC until embedding. The samples were embedded in paraffin by the Harvard Department of Stem Cell

Biology and Regenerative Biology (HSCRB) Histology-Immunohistochemistry Core (Cambridge, MA). The samples were sectioned and stained with hematoxylin and eosin for analysis of cell morphologies from each of the three germ layers.

Statistics: Unless otherwise noted, the significance for the difference between sporadic Alzheimer's disease and normal lines was calculated using a student's *t*-test on Microsoft Excel with the significance level set at $p < 0.05$. All error bars in the figures are the standard error of the mean (SEM) calculated through Excel unless otherwise specified.

Results

A. Genotyping the fibroblast lines for *APOE* and *PSEN1*

The *APOE4* genotype is the most important genetic contributor to sporadic Alzheimer's disease (Corder et al 1993). Therefore, the thirteen fibroblast lines acquired from the Coriell Cell Repository were genotyped at *APOE* to see if different alleles of this gene may affect the cellular mechanisms of AD neurodegeneration and are apparent in this culture system. Restriction digest with HhaI differentiates the three *APOE* alleles, showing that our lines have a wide variety of *APOE4* genotypes (Figure 2.1a, Table 2.1). Of note, two of the SAD lines are *APOE4* homozygotes (SAD1 and SAD5), as well as one *APOE4/E3* heterozygote (SAD6). There is one *APOE4/E3* heterozygote who has escaped the development of AD, NL6. Finally, SAD3 is an *APOE3/E2* heterozygote who still developed SAD with a relatively early onset despite the protective effects of the *E2* allele. The rest of the patients have the most prevalent *APOE3/E3* genotype.

One fibroblast line was acquired from a familial AD patient FAD1 with a putative L286V mutation in presenilin 1. To verify this mutation in the *PSEN1* gene, both the forward and reverse strands of exon 8 were sequenced (Figure 2.1b). Both strands showed a heterozygous

G/C basepair at the position to cause a leucine to valine transposition at amino acid 286 in the presenilin 1 protein. This creates a new *PvuII* restriction site which is apparent in the cleaved products visible in the FAD1 sample, but not the NL5 control individual (Figure 2.1c).

Table 2.1: Summary of Fibroblast Lines

Line	Coriell #	Diagnosis	Age at Biopsy	Gender	*APOE*	AD mutation
NL1	AG04455	Normal	60	F	*E3/E3*	N/A
NL2	AG08125	Normal	64	M	*E3/E3*	N/A
NL3	AG08379	Normal	72	M	*E3/E3*	N/A
NL4	AG08509	Normal	73	M	*E3/E3*	N/A
NL5	AG14244	Normal	75	F	*E3/E3*	N/A
NL6	AG09173	Normal	92	F	*E4/E3*	N/A
SAD1	AG06869	Sporadic AD	60	F	*E4/E4*	N/A
SAD2	AG07376	Sporadic AD	60	M	*E3/E3*	N/A
SAD3	AG21158	Sporadic AD	69	F	*E3/E2*	N/A
SAD4	AG08243	Sporadic AD	72	M	*E3/E3*	N/A
SAD5	AG10788	Sporadic AD	87	F	*E4/E4*	N/A
SAD6	AG14149	Sporadic AD	80	F	*E4/E3*	N/A
FAD1	AG08541	Familial AD	59	F	*E3/E3*	PSEN1 L286V

Figure 2.1: Genotyping of Fibroblast Lines

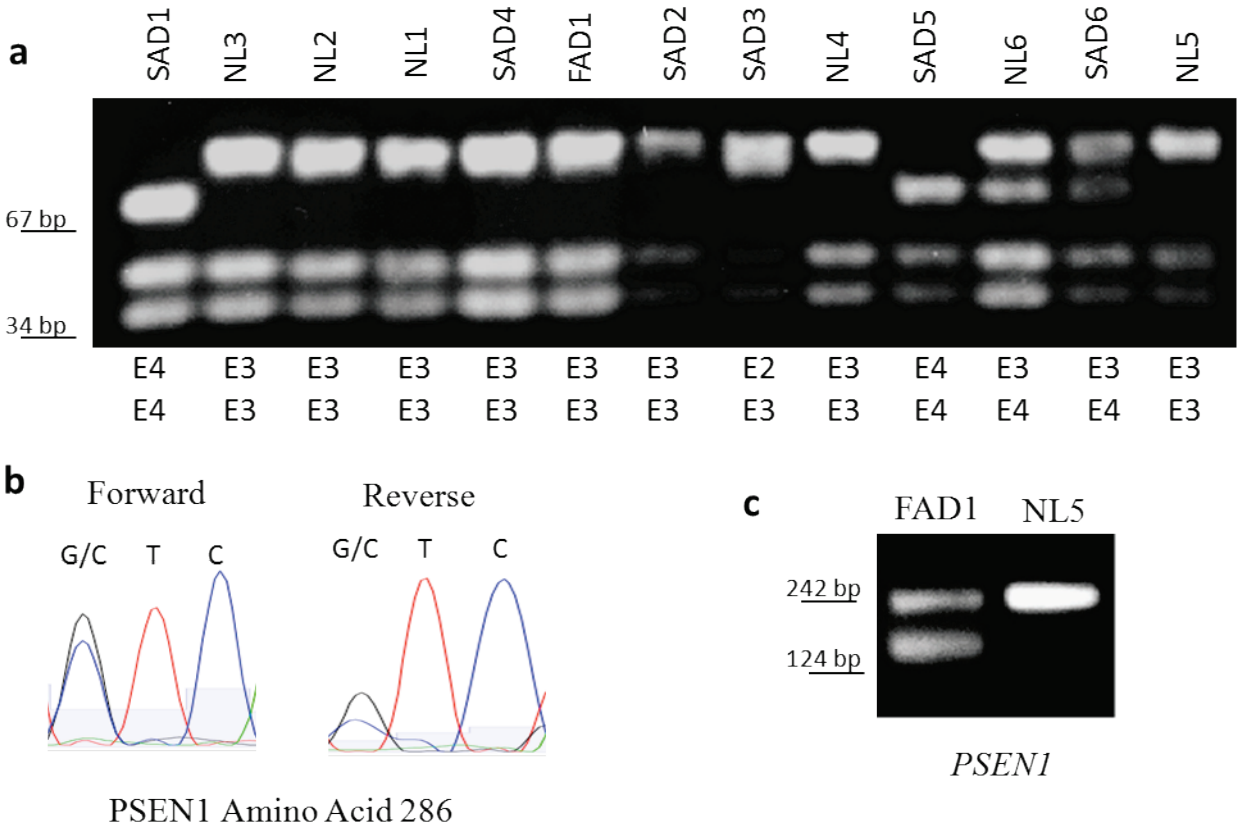

Figure 2.1: Genotyping of Fibroblast Lines (a) *APOE* genotyping in fibroblasts. The *APOE* gene was amplified through PCR and restriction digested by Hha1, creating fragments of 91 and 83 base pairs (bp) for *APOE2,* 91, 48, and 35 bp fragments of *APOE3*, and 72, 48, and 35 bp for *APOE4*. (b) Sequencing of FAD1 in *PSEN1* shows a heterozygous mutation coding for amino acid 286. This shows the sequence of the three base pair codon for amino acid 286 of the PSEN1 protein using both forward and reverse primers. The reverse primer sequence is converted to the reverse complement. (c) Restriction digest in *PSEN1* confirms the mutation. L286V creates a new *PvuII* restriction site, resulting in products of 149 bp and 113 bp in FAD1 (and the full length 262 bp), while the control line NL5 only has the full length *PSEN1* amplified product. The 113 bp product is not visible on this gel.

B. Gene expression in fibroblast cells

Microarray profiling of a subset of the fibroblast lines (NL1, NL2, NL3, NL4, SAD1, SAD2, SAD4, and FAD1) shows a difference in mRNA expression in the SAD and NL lines (Figure 2.2a). The gene expression was measured on an Affymetrix U133 Plus 2.0 array and background adjusted and normalized using robust multi-array averaging (RMA) before preprocessing to remove genes that showed little variation and thus differences that may be due to platform noise or are not biologically relevant. The normalized and preprocessed expression data was analyzed for differences between the normal and SAD lines. Since there is only one FAD line, it was not directly included in the comparison between SAD and NL, since it may have a different mechanism by which the patient developed AD. However, it was included in all post-hoc analyses to see if it correlates more closely with the SAD or NL line. The results were corrected for multiple hypothesis testing using the Q-value (Storey & Tibshirani 2003) calculated with an asymptotic p-values (due to the small number of samples in each group).

150 annotated probes showed differentially expression between the SAD and NL lines using a significance cut-off of q-value ≤ 0.15 which corresponds to a p-value ≤ 0.012 (Supplementary Table 1). In this statistical measure, 15% of the genes on the list are expected to be false positives. This less stringent cut-off was chosen to be consistent with later stages of analysis. Correlation analysis between the expression of the fibroblast lines shows intra-group correlation for both the AD lines and NL lines (Figure 2.2e). The expression in FAD1 correlated most with the SAD lines (Pearson correlation coefficient r between 0.32 and 0.50), rather than the normal lines. The SAD lines correlated with each other ($r = 0.30$-0.62), while the expression of normal lines correlated as well ($r = 0.31$-0.44).

Figure 2.2: Gene Expression Profile of Fibroblasts (a) Heat map of significant genes differentially expressed between SAD and normal fibroblast lines with a q-value of less than 0.15. (b) The ten most significant biological processes evaluated through enrichment analysis in the gene ontology (GO) database using MetaCore. (c) The fold changes of the individual genes for one of the significant gene ontology biological processes, nervous system development, show a predominate down-regulation of genes in SAD fibroblasts. (d) Analysis using the Database for Annotation, Visualization, and Integrated Discovery (DAVID) for functional annotation clustering in the significant fibroblast gene list. Included annotation clusters had an enrichment factor greater than one and are annotated through the first novel descriptor. D: domain, CC: cellular compartment, BP: biological process. (e) A heat map of Pearson correlation coefficients shows that gene expression of FAD1 in the differentially expressed fibroblast genes clusters with the three SAD lines, while the four normal lines are most similar to each other. (f) Interactome analysis using MetaCore shows enrichment of interaction hubs in the genes differentially expressed in the fibroblasts. The hubs selected were the only significant interactions in the gene set. The ratio refers to the number of interaction partners in the gene list divided by the expected number of interactions in a random gene list of equal size. (g) Analysis of upstream regulators by Ingenuity Pathway Analysis (IPA) calculates the regulators that are predicted to be more or less activated due to the difference in gene expression of the significant gene list. The upstream regulators selected were the only ones to show an activation or inactivation score and thus a predicted difference in activity levels in the SAD fibroblasts.

Figure 2.2: Gene Expression Profile of Fibroblasts (cont.)

a

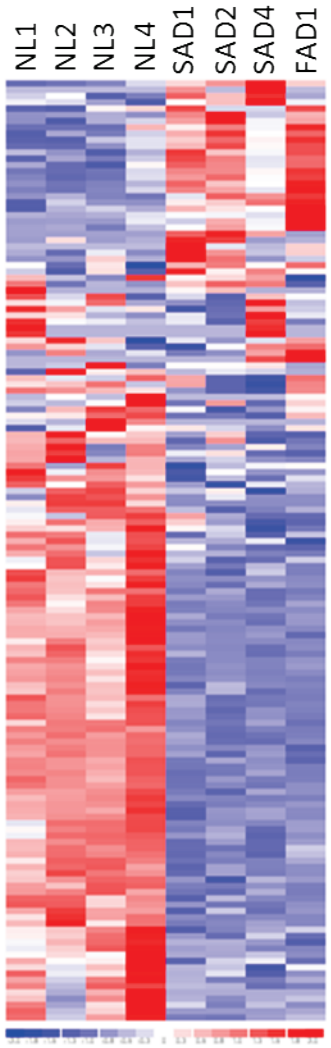

b

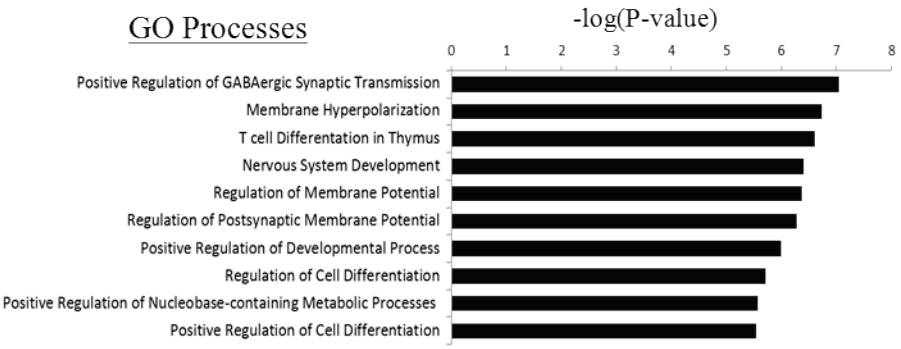

c

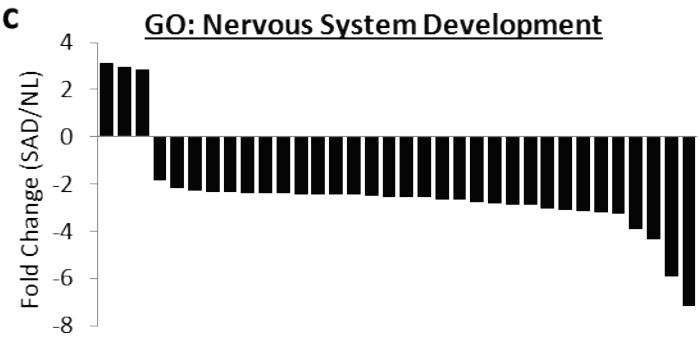

d

Annotation Cluster	Type	Enrichment
Fibronectin, type III-like fold	D	2.43
Integral to Plasma Membrane	CC	1.60
Signal Peptide	BP	1.49
Glucose Homeostasis	BP	1.34
Positive Regulation of Developmental Process	BP	1.13
Cell Adhesion	BP	1.09

e

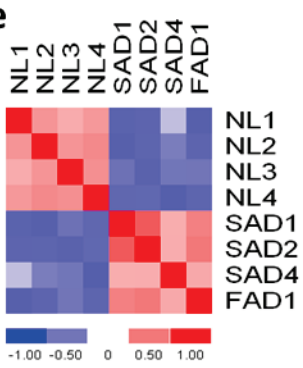

f

Interactions

Category	Object	P-value	Ratio
Receptor	TNFRSF6B	4.55E-04	59.9
Receptor	IGVL1	4.55E-04	59.9
Kinase	FAK1	2.56E-04	4.9
Enzyme	DCoHM	4.22E-05	20.5
Enzyme	BRG1	2.45E-04	3.6

g

Upstream Regulators

Upstream Regulator	Type	Activation	P-value
TP53	transcription regulator	1.90	4.65E-01
E2F1	transcription regulator	1.19	9.47E-03
ADCYAP1	other	0.64	3.07E-03
TCF3	transcription regulator	-0.45	2.86E-03
RUNX2	transcription regulator	-0.69	3.22E-04
INHBA	growth factor	-1.00	2.30E-02

Enrichment analysis using MetaCore software shows that five of the ten most significant gene ontology (GO) biological processes relate to neuronal function (Figure 2.2b). This is surprising since fibroblasts are not expected to express many neuronal genes. These neuronal genes are mainly down-regulated in the SAD fibroblasts, as visualized through the differential expression of the genes in the nervous system development GO group (Figure 2.2c). Annotation clustering analysis using the Database for Annotation, Visualization, and Integrated Discovery (DAVID) did not show enrichment for neuronal processes, but greater than expected expression of genes with fibronectin domains and those that localize to the plasma membrane (Figure 2.2d).

Interaction and upstream regulator analysis was performed using MetaCore and Ingenuity Pathway Analysis (IPA) respectively (Figure2.2e,f). The interaction analysis evaluates the gene list for overconnected interactions, listed by the protein that serves as a hub for that network. Several of the overconnected interaction hubs relate to neuronal function, including the two with the highest number of interactions, focal adhesion kinase (FAK1/PTK2), which functions at focal adhesions downstream of many extracellular matrix receptors and is important in neural functions (Nikolic 2004) and BRG1, an ATPase which belongs to a neural progenitor-specific chromatin remodeling complex (Lessard et al 2007). The upstream regulators calculated by IPA include an activation score to show whether the gene expression differences are consistent and show increased or decreased activity of the upstream regulators in the SAD lines. The activated upstream regulators are the transcription regulators p53 and E2F1, which can act together in both cell proliferation and cell death (Polager & Ginsberg 2009).

C. Reprogramming into induced pluripotent stem cells

Fibroblasts were reprogrammed into iPS cells using retroviral transduction of the Yamanaka factors (*SOX2, KLF4, cMYC,* and *OCT4*). Multiple clones were formed for most lines through distinct viral integration events and distinguished by a numeral following the individual name (*e.g.* SAD2.1, SAD2.2, and SAD2.3). Clones from each individual were evaluated for their expression of pluripotency markers and differentiation capability (Table 2.2). Every clone showed ESC-like morphology and each tested line expressed the pluripotency markers NANOG, SOX2, TRA-1-81, and OCT4 as well as the elevated alkaline phosphatase activity indicative of a undifferentiated, pluripotent stem cell (Table 2.2, Figure 2.3a,b). All analyzed lines maintained a normal karyotype except SAD1.1, which had a balanced translocation between chromosome 3 and chromosome 5 (Figure 2.3c). The karyotype of SAD1 fibroblasts was normal when analyzed by the Coriell Cell Repository, indicating that the translocation may have occurred during the reprogramming process.

To evaluate inactivation of the transduced reprogramming factors, actual mRNA expression levels of both the transgenic and endogenous reprogramming genes were measured using qRT-PCR to a quantified cDNA standard curve specific to each gene product (Figure 2.4a, b). In the iPS cell lines tested (one per individual), the *cMYC* transgene was expressed at less than 15% of the endogenous locus, *SOX2* was expressed at less than 4% of the endogenous locus, and *OCT4* transgene expression was less than 8% of the endogenous locus. Even *KLF4*, which had the lowest levels of endogenous expression, showed less than 30% expression of the transgene compared with endogenous *KLF4*. Most importantly, there is no difference in transgene inactivation between the SAD and normal iPS lines.

Table 2.2: Characterization of iPSCs: Clones and Passage Number

Line	Immuno-fluoresence		Alkaline Phosphatase		Karyotyping		Transgene Inactivation	
	iPS Clone	Passage	iPS Clone	Passage	iPS Clone	Passage	iPS Clone	Passage
NL1	1, 2, 4	3	1,2,3	3	1	23	1	7
NL2	1	3	1,4	3	1	11	1	9
NL3	1,2,3	3	1,2,3,4,5	3	1	12	2	10
NL4	1	19	1	19	1	19	1	11
NL5	1	21	1	21	-	-	1	8
NL6	1	12	1	12	-	-	1	6
SAD1	2	3	1,2,3	3	1	20	1	11
SAD2	1,2,3	3	1,2,3	3	1	14	1	10
SAD3	1	13	1	13	1	13	1	8
SAD4	1	3	1,2	3	1	15	1	9
SAD5	1	21	1	21	1	13	1	8
SAD6	-	-	-	-	2	8	1	6
FAD1	1,3	3	1,2,3	3	1	20	1	11

Line	EB RT-PCR		Teratoma		Microarray	
	iPS Clone	Passage	iPS Clone	Passage	iPS Clone	Passage
NL1	1	26	1	22	1	7
NL2	1	24	1	17	1	9
NL3	1	23	1	13	2	10
NL4	1	22	1	17	1	11
NL5	1	24	1	18	1	8
NL6	1	17	1	22	1	6
SAD1	1	19	1	29	1	11
SAD2	1	17	1	12	1	10
SAD3	1	25	1	19	1	8
SAD4	1	18	1	12	1	9
SAD5	1	24	1	21	1	8
SAD6	2	15	2	9	1	6
FAD1	1	28	1	16	1	11

Figure 2.3: iPS Cell Characterization (a) iPS cell lines express the pluripotency markers OCT4, Tra-1-81, NANOG, and SOX2. Images were acquired at 200x magnification. (b) The iPS cells show enhanced alkaline phosphatase activity with the ability to create a histochemical substrate from naphthol AS-BI phosphate, visualized by staining with Fast Red Violet. The images were acquired using a brightfield microscope coupled to a CCD camera at 100x magnification. (c) Cytogenetic analysis of the iPS lines revealed normal karyotypes in all the tested lines except SAD1.1 which has a balanced translocation between the short-arm of chromosome 3 at band p21 and the long-arm of chromosome 5 at band q13.

Figure 2.3: iPS Cell Characterization (cont.)

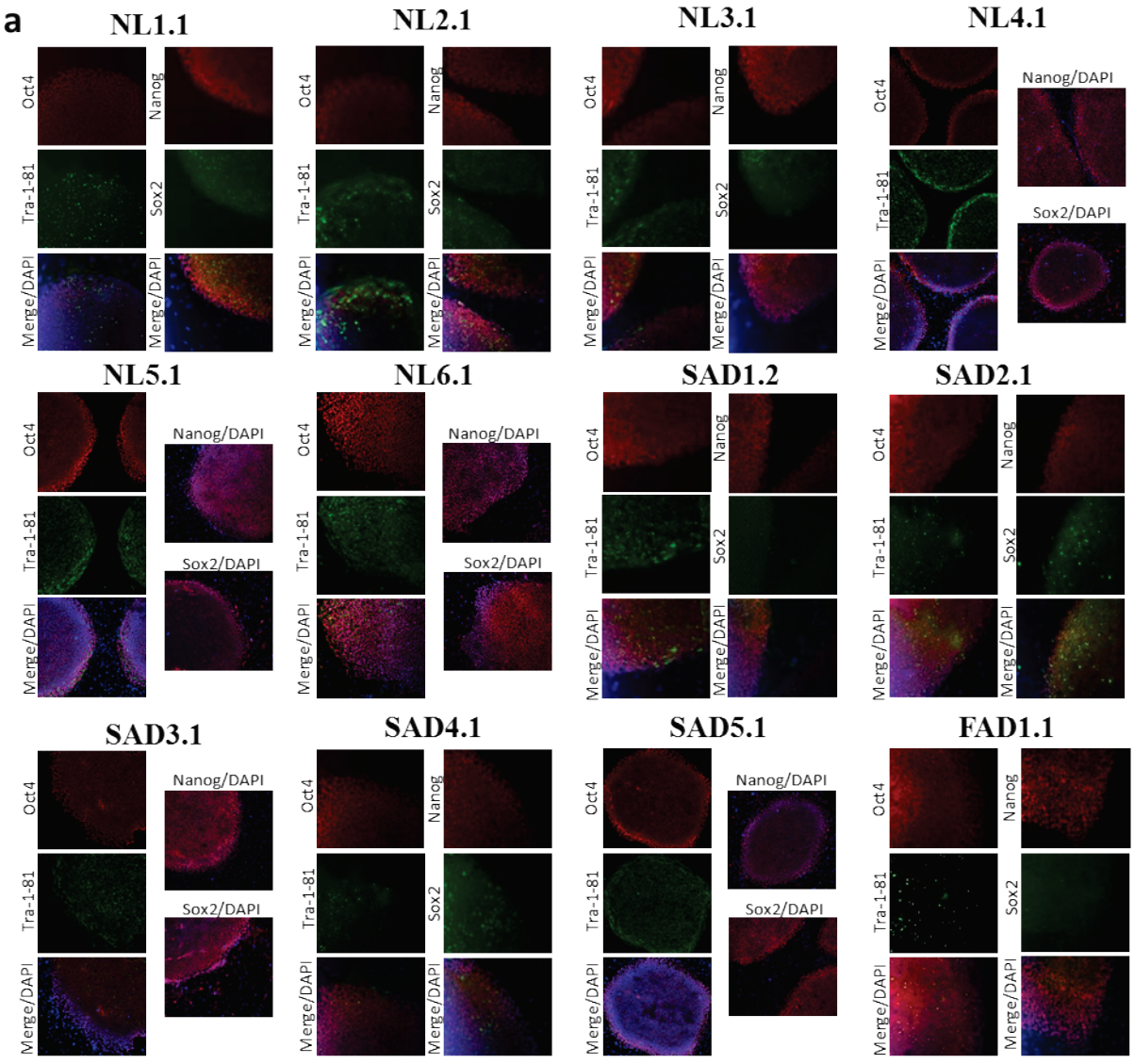

Figure 2.4: iPS Cells Inactivate the Viral Transgenes (a) cDNA from the reverse transcription-PCR of the endogenous and transgenic reprogramming factors *KLF4*, *cMYC*, *SOX2*, and *OCT4* were separated and extracted from an agarose gel. All the PCR reactions produced a single band product except *cMYC* endogenous, which had a lesser secondary band. Only the major cDNA product was used to make a standard curve. (b) All the reprogramming factors have lower levels of transgene expression than the endogenous gene, indicating transgene inactivation. Actual mRNA levels of each gene for one IPSC line per individual were measured through qRT-PCR and comparison to a quantified cDNA standard curve. (c) Expression of *GFP* from pMIG-Reprogramming factor-IRES-GFP in all the evaluated iPSC lines was less than 0.05% the levels of a human fibroblast retrovirally transduced with pMXs-IRES-GFP, supporting strong inactivation of the four transgene reprogramming factors. All expression values were normalized to *GAPDH*.

Figure 2.4: iPS Cells Inactivate the Viral Transgenes (cont.)

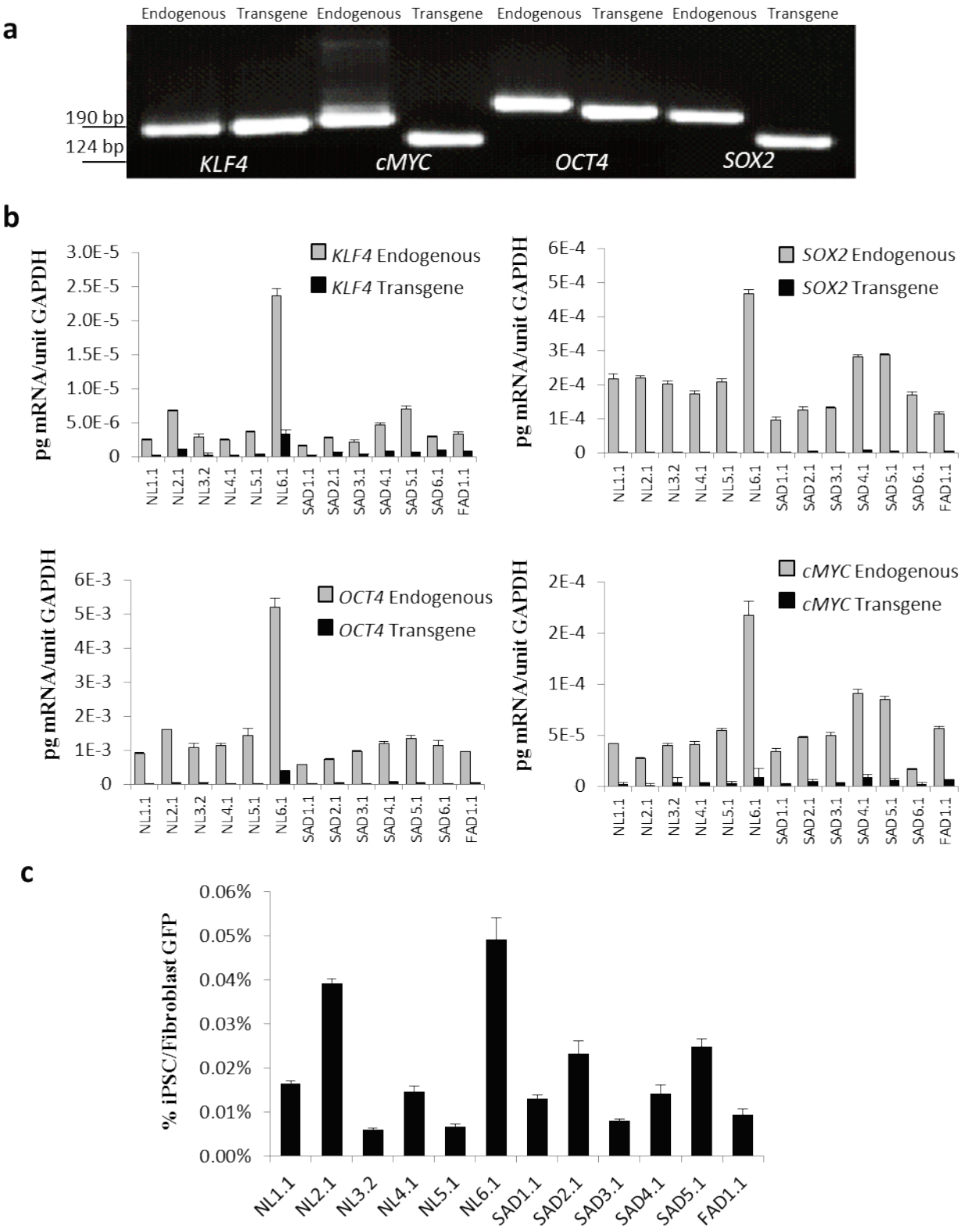

To evaluate the overall transgene inactivation levels compared to a recently transduced control, *GFP* expression was measured for each line (Figure 2.4c). All four of the reprogramming factors have an IRES-GFP element which should be expressed in tandem with the reprogramming gene. Immediately following transduction, the fibroblasts express GFP, but the GFP expression in the mature iPS cells is below detectable limits through epifluorescent microscopy, indicating inactivation (data not shown). The levels of *GFP* mRNA were measured in iPS cells using qRT-PCR and compared to a human fibroblast control line transduced with pMXs-GFP. The pMXs promoter is similar, but not identical to the pMIG plasmids used for reprogramming, since the MMLV 5' long terminal repeat (LTR) of pMXs differs in several basepairs from the MSCV 5' LTR of pMIG (Cherry et al 2000). The *GFP* of the reprogramming factor vectors was expressed at less than 0.04% the levels of the *GFP* in the fibroblasts, indicating that the transgenes are inactivated not only compared to the endogenous genes, but also quite strongly compared to the levels following transduction.

In order to prove that the reprogrammed iPS cells are in fact pluripotent, we tested their ability to form tissues of the three germ layers formed during embryogenesis: ectoderm, endoderm, and mesoderm. iPSC colonies were grown in suspension for one week without basic fibroblast growth factor (bFGF) to form embryoid bodies (EBs), a three-dimensional cellular aggregate in which differentiation to more specialized cells starts to occur. The EBs were plated and differentiated for one more week in serum-containing media to induce further differentiation, forming diverse morphological structures (Figure 2.5b). All iPSC lines tested (one per individual) were able to differentiate into the three germ layers *in vitro*, showing mRNA expression of the ectodermal markers β-tubulin III and *NCAM*, the endodermal markers *AFP* and

GATA4, and the mesodermal markers *Flk* and *GATA2* through semi-quantitative RT-PCR (Figure 2.5a).

The ability to form all three germ layers was also recapitulated *in vivo*, when iPS cells injected under the renal capsule of NOD-SCID mice formed teratomas, a tumor which contains diverse tissue types from more than one germ layer (Figure 2.6). All thirteen lines tested (one per individual) formed teratomas containing tissues derived from each of the three germ layers, confirming that the iPS cells are pluripotent.

Figure 2.5: Differentiation of iPS cells into all germ layers *in vitro*

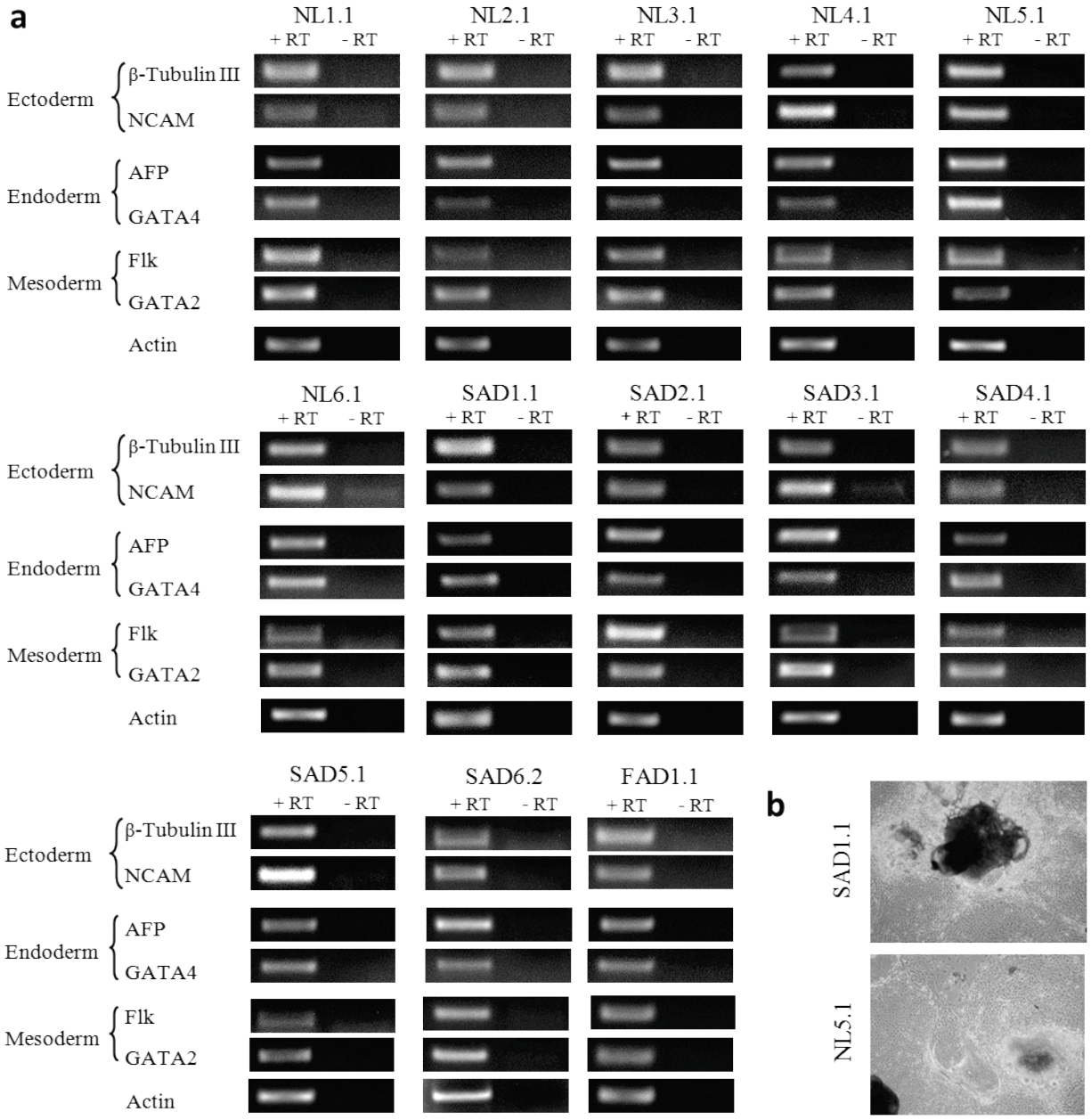

Figure 2.5: Differentiation of iPS Cells into three germ layers *in vitro*. (a) Semi-quantitative RT-PCR shows 2-week differentiated iPS cells express markers of all three germ layers *in vitro*. RNA was harvested from differentiated iPS cells that had been grown in suspension as embryoid bodies (EBs) for seven days and then on gelatin in serum-containing media for seven days. RT-PCR was run both with and without reverse transcriptase (RT) to control for DNA contamination. (b) Representative phase contrast images of plated EBs after two weeks differentiation from iPS cells.

Figure 2.6: Differentiation of iPS cells into all germ layers *in vivo*

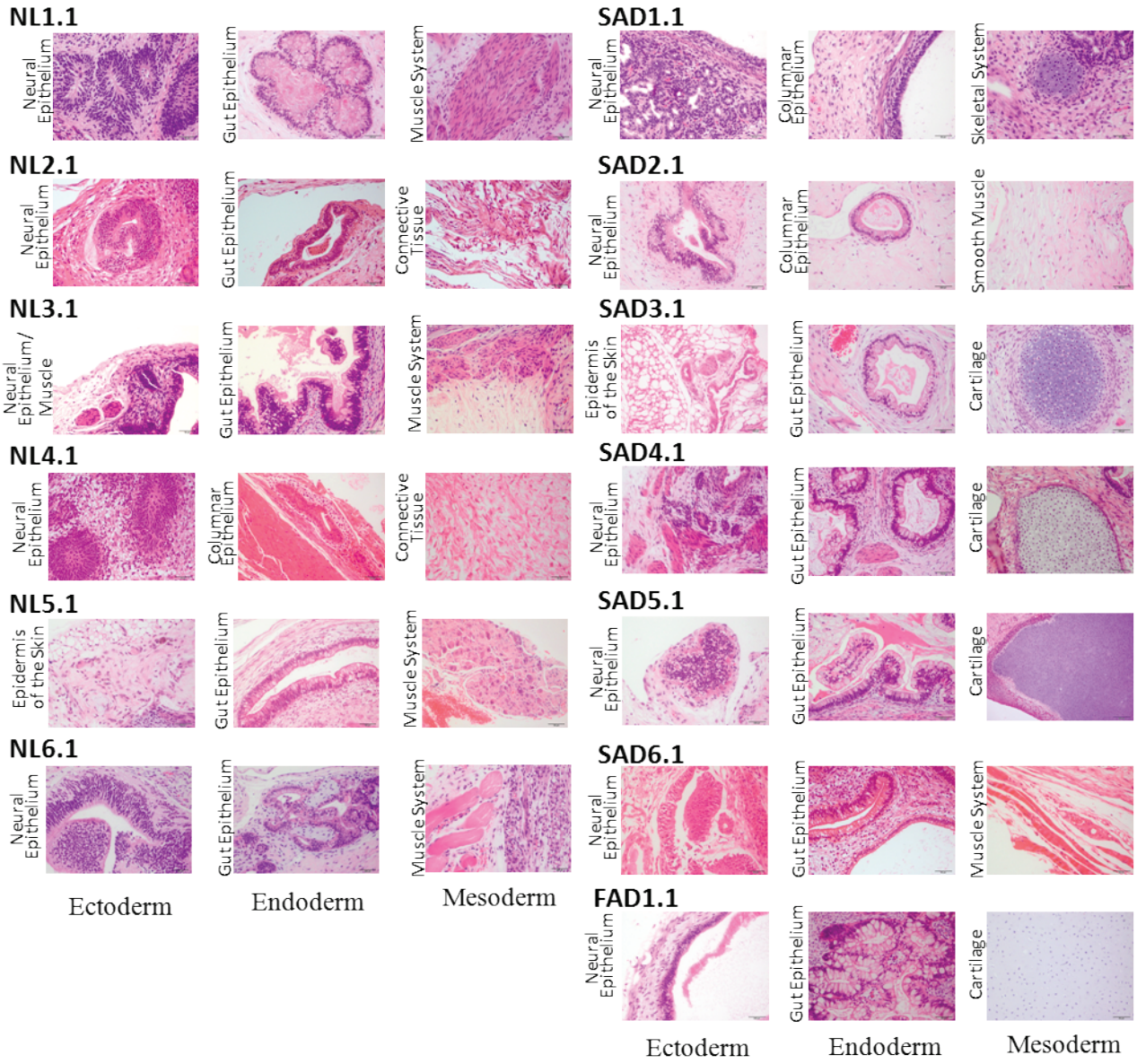

Figure 2.6: Differentiation of iPS cells into all germ layers *in vivo*. One iPS cell line per individual was injected into the kidney subcapsule of NOD-SCID mice to evaluate *in vivo* pluripotency. Tumors formed for each line which contained tissues from each of the germ layers. The teratomas were embedded in paraffin and stained with hematoxylin and eosin to show structures including ectodermal neural epithelium and skin epidermis, endodermal gut and columnar epithelium, and mesodermal muscle, cartilage, and connective tissue.

D. Gene Expression in iPS Cells

Gene expression in iPS cells was evaluated using the same approach as the fibroblast lines, but including more individuals (Table 2.2). One clone per individual was included in the analysis. Despite the increased number of samples, there were no genes that met the statistical criteria of q-value less than 0.15 (Supplementary Table 2). In fact, all of the q-values were close to 1, indicating that any significant gene differences indicated through p-value analysis have a high probability of being a false positive.

Conclusions and Discussion

We have established the largest group of iPS cells from sporadic AD and age-matched control patients to date from the fibroblasts of 6 NL and 6 SAD individuals, as well as one FAD *PSEN1* mutant. These patients are enriched for an earlier age of onset to increase the likelihood of recognizing differences in cellular mechanisms that may lead to AD neurodegeneration. They also have a variety of *APOE* genotypes, including two *E4/E4* homozygotes and one *E2/E3* individual that may provide evidence for the effects of APOE isoform on AD development.

The subset of AD fibroblast lines tested show a distinct gene expression profile from the control lines using microarray analysis. Although this difference was seen in a relatively small group of genes, this result was surprising since AD is predominantly a disease of the central nervous system and does not have any known effects in the skin. However, it has been previously asserted that fibroblasts from familial AD patients share a distinctive gene expression profile, irrespective of the starting mutation (Nagasaka et al 2005). Unfortunately, this gene profile was not published, therefore we are unable to see if it correlates with our findings.

Using enrichment analysis, the distinctive genes of AD fibroblasts are enriched for neuronal and differentiation genes. The top ten most significant gene ontology biological

processes included five related to neuronal function and development and three related to cell differentiation. All of these GO groups feature genes that are predominantly down-regulated in the AD lines, suggesting these processes could be disrupted in AD patients. However, annotation clustering analysis using DAVID supported a more important enrichment of plasma membrane-related genes, including those involved in signaling, cell adhesion, and containing fibronectin domains. It is unclear what functional effects these differences may have in human fibroblasts, but they remain important areas to explore throughout the later stages of differentiation.

Two possible explanations for the difference in gene expression are that 1) the gene expression differences may just be due to the advanced stage of the disease affecting the overall health of the patient or 2) this difference reflects fundamental variance in the genetic or epigenetic state of the individual that led to the development of AD. To control for the gene expression differences due to the poor health of the patient, the gene expression profile should be compared to patients with other diseases, especially neurological such as Parkinson's or Huntington's. If instead these gene expression differences may contribute to the development of AD, the gene expression changes should be seen in the later stages of differentiation and provide more insight to the effects on the brain.

All thirteen iPS lines are pluripotent, expressing pluripotency markers and differentiating into all three germ layers. They also silenced the reprogramming factors, indicating that the lines are suitable for differentiation. Despite any remaining epigenetic modifications after reprogramming, the difference in gene expression between the SAD and NL fibroblasts was completely erased in the iPS cells. Although there still could be epigenetic modifications that could affect expression in later stages of differentiation, this homogenous gene expression

supports that reprogramming returns the cells to a more embryonic state and that gene expression in later stages of differentiation will be primarily dependent on the genetic differences between the individuals.

Contributions

Nicholas Bishop reprogrammed the fibroblasts into iPS cells. He also characterized half of the iPS cell lines for pluripotency markers and alkaline phosphatase activity (NL1.1, NL2.1, NL3.1, SAD1.2, SAD2.1, SAD4.1, and FAD1.1). He prepared the RNA samples for the fibroblast and iPS microarray. Karyotype analysis was performed by Cell Line Genetics (Madison, WI). Semi-quantitative RT-PCR of the differentiated iPS cells *in vitro* was performed by the Harvard Stem Cell Institute's iPS core facility in collaboration with Laurence Daheron. Teratoma formation was performed by Zhenjuan Wang at the Harvard University Genome Modification Facility and embedding, sectioning, imaging, and analysis was performed by Cathy MacGillivray at the HSCRB Histology-Immunohistochemistry core.

Chapter 3: Differentiation and characterization of neural progenitors

Abstract

Neural progenitors (NPs) were differentiated from iPS cells derived in three different labs and expressed the neural progenitor markers nestin, musashi, and SOX2. Gene expression profiling using microarray analysis shows a robust difference between the SAD and NL neuronal progenitor lines, with a surprising up-regulation of neuronal differentiation genes in the SAD neural progenitors. This difference was verified through qRT-PCR and western blotting and was confirmed to be isolated to a subset of cells through immunostaining and fluorescent-activated cell sorting (FACS) analysis. Furthermore, this difference was confirmed using NP cells derived from multiple iPSC clones from the same patients, confirming that SAD neural progenitor lines have increased expression of neuronal differentiation markers compared with the NL patient age-matched controls.

Introduction

Now that we have successfully reprogrammed fibroblasts into induced pluripotent stem cells, we want to differentiate the cells into neurons to test if there are any differences between the SAD and NL patient cells. The neural differentiation process can be paused at a neural progenitor intermediate that is stable and self-renewing. This type of cell is easier to culture than iPS cells or neurons and differentiation into neurons can be readily initiated. It will also allow us to see if there are any differences between the AD and NL cells earlier in differentiation before the cells become mature neurons.

Neural development is a complicated and incompletely understood process *in vivo* (Jessell 2000), which may make it difficult to replicate *in vitro*. First, the neural lineage must be induced in cells to create a population of neural progenitors. Then, the progenitors are

committed to a neuronal fate and the immature neurons must migrate, grow dendrites and axons, guide the axonal growth cone to postsynaptic partners, and generate synapses to become mature neurons.

After gastrulation during which the three germ layers form, a neural plate forms in the ectoderm. The neural plate folds into the neural tube that will become the cells of the central nervous system. Neural differentiation seems to be the default state of these cells, but is suppressed by bone morphogenic proteins (BMP) 2 and 4 (Varga & Wrana 2005). The BMPs are suppressed by noggin and chordin which are produced in the mesoderm and diffuse to the cells of the neural tube, allowing neural induction to occur (Chitnis 1999).

However, positive inducers of neuronal induction including Wnt and factors that activate MAPK including fibroblast growth factor (FGF) family members and insulin-like growth factor (IGF) may also play a role in the neural induction process (Gaulden & Reiter 2008). After neural induction has occurred, the cells may now be considered neural progenitors and have the capacity to become several different cell types of the central nervous system including neurons, astrocytes, and oligodendrocytes. The commitment to the neural fate occurs during neurogenesis in which neural progenitors are selected through a lateral inhibition process reliant on Notch-Delta signaling at distinct regions of the neural plate (Bally-Cuif & Hammerschmidt 2003). Delta expression is up-regulated in differentiating neurons and activates Notch signaling in neighboring progenitors, which inhibits differentiation in those neighboring cells (Kageyama et al 2009).

These regions where the production of neurons and glial cells occur are defined by a variety of secreted morphogens including sonic hedgehog, Wnt, BMPs, FGF, and retinoic acid which form gradients in a process called neural patterning (Takahashi & Liu 2006). This neural

patterning causes combinatorial expression of pro-neural transcription factors, leading to the wide variety of different types of CNS cells (Corbin et al 2008). These transcription factors include members of the homeoprotein family such as HOX and PAX, TALE transcription factors such as MEIS, zinc-finger family such as GLI and ZIC, and basic helix-loop-helix (bHLH) family such as HES, ID, ASCL1 and neurogenins (Bally-Cuif & Hammerschmidt 2003). Expression of these various transcription factors and others are spatially and temporally regulated to control the location and type of cells produced by differentiation.

Neural progenitors are a diverse group of cells in the developing brain. In the telencephalon, from which most of the regions affected during Alzheimer's disease arise including the cerebral cortex, hippocampus, and olfactory bulb, there are two distinct classes of neural progenitors: 1) the progenitors dividing at the ventricular surface including neuroepithelial cells and radial glia and 2) the progenitors that divide predominantly in the basal region called basal or intermediate progenitors (Gotz & Huttner 2005). These progenitors remain incompletely understood, but are known to generate other progenitors, neurons, and glia.

The neuroepithelial progenitors (NEPs) are the earliest of the stem cells and most similar to the kind we attempt to differentiate in culture from the iPS cells. Prior to the onset of neurogenesis, the proliferating neuroepithelial progenitors primarily undergo symmetric divisions, expanding the pool of NEPs (Huttner & Kosodo 2005). They are polarized cells which are anchored to the basal lamina through integrins and to each other through tight junctions and adherens junctions (Gotz & Huttner 2005). However, in later stages of development, the NEPs asymmetrically divide to produce neurons and glia, but also another type of neural progenitor: the radial glia cells.

Radial glia cells (RGCs) have a bipolar morphology and are multifunctional. They act as both a scaffold for migration of the newly generated neurons, but also the most important neuronal progenitor, accounting directly or indirectly for most of the neurons in the cerebral cortex (Guillemot 2005). RGCs express many markers of glial cells, including expression of GFAP, and are not bound together by tight junctions like the neuroepithelial progenitors (Barry et al 2014). However, they still express the progenitor marker of nestin. The PAX6 transcription factor is important for the development of radial glia cells; forced expression in murine neuroepithelial cells triggers differentiation into radial glia and neurons, while knockdown decreases the production of RGCs (Suter et al 2009). RGCs produce postmitotic neurons, astrocytes, or a third class of neuronal progenitors: the basal or intermediate neuronal progenitors.

Intermediate neuronal progenitors (INPs) are not adhered to the ventricular zone like the NEPs and RGCs and are instead located in the basal region where the apically derived neurons are migrating. They have limited proliferative potential, only undergoing 1-3 mitotic cycles and generate exclusively neurons (Kowalczyk et al 2009). They are positive for the transcription factor Tbr2 and are thought to be important in increasing the number of neurons generated from a given ventricular-zone progenitor at the basal site of inclusion and possibly in balancing the generation of glutamatergic and GABAergic neurons (Haubensak et al 2004, Sessa et al 2010). A subset of INPs is also found at the apical ventricular zone, which may be equivalent to the short neuronal precursers seen in rodents. These ventricular zone INPs have a distinct morphology and are incompletely understood (Kowalczyk et al 2009).

Even with these classifications of the neuronal progenitors seen *in vivo* during cortical development, there is a lot of heterogeneity with many subsets with distinct gene expression

profiles (Kriegstein et al 2006). This variance may be due to differences in morphogen signaling and resulting transcription factor expression.

In adult neurogenesis, neural stem cell (NSC) populations are found in two regions: the subventricular zone (SVZ) that feeds into the olfactory bulb and the subgranular zone (SGZ) which feeds into the dentate gyrus. The predominant NSC population in the SVZ expresses GFAP and CD133 which will asymmetrically generate transit amplifying cells that migrate into the olfactory bulb (Faigle & Song 2013). The predominant population in the SGZ expresses GFAP, nestin, and SOX2 and is considered radial glia-like (RGL) cells (Type 1 cells). This population can give rise to more RGL cells, glia, and a more restricted but still mitotically active intermediate progenitor that no longer expresses GFAP and expresses the transcription factor ASCL1 (Type 2A cells). As the intermediate progenitor matures it will begin to express the microtubule-binding protein doublecortin and the neurogenin transcription factor (Type 2B cells) (Hodge et al 2008, Kempermann et al 2004). When the cells no longer express nestin and only express doublecortin, they are considered Type 3 neuroblasts. This intermediate will differentiate into post-mitotic glutamatergic dentate granule cells (Faigle & Song 2013). In the adult brain, the NSCs are predominantly quiescent, maintained by many factors including BMP and Notch signaling, cell adhesion molecules, G-protein coupled receptors (GPCRs), and cell cycle inhibitors (Giachino & Taylor 2014).

It is difficult to replicate a specific population of neural stem cells (NSCs) *in vitro* due to the many factors that control stem cell character. Small changes in secreted morphogen levels or substrate could have a large effect on the resulting neural stem cell population. Replicating the three dimensional architecture that occurs during corticogenesis *in vivo* is technologically infeasible meaning that important feedback will be missing during the development of these

neural stem cells *in vitro*. Therefore, our goal was to create a population of neural progenitors that is positive for the ubiquitous neural stem cell marker nestin, but may remain heterogenous. Other groups studying AD using iPS cells used FACS sorting to obtain a more homogenous population of NSCs (Israel et al 2012), but by only taking a small subset of the cells expressing nestin, that method may miss important populations of cells that are different between the AD and control groups.

We also acquired additional iPS lines from other labs: two normal patients from the Eggan laboratory and multiple clones from four patients from the Goldstein laboratory with two unaffected by AD and two with sporadic Alzheimer's disease (Table 3.1) (Boulting et al 2011, Israel et al 2012). It highly strengthens our results using iPS lines derived from multiple labs since laboratory of origin is known to affect gene expression (Newman & Cooper 2010).

Table 3.1: Additional iPS Lines

Line	Clones	Lab of Origin	Diagnosis	Age at Biopsy	Gender	*APOE*	Reference
17	a	Eggan	Normal	71	F	*E3/E3*	Boulting et al. 2010
20	b	Eggan	Normal	55	M	*E3/E3*	Boulting et al. 2010
NDC1	1,2,3	Goldstein	Normal	86	M	*E2/E3*	Israel et al. 2012
NDC2	2,3	Goldstein	Normal	86	M	*E3/E3*	Israel et al. 2012
SAD1	1,2	Goldstein	Sporadic AD	83	F	*E3/E3*	Israel et al. 2012
SAD2	1,2,3,4	Goldstein	Sporadic AD	83	M	*E3/E3*	Israel et al. 2012

Materials and Methods

Additional iPS Lines: iPS lines derived from the Eggan and Goldstein laboratories were acquired from the HSCI iPS Core Facility and directly from the Goldstein laboratory, respectively.

Differentiation and Culture of Neural Progenitors: The neural progenitor differentiation protocol developed was adapted from several sources (Marchetto et al 2010, Swistowski et al 2009). Culture conditions for neural progenitors were based on previous published work (Shin et al 2006). High density iPS cells growing on iMEF feeders (30-60 cm^2) were primed for neural differentiation two days before passaging by supplementing the hESC media with 1x N-2 supplement (Life Technologies) and the day before passage with 1x N-2 and 1 μM AMPK inhibitor (Calbiochem). The iPSC colonies were detached with dispase and transferred intact using a glass pipette to be washed twice with DMEM/F-12 to remove any residual dispase. The colonies were grown in suspension on 10 cm petri dishes (not treated for tissue culture) to form embryoid bodies (EB) in neural EB (NEB) media (DMEM/F-12 with 20% knockout serum, 1x N-2 supplement, 1 μM AMPK inhibitor, 1 mM L-glutamine, 100 μM non-essential amino acids, 100 μM 2-mercaptoethanol, 50 U/mL penicillin, and 50 mg/mL streptomycin). Media was changed every 2-3 days until day 8 when media was changed to neural induction media (NIM; DMEM/F-12 with 20% knockout serum, 1x N-2 supplement, 10 ng/mL bFGF, 1 mM L-glutamine, 100 μM non-essential amino acids, 100 μM 2-mercaptoethanol, 50 U/mL penicillin, and 50 mg/mL streptomycin). After three more days culture in suspension, the EBs were plated on 10 cm^2 CELLstart-coated (Life Technologies) tissue culture dishes in NIM. The NIM was changed every 2-3 days until neural rosettes formed (1-4 days).

The neural rosettes are manually harvested and transferred intact onto 0.002% polyornithine (Sigma Aldrich) and 5 ug/mL laminin (Sigma Aldrich) coated plates. The plates

were coated for 2 hours with polyornithine diluted in sterile, distilled water at 37º before washing and coating with 5 µg/mL laminin diluted in 4º Dulbecco's PBS without calcium or magnesium (Life Technologies) for 2 hours at 37º. The rosettes are grown in neural progenitor media (NPM) (Neurobasal media with 1x B-27 without vitamin A (Life Technologies), 1 mM L-glutamine, 10 ng/mL bFGF, 10 ng/mL leukemia inhibitory factor (LIF, Millipore), 50 U/mL penicillin, and 50 mg/mL streptomycin). Once confluent, the neural rosettes are broken apart and passaged using accutase (StemCell Technologies). The resulting NP cells are plated on polyornithine/laminin and NPM is changed every 2-3 days. The NPs are split with accutase when confluent.

DNA Fingerprinting: DNA fingerprinting was performed by Cell Line Genetics (Madison, WI) using the Powerplex 16 kit (Promega). Samples were run in duplicate and the interpreter blinded to confirm results.

Immunofluorescence (IF) and Antibodies: IF was performed as described in Chapter 2 on neural progenitors growing on glass coverslips coated with polyornithine and laminin. For all quantification, at least five randomized fields were imaged per coverslip and the cells expressing each marker were counted using MetaMorph (v7.7.0.0) software. First, the channels were separated into a separate image for each fluorophore using the command "Color Separate". Then, the number of cells expressing each marker was counted using the "Multi Wavelength Cell Scoring" application and consistent inclusion criteria throughout all coverslips.

Target	**Host**	**Source**	**Catalogue #**	**Dilution**
Nestin	Mouse	Millipore	MAB5326	1:200
Musashi	Rabbit	Millipore	AB5977	1:250
Sox2	Millipore	Rabbit	AB5603	1:250

β-tubulin III	Mouse	Chemicon	MAB1637	1:250
Doublecortin	Rabbit	Cell Signaling	4604S	1:400

Microarray Analysis: RNA was extracted using TRIzol reagent (Life Technologies) from confluent neural progenitors. mRNA was measured on Affymetrix U133 Plus 2.0 arrays by the Molecular Biology Core Facility at Dana Farber (Boston, MA) and the data was analyzed as described in Chapter 2. For the additional clones, the increased sample size allows for permutation testing, therefore 10,000 permutations were performed to calculate the p- and q-values.

Quantitative RT-PCR and Primers: Primers were designed for 100-250 bp segments spanning exon boundaries highly conserved between alternative transcripts using Ensembl gene mapping information and Primer3 to optimize G/C concentration and melting temperature. The primer products were verified by agarose gel electrophoresis and a standard curve was established for each primer pair using serial dilution of a titrated RNA sample to account for primer efficiency. RNA was harvested from NP cells using either TRIzol reagent or Cells-to-cDNA II kit with DNase treatment. The mRNA was quantified using QuantiTect SYBR Green PCR kit according to the manufacturer's guidelines and run in a one-step RT-PCR cycle in an iQ5 (Bio-Rad) (reverse transcription at 50º for 30 minutes, denatured at 95ºC for 12 min, and then subjected to 35 cycles of amplification (20 seconds at 95ºC, 30 seconds at 55ºC, and 30 seconds at 68ºC) before a final extension of 65ºC for 10 minutes). The purity of the PCR products was determined by single peak melting curves. The relative cDNA was quantified using the standard curve established for each primer pair and normalized to *GAPDH* or *β-actin*. Statistical

differences between the SAD and NL lines were calculated using a two tailed student's *t*-test assuming unequal variances for both the normalized relative mRNA concentration and its $\log_2$.

Primer Target	Forward Sequence	Reverse Sequence
GAPDH	AGCCACATCGCTCAGACACC	GTACTCAGCGCCAGCATCG
Doublecortin	GAACTGGAGGAAGGGGAAAG	GCTCAAAAGAGTGGGCTGTC
ASCL1	AACAGTCAACCAACCCCATC	GCTGTGCGTGTTAGAGGTGA
CD24	ATGTGGCAAGGAAAAACAGG	CTCCATTCCACAATCCCATC
EPHB1	GGCCCATCGCATCTACAC	ATCAGCCTTCCCCCAAAG
COL11A1	ATGGAATCACGGTTTTTGGA	AGGTTCCTGAGCTTGAGCAG
CD44	GCAGGTATGGGTTCATAGAAGG	GTCATACTGGGAGGTGTTGGAT
Actin	TTCTACAATGAGCTGCGTGTG	AGAGGCGTACAGGGATAGCA

Western blotting: Confluent cultures of neural progenitor cells were washed with PBS before manual harvest with a cell scraper. Samples were resuspended in lysis buffer (RIPA-DOC (50 mM Tris-Cl (pH 7.2), 150 mM NaCl, 1% Triton x-100, 0.1% SDS, and 1% deoxycholate) with 1x PhosSTOP (Roche) and 1x cOmplete protease inhibitor (Roche)). Lysed samples were sonicated for 15 seconds each with a 550 Sonic Dismembrator (Fisher). Protein concentration for each sample was measured using D_C protein assay kit (Bio-Rad) and adjusted to 0.8-1.5 µg/µL in 5x SDS-reducing sample buffer. Equivalent amounts of protein were loaded per lane and resolved by 4-20% SDS-PAGE. Protein was transferred to PVDF membrane and blocked with 5% nonfat milk in PBS with 0.02% Tween-20 (PBST) for 1 hour at room temperature with shaking. Membranes were cut to allow targeting of multiple size proteins on the same blot and incubated overnight with primary antibody diluted in PBST with 5% bovine serum albumin and 0.05% sodium azide at 4ºC with shaking. The membranes were thoroughly washed with PBST before incubation for 1 hour with peroxidase-conjugated secondary antibody against the host species (Jackson ImmunoResearch, 1:2500) in 5% nonfat milk in PBST. After 1 hour, the membranes were washed thoroughly with PBST before visualization by chemiluminescence

(ECL or ECL Prime, GE Healthcare). Intensities of the immunoreactive bands were quantitatively analyzed on a gel documentation system (SynGene). All quantified proteins were normalized to GAPDH or β-actin and, if multiple membranes were necessary, also to control samples common to blots. Significance between groups was calculated using a two tailed student's *t*-test assuming unequal variances.

Target	Host	Source	Catalogue #	Dilution
Doublecortin	Rabbit	Cell Signaling	4604S	1:1000
GAPDH	Mouse	Abcam	ab8245	1:2500

Fluorescence-activated Cell Sorting (FACS): Confluent neural progenitor cells were dissociated from 10 cm^2 tissue culture dishes with accutase at 37º and triturated in Neurobasal media. They were incubated for 10 minutes with 10 U/mL DNase. The cells were filtered in a 40 μm filter, spun down, and resuspended in 100 μL NPM with 5 μM EDTA and 0.5% bovine serum albumin (BSA) (about $1x10^6$ cells). 20 uL (1 test) of mouse anti-human CD24-FITC (BD Biosciences, 560992) was added per sample and incubated in the dark on ice for 30 minutes. The cells were then washed twice with Neurobasal with EDTA and BSA and resuspended in NPM with EDTA and BSA at 2.5 $x10^5$ cells/mL. Cells were stored on ice in the dark until analyzed on a FACSCalibur unit (BD Biosciences) omitting forward and side scatter. Cells incubated without antibody were used as a negative control to adjust settings above autofluorescence. Significance between groups was calculated using a two tailed student's *t*-test assuming unequal variances.

Results

A. Generation of neural progenitor cells

When this project was established, protocols for differentiating iPSCs into glutamatergic neurons had not been published, therefore a variety of hESC differentiation protocols were tested for our lines. We wanted to establish a protocol for a stable, self-renewing neural progenitor population so that neural differentiation could be readily initiated from cells that are easier to culture than iPSCs. We adapted the protocol from Swistowksi et al. (2009) with further modifications based on Marchetto et al. (2010) and personal correspondences with an author of that paper (C. Carromeu). For the protocol that established the highest yield of neural rosettes that could be harvested to form neural progenitors, iPSCs were cultured in suspension as embryoid bodies (EBs) for 8 days in a culture media containing the AMPK inhibitor dorsomorphin and neuronal N-2 supplement to predispose the EBs to neural differentiation (Figure 3.1). The AMPK inhibitor inhibits TGF-β superfamily receptors, blocking activin and BMP signaling and inducing neuroectoderm formation (Zhou et al 2010). For the next three days, the EBs were cultured in a neural induction media without AMPK inhibitor and with basic fibroblast growth factor (bFGF) to begin transitioning to a stable neural progenitor cell type. bFGF is a mitogen for neural progenitors, increasing the rate at which they divide (Kitchens et al 1994), but prevents differentiation of ESCs, thus it was removed from the media during early neural differentiation (Xu et al 2005).

The EBs are then plated on CELLstart, a proprietary xeno-free substrate for stem cell growth. On this substrate, neural rosettes form which are radial arrangements of columnar cells that have a broad neural differentiation potential (Elkabetz et al 2008, Wilson & Stice 2006). These rosettes can be harvested and maintained in a neural progenitor media containing bFGF

Figure 3.1: Protocol for Neural Progenitor Generation

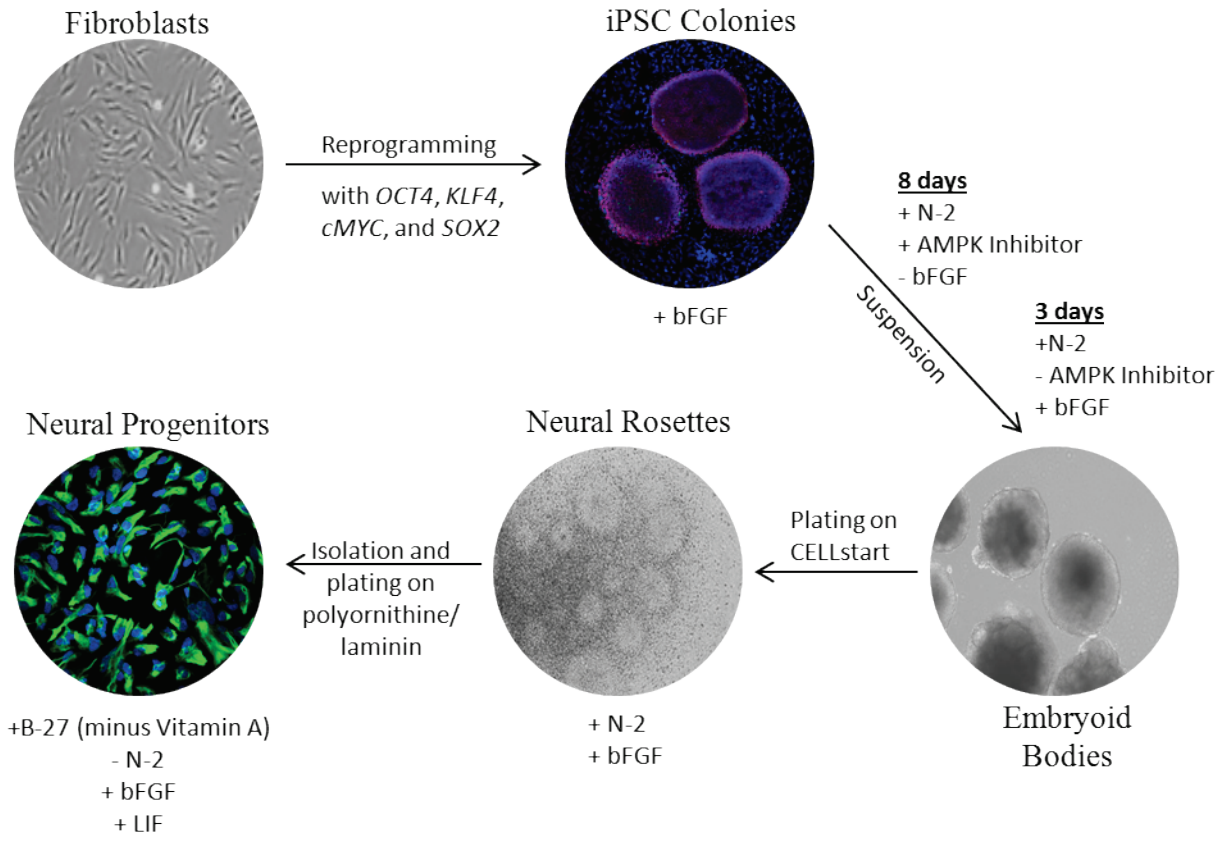

Figure 3.1: Protocol for Neural Progenitor Generation. Schematic of the protocol to differentiate neural progenitors from patient fibroblasts. Patient fibroblasts were reprogrammed using OCT4, KLF4, cMYC, and SOX2, forming iPS colonies. The representative composite image shows iPS colonies stained for OCT4 (red), Tra-1-81 (green), and DNA (DAPI, blue). The colonies are detached with dispase and then grown in suspension in a neural-enhancing EB media for 8 days. The EBs are grown in suspension for an additional 3 days in neural induction media before plating on CELLstart coated cell culture plates. Neural rosettes form after about 3 days and are manually harvested when mature and grown on polyornithine/laminin coated plates in NP media. In subsequent passages, the NPs are dissociated to single cells. The NP image shows representative NPs stained with the NP marker nestin (green) and DNA with DAPI (blue).

and leukemia inhibitory factor (LIF), which is a member of the IL-6 cytokine family and increases NP expansion rates and prevents senescence while inhibiting terminal differentiation (Wright et al 2003). The NP media also contains B-27, a neuronal support supplement, but without vitamin A, which can be metabolized into retinoic acid, a potent enhancer of neural differentiation. The rosettes can be dissociated to form a population of cells positive for the neural progenitor markers nestin, musashi, and SOX2 (Figure 3.2a,b). More than 95% of the NP cell population is positive for these markers, while none of the cells are positive for the earlier pluripotent stem cell markers including nanog, Oct3/4, and Tra-1-81 or the glial marker GFAP (data not shown). Based on the markers, the cells seem most similar to neuroepithelial progenitors that arise during corticogenesis or nonquiescent adult neural stem cells of the SGZ. These NP cells can be passaged for many months without loss of proliferative potential. One clone per individual was DNA fingerprinted following NP differentiation to ensure that the lines used still correspond with the original fibroblasts of the patient (Table 3.2).

Although most of the NP lines showed similar morphology, one line derived from SAD6.1 has a large population of cells with an aberrant shape: elongated cells with a spindle-like morphology. To determine what kind of cells these are, we immunostained for an early neuronal marker (β-tubulin III), a glial marker (GFAP), and an endothelial marker (lectin) (Figure 3.3a). The aberrant cells were positive for β-tubulin III, but negative for GFAP and lectin, indicating they may be some kind of early bipolar neuron. Due to their morphology, the aberrant cells could also be a radial glia like the small subset that expressed β-tubulin III *in vivo*, but it is unlikely since it does not express GFAP. Multiple differentiations from this clone as well as from SAD6.2 showed the same aberrant morphology not seen in other lines, so it was not used for any later analysis.

Figure 3.2: Characterization of Neural Progenitor Cells (a) Representative images of neural progenitors stained for the neural stem cell markers nestin (green), musashi (red), and SOX2 (red) with DAPI (blue) staining cell nuclei. (b) Unbiased quantification of a representative immunocytochemical experiment shows that greater than 95% of the cells considered neural progenitors are positive for nestin, greater than 99% are positive for musashi, and more than 96% of nuclei are positive for SOX2. There is no difference between the NL and SAD NP cells for these markers. The error bars represent the standard error of the mean.

Figure 3.2: Characterization of Neural Progenitor Cells (cont.)

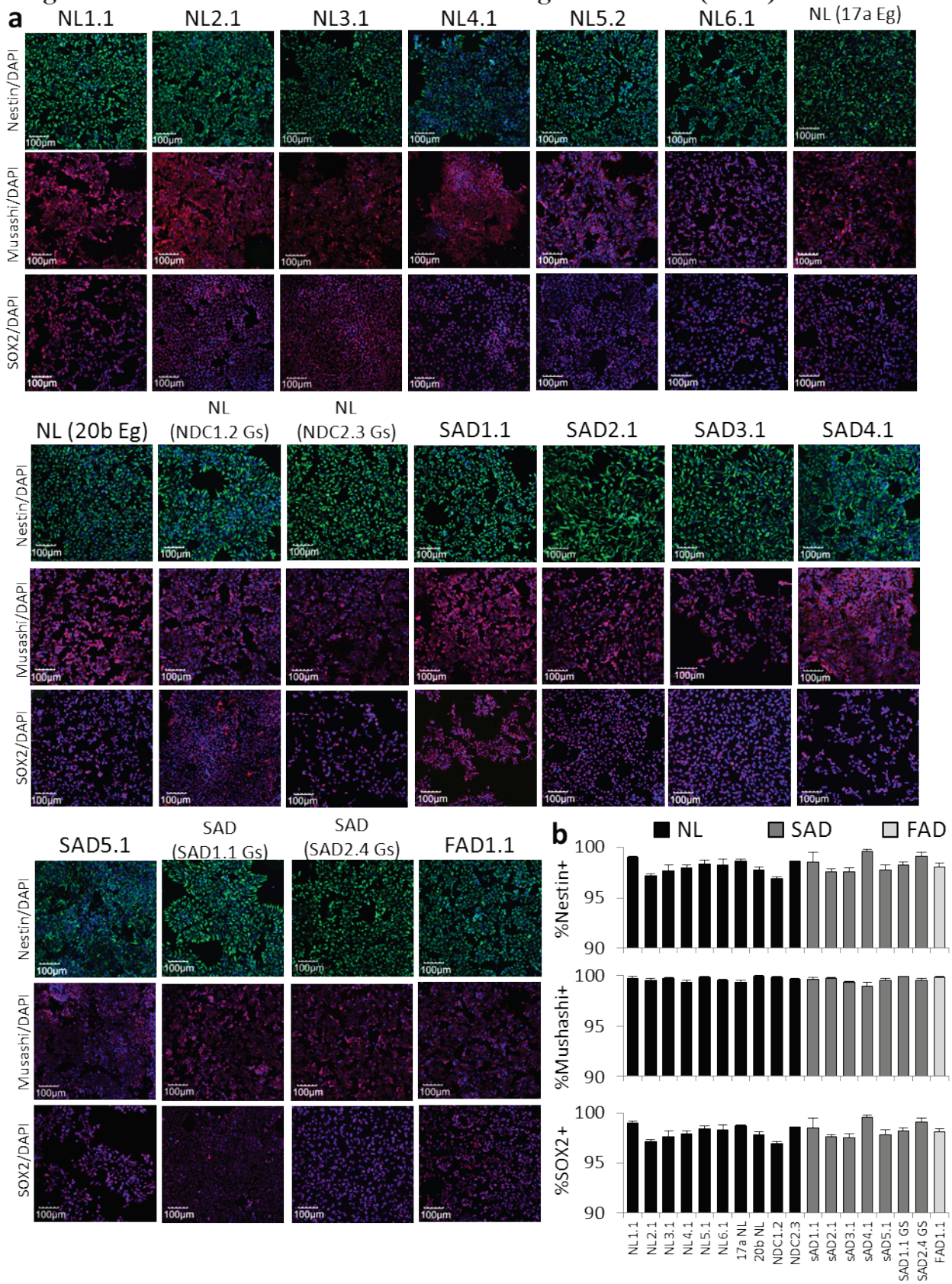

Table 3.2: Passages for NP characterization

Line	DNA Fingerprinting		Immunocytochemistry		Transgene Inactivation		Microarray I	
	NP Clone	Passage	NP Clone	Passage	NP Clone	Passage	NP Clone	Passage
NL1	1	12	1	22, 26	1	16	1	16
NL2	1	11	1	9, 10, 22	1	8	1	8
NL3	1	11	1	8, 10, 22	1	9	1	9
NL4	1	18	1	6, 19	1	14	1	14
NL5	1 (iPS)	22	2	3, 19	2	6	-	-
NL6	-	-	1	15, 23	1	13	1	13
NL (17 Eg)	-	-	a	10, 12, 19	-	-	a	7
NL (20 Eg)	-	-	b	7, 8, 22	-	-	b	11
NL (NDC1 Gs)	-	-	2	21	-	-	-	-
NL (NDC2 Gs)	-	-	3	19	-	-	-	-
SAD1	1	16	1	10, 14, 25	1	12	1	12
SAD2	1	14	1	11, 14, 22	1	12	1	12
SAD3	1	13	1	9, 12, 24	1	10	1	10
SAD4	1	15	1	14, 15, 28	1	13	1	13
SAD5	1	13	1	8, 14, 25	1	9	1	9
SAD6	1	6	1	10	-	-	-	-
SAD (SAD1 Gs)	-	-	1	20	-	-	-	-
SAD (SAD2 Gs)	-	-	4	19	-	-	-	-
FAD1	1	18	1	15, 18, 27	1	12	1	12

Line	qRT-PCR		Western Blotting		FACS	
	NP Clone	Passage	NP Clone	Passage	NP Clone	Passage
NL1	1	16	1	18, 23, 23	1	18, 19, 22
NL2	1	8	1	8, 11, 14	1	5, 6, 9
NL3	1	9	1	11, 14, 20	1	6, 7, 10
NL4	1	14	1	16, 17, 20	1	11, 12, 15
NL5	2	6	2	9, 11, 18	2	4, 5, 8
NL6	1	13	1	16, 21, 21	1	14, 15, 18
NL (17 Eg)	a	7	a	15, 15, 17	a	7, 8, 11
NL (20 Eg)	b	11	b	10, 12, 18	b	5, 6, 9
NL (NDC1 Gs)	2	8	2	11, 12	2	6, 7, 10
NL (NDC2 Gs)	3	8	3	12, 14	3	6, 7, 10
SAD1	1	12	1	10, 17, 18	1	6, 7, 10
SAD2	1	12	1	8, 15, 21	1	6, 7, 10
SAD3	1	10	1	11, 16, 18	1	8, 9, 12
SAD4	1	13	1	10, 16, 20	1	6, 7, 10
SAD5	1	9	1	14, 16, 22	1	5, 6, 9
SAD6	-	-	-	-	-	-
SAD (SAD1 Gs)	1	9	1	13, 13	1	7, 8, 11
SAD (SAD2 Gs)	4	9	4	11, 12	4	6, 7, 10
FAD1	1	12	1	13, 13, 18	1	7, 8, 11

To verify that the reprogramming transgenes remain inactivated in the NP cell population, *GFP* expression was measured for each line using qRT-PCR (Figure 3.3b). All four of the reprogramming factors have an IRES-GFP element which should be expressed in tandem with the reprogramming gene. Levels of *GFP* mRNA were compared to a human fibroblast control line transduced with pMXs-GFP. The *GFP* of the reprogramming factor vectors was expressed at less than 0.2% the levels of the *GFP* in the fibroblasts. This level is slightly higher than in the iPS cells (highest relative *GFP* expression ~0.04%), however the transgenes remain inactivated quite strongly compared to the levels following transduction and most importantly, there is no difference between the AD and NL lines.

Figure 3.3: Aberrant NP Cells and NP Transgene Inactivation

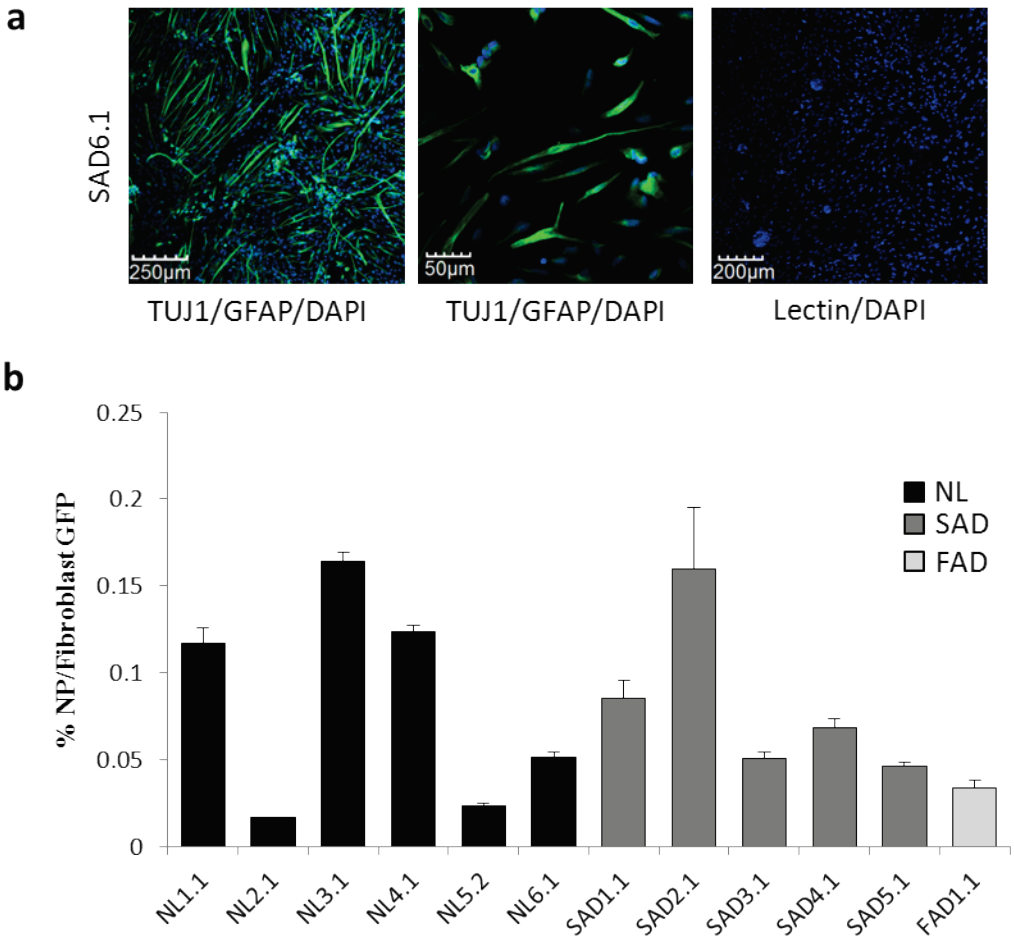

Figure 3.3: Aberrant NP Cells and Transgene Inactivation. (a) Cells with an aberrant morphology in SAD6.1 NP cultures stained positive for the early neuronal marker β-tubulin III (green), but negative for the glial marker GFAP (red) and the endothelial marker lectin (green) when co-stained with DAPI (blue). (b) Expression of *GFP* mRNA from pMIG-Reprogramming factors-IRES-GFP in all the NP lines evaluated using qRT-PCR and normalized to GAPDH was less than 0.2% the levels of a human fibroblast retrovirally transduced with pMXs-IRES-GFP, supporting continued strong inactivation of all four of the transgene reprogramming factors.

B. Divergent expression of neural differentiation genes in SAD NPs

Microarray profiling of neural progenitor cells between 7 and 16 passages was performed on Affymetrix U133 Plus 2.0 arrays for most of our NP lines and the two control lines derived from iPS cells from the Eggan laboratory (Table 3.2) with NP lines derived from one iPS clone per individual. The gene expression was analyzed according to the same methods described for fibroblasts and iPS cells. The SAD neural progenitors showed a strong gene expression difference compared to the normal controls with 326 annotated probes showing differential expression from the NL lines using a significance q-value of ≤ 0.15, which corresponds with a p-value $\leq$ 0.020 (Supplementary Table 3, Figure 3.4a). Using a q-value of 0.15 allows for the inclusion of most of the genes that appear to be biological significant due to their functional similarities to other significant genes and presence of multiple significant probes corresponding to the same gene.

Correlation analysis for the significant gene list shows intra-group correlation for both the SAD (Pearson correlation coefficient r between 0.37 and 0.80) and NL lines (r = 0.24-0.63, except NL4.1), however the FAD1.1 correlates with neither group and NL4.1 diverges from the other controls (Figure 3.4b). The normal NP lines derived from the Eggan iPS lines correlated well with each other (r = 0.49) and other NL lines (r = 0.24-0.53, except NL4.1), indicating that laboratory origin of the iPS does not affect the normal NP gene expression.

Enrichment analysis of the differentially expressed genes shows that biological processes related to nervous system development and development in general are highly enriched in the gene list (Figure 3.4c). This strong bias towards neuronal differentiation genes is supported by secondary analysis using DAVID, which shows an enrichment factor of 8.86 for the neuron development annotation cluster, much higher than any other cluster (Figure 3.4d). Unlike in the

Figure 3.4: Gene Expression Profile of Neural Progenitors (a) Heat map of significant genes differentially expressed between SAD and normal NP lines (derived from one clone per iPS line) with a q-value of less than 0.15. (b) A heat map of Pearson correlation coefficient shows that the gene expression of SAD and NL neural progenitors correlate within their respective groups, but FAD1.1 does not correlate with either group. NL4.1 is also an outlier. (c) The ten most significant biological processes evaluated through enrichment analysis in the gene ontology (GO) database using MetaCore. (d) The ten most significant annotation clusters using the Database for Annotation, Visualization, and Integrated Discovery (DAVID) in the significant NP gene list. BP: biological process, CC: cellular compartment. (e) The fold changes of the individual genes for the most significant gene ontology biological process, nervous system development. (f) Comparison of the significant differentially expressed genes between the fibroblasts and NP does not show a large overlap. FC Fib = fold change fibroblasts, FC NP = fold change neural progenitors. All fold changes are SAD/NL.

Figure 3.4: Gene Expression Profile of Neural Progenitors (cont.)

a

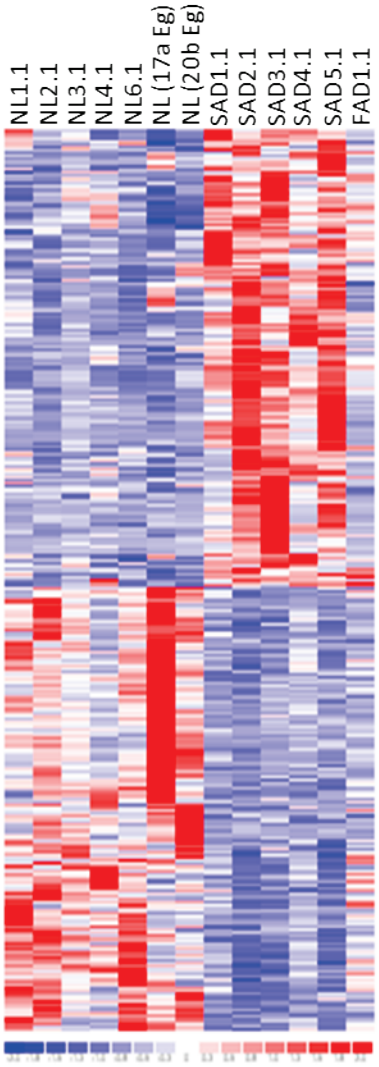

b

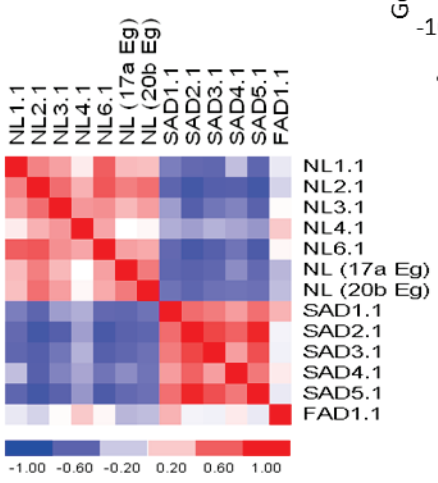

c

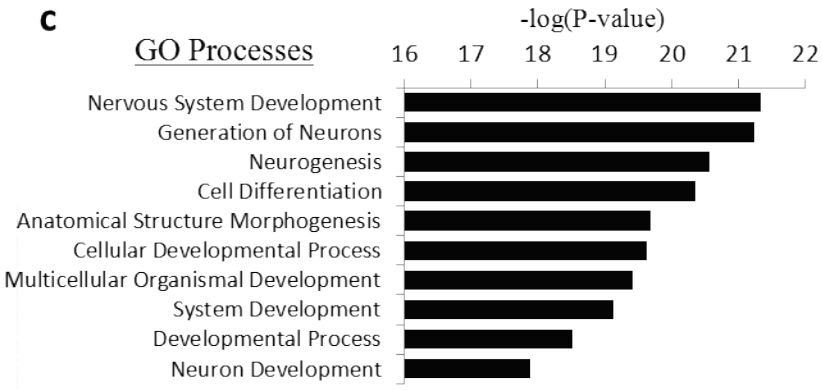

d

Annotation Cluster	Type	Enrichment
Neuron Development	BP	8.86
Cell Motion	BP	2.87
Blood Vessel Development	BP	2.83
Pattern Specification Process	BP	2.71
Cranial Nerve Morphogenesis	BP	2.71
Regulation of Neurogenesis	BP	2.25
Skeletal System Morphogenesis	BP	2.25
Neuron Projection	CC	2.22

e

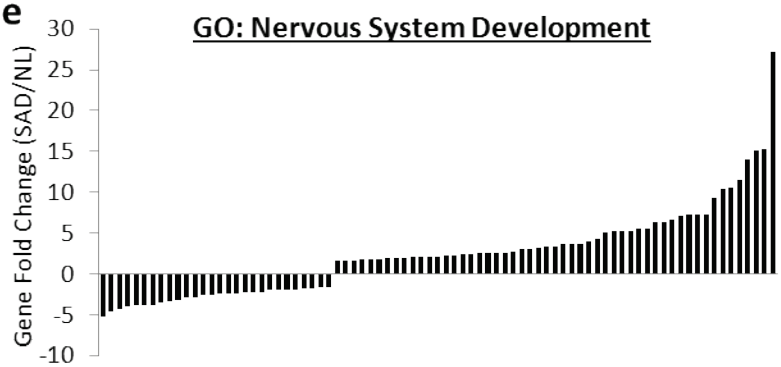

f

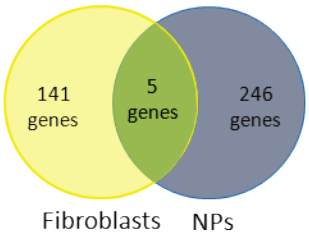

Overlapping Genes

Gene	Protein Descripiton	FC Fib	FC NP
CD44	CD44 Antigen	-2.42	-3.42
DLL3	Delta-like 3	-2.53	2.69
FGF18	Fibroblast Growth Factor 18	-2.54	-2.86
PPP1R3B	Protein phosphatase 1 Regulatory Subunit	2.05	-1.84
RPRML	Reprimo-like	-3.78	2.88

fibroblasts in which nervous system development genes were predominantly down-regulated, the genes associated with that cluster for NPs have more up-regulated genes, including some that are increased more than 10-fold in the SAD neural progenitors (Figure 3.4e). Comparison of the two stages of differentiation shows very little gene overlap (Figure 3.4f). Only five genes are in both the fibroblast and NP gene list and three of those are regulated in different directions. The only genes that are down-regulated in both significant gene lists are CD44, a cell adhesion molecule found in many tissues, and FGF18, a growth factor important in skeletal development (Goodison et al 1999, Haque et al 2007). Therefore, there seems to be little overlap between the mechanisms affecting gene expression in SAD fibroblasts and SAD neural progenitors.

Using MetaCore software to identify interacting proteins that are over-represented in the SAD neural progenitor gene list shows a large number of highly significant interactors (Supplementary Figure 5). The most significant transcription factors include ASCL1/MASH1, which is highly up-regulated in the SAD neural progenitors and REST/NRSF, an important repressor of neuronal genes (Jones & Meech 1999), as well as many other transcription factors involved with development (Figure 3.5a). The two most significant interacting proteases are BACE1 and BACE2, which both have been associated with the generation of Aβ, although BACE1 is the primary beta-secretase for APP (Ahmed et al 2010). The receptor and ligand category are both enriched for cell surface proteins, including semaphorin and ephrin receptors, which are involved in neuronal axon growth and guidance, and TGF-β type II receptor, which modulates the proliferation, survival, and differentiation of many different cell types. All three of these signaling systems have genes differentially expressed in the NP gene list, including the down-regulation of the TGF-β type II receptor, the up-regulation of the ephrin receptors A4, A7, and B1, and the up-regulation of semaphorin 6 (Supplementary Figure 3).

Figure 3.5: Analysis of the Gene Expression Profile of Neural Progenitors

a

Interactions

	Object	P-value	Ratio
Transcription Factors	Androgen receptor	6.86E-09	2.8
	BLIMP1	1.49E-07	8.0
	REST	2.92E-07	3.9
	PREP1	6.37E-07	14.0
	SP1	1.51E-06	2.3
	HOXB1	2.06E-06	11.8
	PAX3	4.39E-06	7.3
	PBX1	5.52E-06	6.2
	CREB1	7.89E-06	1.6
	HES1	2.19E-05	5.3
	C/EBPdelta	2.57E-05	4.7

Category	Object	P-value	Ratio
Transcription Factors	p63	2.76E-05	3.0
	POU3F2 (BRN2)	3.14E-05	6.6
	c-Myc	4.24E-05	1.7
	Oct-3/4	4.78E-05	2.1
	ASCL1	9.94E-05	5.6
Proteases	BACE2	4.07E-07	14.9
	BACE1	1.96E-06	5.6
Receptor	SEMA3G	2.06E-05	49.0
Receptor/Kinase	TGF-β receptor type II	5.27E-05	5.3
Receptor/Kinase	Ephrin-A receptor 2	9.52E-05	8.2
Ligand	Ephrin-A2	1.33E-05	26.1

b

	Upstream Regulator	Type	Activation	P-value
Activated	RARA (Retinoic Acid Receptor)	ligand-dependent nuclear receptor	2.24	1.25E-02
	HOXA9	transcription regulator	2.16	2.35E-03
	NKX2-3	transcription regulator	2.13	1.04E-04
	HLX	transcription regulator	1.99	8.32E-04
	NEUROG1	transcription regulator	1.63	2.50E-04
	Estrogen Receptor	group	1.46	3.68E-03
	Growth Differentiation Factor 2	growth factor	1.46	9.50E-04
	ASCL1	transcription regulator	1.39	5.08E-04
Inhibited	Collagen type I	complex	-1.982	1.21E-03
	Angiotensin	growth factor	-2.05	2.87E-04
	Tumor Necrosis Factor	cytokine	-2.126	1.27E-03
	TGFBR2	kinase	-2.196	1.00E-02
	Androgen Receptor	ligand-dependent nuclear receptor	-2.219	3.04E-03
	Interleukin 1B	cytokine	-2.382	6.22E-04
	CNR1 (cannibinoid receptor)	G-protein coupled receptor	-2.390	6.43E-03
	Interferon alpha	group	-2.608	5.54E-03
	Akt	group	-2.828	1.59E-03
	Interferon Gamma	cytokine	-2.843	9.13E-04

Figure 3.5: Analysis of the Gene Expression Profile of Neural Progenitors. (a) Table of the most significantly connected transcription factors, proteases, receptors, and ligands using MetaCore Interactome analysis. The ratio refers to the number of interaction partners in the gene list divided by the expected number of interactions in a random gene list of equal size. P-value had to be less than $1x10^{-4}$ to be included. (b) Table of the most significant activated and inhibited upstream regulators calculated by Ingenuity Pathway Analysis (IPA). Upstream regulators with a p-value less than .02 were included.

Many of these interactions are supported using Ingenuity Pathway Analysis (IPA), which uses an algorithm to distinguish upstream regulators which may cause the gene expression changes seen in the gene list (Supplementary Figure 6). One strength of IPA is that it evaluates whether the upstream regulator is up- or down-regulated through its activation score. Considering the most strongly activated and inactivated regulators (Figure 3.5b), there are some clarifications of the hubs identified through interactions analysis, including that TGF-β receptor II signaling is down-regulated, while ASCL1 is activated, both consistent with their expression levels in SAD neural progenitors. Interferon signaling is also down-regulated, seen also in MetaCore by the significance of the BLIMP1 transcription factor, a repressor of interferon signaling (Doody et al 2010). The strongest activated upstream regulator is the retinoic acid receptor, a well-known pathway for inducing the induction of neural differentiation.

To further explore which genes and pathways are up- and down-regulated in the sporadic AD NPs, the genes were analyzed separately. Tables of the most significant up- and down-regulated genes show that the down-regulated genes are enriched for components and modulators of the extracellular matrix, including three different alpha chains of collagen (11, 13, and 23), matrilin 3, ependymin-like, the alpha subunit of the integrin receptor, and neuroserpin (Figure 3.6a). The gamma 1 subunit of laminin is also down-regulated 2.3-fold in the SAD neural progenitors. Enrichment analysis using the MetaCore Process Network Ontology shows the greatest enrichment for cell-matrix interactions in the down-regulated genes, as well as cell cycle regulation (Figure 3.6b). Also down-regulated are genes associated with various growth signaling pathways, including *CNPY1*, which modulates FGF signaling, and *BMP5*, in the TGF-β superfamily. The EGF receptor is also down-regulated 2.4-fold.

Many of the up-regulated genes are specific or increased in early neural development, including doublecortin, *MEIS1*, *ASCL1*, *CD24*, stathmin 2, and ephrin receptor B1, while *KCNIP4*, the neuropeptide Y receptor, and *LGI1* are also enhanced in mature neuronal tissues (Figure 3.6c). Other of the highly up-regulated genes includes the developmental transcription factors *HOXA3*, *HOXA2*, *MAFB*, and *SP8*. Many other transcription factors that belong to families associated with neural induction or patterning are up-regulated in the SAD neural progenitors, including *HOX*(*A1, A2, A3, B2*), *PAX6*, *ID*(*2,3*), *HES*(*4,6*), *TSHZ1*, and *MEIS*(*1,2*) (Supplementary Table 3).

Enrichment analysis for the up-regulated gene list supports this connection to neuronal development with the most significant process networks including neurogenesis, axonal guidance, and synaptic contact (Figure 3.6d). The only significant process network in both the up- and down-regulated NP genes is attractive and repulsive receptors. In summary, there is a robust and significant difference in NP gene expression between the SAD and NL lines in which neuronal differentiation genes are predominantly up-regulated and genes related to the extracellular matrix and growth factors are mostly down-regulated.

Figure 3.6: Up- and Down-regulated Genes of SAD Neural Progenitors

a

Most Down-regulated Genes in SAD

Gene	Protein Description	Average FC	Probes
MUM1L1	Melanoma-associated antigen (mutated) 1 like	-6.40	1/1
MATN3	Matrilin 3	-5.88	1/1
COL11A1	Collagen 11 alpha 1	-5.79	3/3
TM4SF18	Transmembrane 4L Six (tetraspanin)	-5.75	2/2
EPAS1	Endothelial PAS domain protein (HIF2A)	-5.69	1/2
ADM	Adrenomedullin	-5.24	1/1
COL23A1	Collagen 23 alpha 1	-4.66	1/1
CNPY1	Canopy FGF Signaling Receptor	-4.24	1/1
EPDR1	Ependymin Related 1	-3.94	1/1
TRIM22	Tripartite Motif containing 22	-3.93	1/1
ITGA1	Integrin alpha 1	-3.90	1/2
SERPINI1	Neuroserpin	-3.87	1/1
COL13A1	Collagen 13 alpha 1	-3.79	2/3
BMP5	Bone Morphogenic Protein 5	-3.66	2/2
SLC25A43	Solute Carrier (mitochondrial)	-3.66	1/1
HHIP	Hedgehog Interacting Protein	-3.53	3/4
CCND2	Cyclin D2	-3.25	3/4

b

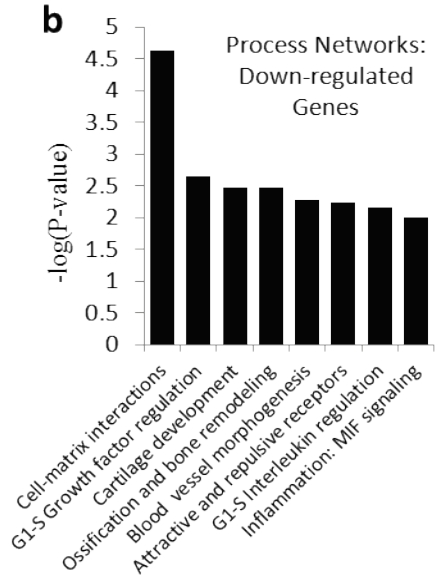

c

Most Up-regulated Genes in SAD

Gene	Protein Description	Average FC	Probes
NPY5R	Neuropeptide Y Receptor	15.37	1/1
DCX	Doublecortin	14.78	2/2
ASCL1	Achaete-Scute Complex Homolog 1/MASH1	14.67	3/4
CD24	CD24 signal transducer	12.43	6/6
HOXA3	Homeobox A3	11.53	1/2
KCNIP4	Voltage-gated Potassium Channel Interacting	11.04	1/2
SP8	SP8 transcription factor	10.16	1/2
STMN2	Stathmin 2	9.55	2/2
HOXA2	Homeobox A2	7.33	1/1
LAMP5	Lysosomal-related membrane Protein	7.25	1/1
LGI1	Leucine-rich, glioma Inactivated	6.75	1/1
DLL1	Delta-like 1	6.43	1/2
EPHB1	Ephrin receptor B1	6.21	2/3
MEIS1	Meis Homeobox 1	6.11	2/2
MAFB	MAFB Transcription Factor	5.11	2/2
EDNRB	Endothelin Receptor Type B	5.03	3/3

d

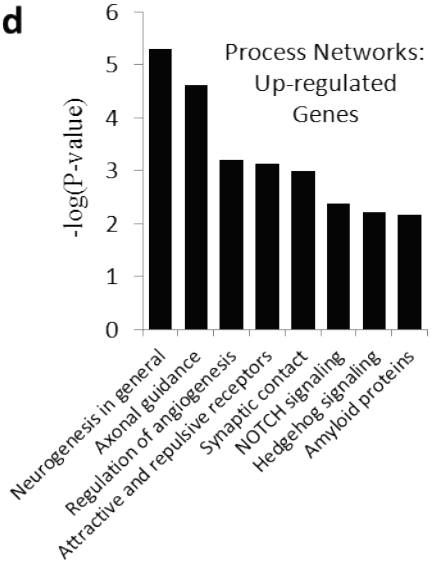

Figure 3.6: Up- and Down-regulated Genes of SAD Neural Progenitors. (a,c) Tables of the most strongly up-regulated and down-regulated genes in the SAD lines. The fold change (FC) represents the average of all probes for the specific gene, while probes refers to the number of probes that reach the significance threshold for NP expression out of all the probes annotated for that gene on the Affymetrix U133 Plus 2.0 array. The tables consist of genes with at least one probe showing less than 3.5 fold decrease or greater than 5.5 fold increase respectively as well as at least 50% of probes for that gene in the significant gene list. (b,d) Enrichment analysis using MetaCore software for process networks that are significantly enriched in the up- and down-regulated genes. Included are only networks with a p-value less than 0.01.

C. SAD neural progenitor gene expression differences verified through qRT-PCR

To confirm the differences in gene expression identified through microarray analysis, mRNA from the neural progenitors for several key genes was measured using quantitative real-time PCR (qRT-PCR). RNA samples were included from one clone per individual, including the individuals that were not analyzed by microarray: NL5 and the four patients from the Goldstein study (Table 3.2). Thus neural progenitor cells from a total of 18 patients (10 normal, 7 SAD, and 1 FAD) were evaluated from iPS cells derived in three different laboratories, the largest number of individuals studied in neural cells from AD patients thus far.

Most of the microarray findings are confirmed with the increased number of individuals (Figure 3.7). *DCX* expression is 9-fold higher in the SAD neural progenitors than the NL cells. Doublecortin is a microtubule binding protein which is expressed transiently in immature neurons during neurogenesis and migration, but is not expressed in mature neurons (Gleeson et al 1999). It is widely used as a marker for adult neurogenesis (Couillard-Despres et al 2005). (Figure 3.7). *ASCL1* expression is 4.7-fold higher in the SAD neural progenitors. It is a basic-loop-helix transcription factor which has been shown in mice to promote neuronal fate determination through sustained expression (Imayoshi et al 2013). It is also widely used for the transdifferentiation of fibroblasts and other somatic cells into neurons using induced expression of transcription factors (Pang et al 2011, Vierbuchen et al 2010). Together, expression of these two genes is used to identify the maturing intermediate cells of neurogenesis in the SGZ during adult neurogenesis (Hodge et al 2008, Kempermann et al 2004).

CD24 is 7.1-fold higher in the SAD neural progenitors. It is a glycosylphosphatidyl-inositol (GPI)-anchored cell adhesion protein which is expressed in regions of developmental and adult neurogenesis (Calaora et al 1996). Its increased expression during neuronal

Figure 3.7: mRNA of Differentially Expressed Genes in Neural Progenitors

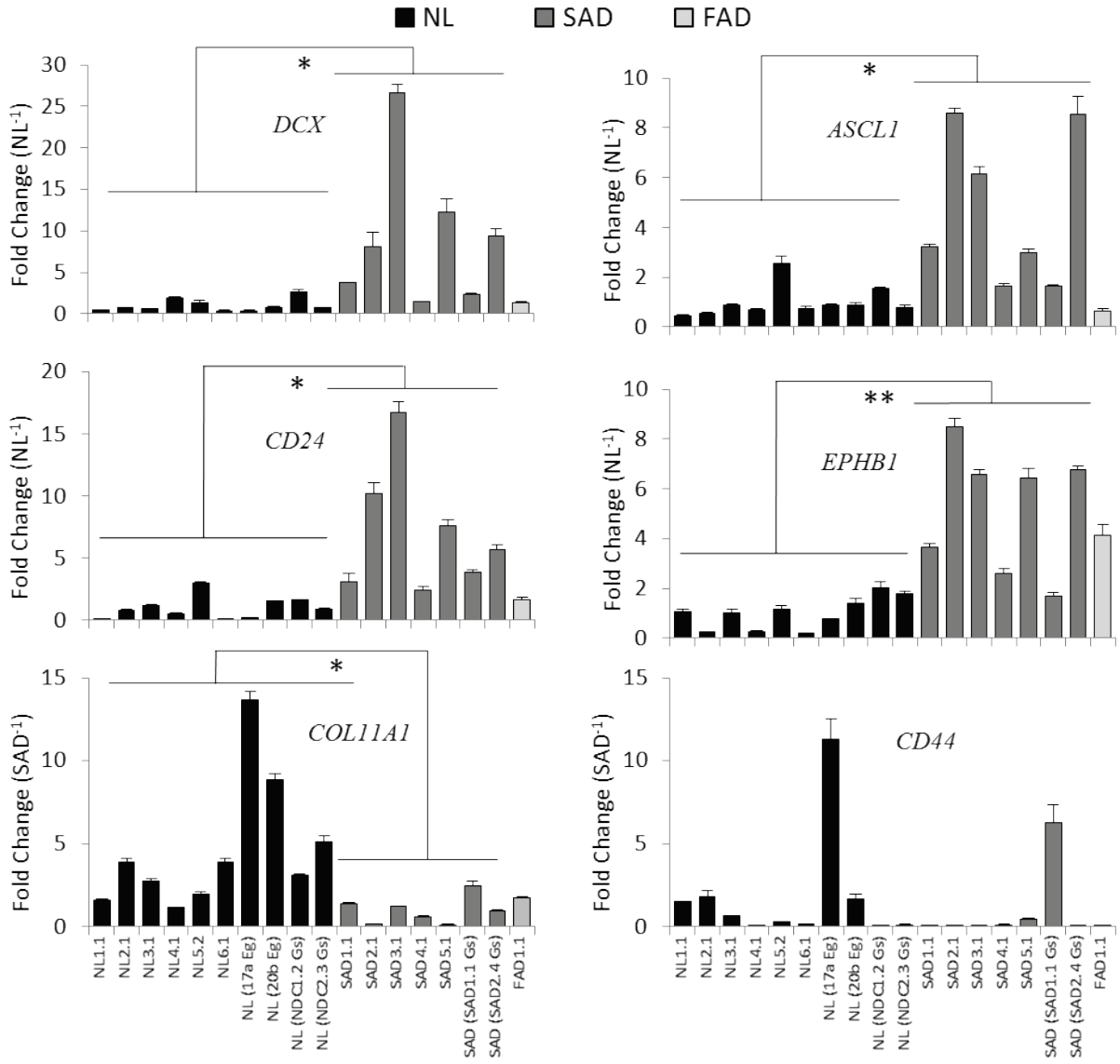

Figure 3.7: mRNA of Differentially Expressed Genes in Neural Progenitors. Representative quantitative RT-PCR shows differential mRNA expression in the SAD neural progenitors compared to the controls for *DCX, ASCL1, CD24, EPHB1,* and *COL11A1,* but not *CD44*. mRNA values were calculated using the relative standard curve method and normalized to *GAPDH*. Fold change was calculated relative to the average normalized expression of all the NL lines except for *COL11A1* and *CD44*, where it is relative to the average normalized expression of all the SAD lines. Errors are the standard error of the mean for multiple wells. *DCX*: p=0.047, Log_2 p=0.001; *ASCL1* p=0.019, Log_2 p<0.001; *CD24* p=0.013, Log_2 p<0.001; *EPHB1* p= 0.004, Log_2 p=0.001; *Col11A1* p=0.017 Log_2 p=0.006; *CD44* p=0.59 Log_2 p=0.16. *p<0.05, **p<0.01

differentiation is widely used as a marker of immature neural lineage during FACS sorting (Pruszak et al 2009, Yuan et al 2011). *EPHB1* expression is increased 5.2-fold in SAD neural progenitors. EPHB1 is a receptor for ephrins that plays a diverse role in neural development, including possible roles in neuronal migration and axon targeting cones through repulsion and regulation of cell adhesion (Wilkinson 2001).

COL11A1 is down-regulated 4.6-fold in the SAD lines. It is not associated with neural tissue, but rather encodes a component of type XI collagen which is enriched in cartilage and the vitreous of the eye (Richards et al 2010). *CD44* was an interesting candidate gene to investigate because its down-regulation was one of the few changes conserved from fibroblasts to neural progenitors and its role in regulating the extracellular matrix to maintain the stem cell niche (Wagner et al 2008). However, only a few of the probes for *CD44* were significant in both the fibroblasts (1/13) and NPs (3/13). qRT-PCR confirmed that this is not a significant difference between the SAD and NL neural progenitors with a $\log_2$ p-value of 0.16. Although *CD44* trends higher in the normal lines, expression levels are highly variable and one SAD line (SAD (SAD1.1 Gs)) shows quite high expression. This does not exclude the possibility that an alternatively spliced product not recognized by the qRT-PCR primers could be differentially expressed in the SAD neural progenitors.

Although the average levels of the early neuronal markers tested showed a significant increase in the SAD neural progenitors, not all the lines had the same amplitude of increase. The four strongest lines were SAD3.1, SAD4.1, SAD5.1, and SAD (SAD2.4 Gs), while SAD1, SAD4, and SAD (SAD1.1 Gs) had weaker phenotypes although still generally higher than NL. There is no clear correlation between the four stronger lines; out of the two *APOE4/E4* individuals (SAD1 and SAD5), one is a strong expresser and the other is a weaker expresser of

the neural genes. From the sporadic iPS lines derived in the Goldstein laboratory, one of them is a strong expresser and the other is a weak expresser. Interestingly, the strong expresser, SAD (SAD2.4 Gs), is also the individual identified in their study as having stronger AD phenotypes: increased phosphorylated tau, secreted Aβ40, and active GSK3β (Israel et al 2012). FAD1.1, with a L286V PSEN1 mutation, has an intermediate expression level for the neuronal markers, in line with the weaker SAD expressers and higher NL individuals.

D. A subset of neural progenitors expresses neuronal differentiation markers

Since it is clear that the mRNA levels are higher for early neuronal differentiation markers in the SAD neural progenitor cells, we next wanted to evaluate if that difference is maintained through protein expression. Western blotting for doublecortin shows an increase in protein levels in the SAD neural progenitors, although at a slightly lower magnitude than seen for the mRNA expression with a fold change of 1.2 to 5-fold over NL lines (Figure 3.8a,b). FAD1.1 again falls in the middle of the SAD and NL with doublecortin protein expression increased 1.2-fold over NL.

Immunofluorescent staining for doublecortin shows that the increase is not due to all cells expressing more doublecortin, but rather a small number of cells highly expressing doublecortin (DCX^{HIGH}, Figure 3.8c). Most cells remain positive for the neural progenitor marker nestin, showing despite the premature differentiation in a few cells, the culture is still predominantly progenitors. Staining for another marker of early neuronal differentiation, β-tubulin III, which was not differentially expressed at the mRNA level, shows a similar pattern where a few cells are highly positive ($TUBB3^{HIGH}$), while the majority remain positive for the neural progenitor marker musashi (Figure 3.8d). Co-staining for DCX and TUBB3 shows that the same small population of cells are positive for both DCX and TUBB3, although individual cells may show

Figure 3.8: Early Neuronal Proteins in Neural Progenitors. (a) Representative western blots for doublecortin (DCX) in neural progenitors show increased expression of doublecortin in the SAD NP lines. GAPDH is used as a loading control on the same blot. (b) Average fold change of doublecortin protein levels from three different western blots, normalized to GAPDH, shows increased expression of DCX in the SAD lines. Fold change was calculated relative to the average normalized expression of all the NL lines. n = 3, except for the four Goldstein lines (n = 2). p = 0.026. (c) Representative images of neural progenitors stained for nestin (green), doublecortin (red), and DAPI (blue) shows that most cells are positive for the neural progenitor marker nestin and a small proportion are highly positive for the early neuronal marker DCX (DCX^{HIGH}). (d) Representative images of neural progenitors stained for β-tubulin III (TUBB3, green), musashi (red), and DNA (DAPI, blue) shows that most cells are positive for the neural progenitor marker musashi and a small proportion is highly positive for the early neuronal marker β-tubulin III ($TUBB3^{HIGH}$). (e) Representative images of neural progenitors co-stained for TUBB3 (green) and DCX (red) with a DAPI DNA dye (blue). (f) Quantification of the percent cells positive for the early neuronal markers DCX and TUBB3 shows an insignificant trend towards more DCX^{HIGH} ($p=0.096$) and $TUBB3^{HIGH}$ ($p=0.11$) in the SAD neural progenitor cells. n = 1 (NL1.1, NL6.1, NL (NDC1.1 Gs), NL (NDC2.3 Gs), SAD (SAD1.1 Gs), SAD (SAD2.4 Gs)); n = 2 (NL5.2); n = 3 (NL3.1, SAD5.1); n = 4 (NL2.1, NL4.1, NL (17a Eg), NL (20b Gs), SAD1.1, SAD2.1, SAD3.1, SAD4.1, FAD1.1) (g) Representative FACS plots for CD24 (x-axis) after presorting for single cells. For this experiment, $CD24^{HIGH}$ was defined as greater than $2x10^2$. The y-axis is the side light scatter (SSC-H). (h) Averages from three FACS experiments shows an increased number of $CD24^{HIGH}$ cells in the SAD lines. $P=0.012$. *$p<0.05$

Figure 3.8: Early Neuronal Proteins in Neural Progenitors (cont.)

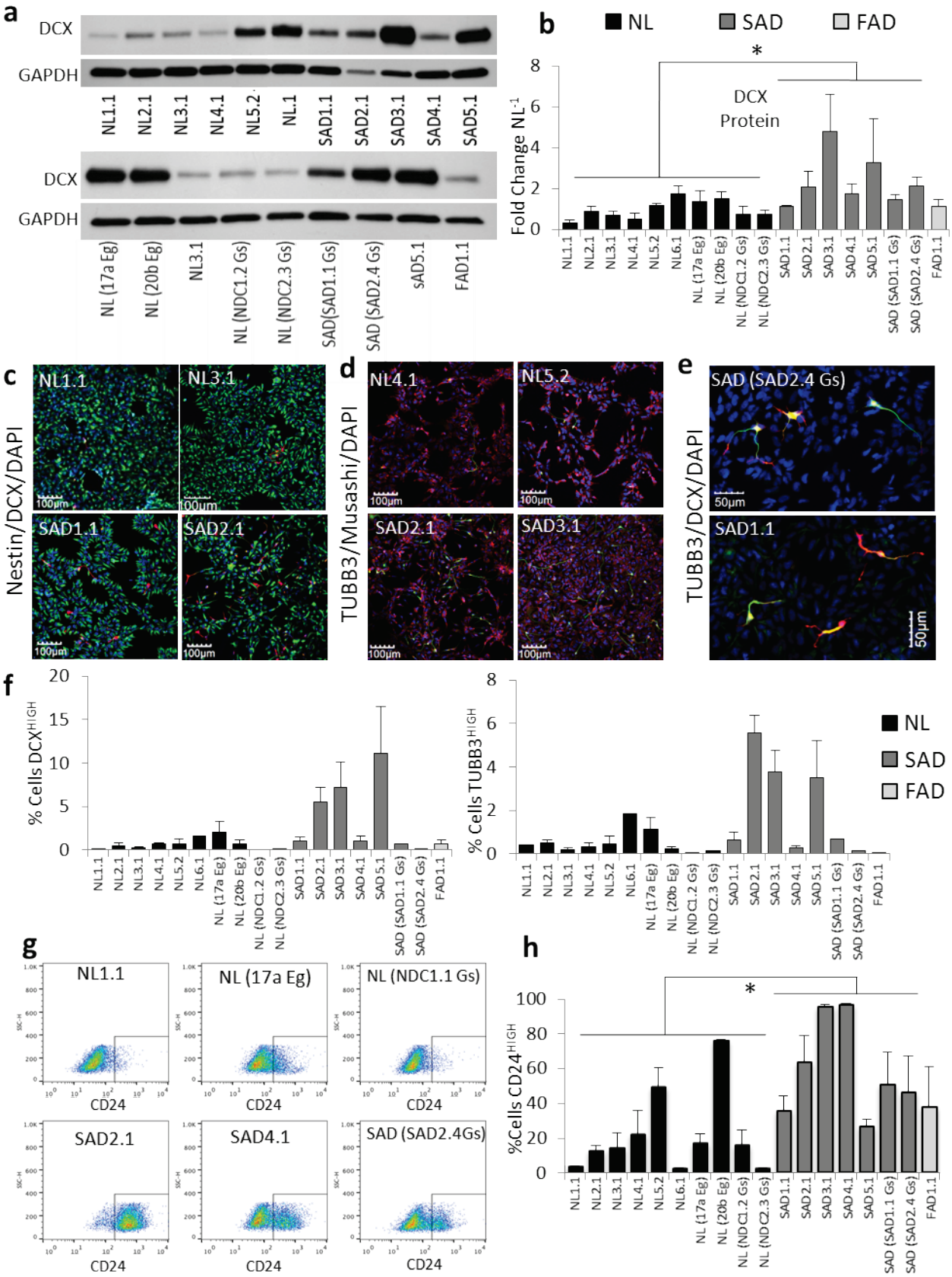

higher levels of one or the other (Figure 3.8e). These cells have also started to form processes, further supporting that the DCX^{HIGH} and $TUBB3^{HIGH}$ population of cells are early neurons that have differentiated out of the neural progenitor pool. Quantification of the number of cells DCX^{HIGH} and $TUBB3^{HIGH}$ shows a trend towards increased number of early neuronal cells in the SAD lines, but it is not statistically significant ($p=0.096$, $p=0.11$) (Figure 3.8f). This suggests that although there may be a difference in some lines for the number of DCX^{HIGH} and $TUBB3^{HIGH}$ neural progenitors, more important is that the SAD lines have a higher level of DCX expression in those cells, leading to the significantly higher overall protein levels.

To further differentiate the SAD and NL neural progenitors by protein expression, FACS analysis was performed for CD24, a cell surface adhesion protein with mRNA levels significantly enriched in SAD neural progenitors. It is expressed in regions of neurogenesis and has widely been used as a marker of immature neural lineage during FACS sorting in tandem with other cell surface proteins (Pruszak et al 2009, Yuan et al 2011). CD24 expression was widely varying between the neural progenitor lines (Figure 3.8g,h). There are two clear populations of $CD24^{LOW}$ and $CD24^{HIGH}$ for most lines after the data is presorted to include only single cells through the amount of forward and side scatter. Most of the control lines are predominantly $CD24^{LOW}$, while some of the SAD lines are almost entirely $CD24^{HIGH}$. The large number of $CD24^{HIGH}$ cells in the SAD neural progenitors indicates that it isn't the same population as smaller proportion of DCX^{HIGH} and $TUBB3^{HIGH}$ cells, although it may overlap. There are a few outliers (NL5.1 and NL (20b Eg) are more $CD24^{HIGH}$ than other NL), but overall the number of $CD24^{HIGH}$ neural progenitors is significantly increased in the SAD lines ($p = 0.012$), further supporting that the SAD neural progenitors are skewed towards a further neural differentiation state than the NL controls.

E. The difference between SAD and NL differentiation is specific to the neural lineage

The next question we wanted to answer is whether this difference in propensity to differentiate is true for all types of differentiated cells or specific for the neural lineage. We have already tested the differentiation capabilities of these lines when we evaluated the pluripotency of the iPS cells. The semi-quantitative RT-PCR for markers of the three germ layers after undirected differentiation into EBs did not show a difference (Figure 2.5), but using quantitative real-time RT-PCR may pick up a more subtle difference.

qRT-PCR for *DCX* and *ASCL1* in the 2-week differentiated EBs that did not contain reagents to induce the neuronal lineage (such as AMPK inhibitor and N-2 supplement) does show a trend towards increased neuronal differentiation markers, but it is not statistically significant (*DCX*: $p = 0.12$, *ASCL1*: $p = 0.29$) (Figure 3.9a). With more lines, this may become significant, but at this point more evidence is needed to conclude whether the difference in neuronal propensity is intrinsic to the differentiating iPS cells without any chemical inducement.

Another assay that may give insight into the inclination to differentiate is the *in vivo* teratoma assay (Figure 2.6). Teratomas consisting of all three germ layers formed from each of iPS lines, but if there was a difference in the rate of differentiation, the SAD lines may form teratomas more rapidly than the NL iPS cells. However, there was no difference in the rate at which teratomas formed (Figure 3.9b). One complication of this analysis is that the quantified output is when the teratoma becomes visible and differing rates of growth may not be dependent on differentiation state. Therefore, although we can conclude that there is no difference in the rate at which teratomas grow to a visible size, we cannot conclude that this is due to equivalent propensity to differentiate.

Figure 3.9: Neural Markers in EBs and Differentiation Time *in Vivo*

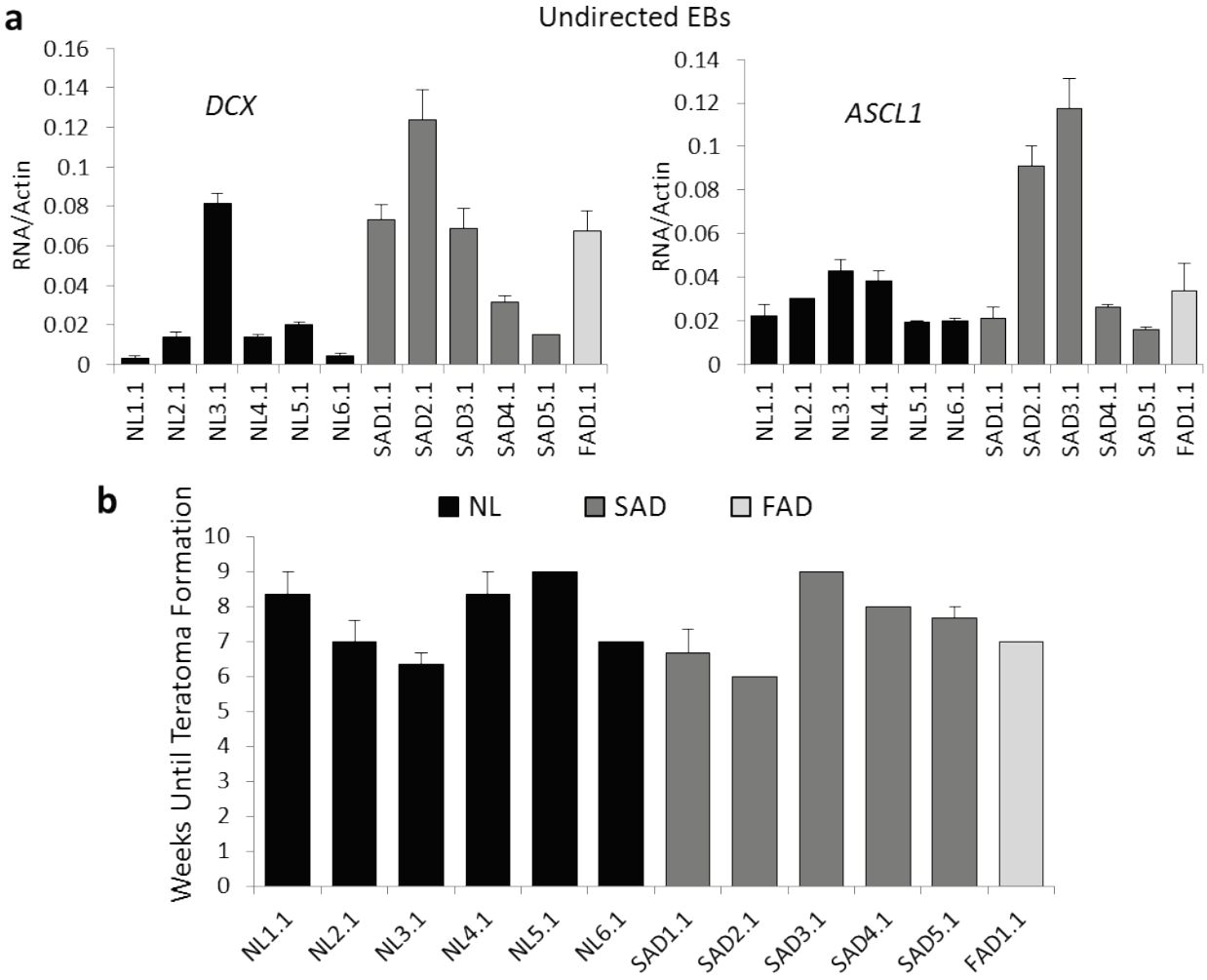

Figure 3.9: Neural Markers in EBs and Differentiation Time *in Vivo*. (a) qRT-PCR for 2-week differentiated EBs that were not directed down the neuronal lineage with AMPK inhibitor and N-2 supplement show an insignificant trend towards increased neuronal markers. (DCX: $p = 0.12$, ASCL1: $p = 0.29$) RNA was harvested from differentiated iPS cells that had been grown in suspension as embryoid bodies (EBs) for seven days and then on gelatin in serum-containing media for seven days. Units are relative RNA units (from standard curve) normalized to relative β-actin mRNA levels. (b) The timeline for the development of teratomas in mice from the iPS lines is not different between the SAD and NL lines. One iPS cell line per individual was injected into the kidney subcapsule of three NOD-SCID mice. This plot shows the time in weeks until the teratomas had grown apparent. $n = 3$ (except SAD2.1, where $n = 1$) $p = 0.77$

F. Gene expression profiles of neural progenitors from additional iPSC clones of four SAD and four NL individuals

One concern is that we have only made neural progenitor cells from one iPS clone per patient. Therefore, the difference in neural differentiation state that we see may be due stochastic differences during the NP differentiation process and not specific to the individual patient. Therefore, we derived NP lines from additional clones from eight of the patients: NL2, NL5, SAD2, SAD3, NL (NDC1 Gs), NL (NDC2 Gs), SAD (SAD1 Gs), and SAD (SAD2 Gs) (Table 3.3). With this data, we will now have full NP gene expression information for every Goldstein patient, as well as our own that were not quantified in the first NP microarray (NL5). The NP lines that were duplicated (NL2.1, SAD2.1, and SAD3.1) were from separate RNA harvests and passages than the original microarray. The gene expression was analyzed on Affymetrix U133 Plus 2.0 arrays in the same manner as the fibroblast, iPS cells, and other neural progenitors (Table 3.4). With the larger sample size (12 NL and 13 SAD), permutation analysis is now statistically relevant, so the p- and q-values were derived through 10,000 permutations.

294 probes are differentially expressed between the SAD and NL NP lines with a q-value less than 0.15, which corresponds to a p-value of 0.0096 (Supplementary Table 7, Figure 3.10a). The SAD and NL lines have intra-group correlation, but not as strongly as when one clone per individual was analyzed (Figure 3.10b). The gene expression correlates more closely by AD diagnosis than by individual, indicating that the significant changes identified through the statistical analysis are not specific to the patient.

The overlap of significant genes between the original NP microarray (one clone per individual) and new multiple clones doesn't have a large number of genes overlapping (36) (Figure 3.10c). However, the genes that do overlap are all differentially expressed in the same

Table 3.3: Additional Clones and Passage Number

Line	Clones	Lab of iPS Origin	Diagnosis	Age at Biopsy	Gender	*APOE*	Reference
NL2	1, 2, 3, 4	Yankner	Normal	64	M	*E3/E3*	This thesis
NL5	1, 2, 3	Yankner	Normal	75	F	*E3/E3*	This thesis
SAD2	1, 2, 3, 4	Yankner	Sporadic AD	60	M	*E3/E3*	This thesis
SAD3	1, 2,3	Yankner	Sporadic AD	69	F	*E2/E3*	This thesis
NL (NDC1 Gs)	1, 2, 3	Goldstein	Normal	86	M	*E2/E3*	Israel et al. 2012
NL (NDC2 Gs)	2, 3	Goldstein	Normal	86	M	*E3/E3*	Israel et al. 2012
SAD (SAD1 Gs)	1, 2	Goldstein	Sporadic AD	83	F	*E3/E3*	Israel et al. 2012
SAD (SAD2 Gs)	1, 2, 3, 4	Goldstein	Sporadic AD	83	M	*E3/E3*	Israel et al. 2012

	Microarray II and qRT-PCR		Microarray II and qRT-PCR
Clone	**NP Passage**	**Clone**	**NP Passage**
NL2.1	9	NL (NDC1.1 Gs)	4
NL2.2	9	NL (NDC1.2 Gs)	8
NL2.3	4	NL (NDC1.3 Gs)	4
NL2.4	5	NL (NDC2.2 Gs)	4
NL5.1	5	NL (NDC2.3 Gs)	8
NL5.2	7	SAD (SAD1.1 Gs)	9
NL5.3	4	SAD (SAD1.2 Gs)	2
SAD2.1	4	SAD (SAD2.1 Gs)	4
SAD2.2	5	SAD (SAD2.2 Gs)	4
SAD2.3	8	SAD (SAD2.3 Gs)	5
SAD2.4	4	SAD (SAD2.4 Gs)	9
SAD3.1	4		
SAD3.2	11		
SAD3.3	3		

Figure 3.10: Gene Expression Profile of Additional Clones Neural Progenitors. (a) Heat map of significant genes differentially expressed between SAD and normal NP lines with additional clones from each individual with a q-value of less than 0.15. (b) A heat map of Pearson correlation coefficient shows that the gene expression of SAD and NL NP cells correlate within their respective groups, although NL (NDC1.1 Gs) and SAD (SAD1.1 Gs) are outliers. (c) Comparison of the significant differentially expressed genes between the original NP microarray and the additional clones, shows a small but robust overlap of genes. The numbers shows the fold change of the genes in each microarray set with average SAD over average NL. If multiple probes were significant for the same gene, the average fold change was taken. d) The six most significant annotation clusters (enrichment greater than 1.8) using the Database for Annotation, Visualization, and Integrated Discovery (DAVID) in the significant additional NP clone gene list. BP: biological process, CC: Cellular compartment, D: Domain.

Figure 3.10: Gene Expression Profile of Additional Clones Neural Progenitors (cont.)

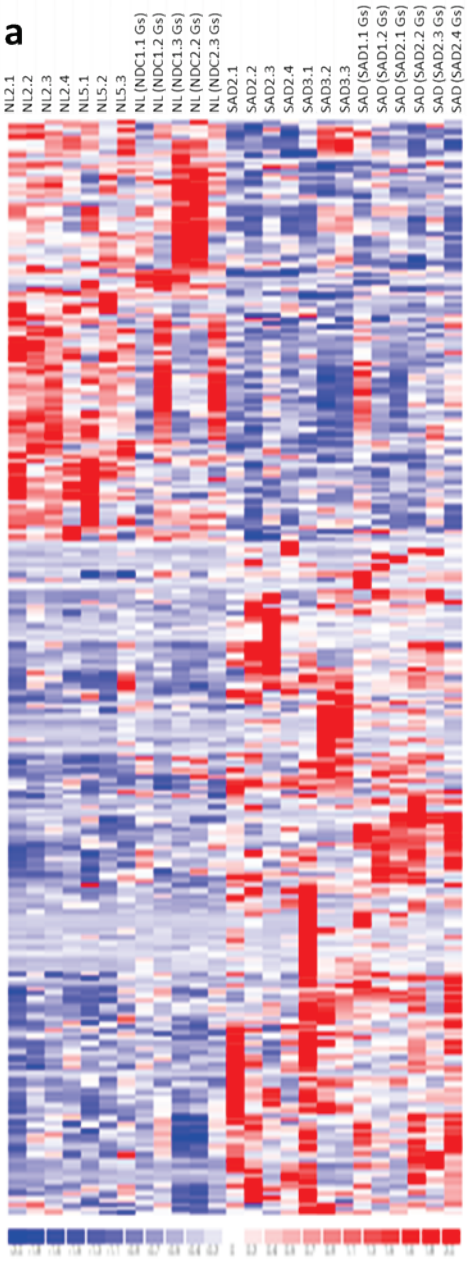

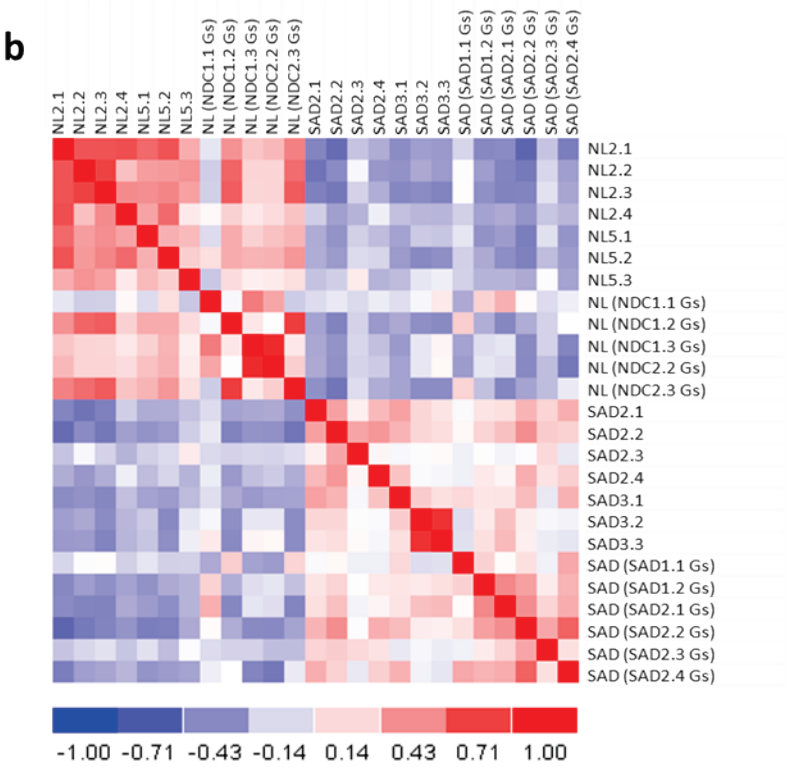

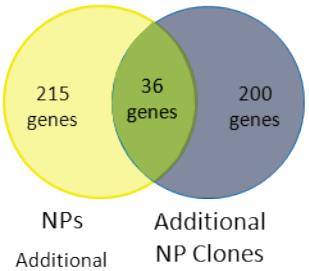

	NPs	Additional NP Clones
ADA	-2.39	-1.48
ASCL1	14.67	2.27
ASXL3	2.43	1.71
BACH2	1.85	1.31
BTN3A2	-2.39	-1.77
C14orf132	1.79	1.60
C1orf21	1.58	1.39
CNR1	7.30	5.23
COL13A1	-3.79	-2.30
CSRNP3	3.05	1.94
DCX	14.78	3.58
DLL3	2.69	2.62
DPYD	-2.63	-2.23
ECM1	-3.19	-2.00
EPHA7	3.09	3.08
GKAP1	1.86	1.55
LAMC1	-2.32	-1.89
LOC100509635	3.56	2.25

	NPs	Additional NP Clones
LSAMP	1.99	2.19
MAFB	5.11	2.77
MEIS2	4.69	2.41
NRP1	-2.57	-1.68
NRP2	-2.07	-1.90
OTTHUMG00000175759	3.73	1.95
PLA2G3	-2.18	-1.77
PLXDC2	2.58	1.94
PTPRJ	-2.54	-1.74
REEP1	3.29	1.59
SEMA6A	2.48	2.04
SNCAIP	2.92	2.04
SOX11	1.85	1.45
STMN2	9.55	4.38
SYT4	2.89	2.05
TLR4	-1.92	-2.50
TSHZ1	2.98	2.30
ZNF503	3.27	2.58

d

Annotation Cluster	Type	Enrichment
Neurogenesis	BP	5.49
Regulation of Cell Differentiation	BP	2.97
Neuron Projection	CC	2.32
Fibronectin, type III	D	2.11
Amino Acid Biosynthesis	BP	2.07
Homeobox	D	1.86

direction, indicating that the regulation is the same in this set of neural progenitors. Some key gene expression differences shared between the two analyses include *ASCL1*, *DCX*, *COL13A1*, and *STMN2*. Some genes identified in the first NP microarray are not significant at the 0.15 q-value threshold for the multiple clones, but still trend in the same direction. For example, *CD24* (FC 1.8-2, p-value 0.02-0.05 for the different probes), *EPHB1* (FC1.6-2.3, p-value 0.09), and *MEIS1* (FC 1.9-2, p-value 0.013-0.017) are still up-regulated in the additional clones but do not reach q-value significance. This is not true for all the strong hits from the initial NP gene list. Although *COL13A1* is down-regulated in SAD in both gene lists, *COL11A1* is not differentially expressed in the additional clones in the microarray analysis.

Enrichment analysis using DAVID shows that the most enriched annotation cluster is for neurogenesis, while genes localized to neuronal projections, and homeobox genes are also in the top six (Figure 3.10d). Using MetaCore software to identify interactors that are over-represented in the genes differentially expressed in the additional NP clones shows some overlap with the first NP microarray, but it is not robust (Supplementary Figure 8, Figure 3.11a). The c-Myc, Oct-3/4, CREB1, and SP1 transcription factors are significant interactors in both groups, while BACE 1 is a top protease. Other top interactors include a different TGF-beta receptor (type III) and the plexin A4 receptor, which interacts with neuropilins (down-regulated in SAD neural progenitors) and transduces signals from semaphorins (up-regulated in SAD neural progenitors) (Suto et al 2005).

Using Ingenuity Pathway Analysis to calculate the strongest activated and inhibited upstream regulators also shows some similarity to the initial NP microarray (Supplementary Figure 9, Figure 3.11b). Retinoic acid is one of the top activated upstream regulators and its receptor was strongly activated in the original NP microarray. The neurogenin 3 transcription

Figure 3.11: Analysis of the Gene Expression Profile of Additional Clones

a

	Category	Object	P-value	Ratio
Interactions	Transcription factor	c-Myc	3.44E-09	2.2
	Transcription factor	GCR-alpha	1.88E-07	2.7
	Transcription factor	Oct-3/4	5.82E-06	2.4
	Transcription factor	FOXO1	4.83E-05	4.0
	Transcription factor	Neurogenin 2	5.15E-05	12.3
	Transcription factor	CREB1	1.15E-04	1.5
	Transcription factor	PAX6	1.41E-04	4.7
	Transcription factor	SP1	1.94E-04	2.0
	Transcription factor	NANOG	1.96E-04	2.5
	Receptor/Kinase	TGF-beta receptor type III	9.16E-06	12.3
	Receptor	Plexin A4	9.70E-09	36.2
	Protease	BACE1	1.57E-04	4.6

b

	Upstream Regulator	Type	Activation	P-value
Activated	ALDH2	enzyme	2.236	2.19E-06
	Retinoic Acid	chemical - endogenous	2.217	2.45E-02
	Estrogen Receptor	group	1.4	1.59E-02
	NEUROG3	transcription regulator	1.103	6.10E-03
	POR (Cytochrome P450)	enzyme	1.067	2.42E-03
	SFTPA1 (surfactant)	transporter	1	8.87E-03
Inhibited	TGFB1	growth factor	-1.521	2.68E-04
	CD38	enzyme	-1.709	1.66E-03
	Tumor Necrosis Factor	cytokine	-2.173	7.31E-04
	PDGF BB	complex	-2.247	7.22E-03
	Interleukin 5	cytokine	-2.339	2.53E-03
	ATF4	transcription regulator	-2.401	4.41E-05
	SYVN1	transporter	-2.449	4.92E-03
	EGF	growth factor	-2.563	3.68E-03
	FGF2	growth factor	-2.769	1.05E-02
	Vegf	group	-2.778	6.51E-03
	Interleukin 1B	cytokine	-3.225	7.20E-06

Figure 3.11: Analysis of the Gene Expression Profile of Neural Progenitors. (a) Table of the most significantly connected transcription factors, proteases, and receptors using MetaCore Interactome analysis. The ratio refers to the number of interaction partners in the gene list divided by the expected number of interactions in a random gene list of equal size. P-value had to be less than $2x10^{-4}$ to be included. (b) Table of the most significant activated (greater than 1 activation score) and inhibited (less than 1.5) upstream regulators calculated by Ingenuity Pathway Analysis (IPA). Upstream regulators with a p-value less than .025 were included.

factor is activated, whereas the neurogenin 1 was activated in the first microarray. Interestingly, estrogen receptor activity is activated in both NP microarray differential gene lists. The inhibited upstream regulators are strongly enriched for growth factors and cytokines, including VEGF, interleukin 1B, fibroblast growth factor 2, EGF, interleukin 5, platelet-derived growth factor, tumor necrosis factor, and TGFB1. The inhibition of TNF and IL1B activity is shared between the original NP microarray and the additional clone microarray.

To further explore whether similar genes and pathways are up- and down-regulated in the additional neural progenitor clones, the genes with the largest fold changes were emphasized (Figure 3.12a,c). The most down-regulated genes several genes are related to the extracellular matrix: *COL13A1*, *TIMP4* (an inhibitor of metalloproteinases), *ECM1*, and laminin gamma 1. Several of the genes are also related to VEGF signaling: *KDR* and neuropilin 1 and 2 are all down-regulated receptors for VEGF. MetaCore analysis identifies cytoskeleton rearrangement and actin filaments in addition to cell-matrix interactions as process networks enriched in the down-regulated genes (Figure 3.12b).

The top up-regulated gene in the SAD additional clones is a homeobox gene, *HOXA9*. *HOXA10* and *HOXA5* are also up-regulated, compared to the initial NP microarray in which *HOXA1*, 2, and 3 were up-regulated. The highly up-regulated genes include neuronal genes shared with the initial microarray: *STMN2*, *DCX*, and *EPHA7*. Other up-regulated neuronal genes include *SEMA6D* (interacts with the down-regulated neuropilins), *EPHA3*, and *ROBO2*, all of which are involved with axon guidance. MetaCore analysis shows the most significant process networks of the up-regulated genes is neurogenesis and axonal guidance, with cell adhesion and attractive and repulsive receptors also significant (Figure 3.12d).

Figure 3.12: Up- and Down-regulated Genes of Additional Clones NPs

a

Most Down-regulated Genes in SAD

Gene	Protein Description	Average FC	Probes
KDR	VEGF receptor 2	-4.02	1/1
VGF	Nerve growth factor inducible	-2.41	1/1
COL13A1	**Collagen 13 alpha 1**	**-2.30**	**3/3**
DPYD	**dihydropyrimidine dehydrogenase**	**-2.23**	**1/3**
SLC7A5	solute carrier family 7 A5	-2.19	1/1
SNHG5	small nucleolar RNA host gene 5 (non-protein coding)	-2.15	1/1
TIMP4	Tissue Inhibitor Of Metalloproteinase 4	-2.04	1/1
ECM1	**Extracellular Matrix Protein 1**	**-2.00**	**1/1**
NQO1	NAD(P)H dehydrogenase	-1.96	3/3
NRP2	**neuropilin 2**	**-1.90**	**3/10**
LAMC1	**Laminin, Gamma 1**	**-1.89**	**1/2**

b

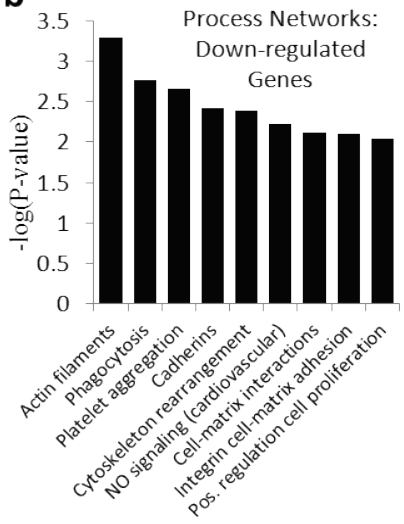

c

Most Up-regulated Genes in SAD

Gene	Protein Description	Average FC	Probes
HOXA9	Homeobox A9	4.95	2/2
SEMA6D	Semaphorin 6D	4.42	2/5
STMN2	**Stathmin 2**	**4.38**	**2/2**
EPHA3	EPH Receptor A3	3.90	1/3
DCX	**Doublecortin**	**3.58**	**2/2**
EPHA7	**EPH Receptor A7**	**3.08**	**3/4**
ROBO2	Roundabout 2	2.97	2/3
LOC283788	unknown	2.91	2/6
MLLT3	Mixed-lineage leukemia	2.71	3/3
FGFR2	Fibroblast Growth Factor Receptor 2	2.39	3/11
KCNMA1	K+ large conductance Ca++-activated channel subunit	2.15	2/4

d

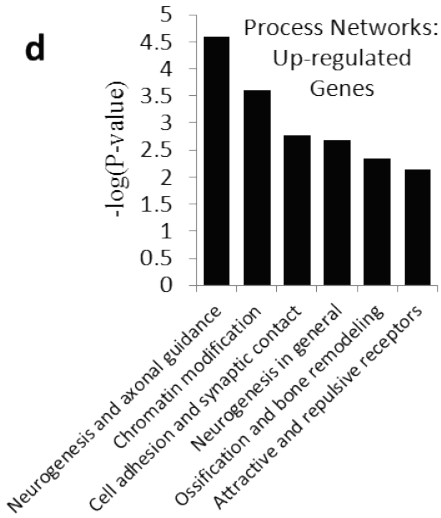

Figure 3.12: Up- and Down-regulated Genes of Additional Clones NPs. (a,c) Tables of the most strongly up-regulated and down-regulated genes in the SAD lines. The fold change (FC) represents the average of all probes for the specific gene, while probes refers to the number of probes that reach the significance threshold for NP expression out of all the probes annotated for that gene on the Affymetrix U133 Plus 2.0 array. The tables consist of genes with at least one probe showing less than 1.8 fold decrease or greater than 2.8 fold increase respectively as well as greater than 25% of probes for that gene in the significant gene list. Bolded genes are also significant in the first NP microarray analysis. (b,d) Enrichment analysis using MetaCore software for process networks that are significantly enriched in the up- and down-regulated genes. Included are only networks with a p-value less than 0.01.

One interesting SAD up-regulated gene is the FGFR since upstream regulator analysis shows that FGF signaling is inhibited in these cells. This dichotomy is also seen in TGF signaling, where TGFB2 is up-regulated in the additional clones, but TGFβ signaling is down. This may suggest a disruption in growth factor signaling regulation since despite the higher levels of the FGF receptor and the TGFβ ligand, downstream gene expression from these signaling pathways remains inhibited.

Neuronal gene expression differences were confirmed through qRT-PCR for *DCX, ASCL1,* and *CD24* (Figure 3.13). All three genes had a p-value less than 0.01 for the difference in expression between the SAD and NL neural progenitor lines.

Figure 3.13: mRNA of Differentially Expressed Genes in Additional Clones

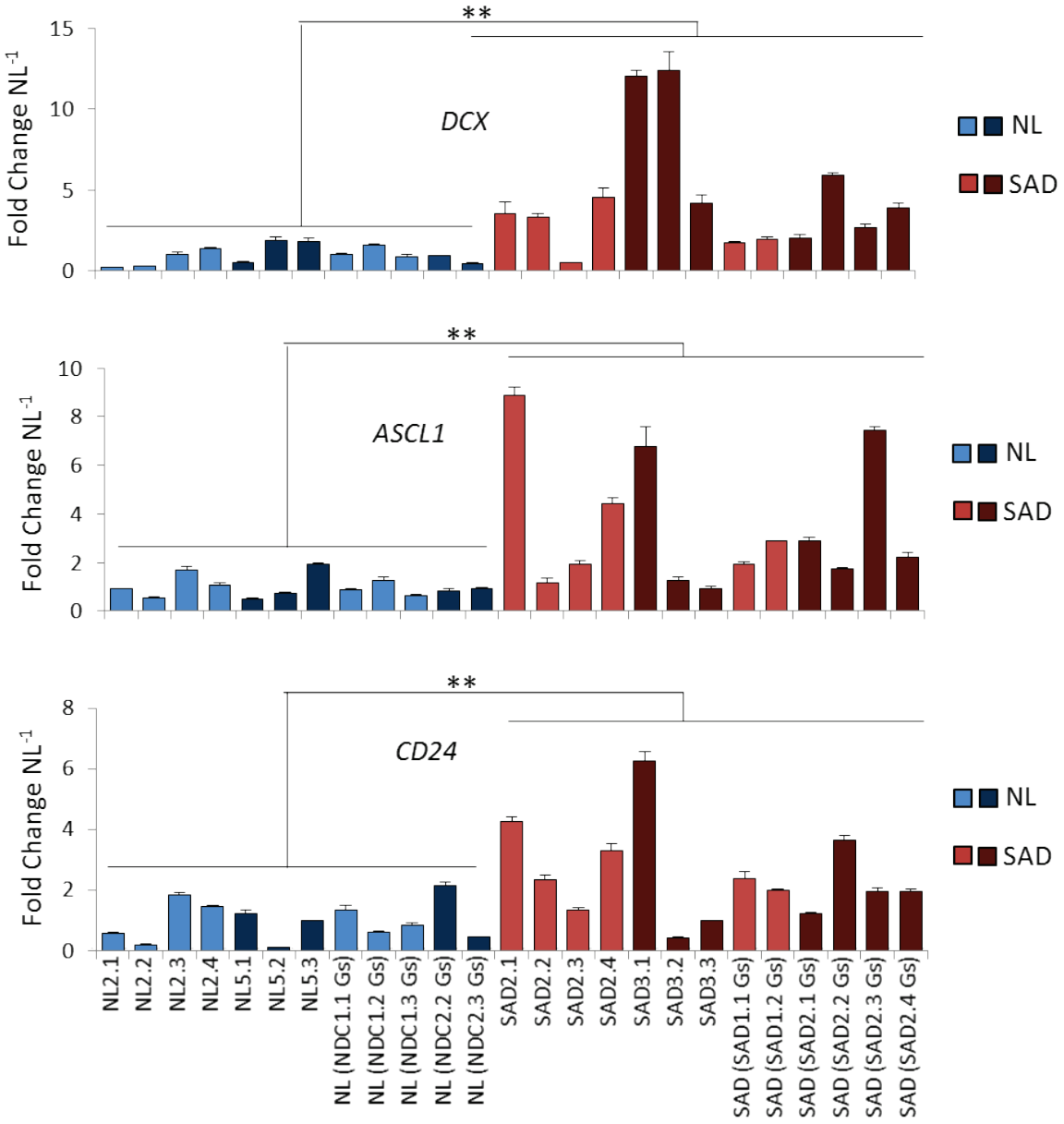

Figure 3.13: mRNA of Differentially Expressed Genes in Additional Clones. Representative quantitative RT-PCR shows differential mRNA expression in the SAD neural progenitors compared to the controls for *DCX, ASCL1,* and *CD24* in multiple clones per patient. mRNA values were calculated using the relative standard curve method and normalized to *GAPDH*. Fold change was calculated relative to the average normalized expression of all the NL lines. Errors are the standard error of the mean for multiple wells. *DCX*: $p=0.005$ Log_2 $p<0.001$; *ASCL1* $p=0.006$ Log_2 $p<0.001$; *CD24* $p=0.006$, Log_2 $p=.005$; **$p<0.01$

Conclusions and Discussion

The increase in neuronal differentiation genes in the SAD neural progenitor lines was a surprising result. Despite the intensive research into Alzheimer's disease, few studies have shown increases in the propensity for neural differentiation affecting the development of AD. Our own fibroblast microarray results show a down-regulation of neuronal genes in the SAD patients. Therefore, the difference in the SAD neural progenitor was carefully confirmed. Despite still showing predominant expression of neural progenitor markers such as nestin, musashi, and SOX2, the SAD lines showed increased mRNA and protein levels for markers of later neuronal differentiation, including doublecortin, ASCL1, and CD24. These markers seem to be localized to a subset of cells, suggesting that the premature differentiation in a small number of cells is accounting for the larger differences in gene and protein expression.

These results were confirmed using neural progenitors differentiated from iPS cells derived from three different laboratories, precluding the possibility of lab-specific iPSC effects. The mRNA results were further confirmed using multiple clones from eight different patients: four SAD and four NL patients. The SAD lines showed a highly significantly significant increase in neural differentiation markers, supporting that these results were not artifacts from random differences in the differentiation process, but due to the intrinsic propensity of the SAD lines to neuronal differentiation.

However, despite the clear overall increase in the SAD lines, there is significant line-to-line variability. In fact, the two NP microarrays, although showing a strong overlap of neuronal differentiation genes, did not share that many other genes. This supports a model in which different upstream mechanisms lead to the same results: increased neuronal differentiation. However, later markers of differentiation such as *TBR2*, which is seen in INPs and more matured

SGZ neural stem cells, are not differentially expressed, suggesting that the increase is in the earliest stage of committed progenitors.

There are many candidates for what may cause the difference in neuronal differentiation. Many different signaling pathways that affect neuronal differentiation are differentially expressed in the SAD neural progenitors. The transcription factors that are differentially expressed include *ASCL1*, *MEIS1/2*, *DACH1*, *MAFB*, and *TSHZ1*. Upstream regulator analysis also identifies the activation of Hox genes, neurogenins, and various ubiquitous differentiation regulators. The up-regulated *DLL3*, a delta-like protein, is a target of ASCL1 and is found in enriched in early post-mitotic neurons where it may inhibit notch signaling, thus enhancing neural differentiation (Henke et al 2009). HES6, unlike the rest of the notch-dependent HES family, actually promotes neurogenesis through binding HES1 and preventing it from inhibiting ASCL1 (Bae et al 2000, Jhas et al 2006). But the inhibited upstream regulators, many of which are implicated in neural patterning, could also play a substantial role in the differentiation of the SAD neural progenitor lines. TGF-β, EGF, VEGF, and FGF2 signaling have all shown evidence for down-regulation which could influence the differentiation state of the neural progenitor cells.

It is clear that it is a complicated story. In addition to the up-regulated neuronal genes, some, such as the neuropilin genes, are down-regulated. Many other genes show differential expression including down-regulation of extracellular matrix genes including collagens, laminin, and integrins. These changes in gene expression could prepare the developing neurons for migration or denote a difference in intermediate neural stem cell state. However, it could also be showing a pathological difference in adhesion properties between the SAD and NL lines.

One important question is why the previous groups that have used iPS cells to study Alzheimer's disease have not seen this difference in neuronal differentiation. There are several

important differences between our approach and the approach used by other groups. Israel et al. (2012), which used some of the same cell lines, did not see a difference in neural stem cell production using the FACS analysis for cells that were CD184+, CD15+, CD44-, and CD271-. However, it is unclear what this population of cells represents since, although based on previous work (Yuan et al 2011), it does not use the same markers for neural stem cells, and is less than 15% of the population of neural progenitor cells. This subpopulation was then used for later differentiation experiments. Furthermore, the protocol for deriving these neural progenitor cells is different than ours, in which they plated the iPS cells on PA6 mouse stromal cells and treated with Noggin and SB431542 (inhibitors of Smad, which is downstream of BMP) to induce neural differentiation. Results may have been further difficult to interpret since there were only two patients in both the SAD and control group and the SAD lines had a relatively high age of onset. Qiang et al. (2011) and Kondo et al. (2013) do not use a neural progenitor intermediate during their differentiation process.

The differences in the neural progenitor gene expression profile did not resemble the fibroblast gene expression profile. In the fibroblasts, neuronal genes were down in SAD, while neuronal genes were predominantly up in the neural progenitors. There were few shared significant genes between the two groups. This suggests that these differences are specific to the neuronal lineage and that the differences in the fibroblasts may reflect that the cells were taken from sick patients. The correlation between FAD and SAD in the fibroblasts, but not the neural progenitors, supports this hypothesis.

The fact that the one FAD line does not more closely mirror the sporadic patients in neural progenitor gene expression is interesting. Although it is difficult to draw conclusions from just one patient, it suggests that this neuronal differentiation phenotype may not be shared

between the sporadic and FAD patients. However, a recent paper looking at iPS cells from M146L and A246E *PSEN1* mutants differentiated into neural progenitors did see an increase in NCAM expression (a marker of neuronal differentiation) and a gene expression profile consistent with a subtle increase in neurogenic potential (Sproul et al 2014). More patients with different mutations in *PSEN1*, *PSEN2*, and *APP* would need to be tested to verify that the difference seen in our SAD neural progenitors are consistent with changes seen in FAD.

The *APOE* genotype does not appear to have a strong effect on the expression of the neural differentiation markers, since SAD5.1 is a strong expresser, while SAD1.1 is a weaker expresser (both *E4/E4*), suggesting that while *APOE* may still contribute to this phenotype; it does not seem to be the primary effector. However, APOE may play a role in neurogenesis, since the levels of doublecortin-positive cells is increased in a mouse model of APOE4, although overall neuronal maturation from adult neurogenesis may be impaired (Adeosun et al 2014, Li et al 2009a). APOE-deficient mice have increased proliferation in the dentate gyrus at an early age before depletion in neural progenitors later in life (Yang et al 2011). Therefore, although it remains unclear the exact effects *APOE* may have during neurogenesis, it does to appear to be important in that process and may be modulating the neuronal differentiation phenotype seen in the *APOE4/E4* SAD lines.

Contributions

Nicholas Bishop differentiated iPS cells into the following NPs: NL1.1, NL4.1, NL6.1, SAD1.1, SAD2.1, and FAD1.1. Tao Lu and Ying Pan differentiated the following NP lines: SAD2.2, SAD2.3, SAD2.4, NL5.2, NL5.3, SAD (SAD2.4 Gs), SAD (SAD1.1 Gs), NL (NDC1.2 Gs), and NL (NDC2.3 Gs). Tao Lu designed the primers for *DCX*, *CD24*, *CD44*, *EPHB1*, *ACTIN*, and

ASCL1. Zhenjuan Wang at the Harvard Genome Modification Facility gathered the data on the teratoma formation timeline.

Chapter 4: Differentiation and characterization of neurons

Abstract

Since neurons are the cell type predominantly affected during Alzheimer's disease, the neural progenitors were next differentiated into a neuronal culture. Neurons expressing the neuronal-specific markers β-tubulin III and MAP2 were generated using a protocol optimized for the generation of glutamatergic neurons. Neuronal cells from all lines were able to form action potentials and had functional sodium and potassium currents in response to depolarization. The neurons were characterized more thoroughly at 6 weeks of differentiation at which point the culture is predominantly β-tubulin III and MAP2-expressing with a subset of cells expressing the glial marker GFAP. They form both glutamatergic and GABAergic neurons, although glutamatergic is the predominant subtype. Gene expression profiling shows a continued robust gene expression difference between the SAD and NL lines, predominantly with an up-regulation of genes involved with mature neuronal functions and a down-regulation of growth factor signaling and cell cycle progression in the SAD neurons. This difference in gene expression is accompanied by a difference in mature neuronal function in the SAD neurons, which form more synapses at 6 weeks of differentiation and are able to generate action potentials earlier than the NL lines.

Introduction

Alzheimer's disease is a disease of the brain, therefore in order to model the disease *in vitro* we want to generate the cells affected by the disease *in vivo*. Using fMRI to map metabolic defects shows that during the preclinical stage of AD, the first region affected is the lateral entorhinal cortex (Khan et al 2014). A combination of clinical post-mortem studies and fMRI shows a loss of metabolism and neurons that extends into the hippocampus and then the cortex as

the disease progresses (Scahill et al 2002). By the time the disease is diagnosed, the numbers of cells in the hippocampus and entorhinal cortex have already been severely diminished.

Since AD is only diagnosed at an advanced stage of dysfunction, there is still some controversy over the most affected cell type. The brain contains many different types of cells, including a diverse plethora of neurons and glial support cells. Glial cells include microglia, an immune cell which acts in the brain, and astrocytes, which are the most numerous cells in the brain and are important in diverse activities including structure, metabolic support of neurons, regulation of the extracellular space, and modulation of synaptic transmission. Other glial cells of the central nervous system (CNS) include oligodendrocytes, which envelop the axons and potentiate the transmission of action potentials, and radial glia cells, which were previously discussed since they act as neural progenitors within the CNS as well as a scaffold of early neuronal migration. Neurons of the central nervous system are highly diverse and usually initially categorized by their neurotransmitter, which includes the predominantly excitatory glutamatergic and the predominately inhibitory GABAergic which make up the vast majority of neurons in the brain. Other neurons of the CNS include those that release cholinergic, dopaminergic, and serotonergic neurotransmitters.

Many of these cells have been implicated in various stages of AD, however, the cell type that is affected during some of the earliest stages of pathology is the loss of function, synapses, and eventual death of the hippocampal pyramidal neurons (Kerchner et al 2010). These are glutamatergic neurons which make up about 90% of the neurons in the hippocampus (Olbrich & Braak 1985, West & Gundersen 1990). In further evidence for their susceptibility to the development of AD, a recent study showed selective toxicity of Aβ for glutamatergic over GABAergic neurons in cultures derived from induced pluripotent stem cells (Vazin et al 2014).

Therefore, the ideal culture will be predominantly glutamatergic, although other cell types will still be useful to test alternative hypotheses for the development of AD.

From the neural progenitor stage of differentiation derived in the previous chapter, the cells must be induced to mature. Neurons are different from most other cells in the body in that they no longer divide and are post-mitotic. In fact, expression of cell cycle genes and a return to cell division results in cell death for neurons both during development and neurodegeneration (Herrup & Yang 2007). Neurons are defined by their capability to propagate electrochemical signals through action potentials and synaptic activity. A mature neuron will be able to respond to depolarization through the induction of sodium and potassium channels, causing first further depolarization as the sodium channels are activated and then repolarization as the potassium channels activate. Action potentials (APs) form as a cyclical depolarization and repolarization through the activity of the sodium and potassium channels and can be measured through the voltage across the membrane using the patch clamp technique. The AP signaling causes neurotransmitters to release and mediates neuronal signaling. Together, the formation of synapses, generation of action potentials, and the formation of neuronal morphology are used to verify the generation of functional neurons *in vitro*.

Materials and Methods

Neuronal Differentiation Tests: The following different surfaces were tested: polystyrene tissue culture plates (Corning), glass coverslips (German, #1.5), and plastic coverslips (Thermanox). Four different coatings were tested. Poly-L-lysine was coated at 0.1 mg/mL in sterile water for 1 hour at room temperature. Polyornithine (Sigma) was coated at 20 µg/mL in sterile water for 2 hours at 37° followed by 5 µg/mL laminin diluted in 4° DPBS without calcium or magnesium (Life Technologies) or 1 mg/mL laminin for two hours at 37°. Matrigel (BD Biosciences) was

diluted to 200 μg/mL in 4° Neurobasal media and coated for one hour at room temperature. Cell concentration was counted using a Z1 Coulter Particle Counter (Beckman Coulter). Three differentiation media were tested. NB media contains Neurobasal media with 1x B-27 (Life Technologies), 1 mM L-glutamine, 50 U/mL penicillin, and 50 mg/mL streptomycin. DBN media contains DMEM/F-12 media with 1x B-27, 1x N-2, 1 mM L-glutamine, 50 U/mL penicillin, and 50 mg/mL streptomycin. 1:3 media contains both DMEM/F-12 and Neurobasal media in a 1:3 ratio along with 1x N-2, 1 mM L-glutamine, 50 U/mL penicillin, and 50 mg/mL streptomycin.

Potassium chloride (Sigma) was tested at 20 nM, BDNF and GDNF were tested at 20 ng/mL each, and kynurenic acid was tested at 1 mM. All the additives were tested in NB media. For glial co-culture, rat glia were cultured in DMEM with 10% FBS, 2 mM L-glutamine, 50 U/mL penicillin, and 50 mg/mL streptomycin and split with trypsin. The Banker method is based on the published protocol (Kaech & Banker 2006) in which glass coverslips have hot paraffin drops applied to the surface (3-4 per coverslip). Once the paraffin is cooled, the coverslips are coated as usual on the surface with the paraffin dots and plated with NPs. The next day, the coverslips are inverted over rat glia so that the NP cells are separated from the rat glia by the paraffin drops. For direct co-culture, the NPs are plated directly onto the rat glia.

Differentiation and Culture of Neurons: Neural progenitors were plated at the desired concentration on plates coated with polyornithine/laminin (20 μg/mL and 5 μg/mL, respectively) or Matrigel (200 μg/mL) in NP media. After 24 hours, the media is changed to NB media. Media is changed every 3-4 days in which approximately half of the media is removed through vacuum aspiration without drying out the differentiating neurons and new NB media is added.

Immunofluorescence (IF) and Antibodies: Neural progenitors were plated on glass or plastic coverslips at $5x10^4$ cells/coverslip unless otherwise specified. Neurons were differentiated for 6 weeks before fixation, unless otherwise specified. IF was performed as described in Chapter 2. For the plastic coverslips, each coverslip was covered with and imaged through a larger glass coverslip. For all quantification, at least five randomized fields were imaged per coverslip and the cells expressing each marker were counted using MetaMorph (v7.7.0.0) software as described in Chapter 3. Synapsin-1-positive puncta were defined as between 1-8 μm and greater than 1500 times the baseline intensity. GABAergic neurons were identified by the presence of GABA in the soma overlapping the nucleus, while GFAP-expressing cells were counted manually.

Target	**Host**	**Source**	**Catalogue #**	**Dilution**
β-tubulin III	Rabbit	Covance	MRB-435P	1:1000
GFAP	Mouse	Cell Signaling	3670	1:300
Nestin	Mouse	Millipore	MAB5326	1:200
β-tubulin III	Mouse	Chemicon	MAB1637	1:250
Doublecortin	Rabbit	Cell Signaling	4604S	1:400
MAP2	Mouse	Millipore	MAB3418	1:500
VGLUT1	Mouse	MediMABS	MM-0016-P	1:400
GABA	Rabbit	Sigma	A2052	1:2000
Synapsin 1	Rabbit	Calbiochem	574777	1:1000

Electrophysiology: Electrophysiology was performed in collaboration with the laboratory of Dr. Li-Huei Tsai (MIT). The excitability of neurons was measured after different periods of

differentiation on glass coverslips coated with polyornithine/laminin using the patch clamp technique on an Axon Axopatch 200B (Molecular Devices). The presence of induced action potentials was confirmed by measuring voltage in response to current steps ranging from -100 pA to +200 pA. Sodium and potassium channel activity was determined by measuring current in response to voltage steps ranging from -50 mV to +55 mV. The external solution was 130 mM NaCl, 4 mM KCl, 2 mM $CaCl_2$, 1 mM $MgCl_2$, 10 mM HEPES, and 10 mM glucose (pH = 7.4, osmolality = 325 mOsm kg^{-1}). The internal solution was 110 mM potassium gluconate, 20 mM KCl, 2 mM MgATP, 10 mM sodium phosphocreatine, 1 mM EGTA, 0.3 mM GTP-Tris, and 20 mM HEPES (pH = 7.3, osmolality = 320 mOsm kg^{-1}). Pipettes were fire-polished to resistances between 2-4 mOhm and series resistance was compensated 75%. Between 4 and 12 cells were tested per coverslip and pClamp10 software was used for data analysis.

Microarray Analysis: RNA was extracted using TRIzol reagent (Life Technologies) from 6-week differentiated neurons plated on polyornithine/laminin, directly on polystyrene 10 cm^2 tissue culture dishes. mRNA was measured on Affymetrix U133 Plus 2.0 arrays by the Molecular Biology Core Facility at Dana Farber (Boston, MA) and the data was analyzed as described in Chapter 2.

Quantitative RT-PCR and Primers: qRT-PCR was performed as described in Chapter 3. All cells were differentiated on polyornithine/laminin coated polystyrene tissue culture plates. The below new primers were used.

Primer Target	Forward Sequence	Reverse Sequence
CCND2	AGTCCCATCTGCAACTCCTG	CGCAAGATGTGCTCAATGAA
ZIC3	GCAAGTCTTTCAAGGCGAAG	CTGTTGGCAAAGCGTCTGT
HOXA3	CAAACAAATCTTCCCCTGGA	ACAGGTAGCGGTTGAAGTGG
SPON1	GCGTCAAACAAGTTGCAGAA	CCATCATGGTCAGGAAGGAC

NESTIN	CAGCGTTGGAACAGAGGTTGG	TGGCACAGGTGTCTCAAGGGTAG
COL11A1	ATGGAATCACGGTTTTTGGA	AGGTTCCTGAGCTTGAGCAG

Cell Count: Neural progenitors were counted on a Z1 Coulter Particle Counter (Beckman Coulter) after dissociation with accutase and plated at $5x10^4$ cells/well in a 24-well plate. Experiments 1 and 3 had one well per time point and experiment 2 had four wells per time point. For the neuronal cell count, two wells per time point were plated on Matrigel at $2x10^4$ cells/well in a 24-well plate. Lines that did not adhere well and had less than $2.5x10^5$ cells at 7 days were removed from the analyses. The neurons were dissociated with trypsin and counted on the Z1 Coulter Particle Counter.

Results

A. Generation of neurons

A variety of conditions were tested to differentiate the NPs into neurons (Table 4.1). The greatest challenge was preventing the differentiating neurons from lifting off the substrate over the course of differentiation up to 12 weeks. Various surfaces were tested: directly on plastic tissue culture dishes, on glass coverslips, and on plastic coverslips. The NPs preferred to differentiate directly onto the tissue culture plates. However, many applications, such as immunocytochemistry and electrophysiology experiments require coverslips. The cells were more likely to remain adhered to plastic rather than glass coverslips, but the plastic coverslips interfere with fluorescent microscopy and changed the morphology of the neurons to a more flattened state, making them more difficult to measure in electrophysiology experiments. Therefore, glass coverslips are used for those applications.

Various coating conditions were also tested including poly-L-lysine, polyornithine with two different concentrations of laminin, and Matrigel. The cells did not remain adhered to poly-

Table 4.1: Neuronal Differentiation Test Conditions

	Condition	Details	Observations
Surface	Plastic Tissue Culture	No coverslip	Most cells stay adhered, but limited for downstream applications
	Glass Coverslip	German glass	Works better for some lines, some lift off
	Plastic Coverslip	Thermanox #174950	More adherent than glass, but difficult for many downstream applications
Coating	Poly-L-lysine	0.1 mg/mL	Cells did not stay adhered during differentiation
	Polyornithine/Laminin	20 µg/mL polyornithine / 5 µg/mL laminin	Most cells remain adhered
	Polyornithine/high concentration laminin	20 µg/mL polyornithine / 1 mg/mL laminin	Cells did not stay adhered during differentiation
	Matrigel	200 µg/mL	Most cells remain adhered, but may affect signaling
Cell Concentration	$5x10^4$ cells/cm^2	Tested in 2 cm^2	Very confluent during differentiation and more likely to lift off
	$2.5x10^4$ cells/cm^2	Tested in 2 cm^2	Best condition, but varies from line-to-line
	$5x10^5$ cells/cm^2	Tested in 2 cm^2	Sparse, but still neuronal, works better for some lines than others
Media	Neurobasal/B-27	1x B-27	Looks good, some glia
	1:3 DMEM F-12/Neurobasal	1x N-2	More processes, some glia
	DMEM F-12/N2/B-27	1x N-2/ 1x B-27	Much more glia, less neurons
Additives	Potassium Chloride	20 mM	No effect
	BDNF/GDNF	20 ng/mL each	Increases glia in culture
	Kynurenic Acid	1 mM	No effect
Media Change	Half Media		Works well
	Full Media		Cells more likely to lift off and die
Frequency of Media Change	Daily		Cells more likely to lift off
	Biweekly		No ill effects from changing media less frequently
Glial Co-Culture	Banker Method	Cells suspended upside down on glass coverslip over rat glia	Cells are very healthy, but some glia migrate onto coverslip
	Direct Co-Culture	With rat glia	Cells healthy, but some assays difficult without marker of human cells

L-lysine during differentiation and unlike in previous reported results, we did not see better adherence with a higher laminin concentration (Shin et al 2006), although this may be due to inadequate distribution of the high concentration laminin. A coating of polyornithine and 5 μg/mL laminin was usually sufficient to keep cells adhered throughout the differentiation process, however Matrigel had the best adherence success as previously found (Uemura et al 2010). One concern with using Matrigel is that it is derived from mouse tumor cells and is not well-defined. It contains multiple growth factors including FGF, EGF, IGF1, TGFβ, PDGF, and nerve growth factor (NGF) which could affect neural differentiation (Vukicevic et al 1992). Therefore, both polyornithine/laminin and Matrigel coating are used for neural differentiation and specified for each experiment.

Various starting cell concentrations of neural progenitors were also tested. Proliferation continues even after the onset of differentiation, making it difficult to predict the ending confluency of post-mitotic neurons. There was significant variability between lines but in general $2.5x10^5$ cells/cm^2 works best for maximizing adherence and still allowing individual cells to be visualized and manipulated on polyornithine/laminin. Higher concentrations can be used when the whole population is being studied such as harvesting mRNA or protein. Cells on Matrigel proliferate more before differentiation, so a lower starting density of NPs was needed.

Three different previously described neuronal differentiation medias were tested: Neurobasal/B27 (NB media), DMEM F-12/N-2/B-27 (DNB media), and 1:3 DMEM F-12: Neurobasal with N2 (1:3 media) (Li et al 2009b, Shin et al 2006, Spiliotopoulos et al 2009). All cultures produced a mixture of β-tubulin III-expressing neurons and GFAP-expressing glial cells (Figure 4.1a). The DNB media had the greatest concentration of glial cells, while NB media provided the most uniform distribution of neuronal processes with only a few glial cells.

Figure 4.1: Neuronal Differentiation Test Conditions

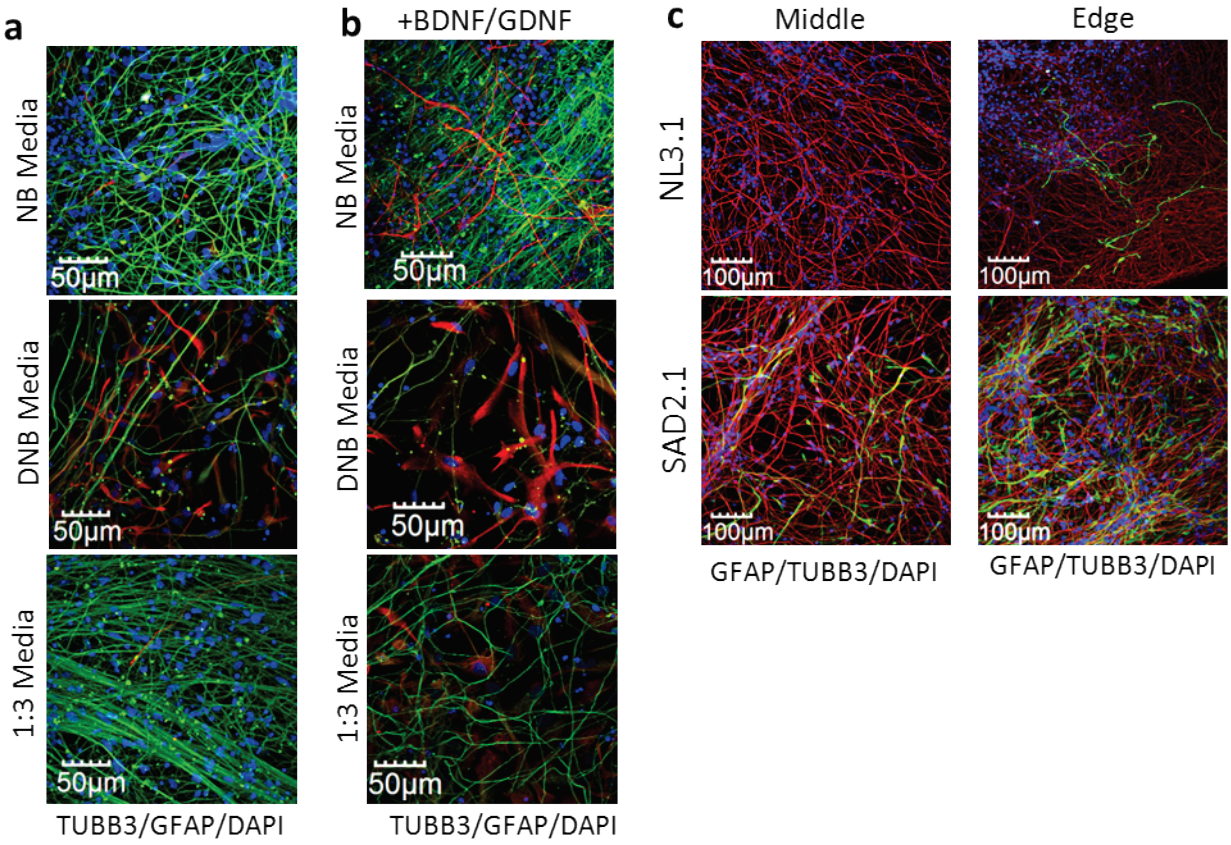

Figure 4.1: Neuronal Differentiation Test Conditions. (a) SAD4.1 neurons differentiated for 5.5 weeks have both β-tubulin III (TUBB3, green) and GFAP (red) cells when co-stained with DAPI (blue) for DNA using several different differentiation conditions. The three tested media were Neurobasal/B27 (NB media), DMEM F-12/N-2/B-27 (DNB media), and 1:3 DMEM F-12: Neurobasal with N2 (1:3 media). (b) SAD4.1 neurons differentiated for 5.5 weeks with the addition of the neurotrophic factors BDNF and GDNF (20 ng/mL) have more GFAP-expressing cells (red), but still produce TUBB3-expressing cells (green). (c) Using the Banker co-culture method for 4 weeks of differentiation, most glia cells positive for GFAP (green) were localized to the edge of the coverslips, possibly due to the migration of rat glia from the underlying substrate. Most cells in the middle of the coverslip are TUBB3-expressing (red), with a few GFAP-expressing. The cells were grown in NB media on glass coverslips coated with polyornithine/laminin.

Various additives were used to optimize the differentiation process. Quite a few cells die during the differentiation process, therefore the addition of 20 nM potassium chloride and 1 mM kynurenic acid were tested. Potassium chloride is a neuroprotective agent that depolarizes neurons, causing elevation of intracellular calcium, and preventing apoptosis (Franklin & Johnson 1992). Kynurenic acid is an NMDA antagonist that prevents excitotoxicity (Li & Stys 2000). However, neither of these treatments improved neuronal cell culture quality. Brain-derived neurotrophic factor (BDNF) and glia cell-derived neurotrophic factor (GDNF) are survival-promoting neurotrophic factors (Yan et al 1999). Addition of these factors to all the tested media caused an increase in cells expressing GFAP (Figure 4.1b). In media containing DMEM F-12, the GFAP+ cells had a more flattened morphology, while in NB media the GFAP+ cells have the bipolar morphology of radial glial cells.

During their growth, neurons condition their media with factors that promote cell survival; therefore changing the media can disrupt cell growth. I tested both changing the full media and only removing half of the depleted media before adding fresh media as well as altered the frequency of media change from daily to every 3-4 days. The neurons thrived when disturbed the least, therefore the half media changes every 3-4 days had the best cell adherence and survival during differentiation.

Finally, to further condition the media, neurons can be cultured with glia. I tested two methods of culture with rat glia: the Banker method in which the cells are grown on an inverted coverslip separated from the glial layer by a paraffin tripod and direct co-culture where the human neurons are differentiated directly on a layer of rat glia (Kaech & Banker 2006). The cells thrived in both conditions; however the methods were complicated by the presence of foreign cells. In the Banker method, GFAP-expressing cells were localized to the edge of the

coverslip and regions near the paraffin, suggesting that rat glia may have migrated onto the neuronal coverslip (Figure 4.1c). In both methods, without a marker for our iPS-derived neuronal cells, it is challenging to make conclusions about differentiation. Therefore, glial co-culture was not used for most of our experiments.

Since the population of cells that we are most interested in is neurons, the optimized conditions for neuronal differentiation of our neural progenitors is first plating at the desired density in NPM, then changing the media the next day to NB media after the cells adhere. Half of the NB media is changed every 3-4 days. The cells are plated directly on the tissue culture plate or glass coverslips as needed, coated with Matrigel or polyornithine/laminin. The capability of the neural progenitors to differentiate into neurons is not affected by the passage numbers tested (Table 4.2). One limitation to the optimization is that most of the differentiation tests were done on SAD lines, and the ideal protocol for AD neurons may not necessarily be the ideal protocol for the control lines.

Table 4.2: Neural Progenitor Passages for Neuronal Differentiation

Line	Microarray		qRT-PCR		Immunostaining		Electrophysiology	
	NP Clone	NP Passage	NP Clone	NP Passage	NP Clone	NP Passage	NP Clone	NP Passage
NL1	1	22	1	22	1	Multiple	1	24
NL2	1	8	1	8	1	Multiple	1, (2)	8, 11, 16 (11)
NL3	1	8	1	8	1	Multiple	1	8, 12, 15
NL4	1	5	1	5	1	Multiple	1	12
NL5	2	5	2	5	2	Multiple	2	22
NL6	1	17	1	17	1	Multiple	1	23
NL (17 Eg)	-	-	a	8	a	Multiple	a	17
NL (20 Eg)	-	-	b	7	b	Multiple	b	14
NL (NDC1 Gs)	-	-	2	18	2	Multiple	-	-
NL (NDC2 Gs)	-	-	3	18	3	Multiple	3	15
SAD1	1	10	1	10	1	Multiple	1	7
SAD2	1	10	1	10	1	Multiple	1	16, 19
SAD3	1	10	1	10	1	Multiple	1	10, 16, 17
SAD4	1	14	1	14	1	Multiple	1	12, 20
SAD5	1	12	1	12	1	Multiple	1	12, 16
SAD (SAD1 Gs)	-	-	1	19	1	Multiple	-	-
SAD (SAD2 Gs)	-	-	4	18	4	Multiple	4	15
FAD1	-	-	1	14	1	Multiple	1	20, 24

B. Characterization of neuronal cells

Using this protocol, all lines form cells with processes positive for the neuron-specific marker β-tubulin III (TUBB3) and MAP2, a neuronal filament that localizes in the dendrites (Figure 4.2a,b) (Caceres et al 1986). The electrical properties of the differentiated neurons were tested using patch clamp to measure the current or potential across the cell membrane. When current was measured following depolarization, the cells re-established the membrane potential using sodium and potassium channels consistent with neurons (Figure 4.2c). When voltage was measured while current was altered, the cells underwent cyclical oscillations to a higher voltage consistent with the depolarization and repolarization that occurs during an action potential (Figure 4.2d). Lines from each individual were able to form these induced action potentials after 4.5-15 weeks differentiation. Together, these data support that activity-capable neurons are derived from all lines.

The neurons were further characterized after 6 weeks of differentiation. This stage of differentiation is used for further analysis since some of the lines have already formed mature neurons with electrical capabilities, although other lines seem to have a later timeline for maturation which will be explored throughout the rest of this chapter. After 6 weeks differentiation, all the lines are predominantly positive for TUBB3, with a small number of cells positive for the glial marker GFAP (Figure 4.3a). There is a significant increase in the number of GFAP-expressing cells in the SAD 6-week differentiated neurons with the SAD cultures having between 1% and 13% and the NL cultures having between 0% and 5% after 6 weeks of differentiation (Figure 4.3b) ($p = 0.023$). The GFAP-expressing cells do not have the typical morphology of astrocytes, raising the possibility that they are a type of GFAP-expressing

Figure 4.2: Characterization of Neurons. (a) Representative images (one per individual) of 6-week differentiated neurons plated on Matrigel and glass coverslips stained for the neuronal marker β-tubulin III (red) with DAPI (blue) dye marking cell nuclei. (b) Representative images of 6-week differentiated neurons plated on polyornithine/laminin and glass coverslips stained for the neuronal marker MAP2 (green) and DAPI (blue) marking cell nuclei. (c) Representative plots of current following cell depolarization by voltage steps from -50 mV to +55 mV, showing that there are active sodium and potassium channels consistent with neurons in the differentiated cells. SAD (SAD1.1 Gs) was differentiated for 10.5 weeks before measurement and NL5.2 was differentiated for 15 weeks. (d) Representative plots of cell membrane potential following induction of action potentials with current steps from -100 pA to +200 pA, confirming that the differentiated cells are capable of forming action potentials.

Figure 4.2: Characterization of Neurons (cont.)

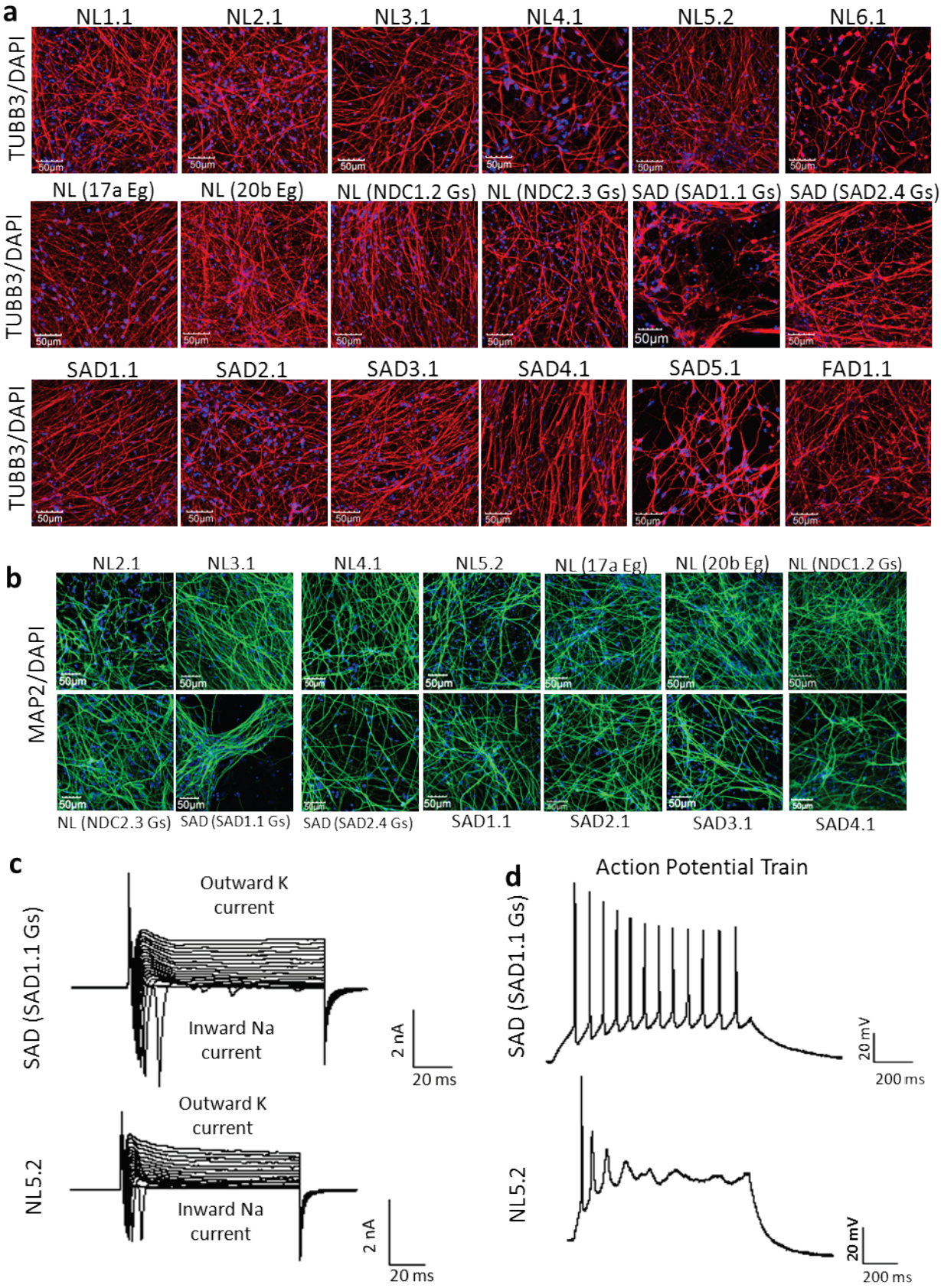

Figure 4.3: Characterization of 6-week Differentiated Neurons. (a) Representative images of 6-week differentiated neurons plated on Matrigel and glass coverslips stained for the neuronal marker β-tubulin III (red) and the glial marker GFAP (green) with DAPI (blue) dye marking cell nuclei. (b) Quantification of cells expressing TUBB3 and GFAP using MetaMorph Multiwavelength Cell Scoring for TUBB3 and cell nuclei and manual counting for GFAP showed increased GFAP+ cells in the SAD neuronal cultures. 5-6 randomized fields per coverslip and two coverslips per line (one plated on polyornithine/laminin and one plated on Matrigel) were quantified, except SAD (SAD1.1 Gs) where only a coverslip coated with Matrigel was quantified . $p = 0.023$ (c) Representative images of 6-week differentiated neurons plated on polyornithine/laminin and glass coverslips stained for the glutamatergic marker VGLUT1(green) and the GABAergic marker GABA (red) with DAPI (blue) marking cell nuclei. (d) Quantification of cells expressing VGLUT1 and GABA using MetaMorph Multiwavelength Cell Scoring for all markers. 5-6 randomized fields per coverslip and one coverslip per included line was quantified. $p = 0.14$ (both VGLUT1 and GABA) (e) Staining of 6-week differentiated neurons plated on polyornithine/laminin and glass coverslips for the neural progenitor marker nestin (green) and intermediate progenitor marker doublecortin (red) with the nuclear DNA dye DAPI (blue).

Figure 4.3: Characterization of 6-week Differentiated Neurons (cont.)

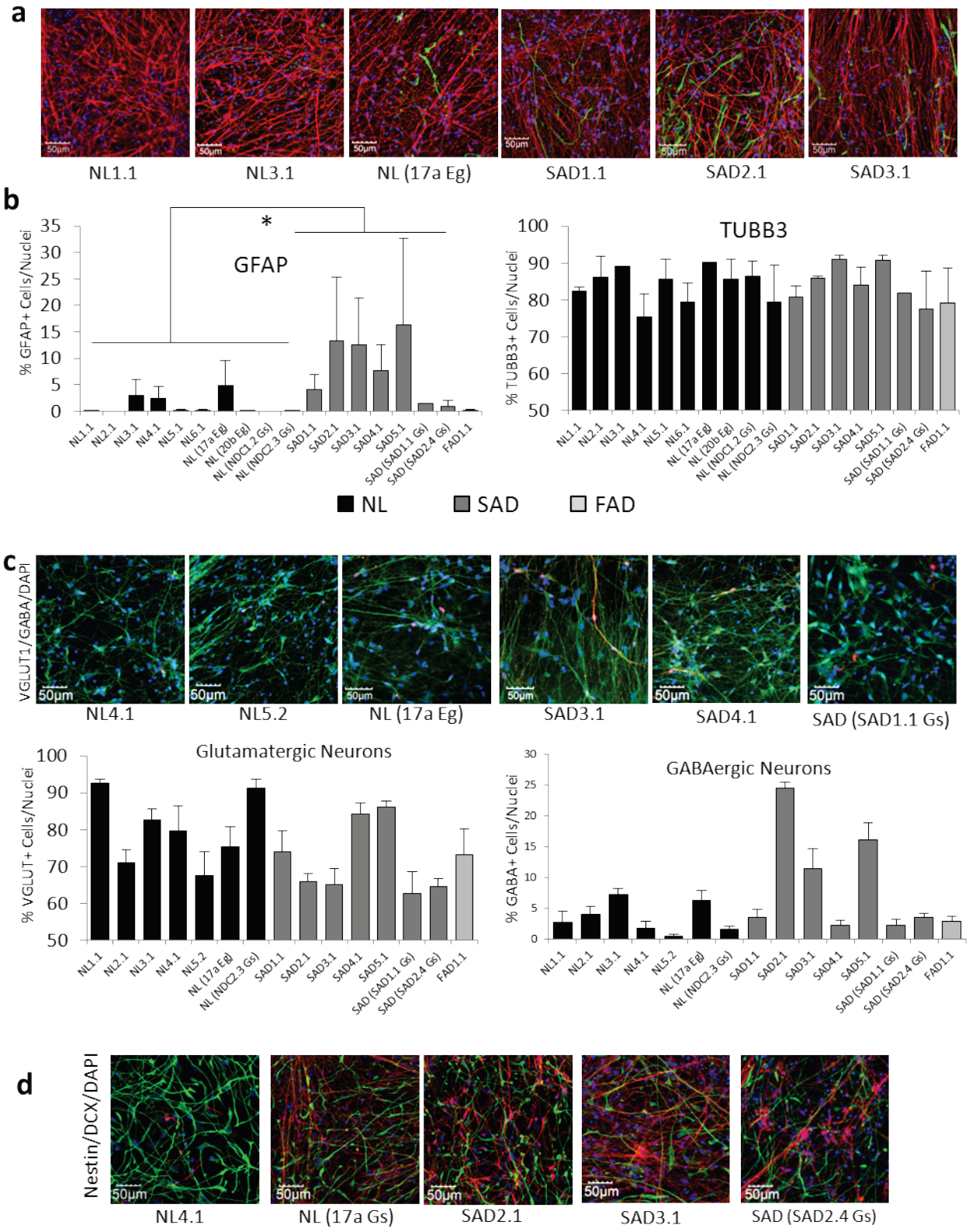

progenitor (Seki et al 2014). However, astrocytes can have distinct morphologies dependent on region and function in the brain, so more markers are needed to fully elucidate the identity of the GFAP-positive cells (Matyash & Kettenmann 2010). Greater than 75% are positive for the neuronal-specific TUBB3 with no difference between the NL and AD lines (Figure 4.3b).

The neurons are a mixture of GABAergic and glutamatergic neurons with the amount of each being variable between lines (Figure 4.3c). In general, greater than 60% of the neurons are positive for the glutamatergic marker VGLUT1, while less than 25% stain for GABA, the neurotransmitter for GABAergic neurons (Figure 4.3d). There is a trend towards increased GABAergic neurons and decreased glutamatergic in the SAD cultures, however it is not significant ($p = 0.14$). A subset of lines was also stained for the more immature marker of neurogenesis, doublecortin, as well as the neural progenitor marker nestin (Figure 4.3d). The 6-week differentiated cultures still have cells that are positive for both markers. The nestin-expressing cells have a different morphology than the NP stage and are bipolar and elongated. This suggests that they may be more mature neural progenitors, such radial glia cells, although work is still lacking to fully elucidate the stages of neural differentiation since it varies in embryonic corticogenesis, each zone of adult neurogenesis, and *in vitro*. In summary, after 6 weeks of differentiation, there is a diverse culture of mostly GABAergic and glutamatergic neurons with some GFAP-expressing cells. The cultures still express the immature markers of doublecortin and nestin, indicating that the cells are still in the process of reaching terminal differentiation. RNA was harvested from these cultures to see if there is a difference in gene expression between the SAD and NL 6-week differentiated neurons.

C. Divergent gene expression in 6-week differentiated SAD neurons

Microarray profiling for 6-week differentiated neurons using the 6 normal and 5 SAD lines derived in our lab was performed on Affymetrix U133 Plus 2.0 arrays with lines derived from one clone per individual (Table 4.2). The gene expression was analyzed as previously described for earlier stages of differentiation. The difference between the SAD and NL 6-week neurons was much more significant than previous stages of differentiation, therefore the more stringent cut-off of $q \leq 0.035$ was used for later analysis, corresponding to a p-value of 0.016. 843 differentially expressed probes met this criterion for significance (Figure 4.4a, Supplementary Table 10).

Correlation analysis for the significant gene list shows intra-group correlation for both the SAD (Pearson correlation coefficient *r* between 0.52 and 0.80) and NL lines ($r = 0.50$-0.74, except NL4.1), except for two outliers: NL5.2 and SAD4.1 (Figure 4.4b). NL5.2 correlated more strongly with the SAD lines ($r = 0.32$-76), while SAD4.1 correlated more weakly with the other SAD lines ($r = 0.16$-0.32).

Enrichment analysis of the differentially expressed genes shows that nervous system development remains one of the most significant gene ontology biological processes enriched differential gene list (Figure 4.4c). Other significant biological processes include regulation of localization and transport, regulation of molecular functions and biological processes, and general system development. The genes of the nervous system development gene ontology group are predominantly up-regulated, with many greater than 5-fold up-regulated in the SAD neurons (Figure 4.4d). This increase in neuronal differentiation gene levels is similar to the pattern seen in the SAD neural progenitors. Analysis using DAVID confirms the enrichment for neuronal-related genes with the cellular compartments of synapse, vesicles, plasma membrane,

Figure 4.4: Gene Expression Profile of Neurons. (a) Heat map of significant genes differentially expressed between SAD and normal 6-week differentiated neurons (derived from one clone per iPS line) with a q-value of less than 0.035. (b) A heat map of Pearson correlation coefficient shows that the gene expression of SAD and NL neurons correlate within their respective groups, but NL5.2 and SAD4.1 are outliers. (c) The ten most significant biological processes evaluated through enrichment analysis in the gene ontology (GO) database using MetaCore. (d) The fold changes of the individual genes for the second most significant gene ontology biological process, nervous system development. (e) The ten most significant annotation clusters using the Database for Annotation, Visualization, and Integrated Discovery (DAVID) in the significant 6-week neuron gene list. BP: biological process, CC: cellular compartment, MF: molecular function.

Figure 4.4: Gene Expression Profile of Neurons (cont.)

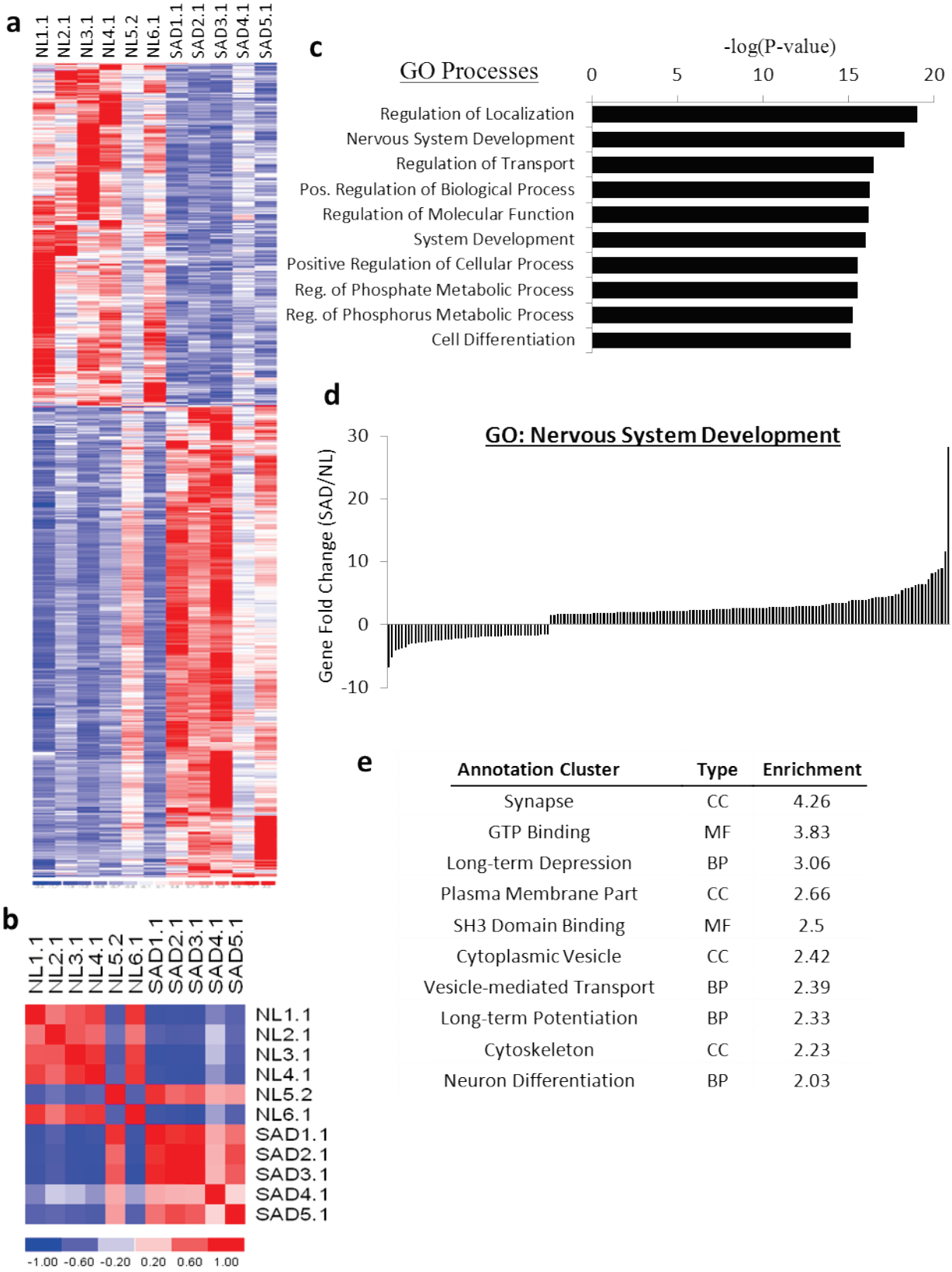

e

Annotation Cluster	Type	Enrichment
Synapse	CC	4.26
GTP Binding	MF	3.83
Long-term Depression	BP	3.06
Plasma Membrane Part	CC	2.66
SH3 Domain Binding	MF	2.5
Cytoplasmic Vesicle	CC	2.42
Vesicle-mediated Transport	BP	2.39
Long-term Potentiation	BP	2.33
Cytoskeleton	CC	2.23
Neuron Differentiation	BP	2.03

and cytoskeleton being among the most enriched, as well as biological processes of long-term depression, vesicle-mediated transport, long-term potentiation, and neuron differentiation (Figure 4.4e). These annotation clusters are associated with the functioning of more mature neurons than seen in the neural progenitors, in which enrichment of processes related to intermediate progenitor function, such as cell motion, neuron projection, and neurogenesis were predominant. Comparison between the two stages of neural differentiation does show some overlap (Figure 4.5a). There are 7 genes that are differentially expressed in all three neuronal lineage microarrays: the 6-week neurons, neural progenitor single clone, and neural progenitor multiple clones. These genes are all up-regulated in the SAD, except for the cannabinoid receptor, which is highly up-regulated in both neural progenitor microarray analyses, but down-regulated in the 6-week neurons (Figure 4.5b). The SAD up-regulated genes include CSRNP3/TAIP2, a cell-death related gene expressed in the brain during development (Yamada et al 2008), LSAMP, a limbic-system associated membrane protein that acts as a cell adhesion molecule in neurite formation and outgrowth (Philips et al 2014), and REEP1 which is specific to neuronal tissues and required for endoplasmic reticulum (ER) network formation and linking to the cytoskeleton (Hurt et al 2014, Philips et al 2014, Yamada et al 2008). STMN2/SCG10 is a microtubule-destabilizing factor involved in neuronal growth during brain development (Sobczak et al 2011), SYT4 (synaptotagmin 4) acts as a postsynaptic calcium sensor which enhances the presynaptic function and is important in scaling synaptic strength in response to network activity (Dean et al 2012, Yoshihara et al 2005), and ZNF503/NOLZ1 is a transcriptional repressor which promotes striatal neurogenesis and increases the number of β-tubulin III and MAP2-positive neurons (Nakamura et al 2008, Urban et al 2010). Clearly, these genes that are up-regulated in both the SAD neural progenitors and neurons are important in neuronal development.

Figure 4.5: Shared Significant Genes Between Neural Progenitors and Neurons

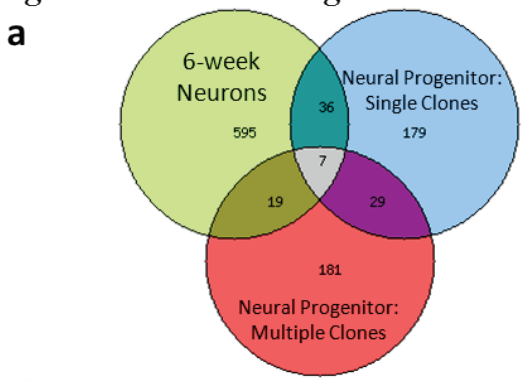

b

Genes Significant in all three Microarray Sets

	Neurons	NPs	Additional NP Clones
CNR1	-2.18	7.30	5.23
CSRNP3	2.79	3.05	1.94
LSAMP	2.63	1.99	2.19
REEP1	4.41	3.29	1.59
STMN2	2.55	9.55	4.38
SYT4	3.43	2.89	2.05
ZNF503	2.46	3.27	2.58

c

Genes Significant in 6-week Neuron and NP (Single Clone) Microarray

	Neurons	NPs	Additional NP Clones
ACSS3	-2.71	-2.67	-1.29
ADM	-3.75	-5.24	-2.56
AFF2	4.62	3.76	1.62
AKR1C1	2.63	1.85	1.07
ASRGL1	1.73	1.93	1.14
BLVRB	-2.46	-2.26	-1.01
CCND2	-2.10	-3.25	-1.53
CNPY1	-4.20	-4.24	-2.21
COL11A1	-9.32	-5.79	-1.02
CTNNA2	2.34	3.27	-1.03
DPH6	-1.87	-1.73	-1.38
DSEL	1.92	-2.09	-1.02
EN2	-5.20	-2.80	-2.22
GFOD1	2.09	-1.75	-1.18
GNPTAB	1.73	-1.43	1.03
HECW2	1.78	-2.32	-1.07
HIST1H2BH	-1.59	1.76	1.03
HOXA2	8.99	7.33	2.31
HOXA3	28.26	11.53	3.00
ITGB8	-2.72	2.12	1.21
KCNC1	2.55	3.69	1.69
LGI1	8.33	6.75	2.35
LOC285812	2.69	-2.12	-1.21
MALT1	-2.09	-1.51	-1.19
NELL1	8.9	3.40	1.53
OLFM1	9.64	2.48	1.05
PLOD2	-1.84	-2.62	1.03
RAB3C	3.38	3.65	1.41
RALYL	3.53	4.13	1.42
SEP6	1.89	2.03	1.19
SERPINI1	5.83	-3.87	-1.37
SHC1	-2.89	-1.76	-1.36
SLC25A43	-3.48	-3.66	-1.03
SLIT3	1.78	2.05	1.54
TENM4	2.98	2.07	1.58
ZCCHC18	3.25	1.99	1.39

d

Genes Significant in 6-week Neuron and NP (Multiple Clones) Microarray

	Neurons	NPs	Additional NP Clones
ARRB1	2.16	-1.21	-1.75
BCAT1	-2.75	1.07	-1.42
CBS	-1.85	-1.06	-1.56
ELAVL4	3.41	3.21	2.21
EPHA3	2.79	1.70	3.90
KCNMA1	8.12	2.55	2.15
KDR	-1.84	-2.73	-4.02
LINC00667	1.79	1.88	1.95
LOC158863	1.65	1.03	1.35
NSG1	3.52	1.78	2.05
OTTHUMG00000160053	1.81	1.07	1.41
RAB30	1.87	-1.05	1.75
RGS8	2.16	1.55	1.34
ROBO2	5.28	1.93	2.97
SCD5	2.17	1.66	1.67
SHMT2	-2.27	-1.16	-1.33
SLC3A2	-2.08	-1.12	-1.45
SNAP25	3.05	1.52	1.98
TGFB2	2.14	2.14	2.66

Figure 4.5: Shared Significant SAD Genes between Neural Progenitors and Neurons. (a) Overlap in the significant gene list between neural progenitors and neurons. (b) The fold changes of the seven genes differentially expressed in all three microarray experiments with average SAD over average NL. If multiple probes were significant for the same gene, the average fold change was taken. (c) The fold changes of the 36 genes differentially expressed between the 6-week neuronal and single clone neural progenitor microarray. (d) The fold changes of the 19 genes differentially expressed between the 6-week neuronal and multiple clone neural progenitor microarray. The fold changes in c and d for the non-significant NP microarrays were derived from the expression values for all probes to the gene even with q-values above 0.15. For all tables, red is up-regulated in SAD, and blue is down-regulated in SAD.

Significant genes that are shared between the 6-weeks neurons and just one of the neural progenitor microarrays contain genes that are both up- and down-regulated in SAD (Figure 4.5c,d). Expression data from the non-significant NP microarray was also included to see if the trend was consistent even if the q-value didn't reach the statistical threshold for significance. Some of the genes that were down-regulated in all three microarray experiments include *ADM* (adrenomedullin), a peptide hormone which plays a role in neural stem cell growth regulation (Martinez-Herrero et al 2012), *CCND2*, a regulator of G1 progression whose mRNA localization affects the self-renewal of neural stem cells (Tsunekawa et al 2012), and *SHC1* which encodes adaptor proteins that are found in neural stem cells, but not differentiated neurons (Conti et al 1997). Other down-regulated genes include *CNPY1* (Canopy1), a positive regulator of FGF signals (Hirate & Okamoto 2006), *EN2* (Engrailed2), a homeobox transcription factor which plays a role in neural patterning and is adjacent to *CNPY1* (Choi et al 2014), and *KDR*, also called *VEGFR2*. Most of the most conserved down-regulated SAD genes through neural differentiation are involved with neural stem cell proliferation and growth factor signaling, which is consistent with the increased neural differentiation phenotype in the SAD lines.

Genes that are up-regulated in SAD cells throughout the neuronal differentiation include the homeobox transcription factors *HOXA2* and *HOXA3*, the potassium channel subunits *KCNC1* and *KCNMA1*, and the surprising *TGFB2*, which is up-regulated despite TGFβ downstream signaling being consistently down-regulated in the SAD lines. Many of the genes that are up-regulated are specific to neurons and the neuronal lineage, including *AFF2/FMR2* which is the gene silenced in fragile X syndrome, *LGI1*, a extracellular matrix protein that may help connect pre- and post-synaptic proteins (Soleman et al 2013), *RALYL* which encodes an RNA-binding protein enriched in the brain (Ji et al 2003), and *TENM4/ODZ4* which is a transmembrane

protein which positively regulates neurite outgrowth (Suzuki et al 2014). Other genes enriched in neurons that are up-regulated in the SAD microarrays include *ELAVL4*/HuD, an RNA-binding gene which is important in hippocampal circuitry and neurite outgrowth (DeBoer et al 2014), *RGS8* which is a brain-specific G-protein regulator (Saitoh et al 1997), and *NSG1* which is a neuron-specific protein involved with receptor recycling (Rengaraj et al 2011). Some of the conserved up-regulated genes are canonical to neuronal pathways, including the *SLIT3*, *ROBO2*, and *EPHA3* of axonal guidance, *RAB3C* in synaptic vesicles, and *SNAP25* of the tSNARE complex which fuses synaptic vesicles to the plasma membrane. Together, the conserved up-regulated genes strongly support an increase in neuronal functions in the SAD neural lineage.

Not all the genes are expressed consistently. *SERPINI1* (neuroserpin) is a regulator of the proteolytic degradation of the ECM during synaptogenesis and is down-regulated in the SAD neural progenitors, but up-regulated in the neurons. *ITGB8* (integrin-β 8) which plays a role in promoting TGFβ activation is up in SAD neural progenitors, but down in neurons. *ARBB1* (β-arrestin 1) regulates the receptor sensitization of GPCR and is down-regulated in SAD neural progenitors and up-regulated in SAD neurons.

D. Neuronal microarray enrichment analysis

Using MetaCore software software to identify interacting proteins that are over-represented in the SAD neural progenitor gene list shows a large number of highly significant interactors (Supplementary Figure 11). Many of the top transcription factors are conserved from earlier stages of differentiation, including CREB1, REST/NRSF, the glucocorticoid receptor, SP1, the androgen receptor, c-Myc, c-Jun, and p53 (Figure 4.6a). There are also some new highly interacting transcription factors, including ATF4, RelA, and NRF2. *ATF4* is induced in response to ER stress or amino acid starvation in a mechanism requiring the kinase

Perk/EIF2AK3, which is down-regulated in the 6-week SAD neurons (Vattem & Wek 2004) and is predicted to be inhibited by Ingenuity Pathway Analysis (Figure 4.6b). *NRF2* is induced by oxidative stress and protects the cells against damage, prevents apoptosis, and promotes cell survival (Kaspar et al 2009). *SMAD3* is induced by TGFβ and is required for the survival of proliferative intermediate progenitor cells in the mouse dentate gyrus (Tapia-Gonzalez et al 2013). All three of those transcription factors are most significant in down-regulated genes, suggesting that their activity is reduced in SAD lines.

The most significant interacting receptors are Synaptotagmin 1, APP, TIE2, and two Dopamine receptors. Synaptotagmin 1 is a calcium sensor which acts in synaptic vesicle docking and at the presynaptic membrane and modulates release probability (Fernandez-Chacon et al 2001). APP is the precursor for the amyloidogenic Aβ, but its endogenous role remains unclear although it has been shown to limit neurite outgrowth and trigger neuronal cell death (Nikolaev et al 2009, Young-Pearse et al 2008). TIE2 is a cell surface receptor that is activated by angiopoietins and is most widely known to act in blood vessel regulation (Fukuhara et al 2009). However, it may also be important in neurogenesis since angiopoeitin-1 increases neural stem cell proliferation and the number of NeuN-positive neurons via Tie2 (Rosa et al 2010). The two most significant kinases are c-Src and GSK3β. Increased levels of active GSK-3β have been shown in Alzheimer's disease brains and in neuronal cultures derived from AD iPS cells (Israel et al 2012, Leroy et al 2007). Plasmin is the most significant interactor of the protease family and it is an activated protein which degrades the extracellular matrix during neuronal cell death as well as cleaving BDNF into an active form during long-term potentiation (Chen & Strickland 1997, Pang et al 2004). The most significant enzyme, EZH2, is a methyltransferase of

Figure 4.6: Analysis of Gene Expression Profile of Neurons

a

Interactions

	Object	P-value	Ratio
Transcription Factors	CREB1	3.56E-14	1.6
	Estrogen Receptor 1	2.09E-12	2.048
	EGR1	6.76E-11	3.049
	REST/NRSF	1.40E-10	3.13
	GCR-alpha	1.81E-09	2.085
	SP1	3.26E-08	1.869
	p53	1.38E-07	1.807
	Androgen receptor	8.89E-07	1.864
	ATF-4	8.94E-07	3.75
	SMAD3	7.73E-06	2.226
	c-Myc	1.00E-05	1.488
	NRF2	1.45E-05	2.995
	RelA	2.72E-05	1.781
	c-Jun	2.74E-05	1.792

Category	Object	P-value	Ratio
Receptor	Synaptotagmin I	4.43E-09	6.316
Receptor	APP	9.37E-08	3.343
Receptor	TIE2	1.38E-05	7.106
Receptor	Dopamine D3 receptor	1.66E-05	8.29
Receptor	Dopamine D2 receptor	1.88E-05	4.777
Kinase	c-Src	1.61E-05	2.077
Kinase	GSK3 beta	2.74E-05	2.409
Protease	Plasmin	2.19E-06	5.391
Protease	BACE1	1.10E-05	3.287
Enzyme	EZH2	8.98E-06	2.042

b

	Upstream Regulator	Type	Activation	P-value
Activated	BCL2	transporter	2.491	1.83E-04
	RBL1	transcription regulator	2.426	5.59E-03
	miR-34a-5p	mature microRNA	2.412	5.11E-03
	Catalase	enzyme	2.392	1.70E-03
	APOE	transporter	2.349	5.18E-03
	NELFB	other	2.236	3.00E-05
	TRIB3	kinase	2.219	7.50E-04
	ANXA2	other	2.213	1.39E-03
	ERBB4	kinase	2.156	1.35E-03
	RB1	transcription regulator	2.155	3.67E-03
	Interferon Gamma	cytokine	-3.055	1.23E-04
Inhibited	ATF4	transcription regulator	-3.056	9.08E-07
	ERK	group	-3.078	3.27E-03
	PDGF BB	complex	-3.185	7.26E-07
	Tumor Necrosis Factor	cytokine	-3.244	1.28E-03
	EGF	growth factor	-3.322	2.93E-07
	FGF2	growth factor	-3.329	3.71E-04
	hydrogen peroxide	endogenous chemical	-3.84	6.46E-05
	F2/Thrombin	peptidase	-3.874	1.76E-05
	Interleukin 1B	cytokine	-4.001	1.58E-03

Figure 4.6: Analysis of the Gene Expression Profile of Neurons. (a) Table of the most significantly connected transcription factors, receptors, kinases, proteases, and enzymes using MetaCore Interactome analysis. The ratio refers to the number of interaction partners in the gene list divided by the expected number of interactions in a random gene list of equal size. P-value had to be less than $3x10^{-5}$ to be included. (b) Table of the ten most significant activated and inhibited upstream regulators calculated by Ingenuity Pathway Analysis (IPA). Upstream regulators with a p-value greater than .025 were excluded.

histone H3K27 which is expressed in dividing neural stem cells and neurons and regulates neurogenesis (Zhang et al 2014).

Ingenuity Pathway Analysis (IPA) of upstream regulators, which calculates the predicted activation or inhibition of the regulators, predicts a strong activation of proteins involved with cell cycle arrest, apoptosis, and neuronal functions (Figure 4.6b). BCL2, RBL1, NELFB, miR-34, and RB1 have all been implicated in the inhibition of cell cycle progression and/or apoptosis. The most strongly activated upstream regulator is BCL2, a regulator of mitochondrial membrane permeabilization which inhibits cell death in developing neurons during normal and ischemic stress conditions (Sasaki et al 2006). It also acts independently of its apoptotic effects to inhibit cell cycle entry (Huang et al 1997). RBL1/p107 is a transcriptional regulator that inhibits cell cycle progression. It limits the precursor pool in both the developing and adult brain by promoting neural progenitor commitment to a neuronal fate (Vanderluit et al 2007). RB1 is related to RBL1 and intrinsic to the regulatory circuit controlling G_1 to S transition, and regulates the interplay between apoptosis, differentiation, and cell cycle progression (Herwig & Strauss 1997). Ectopic expression of the microRNA miR-34a can induce cell cycle arrest, apoptosis, and cell differentiation and has been shown to modulate dendritic spine morphology during neuronal development (Agostini et al 2011, Chen & Hu 2012). NELF-B/COBRA-1 is a negative regulator of transcription which inhibits cell cycle progression (Sun & Li 2010).

The predicted activated proteins related to neuronal activity include APOE, ANXA2, and ERBB4. The activity of APOE, the previously discussed strongest genetic risk factor for sporadic Alzheimer's disease, is predicted to be up-regulated by Ingenuity Pathway Analysis. ANXA2 or annexin A2 regulates actin cytoskeletal rearrangement and cell adhesion, possibly mediating cell migration (Rescher et al 2008). It also plays a key role of the activation of

plasmin by localizing the plasminogen precursor with its activator: tissue plasminogen activator (tPA) (Hajjar & Krishnan 1999). Finally, ERBB4 is a receptor for neuregulin which acts in the nervous system in the release of neurotransmitters by interneurons (Wen et al 2010).

Upstream regulators predicted to be inhibited by Ingenuity Pathway Analysis are predominantly growth factor and cytokine pathways as well as those related to oxidative stress response (Figure 4.6b). Predicted down-regulated growth factor and cytokine upstream regulators include Interleukin-1B, FGF2/bFGF, EGF, TNF, PDGF, and IFN gamma. Although cytokines are traditionally thought to act predominantly in the immune system, they also play a role in regulating neuronal differentiation, although the exact effects remain unclear. Interleukin 1B has been shown to inhibit the proliferation of NP cells and increase apoptosis, as well as impair hippocampal neurogenesis (Wang et al 2007b, Zhang et al 2013a). Interferon gamma (IFNγ) has shown mixed results in regulating neural differentiation with one paper showing enhanced neurogenesis *in vivo* in the absence of IFNγ and while another found that it was a potent inducer of neurogenesis *in vitro* (Leipzig et al 2010, Li et al 2010). Tumor necrosis factor (TNF) increases the proliferation of neural stem cells while decreasing neurogenesis (Takei & Laskey 2008, Widera et al 2006). The receptor of another cytokine, LIF, is significantly down-regulated in the SAD 6-week neurons (Supplementary Figure 10). LIF increases proliferation of neural progenitors, but inhibits terminal differentiation (Moon et al 2002).

Growth factor signaling is also predicted to be inhibited, including most significantly FGF2, EGF, and PDGF, but also TGFβ, IGF1, and VEGF (Supplementary Table 13). Many of these growth factor act through ERK kinases, whose activity are also predicted to be down-regulated by IPA. The effects of these growth factors on neurogenesis are complicated. FGF2 is important for the proliferation of neural progenitors, but inhibits terminal neuronal differentiation

(Chen et al 2007). Expression of both FGF2 and the FGFR are down-regulated in the SAD 6-week neurons (Supplementary Table 10). PDGF signaling is similar: it acts as a mitogen and survival factor for immature neurons, but prevents further differentiation into a post-mitotic state (Enarsson et al 2002). EGF also induces proliferation of neural progenitors, although possible effects on later differentiation have not been fully elucidated (Kitchens et al 1994).

Hydrogen peroxide signaling is also predicted to be highly inhibited by IPA analysis. Endogenous hydrogen peroxide is produced during aerobic metabolism and can both cause oxidative stress to the cell as well as play an important role in redox signaling, acting as a second messenger in several growth-factor-induced signaling cascades (Sies 2014). In fact, neural progenitors have a comparatively high level of reactive oxygen species and low levels of hydrogen peroxide treatment increase multipotent potential and progenitor proliferation (Le Belle et al 2011). These ROS levels are decreased in cells that express ASCL1, but enriched in the cells that express doublecortin. The decreased response to oxidative regulation is supported by the predicted inhibition of ATF4, which is induced by ER stress and the transcriptional down-regulation of the related ATF3 in the microarray of the 6-week SAD neurons. The predicted activation of TRIB3 is also consistent with this decrease in oxidative signaling since it inhibits stress response through a negative feedback loop with the stress-responsive ATF4 (Jousse et al 2007).

F2/thrombin is the active form of a serine protease that is most commonly associated with blood coagulation, however it is also expressed in the nervous system where it has many diverse functions involving growth, maintenance, and morphological changes (Rohatgi et al 2004). It stimulates the proliferation and nestin-expression of radial glia cells while also inhibiting neural differentiation (Jalink & Moolenaar 1992, Wautier et al 2007). Thrombin is also known to

induce the release of growth factors in other cell types, such as smooth muscle cells where after binding to the PAR-1 receptor, thrombin induces secretion of PDGF, FGF2, VEGF, TGFβ, and other growth factors (Bassus et al 2001, Stouffer & Runge 1998). Therefore, the predicted inhibition of its activity is consistent with decreased growth factor signaling.

To further explore the patterns of differential regulation between the SAD and NL 6-week differentiated neurons, the most highly up- and down-regulated genes were analyzed separately. A table of the top down-regulated genes shows down-regulation of genes involved with growth factor response, the extracellular matrix, and protease-related genes (Figure 4.7a). VGLL3 is a transcriptional cofactor and its inhibition decreases proliferation rate and migration properties in soft tissue sarcomas (Helias-Rodzewicz et al 2010). BCAT1 is an enzyme which initiates the catabolism of branched-chain amino acids and promotes proliferation in gliomas (Tonjes et al 2013). CYR61/CCN1 is an extracellular-matrix localized protein that is induced by growth factors and plays diverse roles in cell survival, apoptosis, cell adhesion, and cell proliferation (Lau 2011).

TFPI2 (tissue factor pathway inhibitor) is a matrix-associated inhibitor of serine proteases including trypsin, chymotrypsin, and plasmin. It is suppressed by CD24, which was highly up-regulated in the SAD neural progenitors. Cathepsin C is a serine protease which also acts as a central coordinator for the activation of many other serine proteases, especially in immune cells (Methot et al 2007). PLAT, the tissue plasminogen activator (tPA), is a serine protease that activates plasmin, another serine protease that modulates the extracellular matrix and catalyzes the degradation of laminin during excitotoxic cell death of hippocampal neurons (Chen & Strickland 1997). Its inhibitor, Neuroserpin/SERPINI1 is up-regulated in the 6-week SAD neurons, unlike the neural progenitors, where it is down-regulated. PTX3 is induced by IL-1β

Figure 4.7: Up- and Down-Regulated Genes of SAD Neurons

a

Most Down-regulated Genes in SAD

Gene	Protein Description	Average FC	Probes
COL11A1	**Collagen 11 alpha 1**	**-9.32**	**3/3**
VGLL3	Transcription Cofactor Vestigial-Like Protein 3	-7.20	2/2
TFPI2	Tissue Factor Pathway Inhibitor	-5.79	2/2
ALMS1-IT1	lncRNA	-5.54	1/1
ALPK2	Alpha-Kinase 2	-5.36	1/1
EN2	**Engrailed homeobox 2**	**-5.20**	**1/1**
PLAT	Tissue Plasminogen Activator	-5.02	1/1
CYR61	Cysteine-rich, cell adhesion	-4.99	2/2
PTX3	Pentaxin 3, Induced By IL-1, Tumor Necrosisβ	-4.63	1/1
SGCG	Sarcoglycan gamma	-4.53	1/1
CNPY1	**Canopy FGF Signaling Receptor**	**-4.20**	**1/1**
CTSC	Cathepsin C	-3.73	2/4
ATF3	Activating transcription factor 3 (cAMP-dependent)	-3.43	2/3
SFRP4	Secreted frizzled-related protein 4	-4.04	2/4
LINC00152	lncRNA	-4.08	1/2
PMP22	Peripheral Myelin Protein 22	-3.91	1/1
BCAT1	**Branched Chain Amino-Acid Transaminase 1**	**-2.75**	**4/4**

b

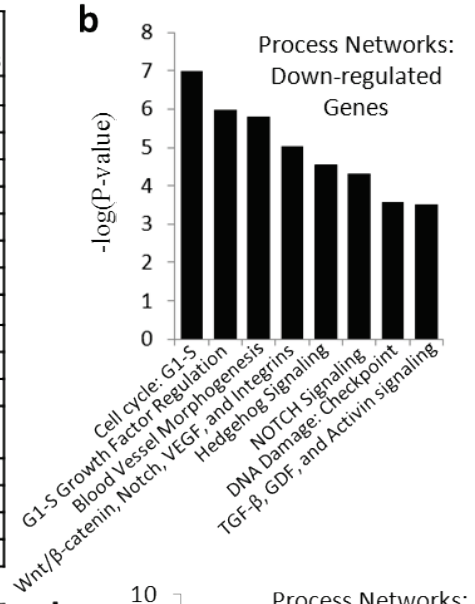

c

Most Up-regulated Genes in SAD

Gene	Protein Description	Average FC	Probes
SPON1	Spondin-1/F-spondin	34.36	3/5
HOXA3	**Homeobox A3**	**28.26**	**1/2**
TMEM200A	transmembrane protein 200A	9.96	1/1
OLFM1	**Olfactomedin 1/noelin**	**9.64**	**2/3**
RIT2	Ras-Like Protein Expressed In Neurons	9.54	1/1
HOXA2	**Homeobox A2**	**8.99**	**1/1**
NELL1	**NEL-Like Protein 1**	**8.90**	**1/2**
OTTHUMG00000175814	lncRNA	8.44	1/1
LGI1	**Leucine-rich, glioma inactivated (neuronal)**	**8.33**	**1/1**
NPY1R	Neuropeptide Y Receptor 1	6.43	1/1
SERPINI1	**Serpin peptidase inhibitor**	**5.83**	**1/1**
ROBO2	**Roundabout, Axon Guidance Receptor 2**	**5.28**	**3/3**
RGS4	Regulator Of G-Protein Signaling	4.93	2/3
SYT17	Synaptotagmin XVII	4.69	1/2
RAB3B	Ras-Related brain antigen	4.08	3/5
SLC8A1	Sodium/Calcium Exchanger	3.28	4/11

d

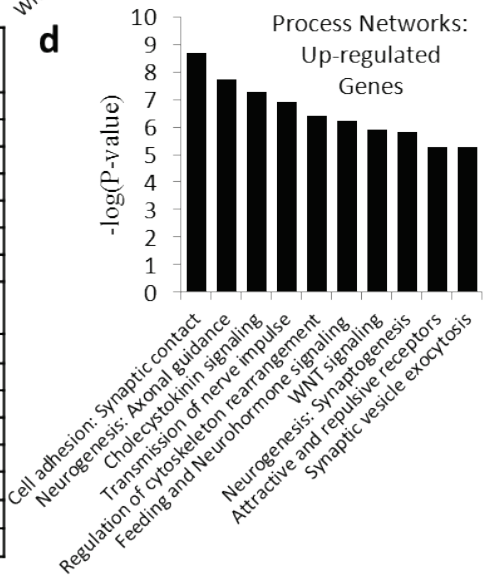

Figure 4.7: Up- and Down-regulated Genes of SAD Neurons. (a,c) Tables of the most strongly up-regulated and down-regulated genes in the SAD 6-week neurons. The fold change (FC) represents the average of all probes for the specific gene, while probes refers to the number of probes that reach the significance threshold for NP expression out of all the probes annotated for that gene on the Affymetrix U133 Plus 2.0 array. The tables consist of genes with at least one probe showing less than 3.8-fold decrease or greater than 5.8-fold increase respectively as well as at least 50% of probes for that gene in the significant gene list. Bold indicates a significant gene that is shared with an earlier stage of differentiation. (b,d) Enrichment analysis using MetaCore software for process networks that are significantly enriched in the up- and down-regulated genes.

and is important for the deposition of extracellular matrix in response to ischemic stress (Rodriguez-Grande et al 2014). Together, these genes show that there is a strong enrichment for genes that modulate the extracellular matrix and especially serine proteases, although the predicted effects of these gene changes are contradictory.

Enrichment analysis of all the down-regulated genes in 6-week SAD neurons using MetaCore does not pick up the enrichment for extracellular matrix modulating serine proteases, but it does show significant down-regulation of G_1-S transition and growth factor signaling (Figure 4.7c). The down-regulation of these processes is consistent with a neuron differentiating to become post-mitotic.

A table of the most robust up-regulated genes in 6-week differentiated neurons is enriched for transcription factors, neuronal genes, guanosine nucleotide-binding proteins (G proteins), and modulators of the extracellular matrix (Figure 4.7b). Many of them are also localized to the extracellular matrix, including the neuronal-enriched OLFM1/Noelin-1, LGI-1/Epitempin, NELL-1, and SPON1. SPON1/F-spondin is the most strongly up-regulated gene in the 6-week differentiated neurons. It is an extracellular matrix protein that is cleaved by plasmin to create two functional fragments that both act to direct axon growth (Tzarfaty-Majar et al 2001, Zisman et al 2007).

Many of the other most significant up-regulated genes are specific to neuronal function. RIT2 is a neuronal-specific GTPase (Zhang et al 2013b). The neuropeptide Y-receptor is a neuronally enriched GPCR and RGS4 is a GTPase-activating protein. One of RGS4 functions is the inhibition of PAR-1, a thrombin receptor (Ghil et al 2014). Normal functioning of this signaling pathway would lead to the up-regulation of thrombospondin/THBS1, an extracellular matrix protein that is down-regulated in the SAD 6-week neurons (McLaughlin et al 2005).

ROBO2 is an axon guidance receptor, SYT17 is a member of the synaptotagmin family that acts in regulation of neurotransmitter release, and RAB3B is a small G-protein which regulates exocytosis in neuronal and other secretory cells (Nishimura et al 2008). SLC8A1/NCX1 is a sodium/calcium exchanger localized to the mitochondrial membrane that may play an important role in regulating postsynaptic calcium transients and protecting the cell from calcium overload and death (Gobbi et al 2007). Together, most significant up-regulated genes in 6-week SAD neurons strongly support an increase in neuronal gene expression, G proteins, and changes in extracellular matrix proteins.

Enrichment analysis of all the SAD up-regulated genes in 6-week neurons shows an increase in neuronal genes involved with synaptic contact and axonal guidance, as well as cytoskeleton rearrangement and Wnt signaling, which was also enriched in the down-regulated genes (Figure 4.7d).

E. SAD 6-week neuron gene expression differences verified through qRT-PCR

To confirm the differences in gene expression identified in the 6-week differentiated neurons derived from iPS lines derived in the Yankner lab in a larger cohort, mRNA from the neurons for several key genes was measured using quantitative real-time PCR (qRT-PCR) (Figure 4.8). RNA samples were included from one clone per individual for all 18 individuals (10 normal, 7 SAD, and 1 FAD).

Most of the microarray findings are confirmed with the increased number of individuals (Figure 4.8). Cyclin D2 (*CCND2)* was down-regulated 2.1-fold in the 6-week differentiated neuron subset and is confirmed to be down-regulated 1.7-fold in the entire cohort. CCND2 is a positive regulator of G_1 cell cycle progression and has been shown to be essential for the expansion of the intermediate progenitor cell pool *in vivo* (Glickstein et al 2009). Furthermore,

Figure 4.8: mRNA of Differentially Expressed Genes in 6-week Neurons

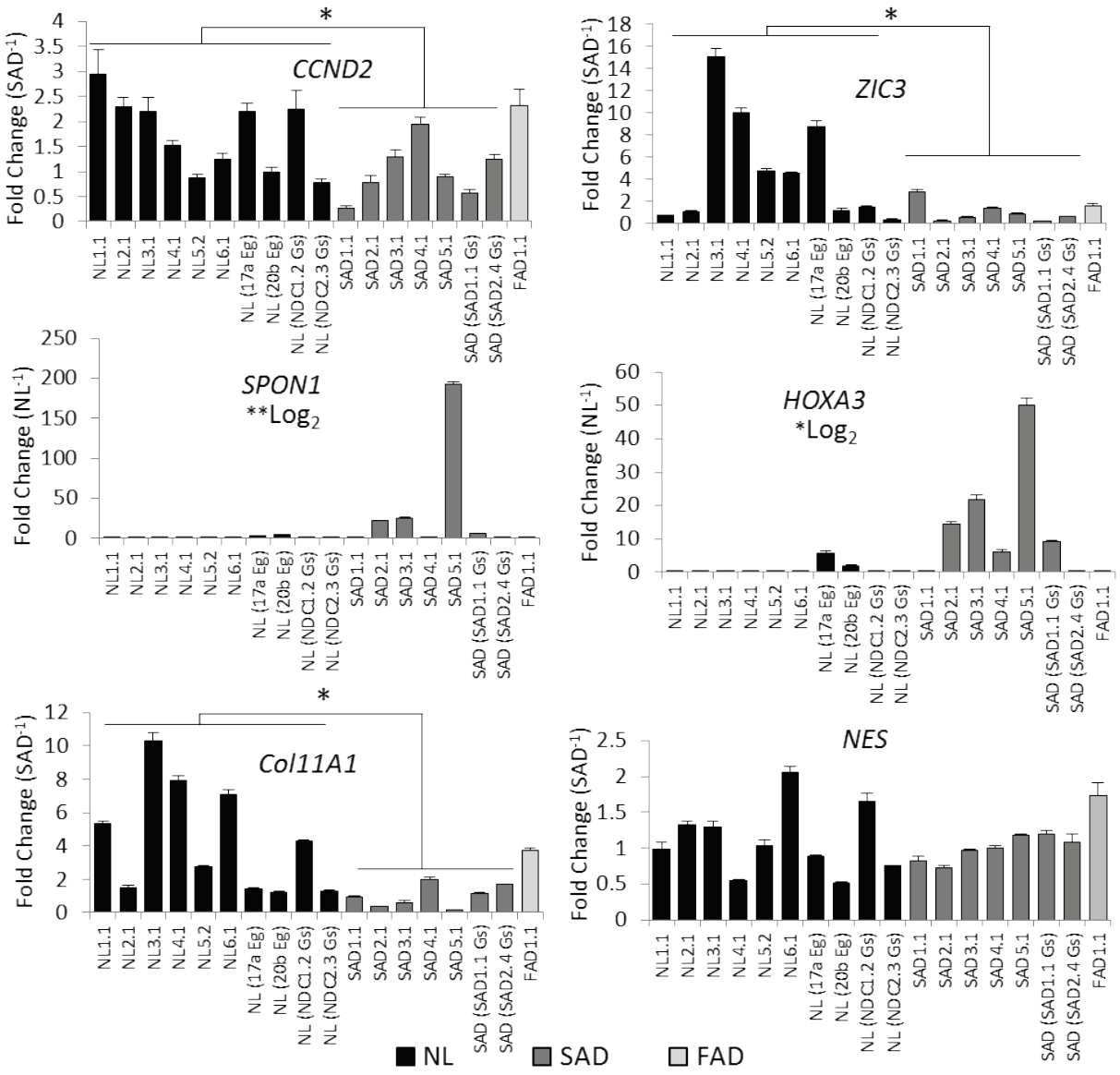

Figure 4.8: mRNA of Differentially Expressed Genes in 6-week Neurons. Representative quantitative RT-PCR shows differential expression of *CCND2 (*cyclin D2*)*, *ZIC3, SPON1* (f-spondin), *HOXA3*, and *Col11A1* but not *NES* (nestin). mRNA values were calculated using the relative standard curve method and normalized to *GAPDH*. Fold change was calculated relative to the average normalized expression of all the SAD lines except for *SPON1* and *HOXA3*, where it is relative to the average normalized expression of all the NL lines. Errors are the standard error of the mean for three wells. *CCND2*: p=0.035, Log_2 p=0.06; *ZIC3:* p = 0.040, Log_2 p=0.024, *SPON1*: p = 0.23, Log_2 p=0.002; *SPON1*: p = 0.084, Log_2 p=0.033; *COL11A1*: p = 0.010 Log_2 p=0.004; *NES:* p=0.54, Log_2 p=0.83; *p<0.05, **p<0.01

uneven inheritance of cyclin D2 protein in neural progenitors supports asymmetric cell division in which a self-renewing daughter cell inherits more cyclin D2 (Tsunekawa et al 2012). Depletion of cyclin D2 results in terminal neuronal differentiation. ZIC3 is a Gli transcription factor which is required for the maintenance of pluripotency in ES cells and is also essential in neural progenitors in maintaining an undifferentiated state by inhibiting neuronal differentiation (Inoue et al 2007, Lim et al 2007). It is down-regulated 6.89-fold in the microarray neurons and 4.81-fold in the expanded qRT-PCR cohort. Together, these markers support a loss of neural progenitor proliferation capabilities in the SAD 6-week neurons.

The two strongest up-regulated genes as well as the most robust down-regulated genes were confirmed in the expanded cohort. *SPON1* and *HOXA3* were up-regulated 34- and 28-fold respectively in the SAD 6-week neuronal microarray, but qRT-PCR confirms that it is a few lines which are highly up-regulated for each gene. *SPON1* is increased 193-fold over the average of the NL lines in SAD5.1, and also noticeable up-regulated in SAD2.1, SAD3.1, and SAD (SAD1.1 Gs). *HOXA3* is up-regulated 50-fold in SAD5.1 with a similar expression profile in the other lines, although it is also increased in SAD4.1. Due to the many orders of magnitude separating the gene expression in the different lines, the difference between these lines is not statistically significant using a student's *t*-test. However, by converting the expression data to $\log_2$ scale, the differences in magnitude are attenuated and both *SPON1* and *HOXA3* are significant in the SAD lines ($p = 0.002$, $p = 0.033$). *COL11A1* is the most robust down-regulated gene, with a decrease of 9.3-fold in the microarray analysis. It is also down-regulated in the expanded cohort with an average fold change of -4.32-fold.

Not all the significant genes from the 6-week neuronal microarray were confirmed using qRT-PCR in the expanded cohort, indicating that there is heterogeneity in the SAD and NL lines.

Nestin (*NES*) was down-regulated in the SAD neuronal microarray, but not using qRT-PCR and *SNAP25* was up-regulated in the microarray, but not differentially expressed using qRT-PCR (only *NES* data shown). Together, these results support that the gene expression differences identified in neuronal cells differentiated from our iPS lines are relevant to an expanded cohort, however some expression changes are more robust and conserved. FAD1.1, with a L286V PSEN1 mutation, appears to have a gene expression profile more closely aligned with the NL differentiated neurons.

F. Functional Differences between SAD and NL Differentiating Neurons

The gene expression differences at 6 weeks of neuronal differentiation strongly support a difference in neuronal function. However, the fact that all lines are capable of forming neurons that generate action potentials (APs) suggests that the difference may be in timeline rather than terminal differentiation capabilities. Therefore, the expression of the early neuronal marker doublecortin was measured in a subset of lines (4 SAD and 4 NL from iPS cells derived from both our laboratory and the Goldstein laboratory) from neural progenitors to 9 weeks of differentiation. Doublecortin is expressed transiently during neuronal development, becoming up-regulated as progenitor cells commit to the neuronal fate and down-regulated at terminal differentiation (Brown et al 2003). During our differentiation protocol, levels of doublecortin increase drastically from the neural progenitor stage of differentiation (0 weeks) to 6 weeks of neuronal differentiation before starting to decline at 9 weeks (Figure 4.9a).

The fold change of *DCX* expression between the AD and NL cells is greatest at 0 weeks (Figure 4.9b). As the culture starts to differentiate into more mature neurons, the doublecortin expression becomes equal between the SAD and NL lines, especially at the 6 and 9 week time

point. Therefore, the NL lines are still capable of expressing differentiation genes like the SAD lines, but just in a delayed timeline.

Since many of the most strongly down-regulated genes affect cell cycle progression and differential expression of some of those genes is conserved from neural progenitors, I tested the proliferation rate of both neural progenitors and neurons. SAD neural progenitors showed a significant decrease in proliferation after 48 hours (Figure 4.9c). This may be due to either the neural progenitors being in a slightly more quiescent state, possibly due to increased resistance to the mitogenic LIF or bFGF in the media, or it could be due to the larger proportion of differentiating cells dividing more slowly. The differentiating neurons also showed a significant difference in proliferation 7 days into differentiation with more NL cells, but this significant difference disappears as differentiation continues (Figure 4.9d). This analysis is complicated by the fact that cell death occurs during the normal differentiation process and in these cultures, thus proliferation isn't the only mechanism affecting cell number. The cells were plated on Matrigel to increase adherence, but this also increases proliferation over the polyornithine/laminin coating on which gene expression results were obtained, complicating interpretation as well. Interestingly, both the SAD and NL lines have a strong outlier in both the neural progenitor and neuronal proliferation rates (SAD1.1 and NL1.1). When those two lines are removed from the analyses, the difference in cell number between the two groups becomes highly significant ($p = 0.034$ at 3 days, 0.015 at 7 days, 0.025 at 14 days, and 0.058 at 21 days), implying that this difference in proliferation is characteristic of some, but not all SAD lines, and is conserved through neuronal differentiation in those lines.

Gene expression differences at 6 weeks indicated an increase in gene expression in many genes involved with synapse formation and function in the SAD lines. To see if there is a

Figure 4.9: Neuronal Differentiation and Proliferation

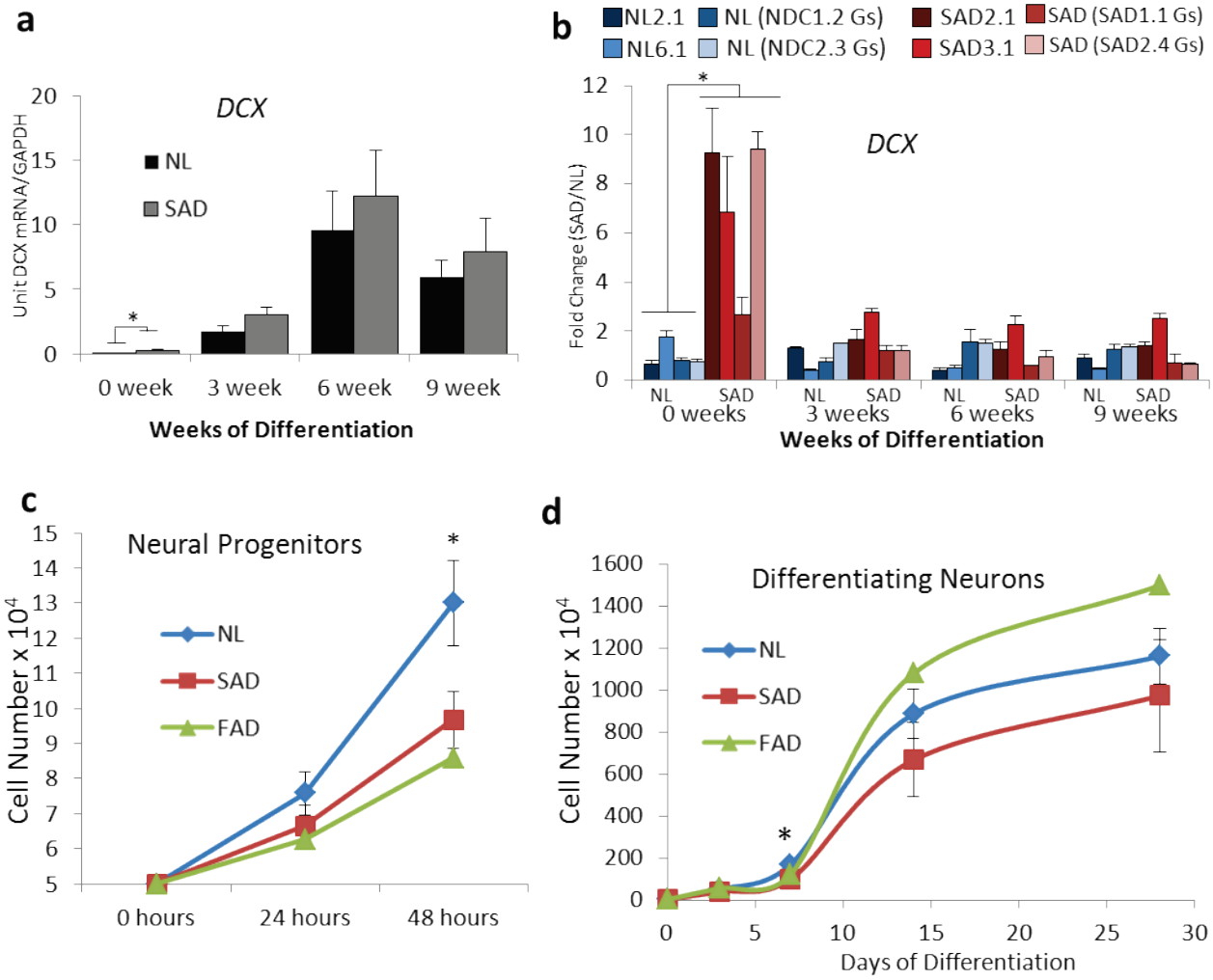

Figure 4.9: Neuronal Differentiation and Proliferation. (a) Quantitative RT-PCR for the expression of doublecortin during the differentiation process. Average of four normal (NL2.1, NL6.1, NL (NDC1.2 Gs) and NL (NDC2.3 Gs)) and 4 SAD lines (SAD2.1, SAD3.1, SAD (SAD1.1 Gs), and SAD (SAD2.4 Gs)) with 2-4 separate differentiations averaged per time point (except 6 week SAD1.1., where n = 1). RNA was quantified using a relative standard curve and normalized to GAPDH expression. $p = 0.029$ at 0 weeks, 0.17 at 3 weeks, 0.59 at 6 weeks, and 0.53 at 9 weeks. (b) Doublecortin expression data converted to fold change using the average of all four normal lines at each time point. (c) Cell number of neural progenitors 24 and 48 hours after plating with the average of 3 experiments of the lines summarized in Table 4.2. $p = 0.043$ (48 hours) (d) Cell number of differentiating neurons at 3, 7, 14, and 28 days. Averages from two wells from 15 lines (Table 4.2). *$p<0.05$

difference in the formation of synapses, the puncta of the pre-synaptic marker synapsin-1 were quantified at 6 weeks of differentiation (Figure 4.10 a,b). At this stage of differentiation there are fewer than two synapsin-1-localized synapses per nuclei, however the SAD lines have significantly more synapses than the NL lines ($p = 0.018$). Cells expressing MAP2, which was used to mark the dendritic neuronal processes, did not show a difference between the AD and NL lines. Synaptic levels of FAD1.1 aligned more with the SAD than the NL neurons.

The gene expression profile of the 6-week differentiated neurons also had an increase in the expression of ion channel genes, indicating that there may be differences in the excitability of the SAD and NL neurons. All the lines are capable of forming induced action potentials, but the time of differentiation may vary between the SAD and NL lines. The ability to form action potentials was first measured at 4.5 weeks of differentiation. At this time of differentiation, half of the SAD lines tested formed action potentials, but none of the NL lines (Figure 4.10c). After 7.5 weeks, all of the SAD lines tested were able to generate action potentials, but none of the NL lines or FAD1.1. At 10 weeks, all tested lines were able to form action potentials, both SAD and NL, and by 15 weeks all lines had formed induced action potentials. The time of differentiation until first measurement of action potentials was significantly lower in SAD ($p = 0.009$) (Figure 4.10d), however an important caveat is that not all the lines were tested at the earlier time points and therefore it may not be an accurate representation of the time at which they are first capable of forming APs. Together, these results support a model whereas the SAD neurons have an accelerated differentiation into functional neurons compared to NL neurons. Based on their ability to form action potentials, it seems possible that the NL neurons do reach an equal level of functioning after sufficient time, but more testing is needed to confirm that hypothesis.

Figure 4.10: Differences in Synapses and Generation of Action Potentials

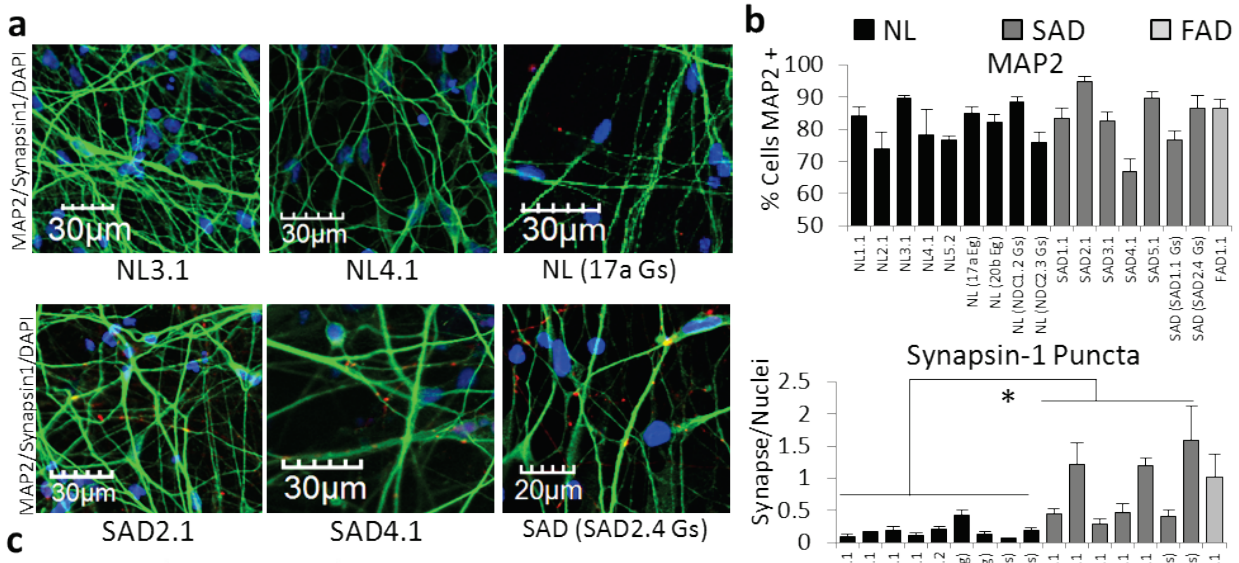

4.5 weeks

Line	AP?
NL2.1	No
NL2.2	No
NL3.1	No
SAD2.1	No
SAD3.1	Yes
SAD4.1	No
SAD5.1	Yes

7.5 weeks

Line	AP?
NL2.1	No
NL2.2	No
NL3.1	No
SAD1.1	Yes
SAD2.1	Yes
SAD3.1	Yes
FAD1.1	No

10 weeks

Line	AP?
NL2.1	Yes
NL3.1	Yes
NL (20b Eg)	Yes
NL (NDC2.3 Gs)	Yes
NL (17a Eg)	Yes
SAD2.1	Yes
SAD3.1	Yes
SAD4.1	Yes
SAD5.1	Yes
SAD5.1	Yes
FAD1.1	Yes

11 weeks

Line	AP?
NL4.1	Yes
NL (NDC2.3 Gs)	Yes
SAD (SAD2.4 Gs)	Yes

15 weeks

Line	APs?
NL1.1	Yes
NL5.2	Yes
NL6.1	Yes

Figure 4.10: Differences in Synapses and Generation of Action Potentials.

(a) Representative images of presynaptic synapsin-1-localized puncta (red) with neuronal processes marked with MAP2 (green) and nuclei with DAPI stain (blue) after 6 weeks of differentiation on polyornithine/laminin. (b) Quantification using MetaMorph unbiased counting for the percentage of cells positive for the marker of neuronal processes MAP2 per total nuclei and number of synapsin-1+ puncta per total nuclei after 6 weeks of differentiation. $p = 0.018$. (c,d) Time of differentiation until induced action potentials (AP) form (Yellow). All data includes the earliest time at which action potentials were measured and any earlier times that action potentials were not detected for the line. All cells were cultured on polyornithine and laminin in the standard protocol except for at 15 weeks differentiation, which were cultured using the Banker method. $p = 0.009$ *$p<0.05$, **$p<0.01$

Conclusions and Discussion

After optimization of the differentiation conditions, a culture of predominantly MAP2+ and TUBB3+ neurons was generated that was able to form functional neurons with sodium and potassium channels capable of forming action potentials. After 6 weeks of differentiation, these cells were predominantly glutamatergic neurons with a small proportion of GFAP-expressing glia and GABAergic neurons. These populations were enriched in the SAD lines, particularly for GFAP. This supports that there is a difference in the differentiation potential and mechanism between the SAD and NL lines. At this stage of differentiation, the neurons are still maturing with cells still expressing doublecortin, a marker of immature neurons, and nestin, a marker of neural progenitors.

Gene expression profiling showed a robust difference between the SAD and NL differentiating cells in a subset of the lines. These differences were enriched for up-regulated genes related to neuronal differentiation, but unlike in the neural progenitors where many of the strongest up-regulated genes were related to cellular migration and axon guidance, the 6-week neurons are enriched for genes related to synapse function and ion channels that could play a role in excitability. This suggests that there continues to be a difference in differentiation timeline between the SAD and NL individuals, which was supported by an increase in synapse number in the SAD lines which was significant for all lines. The SAD and NL lines may also have a different timeline for action potential generation, with SAD lines able to form action potentials earlier than any NL lines tested. However, it is unclear if this difference in neuronal function is just a modulation of development or if there are differences in the functioning of the mature neurons. In support of the first model, all lines tested are able to generate action potentials and the gene expression of the early neuronal marker *DCX* does become equivalent as differentiation

proceeds. However, more study at later points of differentiation is necessary to ascertain if there are any differences in mature neuronal functions.

The down-regulated genes in the SAD neurons show enrichment in genes that regulate cell cycle progression and growth factor regulation. This could correlate with the verified difference in neuronal differentiation, however it could also be pathological to AD. Although growth factors have been extensively studied during the earlier stages of neural patterning and maintenance of the neural progenitor pool, it is less clear what the role of each growth factor may be during the maturation of a neuron. For example, TGFβ signaling is predicted to be down-regulated using Ingenuity Pathway Analysis for expression of downstream targets, however in the microarray analysis TGFβ2 expression is up-regulated in the SAD lines. Furthermore, TGFβ2 has conflicting effects on neuronal precursors dependent on the extracellular milieu (Kane et al 1996). In the presence of serum, it increases progenitor proliferation, while in the absence, it inhibits proliferation. Clearly, the effect of growth factor signaling in neuronal differentiation is complicated and it is difficult to ascertain if any changes in the expression seen in AD neurons are pathological or consistent with normal differentiation.

The decrease in genes promoting cell cycle progression is consistent with enhanced neuronal differentiation. Cell cycle control also plays an important role in apoptotic regulation in the central nervous system with loss of trophic support during development leading to increases in cyclin D and cell death (Freeman et al 1994). During the later highly neurodegenerative stages of Alzheimer's disease, cell cycle genes are up-regulated, unlike the changes we observed in the differentiating neurons (Liu & Greene 2001, Nagy et al 1997). Stress-response genes are also down-regulated in the SAD neurons, including *ATF3* which is induced by oxidative stress and *GADD45A* and *GADD45B* which are induced by DNA damage.

Together, these changes represent a gene expression profile consistent with less cellular stress and cell death, however it is unclear if the cells actually have less stress or are just less responsive.

The FAD1.1 line continues to defy classification. Its gene expression of the selected genes in qRT-PCR more closely resembles the NL lines, however it shows an increase in syanpsin-1-localized puncta at 6 weeks consistent with the SAD lines. This suggests that it may be differentiating more efficiently than the NL lines, however the mechanism may be different than the SAD lines. More lines are needed to test that hypothesis.

Contributions

Rat glia for glial co-culture were isolated by Yoshiho Ikeuchi in the laboratory of Dr. Azad Bonni. Electrophysiology measurements were performed by Susan Su, Sukhee Cho, Jinsoo Seo, and Jun Wang in the laboratory of Dr. Li-Huei Tsai.

Chapter 5: Alzheimer's disease in the culture dish

Abstract

The three pathological hallmarks of Alzheimer's disease in the human brain are amyloid plaques consisting mainly of Aβ, neurofibrillary tangles of predominantly hyperphosphorylated tau protein, and loss of neurons. To test if the SAD lines have increased proclivity for these processes, each was examined in the SAD and NL progenitors and neurons. The SAD neural progenitors have increased production of Aβ40, but the SAD neurons have no significant increase in Aβ40 or Aβ42 production. Both the neural progenitors and neurons show a significant up-regulation of *MAPT* mRNA levels. The neural progenitors have an increase in tau protein levels, but not levels of phosphorylated tau, while the 6-week neurons have increased phosphorylated tau levels, but not total tau. To test whether there is difference in susceptibility to stress, the neural progenitors were treated with oxidative and genotoxic stresses, but there was no decreased cell survival in the SAD lines. SAD gene expression differences seen at 6 weeks differentiation were examined more closely for their association with AD pathology and AD in the human brain. The SAD gene expression differences seen at 6 weeks are enriched for proteins that interact with APP, MAPT, APOE, and other proteins associated with the onset of Alzheimer's disease as well as having an expression profile with some intriguing similarities to the gene changes seen in the human prefrontal cortex during Alzheimer's disease.

Introduction

Now that the differentiated neuronal cells have been characterized *in vitro,* the next question is whether these differences between SAD and NL lines may lead to any of the pathological changes seen in the human brain during Alzheimer's disease. Ever since the

familial mutations were identified as increasing Aβ production, and more specifically increasing the relative production of Aβ42:Aβ40, this difference became the leading hypothesis for the development of Alzheimer's disease (Hardy & Selkoe 2002). The amyloid hypothesis posits that increased Aβ42 production and accumulation causes synaptic and neuritic injury, resulting in oxidative injury, formation of neurofibrillary tangles, and cell death probably due to the toxic nature of the Aβ42 oligomers. In support of this hypothesis, the increased ratio of Aβ42:Aβ40 in *PSEN1* mutations probed in culture correlates with decreasing age of onset (Duering et al 2005). However, despite the strong genetic and molecular evidence for the role of Aβ42 in the development of familial Alzheimer's disease, the data in sporadic AD are less clear.

Although Aβ levels are unquestionably increased in the SAD brain, any modulations of the Aβ42:Aβ40 ratio are less obvious. Aβ levels measured in post-mortem brain tissue shows increased insoluble Aβ42/40 ratio in patients with *PSEN1* mutations, but not SAD patients or patients with an APP mutation (Hellstrom-Lindahl et al 2009). Furthermore, siRNA knockdowns of the genes identified as risk factors for the development of Alzheimer's disease did not affect the Aβ42:Aβ40 ratio in HeLa cells expressing APP with the Swedish mutation, however addition of the familial *PSEN* mutations increased the ratio (Bali et al 2012). Two recent drug trials targeting Aβ in sporadic AD using bapineuzumab and solanezumab failed to produce productive results, suggesting that other mechanisms may be important in the development of sporadic AD, although there could be other factors that contributed to the drug's failure (Callaway 2012).

Neuronal cells from sporadic Alzheimer's disease patients *in vitro* have shown mixed results. Isarel et al. (2012) was unable to measure Aβ42 levels due to the low number of cells, but observing increased Aβ40 in one sporadic AD line, but not the other. Kondo et al (2013)

observed increased accumulation of intracellular Aβ in one of the sporadic patients but no difference in soluble Aβ40 or Aβ42 production in the SAD lines, unlike an APP mutant line. Together, these results suggest that modulations of Aβ42 and Aβ40 production are important for the development of familial AD, especially with *PSEN1* mutations, but whether there are any changes in sporadic AD remains unclear.

In Alzheimer's disease, the brain also forms tangles of hyperphosphorylated and aggregated tau protein. The severity of these tangles during AD is the most highly correlated disease pathology with cognitive decline (Arriagada et al 1992). However, since mutations in *MAPT*, the gene which encodes the tau protein, cause frontal temporal lobe dementia and not Alzheimer's disease, it is hypothesized that these tangles are an effect of Alzheimer's disease and not the cause. Tau is thought to play an important role in the eventual induction of neuronal cell death during neurodegeneration since tau deletion in mice expressing mutant *APP* and *PSEN1* reduces neuronal and synaptic loss (Leroy et al 2012). Israel et al (2012) observed increased phosphorylated tau in proportion to total tau in one of the SAD patient lines, but not the other.

Loss of neurons and synapses in the brain is the third hallmark of the Alzheimer's disease brain, especially in the entorhinal cortex, dentate gyrus, and hippocampus with 64% loss of neurons in Layer II of the entorhinal cortex in mild cognitive impairment when the cognitive deficits of Alzheimer's disease are first becoming apparent (Kordower et al 2001). There are many hypotheses for the mechanism by which cell death is induced in Alzheimer's disease, including mitochondrial dysfunction, excitotoxicity, oxidative stress, and intracellular calcium dynamics however it is unknown if the neurons of sporadic Alzheimer's patients are more susceptible to stress or just undergo greater stress to induce cell death. Therefore, we tested the

neural progenitor cells for increased apoptotic response to oxidative and genotoxic stress to examine if there is increased intrinsic susceptibility to cell death.

Based on our observation of increased neuronal differentiation in the SAD neurons, we wonder if these pathologies could result from aberrant activation of a developmental pathway. There is evidence that the important proteins in the pathogenesis of Alzheimer's disease may also play an important role in neuronal development. APP is the precursor for the amyloidogenic Aβ, but its endogenous role remains unclear although it has been shown to limit neurite outgrowth and trigger neuronal cell death (Nikolaev et al 2009, Young-Pearse et al 2008). Stable overexpression of APP in hESCs causes rapid differentiation along the neuronal lineage to induce expression nestin and β-tubulin III even in the presence of normal ES media through the actions of an N-terminal secreted form of APP (sAPPβ) which is released by the β-secrestase (Freude et al 2011). Clearly, APP can modulate neuronal differentiation in many ways that have yet to be fully elucidated.

Tau phosphorylation also may play a role in neuronal development. Tau is highly phosphorylated in fetal neurons at sites specific to development which decrease with age (Brion et al 1994, Yu et al 2009a). The same developmentally-associated phosphorylation sites are also seen phosphorylated in the pathological tau of Alzheimer's disease. Levels of tau phosphorylation are also quite high in areas of adult neurogenesis, with the hyperphosphorylated tau colocalizing with doublecortin and possibly playing an important role in neuronal migration (Fuster-Matanzo et al 2009). This early neuronal tau phosphorylation may be important in axonogenesis, since tau is differentially expressed along a growing axon where it is highly phosphorylated in the cell body of maturing neurons (about 80% of studied

sites) but not at the growth cone, where only 20% of those sites are phosphorylated (Mandell & Banker 1996).

Thus the pathological proteins of Alzheimer's disease may also affect neuronal development, suggesting that there it could be disruption of the neuronal differentiation process that leads to the development of Alzheimer's disease in the human brain. By comparing the differentially expressed genes from our differentiating neurons to both the genes associated with the onset of Alzheimer's disease and the gene expression changes seen in the AD brain, we may gain insight into the dysfunction that leads to the development of sporadic Alzheimer's disease.

Materials and Methods

Aβ ELISA: Levels of Aβ40 and Aβ42 were quantified in media conditioned for 5 days on either the neural progenitors or neuronal culture using their respective ELISA kits according to the manufacturer's guidelines (Life Technologies). Two dilutions were made for each sample and Aβ levels were compared to a standard curve specific to each experiment. The Aβ levels were normalized to the total protein levels in the culture, harvested immediately after conditioned media harvest and quantified using a D_C protein assay kit (Bio-Rad).

Quantitative RT-PCR and Primers: qRT-PCR was performed as described in Chapter 3. All neurons were differentiated on polyornithine/laminin coated polystyrene tissue culture plates. The below new primers were used.

Primer Target	Forward Sequence	Reverse Sequence
MAPT	TGGCGGAGGAAATAAAAA	GACACCACTGGCGACTTG

Western blotting: Western blotting was performed as described in Chapter 3. The following additional antibodies were used.

Target	Host	Source	Catalogue #	Dilution
APP	Rabbit	Life Technologies	36-6900	1:1000
Actin	Rabbit	Sigma	A2066	1:5000
Total Tau (Tau-5)	Mouse	Life Technologies	AHB0042	1:500
Phospho-Tau (Thr231)	Rabbit	Millipore	AB9668	1:1000
Phospho-Tau (Thr205)	Rabbit	MBL International	AT-5016	1:1000

Cell Viability: Cell viability was measured using the CellTiter 96 Aqueous One Solution Cell Proliferation Assay (Promega) according to the manufacturer's guidelines after treatment with camptothecin, etoposide, or hydrogen peroxide with ferric chloride to induce cell death in confluent neural progenitor cultures in 96-well plates. In this assay, the MTS (3-(4,5-dimethylthiazol-2-yl)-5-(3-carboxymethoxyphenyl)-2-(4-sulfophenyl)-2H-tetrazolium) reagent is converted into a colorimetric formazan product by living cells. The MTS reagent was incubated for 2 hours with fresh NP media in the cells after treatment for 5 or 24 hours. The plates were then mixed on an orbital shaker to evenly distribute the colorimetric product before measuring the product by absorbance at 490 nm. All treatments were compared to untreated controls of the same cell line. At least 4 wells were averaged for every line at each time point and treatment.

Results

A. Generation of Aβ in neural progenitors and neurons

Levels of Aβ40 and Aβ42 were measured in both neural progenitors and neurons. Aβ40 levels were significantly increased in the SAD lines ($p = 0.041$), but Aβ42 levels were below the

accurate detection limits of the ELISA (Figure 5.1a). This difference is not due solely to an increase in APP protein level, since the levels are not significantly different between the SAD and NL lines (Figure 5.1b). However, the SAD line with the highest Aβ40 generation also has the highest APP protein levels (SAD3.1), indicating that this could partially explain the increased Aβ40, at least in that line.

Aβ40 and Aβ42 are not significantly different in 5-week differentiated neurons, although SAD3.1 remains the highest producer of Aβ40 (Figure 5.1c). Interestingly, the most consistent result in the 5-week neurons is a decreased ratio of Aβ42:Aβ40 in the SAD neurons ($p = 0.003$) (Figure 5.1d). FAD1.1 is an important control because the highest ratio of Aβ42:Aβ40 is seen in this line, as has been previously shown for the *PSEN1* L286V mutation (Citron et al 1997). APP protein levels are not significantly different between the NL and SAD neurons, although SAD3.1 continues to have the highest APP levels, possibly indicating a pathogenic method of APP expression regulation.

Figure 5.1: Generation of Aβ. (a) Average Aβ40 generation for two different neural progenitor cultures was measured using ELISAs with media conditioned for 5 days. The Aβ40 production was normalized to total protein in the well quantified using D_C protein assay kit. $p = 0.041$. Aβ42 levels were below accurate detection limits for the neural progenitor culture. (b) APP protein levels in neural progenitors quantified through western blotting are not different between SAD and NL. Average of two separate protein harvests, each independently converted to fold change over the average of the NL lines and normalized to GAPDH protein levels. $p = 0.18$. (c) Average fold change of Aβ40 and Aβ42 generation for three different 5-week neural differentiation cultures was measured using ELISAs with media conditioned for 5 days. Cells were cultured on polyornithine/laminin on polystyrene tissue culture plates. Fold change was calculated relative to the average normalized expression of all the NL lines for each differentiation set. Not all the lines were measured at each time point ($n = 3$ except NL1.1, NL6.1, NL (NDC2.3 Gs), SAD (SAD2.4 Gs) where $n = 1$ and NL (17a Eg), SAD3.1, SAD5.1 where $n = 2$). There was no significant difference between the SAD and NL Aβ generation levels at 5 weeks of differentiation (Aβ40: $p = 0.52$; Aβ42: $p = 0.99$). (d) Average ratio of Aβ42:Aβ40 in the 5-week differentiated neural progenitor cultures with the same number of samples as in (c), except NL6.1 which was an outlier. $p = 0.003$ (e) APP protein levels in 6-week differentiated neurons quantified through western blotting are not different between SAD and NL. Combination of two separate protein harvests, each independently converted to fold change over the average of the NL lines and normalized to GAPDH protein levels. Duplicated samples were averaged (NL2.1, NL3.1, NL5.2, SAD1.1, SAD2.1, and SAD3.1). $p = 0.14$. All errors are the standard error of the mean. $^*p<0.05$, $^{**}p<0.01$

Figure 5.1: Generation of Aβ (cont.)

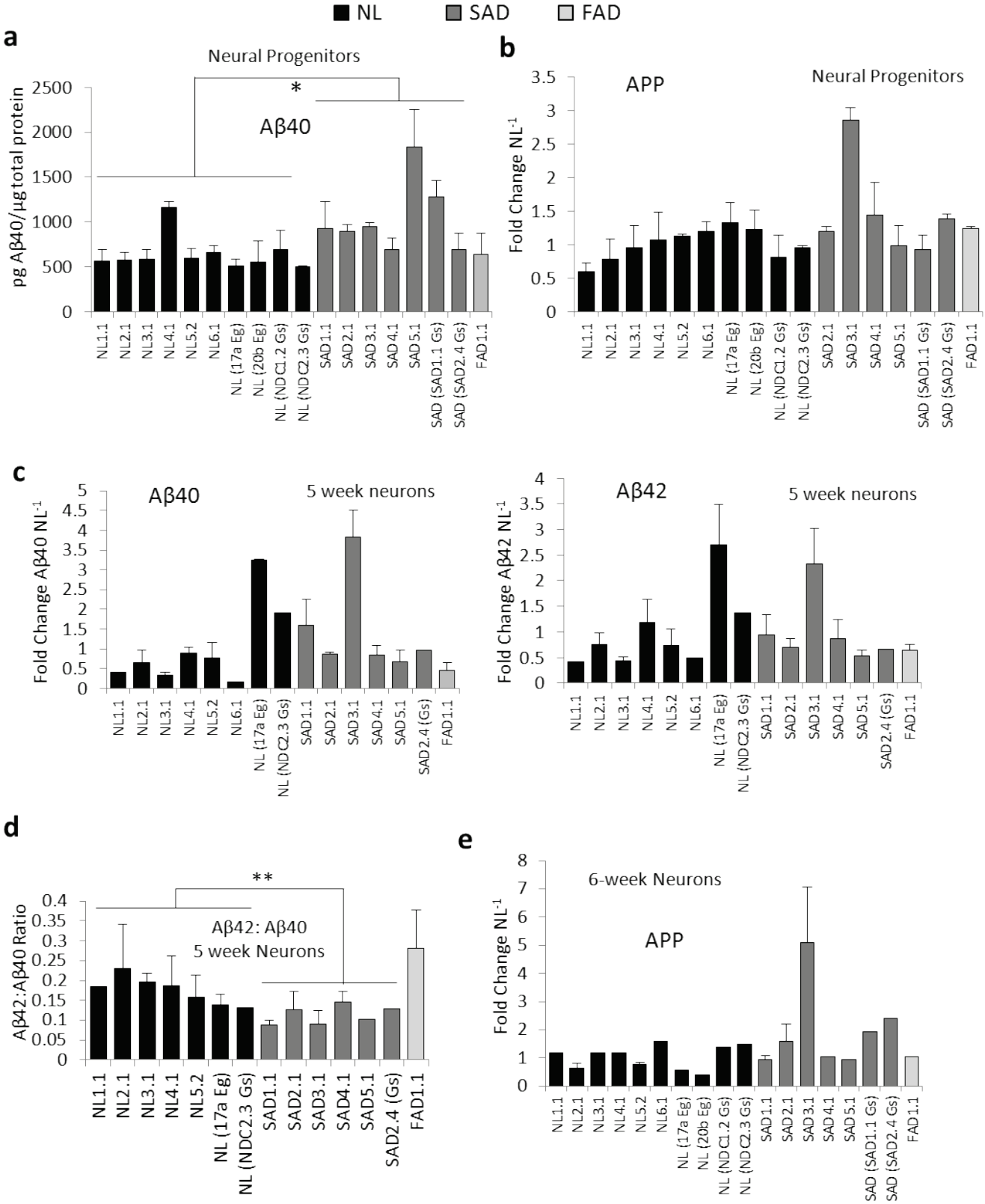

B. Tau in neural progenitors and neurons

MAPT, the gene which encodes the tau gene, was one of the strongest hits in the 6-week neuronal microarray with 4 probes showing an average 3.7-fold increase in *MAPT* expression in the SAD lines (Supplementary Table 10). Therefore, *MAPT* expression levels were measured at both the neural progenitor and 6-week neuronal stage. There was a significant increase in *MAPT* expression in the SAD patient lines even at the neural progenitor stage with both the single clones and multiple clones ($p = 0.048$ and $p = 0.0001$, respectively) (Figure 5.2a,b). The difference at the 6-week neurons was less robust although overall expression levels were highly increased. Although the lines that were analyzed by microarray showed a significant increase in *MAPT* expression in the SAD lines, extending the cohort minimized this differences since NL (17a Eg), NL (20b Eg), and NL (NDC2.3 Gs) all had levels of *MAPT* expression similar to the SAD lines (Figure 5.2c). Since the difference in *MAPT* expression spans many orders of magnitude, the significance of the difference following $\log_2$ transformation shows a significant increase in SAD *MAPT* expression ($p = 0.04$).

Both tau overall protein levels as well as phosphorylation levels at a few important residues were quantified in neural progenitors and neurons using western blotting. Tau is a complicated protein with extensive alternative splicing and over 80 possible phosphorylation sites (Wang et al 2013). In these blots, proteins from 45-75 kDa are shown, corresponding to the adult isoforms of the tau protein (Buee et al 2000). Tau protein levels in neural progenitors are quite low, however a significant increase in total tau expression is seen in the SAD lines ($p = 0.002$) (Figure 5.3a,b). This difference is not seen in blots for antibodies specific for two different phosphorylated tau residues: threonine 231 and threonine 205 (Figure 5.3c-f). Phosphorylation at both Thr231 and Thr205 mediates the assembly of tau filaments which are

Figure 5.2: *MAPT* Expression in Neural Progenitors and Neurons

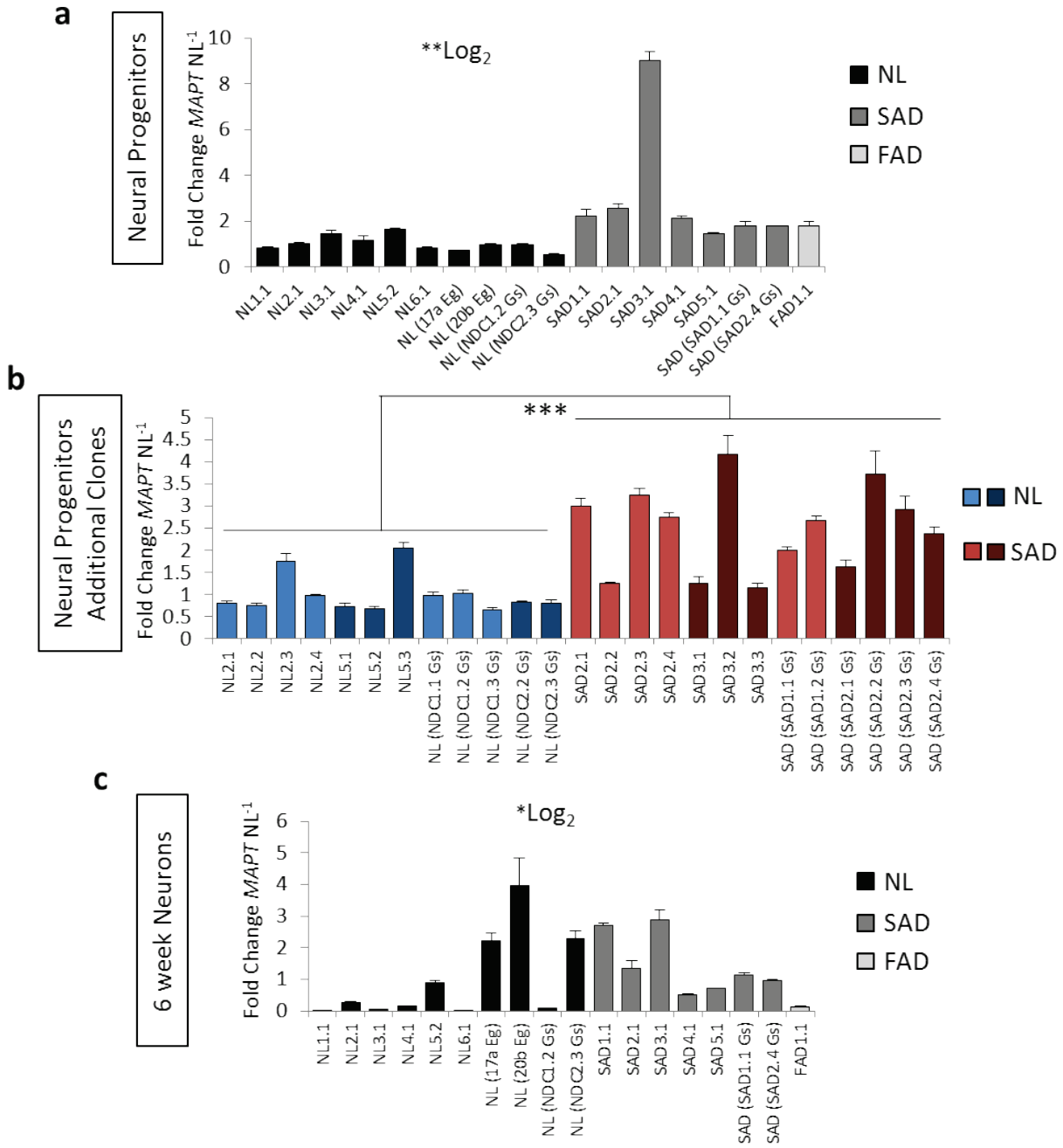

Figure 5.2: *MAPT* Expression in Neural Progenitors and Neurons. (a) Representative *MAPT* expression measured through qRT-PCR in neural progenitors (single clones). p=0.098, Log_2 p=0.005 (b) Representative *MAPT* expression in additional clones from 8 neural progenitors lines shows highly significant increase in tau gene expression. p=0.0001, Log_2 p=$1x10^{-5}$ (c) Representative *MAPT* expression in 6 week differentiated neurons measured through qRT-PCR. p=0.41, Log_2 p=0.04 *p<0.05, ***p<0.001

Figure 5.3: Tau and Phospho-tau in Neural Progenitors

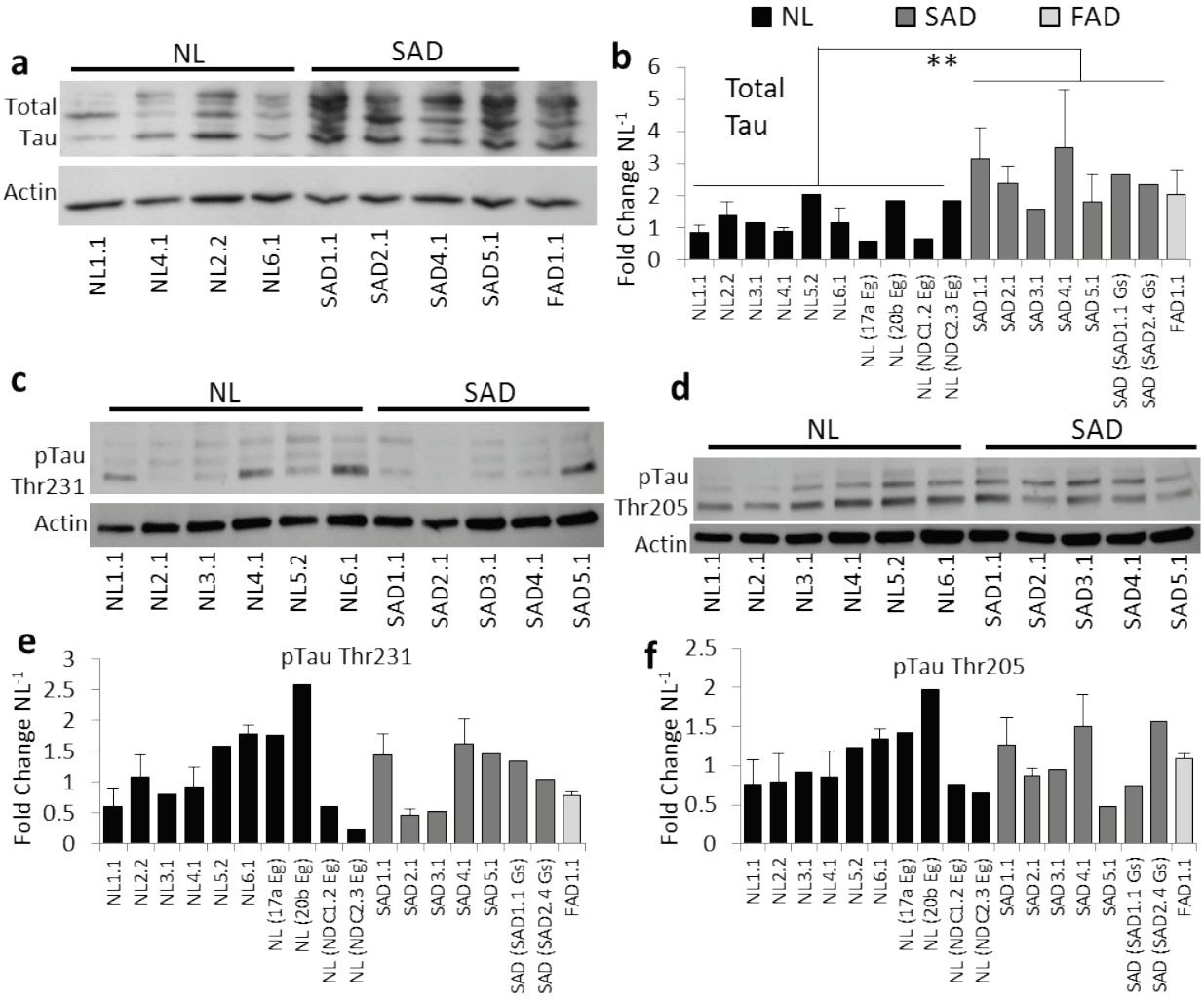

Figure 5.3: Tau and Phospho-Tau in SAD Neural Progenitors. (a,c,d) Representative blots of total tau (Tau-5), tau phosphorylated at residue threonine 231 (pTau Thr231), and tau phosphorylated at threonine 205 (pTau Thr205) in neural progenitors. (b) Total tau protein levels quantified through western blotting are increased in SAD. Average of four separate protein harvests, each independently converted to fold change over the average of the NL lines and normalized to actin protein levels. n = 1 except for NL1.1, NL4.1, NL6.1, SAD1.1, SAD2.1, SAD4.1, and FAD1.1 (n = 4) and NL2.2 (n = 3) and SAD5.1 (n = 2). $p = 0.002$ (e) pTau Thr231 protein levels quantified through western blotting are not changed in SAD neural progenitors. Quantified the same as (b) except SAD5.1 (n = 1). $p = 0.82$. (f) pTau Thr205 levels quantified through western blotting are not changed in SAD neural progenitors. Quantified the same as (e). $p = 0.93$. $^{**}p<0.01$

the major component of neurofibrillary tangles in the AD brain (Rankin et al 2005, Wang et al 2007a). SAD neural progenitors had no change in the levels of phosphorylated tau.

In the 6-week differentiated neurons, there is a trend towards increased total tau protein levels, but it is not statistically significant ($p = 0.085$) (Figure 5.4a,b). Levels of phosphorylated Thr231 tau are significantly increased in the SAD neurons ($p = 0.015$) (Figure 5.4 c,e), although levels of phospho-Thr205 are not increased significantly ($p = 0.17$) (Figure 5.4d,f). Overall, total tau protein and mRNA levels are significantly increased in SAD lines, especially in the neural progenitors, but these differences lessen during differentiation. This is similar to the pattern of other neuronal marker such as *DCX*. However, differences in phosphorylated tau levels at Thr231 are only significant in the differentiating neurons, suggesting that this process may be specific to the SAD neurons.

Figure 5.4: Tau and Phospho-tau in 6-week Differentiated Neurons

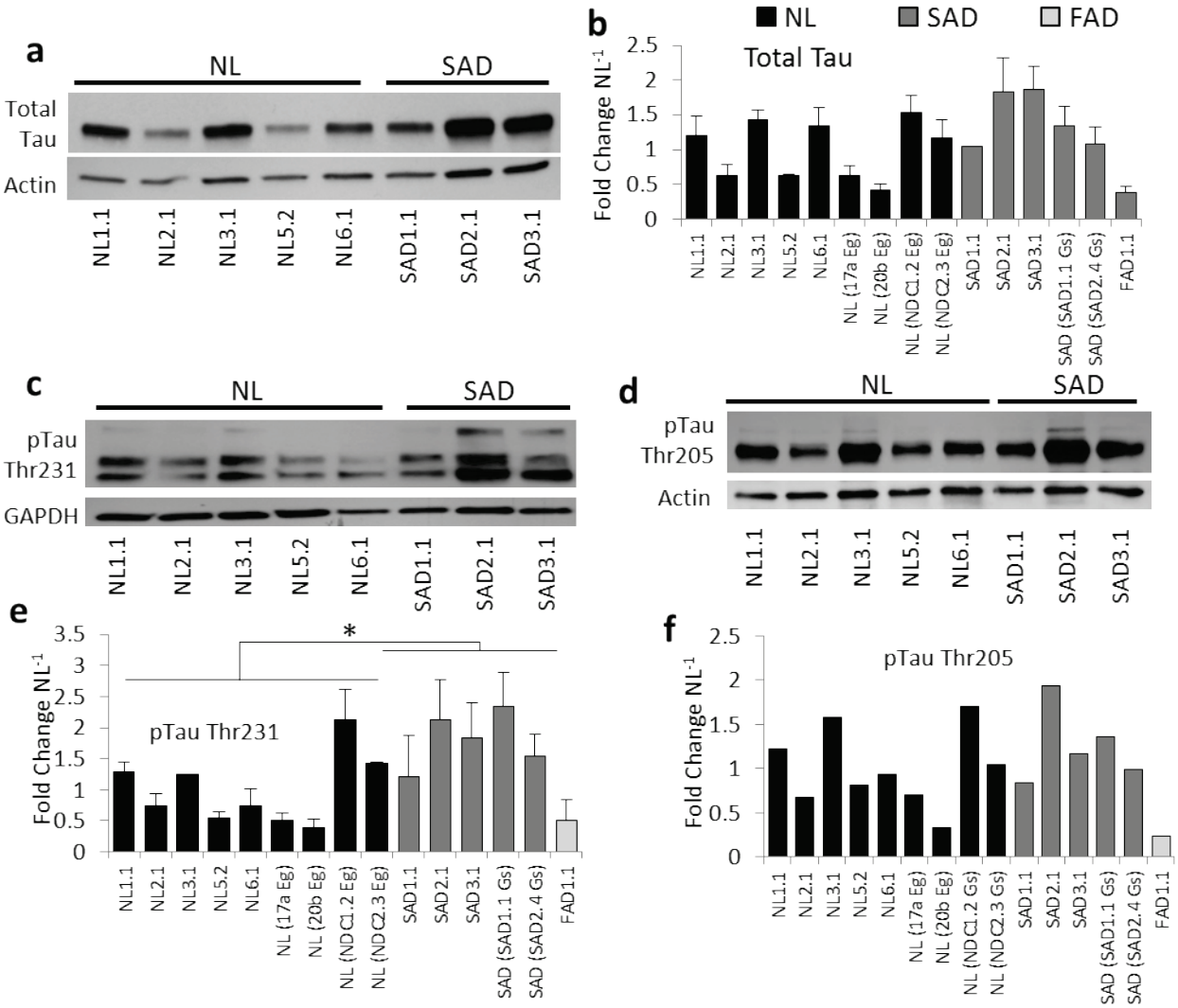

Figure 5.4: Tau and Phospho-Tau in 6-week Differentiated Neurons (a,c,d) Representative blots of total tau (Tau-5), tau phosphorylated at residue threonine 231 (pTau Thr231), and tau phosphorylated at threonine 205 (pTau Thr205) in 6-week differentiated neurons. (b) Total tau protein levels quantified through western blotting are not significantly increased in SAD. Average of blots from the same protein harvest, each independently converted to fold change over the average of the NL lines and normalized to actin or GAPDH protein levels. $p = 0.085$ (e) pTau Thr231 protein levels quantified through western blotting are increased in SAD 6-week neurons. Average of two blots from the same protein harvest. $p = 0.015$. (f) pTau Thr205 levels quantified through western blotting are not changed in SAD neural progenitors. Data quantified from one set of western blots. $p = 0.17$. $^*p<0.05$

C. Cell death in response to stress in neural progenitors

Neurons in the brain are predominantly post-mitotic and irreplaceable, so preventing loss of these cells is an integral process to normal brain functioning. However, loss of neurons is the predominant pathological outcome of Alzheimer's disease, causing severe disruption to normal brain function during the neurodegenerative process. Therefore, we wondered whether SAD neuronal cells had increased susceptibility to stress and were more likely to undergo an apoptotic response. Neural progenitors from three SAD and three NL patients were subjected to oxidative and genotoxic stress. Oxidative stress, induced by hydrogen peroxide in conjunction with ferric chloride to catalyze the production of reactive oxygen, causes a dose-dependent increase in cell death (Figure 5.5a). However, there is no difference between the SAD and NL lines with an insignificant trend towards increased survival in the SAD lines.

Genotoxic stress was induced using camptothecin and etoposide. Both of these drugs are used in the treatment of cancers due to their ability to induce cell death in dividing cells by inhibiting topoisomerase I and topoisomerase II, respectively, and causing damage to the DNA (Baldwin & Osheroff 2005, Pommier 2006). These treatments also reduced cell survival in a dose-dependent manner, but there was no significant difference in response between the AD and NL neural progenitors (Figure 5.5b). Together, these results suggest that differences in apoptotic response to oxidative or genotoxic stress is not important in the pathogenesis of Alzheimer's disease, although the mechanism controlling this response in differentiated neurons may be different.

Figure 5.5: Stress Response and Cell Survival in Neural Progenitors

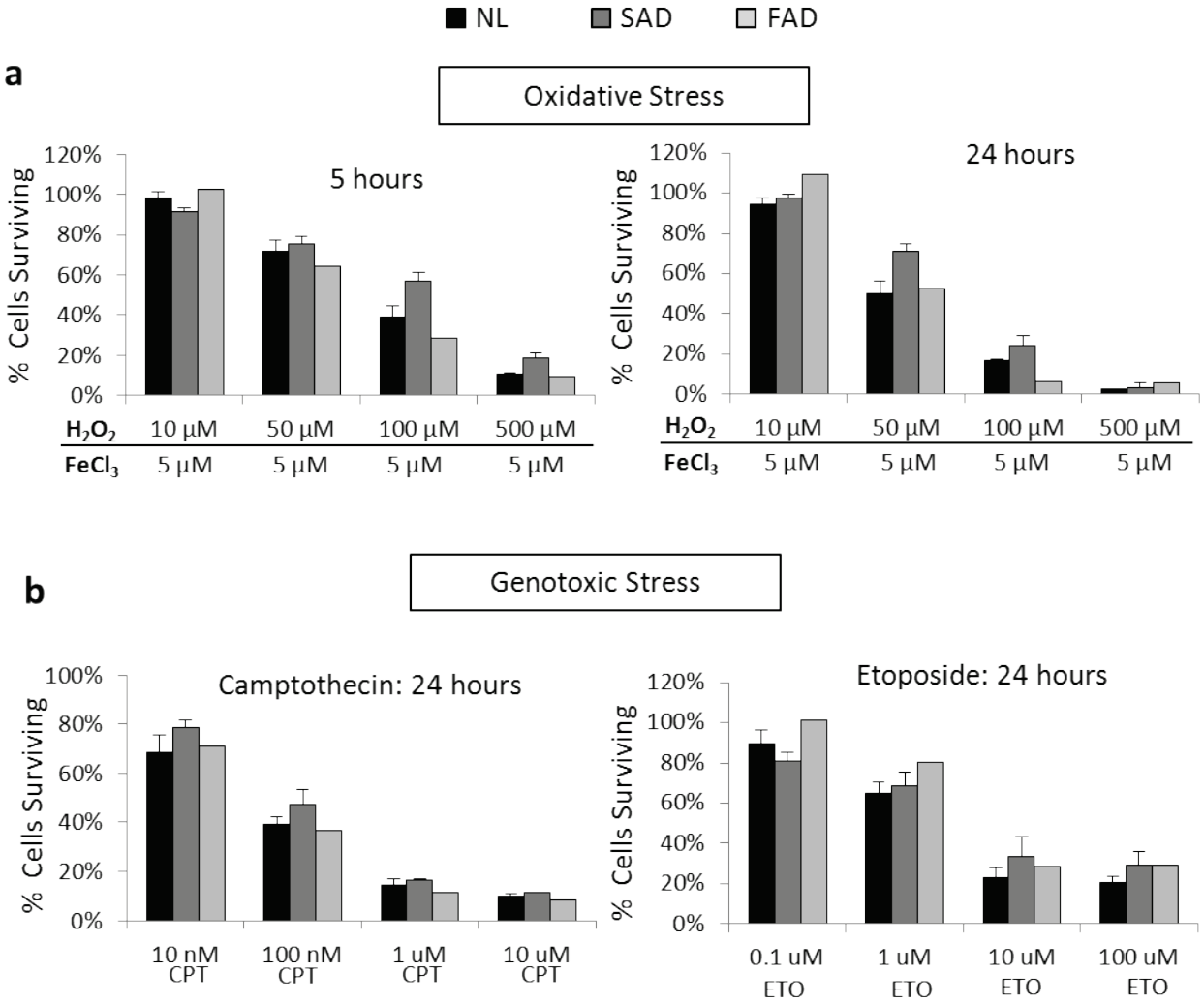

Figure 5.5: Stress Response and Cell Survival in Neural Progenitors (a) Cell viability assay using MTS (3-(4,5-dimethylthiazol-2-yl)-5-(3-carboxymethoxyphenyl)-2-(4-sulfophenyl)-2H-tetrazolium) reagent shows increased cell death with increased oxidative stress from hydrogen peroxide (H_2O_2), but not significant difference between the SAD (SAD1.1, SAD2.1, SAD4.1) and NL lines (NL1.1, NL2.2, NL4.1, NL6.1) in neural progenitors. Ferric chloride ($FeCl_3$) was added with the hydrogen peroxide to catalyze its decomposition and expedite production of reactive oxygen. (b) Genotoxic stress was induced by camptothecin (CPT) and etoposide (ETO) and cell survival was quantified after 24 hours using an MTS assay. All cell survival was normalized to non-treated controls for each line.

D. AD susceptibility genes and the SAD microarray

Multiple genes associated with Alzheimer's disease are differentially regulated in the neuronal cells derived from SAD and NL patients. *APOE* is down-regulated 1.7-fold in the SAD NPs and *MAPT* is up-regulated 3.7-fold in the SAD 6-week neurons. SORL1 (sortilin-related receptor) is up-regulated 1.7-fold in the SAD neurons. SNPs in SORL1 are associated with the development of AD, but they result in the down-regulation of SORL1 expression (Rogaeva et al 2007). It is a cell-surface receptor in the APOE receptor family which has been implicated in the processing of APP (Hoe & Rebeck 2008, Offe et al 2006).

F-spondin (SPON1), the most highly up-regulated gene in the SAD neurons interacts with the APOER2 and APP, causing decreased Aβ production (Hoe et al 2005). The SPON1 gene has been shown to improve memory performance and mice and a SNP in the gene is associated with milder clinical dementia scores and a lower risk of Alzheimer's disease (Hafez et al 2012, Jahanshad et al 2013).

SYT4 (synaptogamin IV) is up-regulated in the SAD neural progenitors (both microarray analyses) and neurons. It has also found to be up-regulated in neurons in a transgenic mouse model of Alzheimer's disease which overexpresses a mutant APP after the formation of plaques (Tratnjek et al 2013).

Some AD risk genes that have been identified by GWAS are not differentially expressed in the 6-week neurons, but closely related genes are (Lambert et al 2013). *EPHA1* has a nearby SNP associated with AD, while *EPHA2* and *EPHA3* are both differentially expressed in the 6-week SAD neurons, and *EPHA3*, *EPHA4*, *EPHA7*, and *EPHB1* are differentially expressed in the SAD neural progenitors (all up-regulated). *PTK2B* is located nearby a SNP associated with AD, and *PTK2* is down-regulated 2.5-fold in the SAD neurons. The PTKs are both kinases that

mediate the attachment of cells to the extracellular matrix, controlling cell migration and adhesion (Lim et al 2008). Finally, a SNP near *CELF1*, an RNA-binding protein, has been associated with the onset of AD, while *CELF4*, *CELF5*, and *CELF6* are all up-regulated in the SAD neurons.

Using Ingenuity Pathway Analysis, APP, MAPT, and APOE were all identified as upstream regulators that are affected in the SAD 6-week neurons (Supplementary Table 13). APOE had an activation score of 2.35, APP had an activation score of -1.4, while MAPT didn't have a predicted activation state, but was highly significant with a p-value of 0.009 in the gene list. The affected downstream genes that were differentially expressed in the 6-week differentiated neurons were extracted and mapped using Cytoscape software (Figure 5.6). This chart shows that the interactions of APP, APOE, and MAPT are highly interconnected and that those interactions are enriched in the genes differentially expressed in the 6-week differentiated neurons.

Together, the relationship between the genes associated with the risk of AD development, AD pathologies, and the gene expression changes in the 6-week differentiated neurons suggest an interconnected pathway that may be disrupted during the development of Alzheimer's disease. The premature differentiation seen the iPS-derived neuronal cells from SAD patients may be a manifestation of the changes that will lead to neurodegeneration during the progression of Alzheimer's disease.

Figure 5.6: Connections of AD Pathologies to Gene Expression Changes

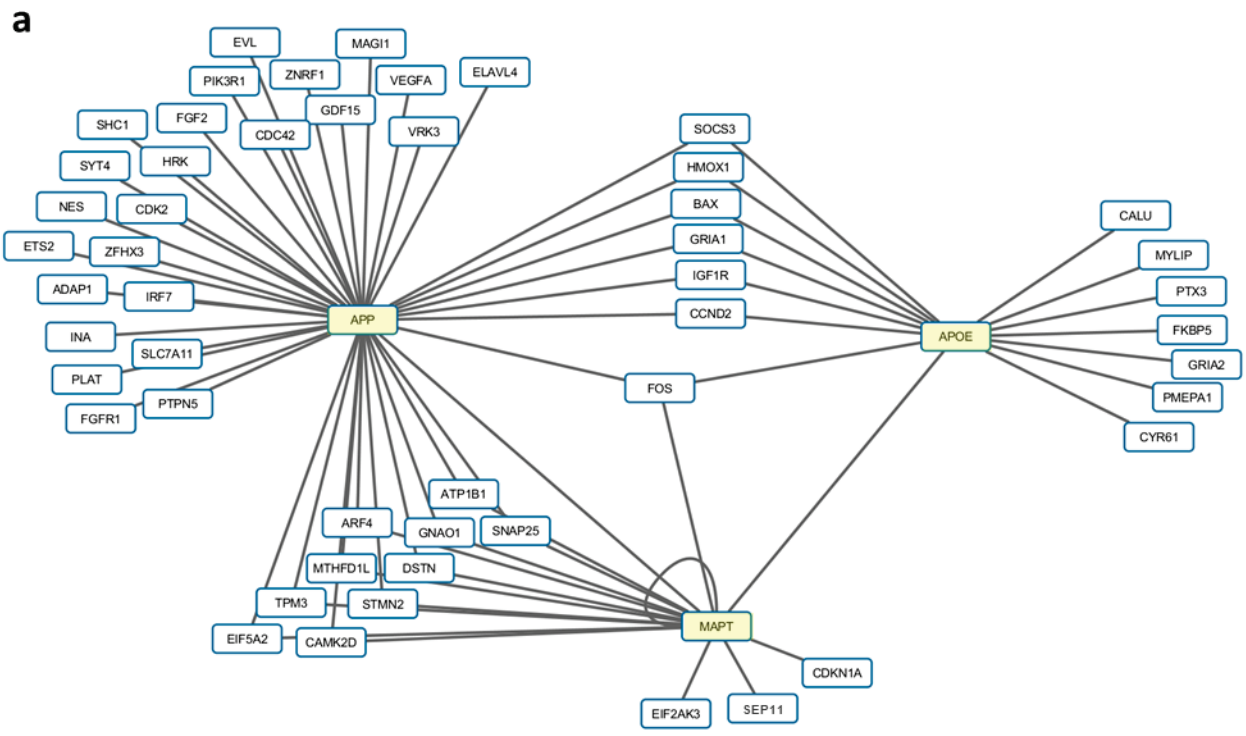

Figure 5.6: Connections of AD Pathologies to Gene Expression Changes. Interconnections of genes differentially expressed in the 6-week differentiated neurons with the proteins responsible for the key pathologies of Alzheimer's disease (APP and MAPT) and the strongest genetic risk factor for sporadic Alzheimer's disease (APOE). The input hubs of the Alzheimer's proteins are indicated by yellow. The connecting genes were identified as downstream targets of the specified hub, using Ingenuity Pathway Analysis of upstream regulators. The diagram was designed using Cytoscape.

E. Gene expression changes in the AD brain

Many studies have shown gene expression changes in the post-mortem AD brain (Blalock et al 2004, Colangelo et al 2002, Ginsberg et al 2000), but there has been some conflicting results. In Colangelo et al (2002), comparison of gene expression in the CA1 region in AD and control show a generalized decrease in transcription, including decreases in transcription factors, neurotrophic factors, and synaptic plasticity genes, but increases in apoptotic and neuroinflammatory genes. In Ginsberg et al (2000), the gene expression in neurons bearing neurofibrillary tangles from the CA1 were compared to normal CA1 neurons from control brains. They saw reductions in gene expression of cytoskeletal, synaptic, and glutamate receptor genes. These results are all dissimilar to the 6-week differentiated neuron microarray in which we observed up-regulation of synaptic and other neuronal genes, however the gene expression changes seen in the advanced stage of Alzheimer's disease may be very different than those seen in the earliest stages.

Studies that attempt to look at the earlier stages of AD development do see an up-regulation of some gene ontology categories. Blalock et al (2004) observed that there was up-regulation of genes involved in proliferation and differentiation as well as adhesion, apoptosis, lipid metabolism, and inflammation in early hippocampal AD neurons. Some of the up-regulated genes were similar to what we observed in the SAD neurons derived from iPS cells, including up-regulation of ASCL1, but there wasn't a large overlap.

A more recent study from Berchtold et al (2014) found that gene expression in four brain regions, but especially the entorhinal cortex, show an increase in synaptic, energy generation, and protein homeostasis genes in mild cognitive impairment that is not seen in age-matched control or later AD brains. Many genes showed a distinct pattern of decreased

expression in the normal aging brains, increased in MCI, and then decreased again in the later stages of AD which may explain the inconsistent results seen in earlier AD brain microarrays. Some of the genes associated with a worse mini–mental state examination (MMSE) score include those up-regulated in our SAD neural progenitors or neurons such as SNAP25 and EPHA4. Many of the MCI up-regulated genes are traditionally associated with enhanced cognitive function, much like the up-regulated genes in the 6-week neurons.

When we overlap the gene expression changes in the SAD 6-week differentiated neurons with the genes that are differentially expressed in the prefrontal cortex during AD (Tao Lu, unpublished results), we see an interesting pattern (Figure 5.7). The up-regulated SAD genes from the 6-week neurons are also up-regulated in AD, but not the aging brain. These same genes are also up-regulated in the young brain, but not to the same extent as the AD brain. The down-regulated 6-week neuronal genes do not show as clear a pattern, with the genes appearing to still be up-regulated in the AD brain with inconsistent expression in the younger brains. Therefore, it seems that the up-regulated genes of the 6-week SAD neurons may be more consistent with the changes occurring in the AD brain and help distinguish the AD brain from age-matched controls. These up-regulated genes are enriched for genes associated with neuronal activities, including synaptic function, neurogenesis, and cell adhesion (see Figure 4.7d). An important caveat is that the gene expression profiles are in the prefrontal cortex which is affected during the later stages of AD, not the hippocampus or entorhinal cortex where most of the AD pathology begins and where Berchtold et al. (2014) saw the strongest up-regulation of neuronal genes in MCI.

Figure 5.7: Gene Expression Changes and the AD Brain

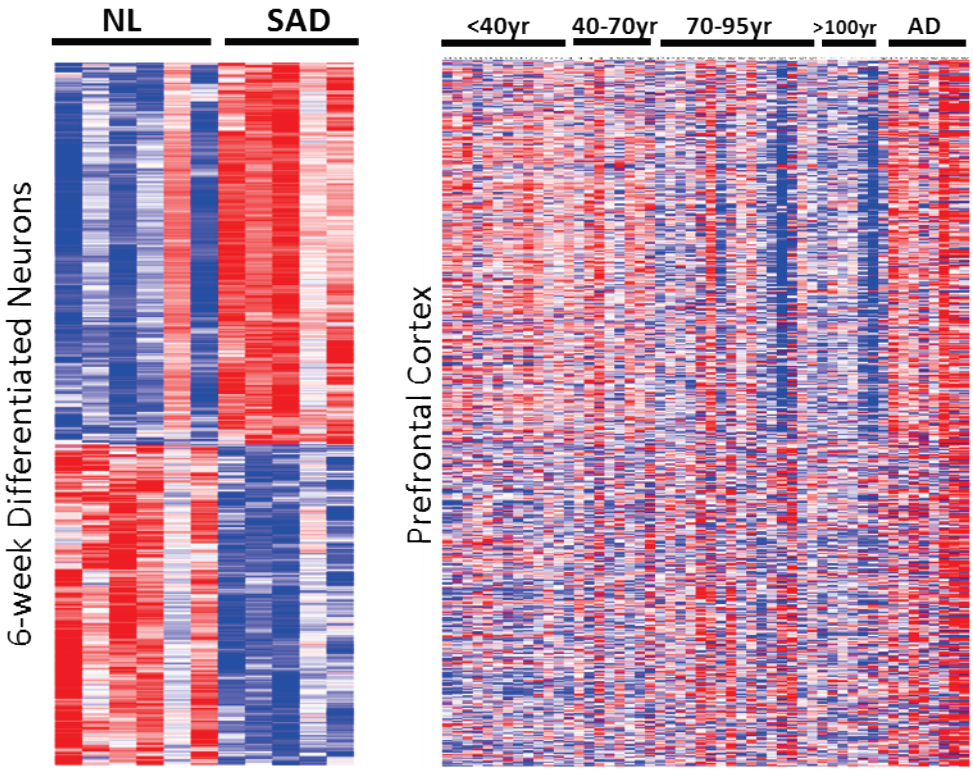

Figure 5.7: Gene Expression Changes and the AD Brain. Overlap of genes differentially expressed in the 6-week differentiated neurons ($q \leq 0.035$, SAD vs. NL) and prefrontal cortex ($p \leq 0.01$, AD vs. aged) during Alzheimer's disease. There are 698 probes that are differentially expressed in both groups.

Conclusions and Discussion

The neuronal cells derived from SAD patients recapitulate some, but not all the pathologies associated with AD in the human brain. These differences provide data in support and opposition to several well-established hypotheses for the development of AD.

Aβ40 production is increased in the neural progenitors, but Aβ40 and Aβ42 levels are not significantly enhanced in 5-week differentiated neurons. However, the ratio of Aβ42:Aβ40 is decreased, which contradicts the amyloid cascade hypothesis in which increased relative generation of Aβ42 and its resulting toxicity is thought to cause AD. Although it may play an important role of the development of FAD, particularly in patients with *PSEN* mutations, based on this data Aβ42 production does not to appear to be modulated in neurons derived from SAD patients. However, there is still a trend towards increased overall Aβ generation and/or decreased clearance which may be more significant at later stages of neuronal differentiation, so a possible difference in overall Aβ levels cannot be ruled out for mature neurons.

Tau protein and mRNA levels are increased in the neural progenitors, consistent with the premature neuronal differentiation seen in the NP culture. This difference is reduced in the differentiating neurons, indicating it may be a transient disparity during differentiation. However, phosphorylated tau levels, specifically at residue Thr231, are increased in the SAD neurons. Although it is unclear what this increased phosphorylation may mean functionally, it is consistent with what is seen in both the developing brain during differentiation and pathologically during Alzheimer's disease.

There is no difference in susceptibility to apoptosis in neural progenitors following genotoxic or oxidative stress, thus providing evidence against the hypothesis that AD neuronal cells have increased vulnerability to these stressors. An important caveat is that these results are

in dividing neural progenitors and not post-mitotic and long-lived neurons which have different priorities for cellular maintenance and preventing apoptosis (Barzilai 2007).

The interconnections between the genes related to AD susceptibility and the differentially expressed genes in the 6-week differentiated neurons suggest that modulations in a common pathway may be causing the development of sporadic Alzheimer's disease. The function of this common pathway has not been fully elucidated, but APP, APOE, their receptors, and other proteins that modulate their activity in the extracellular matrix, such as f-spondin, are highly enriched in both AD susceptibility genes and the gene expression changes seen in SAD iPS-derived neurons. A change in neuronal differentiation is an attractive candidate for an affected pathway, since we observe a functional difference between the SAD and NL patient derived cells in which SAD cells prematurely differentiate out of the neural progenitor stage and show earlier neuronal function through the formation of action potentials and synapses.

Finally, the comparison of the gene expression profile in the 6-week differentiated neurons to the prefrontal cortex of the AD brain shows the greatest correlation in the up-regulated SAD genes, which are down in age-matched controls, but not the young brain. From Chapter 4, the up-regulated genes are particularly enriched for genes related to synaptic and other neuronal functions. Together, with the recent microarray results from Berchtold et al (2014) showing up-regulation of synaptic genes in the entorhinal cortex and the hippocampus during MCI which inversely correlate with cognitive function, it suggests the possibility that the increase in neuronal genes in SAD is not just a difference in neuronal timeline, but may be related to the changes seen during the early stages of AD development.

Contributions

Tao Lu performed all the AD and aging brain microarray experiments and analyzed their similarity to the gene expression differences seen in the 6-week differentiated neurons.

Chapter 6: Investigations into a mechanism

Abstract

Since the phenotype of premature neuronal differentiation is shared by cells from different SAD patients, the next question is whether this difference derives from the same mechanism or different mechanisms in each patient cell line. The transcriptional regulation of the differentially expressed genes is bioinformatically predicted to have a conserved effector during neuronal differentiation: REST/NRSF, a transcriptional repressor which is the most significant regulator of the up-regulated genes. Although expression of this transcription factor is not different between SAD and NL neuronal cells, there is decreased binding in the promoter of the highly up-regulated *DCX* in neural progenitors. Also, overexpression decreases both *DCX* and *MAPT* expression, making it an attractive candidate for modulating the SAD gene expression profile. Other mechanisms tested, including modulations in GSK3β activity and effects of media conditioned by SAD and NL lines have no significant effect on the expression of neuronal differentiation genes.

Introduction

It was quite surprising to discover such a strong shared phenotype in cells derived from patients that developed Alzheimer's disease sporadically without a known genetic cause. The shared gene expression profile of up-regulated early neuronal differentiation genes is strongly conserved throughout the different SAD patients, but the entire gene profile is not shared. This is evidenced by the relative small overlap of significant genes between the neural progenitor microarrays from one clone from many individuals versus multiple clones from fewer individuals. This dichotomy suggests that there may be different mechanisms for the same shared inclination towards neuronal differentiation.

Therefore, multiple signaling pathways were analyzed to investigate possible shared or specific mechanisms that cause the premature differentiation. First, the significant transcription factors predicted to regulate the differentially expressed genes were probed to see if there is consistent and shared change in regulation activity which may explain the gene expression changes seen.

REST/NRSF (repressor element 1-silencing transcription factor/neuron restrictive silencing factor) was identified as a highly significant transcriptional regulator of the up-regulated genes. REST is a transcriptional repressor of neuronal genes, which prevents the expression of those genes in non-neuronal cells (Schoenherr & Anderson 1995). During development, REST coordinates both the transition from pluripotent cell to neural progenitor and from progenitor to mature neuron through changes in both expression levels and binding (Ballas et al 2005). Recently, REST was identified in the Yankner laboratory as an important regulator of aging in the brain, but its activity is lost during Alzheimer's disease (Lu et al 2014). In addition to its role in regulating neuronal differentiation, Lu et al (2014) also found a neuroprotective role for REST, where increased expression protects against oxidative stress and Aβ-mediated toxicity, thus making it a particularly attractive target for affecting the pathogenesis of Alzheimer's disease.

Another signaling pathway that has been long associated with neuronal development is the Wnt signaling pathway (Inestrosa & Varela-Nallar 2014). In the canonical Wnt pathway, Wnt ligands binds its receptor Frizzled (Fz) and the associated co-receptor LRP5/6 to activate disheveled, which inhibits the GSK-3β kinase and preventing the phosphorylation and subsequent degradation of β-catenin. This allows β-catenin to translocate to the nucleus where it activates Wnt target genes, including those genes important in synaptogenesis and synaptic

plasticity, as well as neurogenesis in the adult SGZ and SVZ. GSK3β activation can also be induced by Aβ and increase the phosphorylation of tau (Resende et al 2008). Israel et al. (2012) showed increased activation of GSK3β in neurons derived from the two APP duplication lines and one of the sporadic Alzheimer's disease lines. Also, REST activation is induced by Wnt signaling and inhibition of GSK3β (Lu et al 2014), making modulations in this pathway an attractive target for dysregulation during neuronal development or the progression of Alzheimer's disease.

Neurons and neural progenitors secrete a variety of extracellular factors, including those involved with cell-cell interactions, molecular chaperone proteins, and redox proteins (Schubert et al 2009). To see if the difference in the neuronal differentiation between the SAD and NL lines was due to either increased secretion of a soluble factor or enhanced depletion of a factor in the media, media conditioned on both SAD and NL lines was transferred to SAD neural progenitors to see if this would affect the expression of neuronal markers.

By identifying an upstream pathway that could be modulated, this may allow future therapeutics to be developed that could prevent the onset of Alzheimer's disease.

Materials and Methods

Western blotting: Western blotting was performed as described in Chapter 2. The following novel antibodies were used.

Target	Host	Source	Catalogue #	Dilution
REST	Rabbit	Millipore	07-579	1:500
β-catenin	Rabbit	Cell Signaling	9587	1:2000
β-lamin	Rabbit	Abcam	ab16048	1:5000

Nuclear Fractionation: Cells were harvested in PBS containing protease and phosphatase inhibitors before resuspending in hypotonic buffer (10 mM HEPES and 10 mM KCl) for 15 minutes on ice. The cells were homogenized using a dounce homogenizer with pestle size B. The homogenized sample was spun at 2000 x *g* at 4º for 10 minutes and the nuclear pellet was resuspended in RIPA-DOC buffer with 1x PhosSTOP (Roche), 1x cOmplete protease inhibitor (Roche), 0.5% SDS, and 25 U/100 uL Benzonase (Millipore). The mixture was incubated at room temperature for 10 minutes before addition of sample buffer and loading. For each sample, some of the cells were removed and treated with the nuclease Benzonase (Millipore) following homogenization and centrifugation to obtain cytoplasmic and whole cell fractions to compare to the nuclear fraction to ensure successful fractionation.

Chromatin Precipitation (ChIP) PCR: The ChIP assay was performed as previously described (Lu et al 2014). Neural progenitors cells were cross-linked using 1% formaldehyde at room temperature for 10 minutes. The reaction was stopped by addition of 1.25 M glycine to a concentration of 125 mM and washed twice by centrifugation. The cell pellet was dissolved in SDS lysis buffer (1% SDS, 10 mM EDTA, and 50 mM Tri-HCl, pH 8.1) and the genomic DNA sheared by sonication (Biorupter) at the intensity required to create 300-1000 bp fragments, previously verified for the samples through agarose gel. The sonicated samples were spun down for 10 minutes at 15,000 x *g* at 4º C. The supernatant was diluted 1:10 in ChIP dilution buffer (0.01% SDS, 1.1% Triton X-100, 1.2 mM EDTA, 167 mM NaCl, 16.7 mM Tris-HCl, pH 8.1) and precleared with Protein A Sepharose beads (Life Technologies) before adding REST-antibody conjugation beads. 5% of the sheared DNA was reserved as input control. The sample/beads was incubated for 12 hours with rocking at 4º C and then washed twice with low salt wash buffer and once with high salt wash buffer (0.1% SDS, 1% Triton X-100, 2 mM

EDTA, 150 mM NaCl or 500 mM NaCl, 20 mM Tris-HCl, pH 8.1). The beads were washed once with LiCl wash buffer (0.25 M LiCl, 1% NP-40, 1% deoxycholic acid, 1 mM EDTA, 10 mM Tris-HCl, pH 8.1) and twice with TE buffer (1 mM EDTA, 10 mM Tris-HCl, pH 8.1). The beads were then incubated with elution buffer (1% SDS, 0.1 M $NaHCO_3$) for 30 minutes with rocking and vortexed every 10 minutes. The supernatant was transferred to a new tube and 5 M NaCl was added, followed by de-crosslinking at 65º C for 4 hours. The eluted preparation was treated with RNase A for 10 minutes at room temperature followed by treated with proteinase K and 0.5 M EDTA for 1 hour at 55º. DNA was isolated using the Qiagen PCR purification kit and PCR was run using primers directed to the RE1 binding site of *DCX*.

Antibody:	ChIPAb+ REST	Millipore	Cat. #: 17-641
Primers:	DCX-RE1	**F:** AGGAAGGGAAGCTGGATTGT	**R:** CAAGAGAAAGGCACTGGCATA

REST Overexpression: pHAGE-CMV-Flag-REST-IRES-ZsGreen plasmid was used for REST overexpression (Mulligan et al 2008) and transduced into SY5Y cells and the neural progenitors using lentiviruses.

Conditioned Media Assay: For conditioned media transfer assays, neural progenitor cells from lines NL2.1 and SAD2.1 were grown to near confluency before fresh NP media was added. The NP media was conditioned for 3 days before it was removed and centrifuged to remove any contaminating cells. The media was transferred onto a plate containing neural progenitors of line SAD3.1 with four wells per condition: no media change control, fresh media at 24 hours, 6 hours and 24 hours with SAD-conditioned media, and 6 and 24 hours with NL-conditioned media.

The media on the SAD3.1 cells no media change had been added at the same time as the media for conditioning, for a total of 4 days. It was removed and re-added to the cells to control for any mechanical effects from media removal. RNA was harvested after the prescribed time using Cells-to-cDNA lysis buffer (Life Technologies).

Results

A. Transcription factors regulating SAD gene expression

The MetaCore transcription factor analysis tool uses the transcriptional regulation interactions in its database in order to calculate the significance of each transcription factor. The most significant transcription factors were calculated for the SAD differentially expressed genes in both the neural progenitor (single clone) and 6-week differentiated neuron microarray analyses (Figure 6.1a). There was only one shared transcription factor that was significant for all genes in both the neural progenitors and neurons: REST/NRSF. It was also the most significant transcription factor of the up-regulated genes for both types of neuronal cells with a p-value of $5.7x10^{-9}$ for the NPs and $2.2x10^{-17}$ for the neurons.

Since REST is a transcriptional repressor, the fact that its targets are enriched in the up-regulated genes suggests that REST activity is decreased. However, the MetaCore database only contains a subset of the recognized REST targets. Therefore, the canonical REST target genes identified in Bruce et al (2004) were overlapped with the differentially expressed genes in the three neuronal microarray analyses (Figure 6.1b). The plots show the fold change of each REST target within the differentially expressed gene lists. The majority of the REST-targeted genes are up-regulated in each gene list with fold changes significantly greater than the down-regulated genes. This supports the down-regulation of REST activity, at least at most of its targeted genes.

Figure 6.1: Most Significant Transcription Factors Regulating SAD Gene Expression

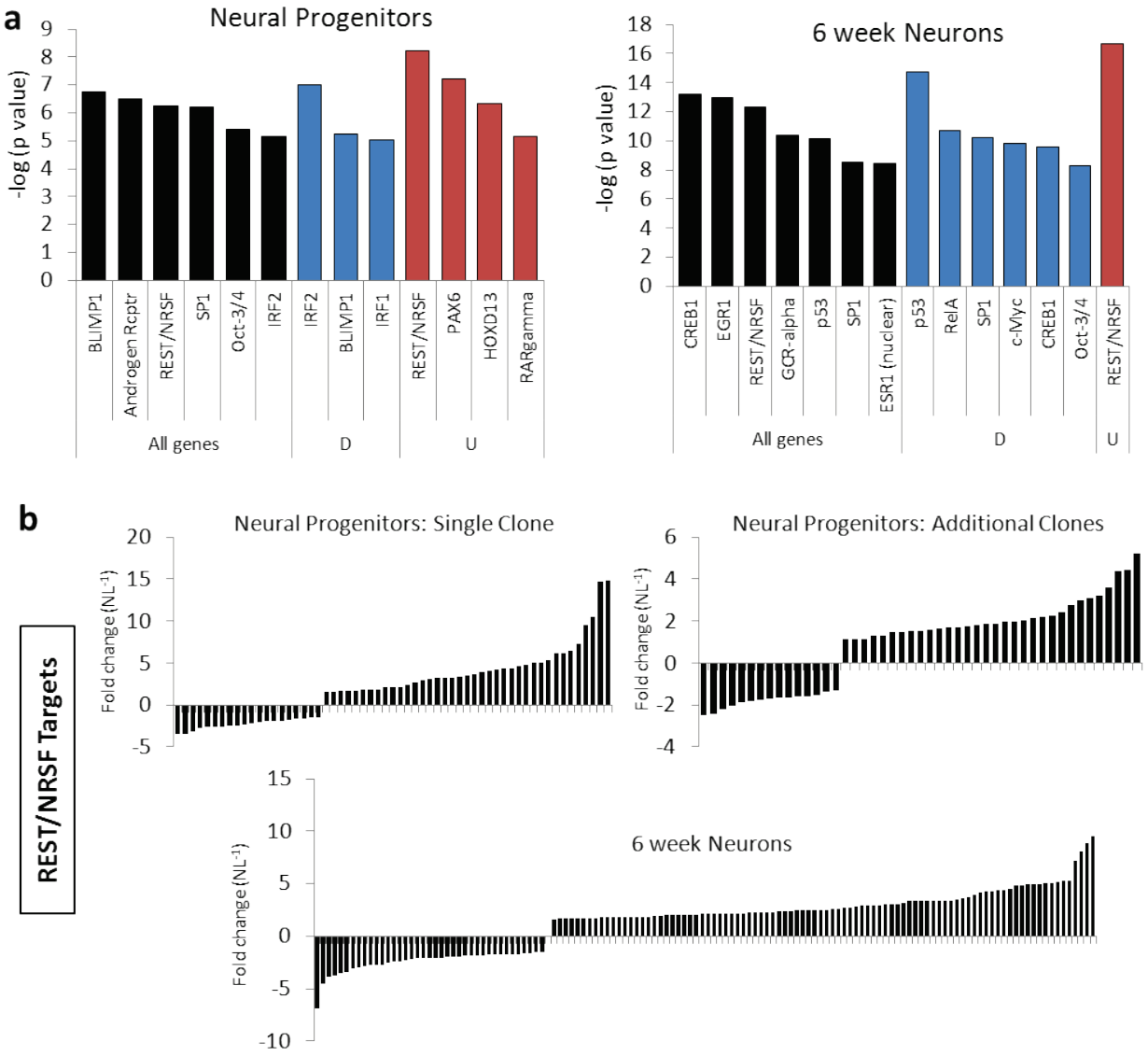

Figure 6.1: Most Significant Transcription Factors Regulating SAD Gene Expression. (a) Most significant transcription factors in the neural progenitor (single clone) and 6 week neurons significant gene list using MetaCore Transcription Factor Analysis. The overall gene list (All genes, black), the down-regulated genes (D, blue), and the up-regulated genes (U, red) were analyzed separately. For the neural progenitors, all transcription factors with a p-value less than 10^{-5} were included and for the 6 week neurons, all transcription factors with a p-value less than 10^{-8} were included. (b) Fold changes of all the targets of the REST/NRSF transcriptional repressor in the significant gene lists. REST targets were identified in Bruce *et al.* 2002.

B. REST expression and activity

In neural progenitors, REST activity is thought to be primarily regulated by expression levels (Ballas et al 2005), however the microarray analyses showed no difference in *REST* mRNA expression between SAD and NL neural progenitors or neurons which was confirmed by qRT-PCR (data not shown). Therefore, western blotting was used to quantify the amount of REST protein to see if there could be a difference in regulation at the protein level, which is decreased in the AD brain (Lu et al 2014). But there was no difference in REST protein levels in either the neural progenitors or neurons in the SAD line (Figure 6.2a,b). REST is active in the nucleus and localization has been shown to be disrupted in AD, so we also looked at REST expression only in the nucleus following cellular fractionation. Unlike in the AD brain, there was no difference in REST levels in the nucleus (Figure 6.2c,d).

However, since so many REST targets are differentially expressed, we decided to look directly at REST binding at the repressor element 1 (RE1) site in the promoter of one the strongest differentially expressed genes in the neural progenitor microarray, *DCX*, which is a REST target. Chromatin immunoprecipitation (ChIP) using antibodies for REST protein was used to isolate the DNA cross-linked to the REST proteins. The DNA was then separated and PCR with primers specific to the *DCX*-RE1 site shows increased REST occupancy in the *DCX* promoter in NL neural progenitor lines ($p = 0.039$) (Figure 6.2e). Therefore, even though there isn't a difference in REST expression or localization, there is a decrease in REST function in the SAD neural progenitors, at least at the *DCX* gene.

Next, the functional effects of modulations in REST activity were tested through REST overexpression in neural progenitors and SY5Y cells, a neuroblastoma cell line. Two neural progenitor lines were transduced with the REST overexpression vector: NL2.1 and SAD

(SAD2.4 Gs). They both showed a substantial increase in REST mRNA levels at 10 days following transduction (Figure 6.2f). Furthermore, REST overexpression decreased *DCX* expression significantly in both lines supporting its role in repressing *DCX* expression. However, even with the increased REST expression, *DCX* levels were still significantly higher in the SAD (SAD2.4) neural progenitors, indicating that either decreased REST is not the only factor mediating the increase in *DCX* expression in SAD (SAD2.4 Gs) or that increasing overall expression of REST isn't enough to change its binding to the *DCX* promoter.

REST was also overexpressed in SY5Y cells and the levels of REST and tau protein were measured using western blotting (Figure 6.2g,h). *MAPT* has an RE1-site and is targeted for repression by REST (Bruce et al 2004). REST overexpression greatly decreased the amount of tau protein expression in the SY5Y cells, supporting that the mechanism of reduced *MAPT* expression in the SAD neuronal cells may be related to decreased REST binding. Although REST expression is not different between SAD and NL cells, differences in REST occupancy and the functional effects of modulating REST expression indicates that it may still play a significant role in regulating the neuronal differentiation in the SAD lines.

Figure 6.2: Characterization and Effects of REST expression. (a) REST protein levels in neural progenitors quantified through western blotting are not different between SAD and NL. Average of two separate protein harvests, each independently converted to fold change over the average of the NL lines and normalized to GAPDH or actin protein levels. $p = 0.12$. (b) REST protein levels in 6-week differentiated neurons quantified through western blotting are not different between SAD and NL. Combination of two separate protein harvests, each independently converted to fold change over the average of the NL lines and normalized to GAPDH or actin protein levels. Duplicated samples were averaged (NL2.1, NL3.1, NL5.2, SAD1.1, SAD2.1, and SAD3.1). $p = 0.35$. (c,d) Nuclear fractionation of neural progenitors shows no difference in REST protein nuclear localization. Normalized to β-lamin (e) Chromatin precipitation and qPCR shows increased binding of REST to the RE1-site in the *DCX* promoter in NL neural progenitors. IgG was used as a negative control to ensure specificity. $p = 0.039$ (f) Representative *REST* and *MAPT* mRNA expression normalized to actin in neural progenitor cells 10 days after transduction with human REST (hREST) or GFP overexpression (OE) vector. Gene expression was measured using qRT-PCR and three out of four experiments showed the same pattern of gene expression. Two lines were infected: NL2.1 and SAD (SAD2.4 Gs). There was a significant difference in *DCX* expression in the normal between control (CTL) and hREST OE ($p = 0.026$) and in the SAD between CTL and hREST OE ($p = 0.003$). There was also a significant difference between the SAD and NL control ($p = 0.009$) and the two hREST OE ($p = 0.005$). (g, h) SY5Y cells stably overexpressing hREST show increased expression of total tau protein expression (Tau-5) by western blotting. GFP overexpression (OE) was used as a control for the overexpression activity and integration. All errors are the standard error of the mean. $^{*}p<0.05$, $^{**}p<0.01$

Figure 6.2: Characterization and Effects of REST Expression (cont.)

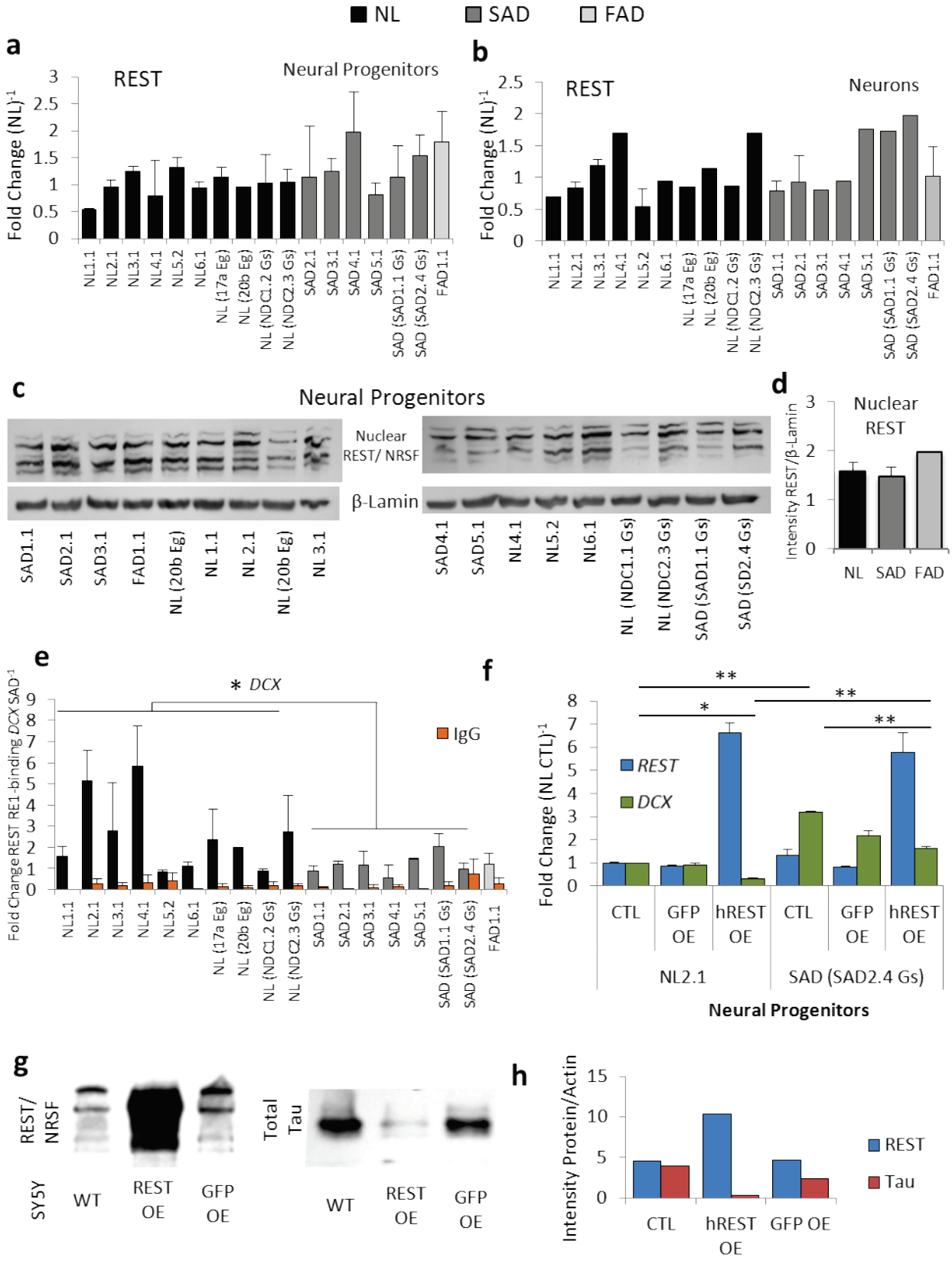

C. β-catenin signaling in neural progenitors

There is some evidence from the gene expression profile for differences in Wnt signaling in the SAD neurons. *WNT4*, a Wnt ligand that has not been widely studied in the CNS, is up-regulated 4.4-fold and *SFRP4* (secreted frizzled-related protein 4), an inhibitor of Wnt signaling, is down-regulated 4-fold in the SAD neurons. Wnt signaling was also identified as an enriched process network in both the up- and down-regulated 6-week neuronal genes. Together, these changes suggest that Wnt signaling may be affected in SAD neurons, although whether the effect is an activation or inhibition remains unclear. GSK3β was shown to be activated in AD neuronal cells (Israel et al 2012) as well as the AD brain, which is consistent with a down-regulation of Wnt signaling.

GSK3β kinase activity was inhibited using lithium chloride (LiCl) and the more specific CHIR9904 at doses recommended as effective to inhibit GSK3β in neuronal cells (Tau Lu, personal communication). Two SAD and two NL lines were treated and there was not a significant difference in *DCX* or *ASCL1* expression following treatment with LiCl or CHIR9904, although levels were quite variable (Figure 6.3a). One time point (7 hours of 5 mM LiCl treatment) showed the strongest variability, leaving the possibility that it was affecting the neuronal gene expression differentially in the SAD and NL neural progenitors. Therefore, that treatment was repeated in more detail using three wells for each line and treatment. *DCX* expression levels were highly consistent between the different wells for each line and LiCl treatment had no effect on its expression (Figure 6.3b). Therefore, GSK3β inhibition does not appear to change the expression on the early neuronal genes in the SAD neuronal cells.

Next, we looked directly at β-catenin localization to the nucleus. When β-catenin isn't phosphorylated by GSK3β, it avoids degradation and translocates to the nucleus where it can

induce gene expression. Therefore, nuclear localization of β-catenin is a direct read-out of Wnt signaling. In SAD and NL neural progenitor nuclei, there is no difference in β-catenin localization (Figure 6.3c,d). Together, the lack of effect on neuronal differentiation genes from GSK3β inhibition and absence of differences in β-catenin in the nuclei of SAD and NL neural progenitors strongly suggests that Wnt signaling is not an important modulator of the increased neuronal phenotype seen in the SAD neuronal cells.

Figure 6.3: β-catenin Signaling in Neural Progenitors

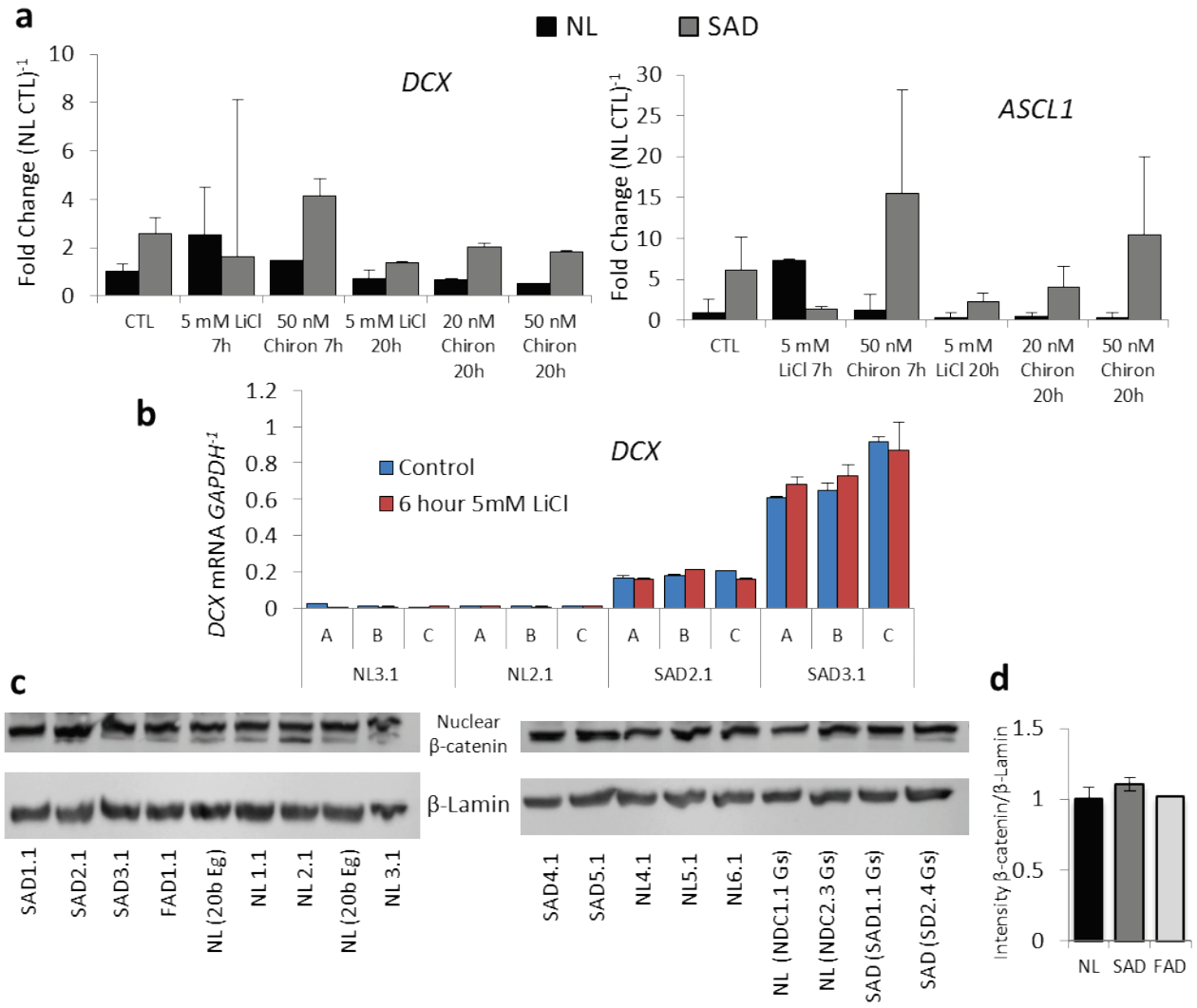

Figure 6.3: β-catenin Signaling in Neural Progenitors. (a) Inhibition of GSK3β using lithium chloride (LiCl) and the more specific inhibitor CHIR9904 (Chiron) caused variability in *DCX* and *ASCL1* expression, but does not appear to significantly change expression levels. Treatment was for 7 or 20 hours (7h, 24h) and RNA was harvested immediately following. All expression is normalized to GAPDH and expressed as fold change over the NL with no treatment control (CTL). NL =NL4.1 and NL5.2, SAD = SAD2.1, SAD3.1 (b) *DCX* expression in neural progenitors treated with 5 mM LiCl for 6 hours shows no decease in *DCX* in response to LiCl. 3 wells (A, B, C) of four lines were treated separately and quantified using qRT-PCR. (c,d) Nuclear fractionation shows that there is no difference in β-catenin protein localization in the nucleus when normalized to β-lamin.

D. Effects of conditioned media on neuronal gene expression

Many of the upstream pathways predicted to be different in the SAD NPs and neurons by Ingenuity Pathway Analysis involve secreted factors. Many growth factor signaling pathways are predicted to be down-regulated, including EGF, FGF2, TGFβ, VEGF, and PDGF, as well as the cytokine IL-1b. The differentially expressed receptor genes for the growth factor and cytokine signaling pathways are all down-regulated in SAD neurons (*KDR, LIFR, FGFR1,* and *IGF1R*), however the ligands have a more complicated expression pattern with TGFB2 up-regulated, although VEGFA and FGF2 are both down-regulated. Significantly, receptors for both of the growth factors added to the NP media to prevent neuronal differentiation are down-regulated in the SAD neurons. Together, these results suggest that there could be a difference in either the production or utilization of growth factors or other secreted compounds in the media.

To test this, media conditioned for three days by either SAD or NL neural progenitor cells were added to a growing culture of SAD3.1 (Figure 6.4). Surprisingly, the strongest decrease in *DCX* and *ASCL1* expression was seen simply through the exchange for fresh media in the control, indicating that depletion of factors in the media, such as bFGF/FGF2 and LIF, may be allowing the SAD lines to express more neuronal genes. The conditioned media may also have an effect, although results were not significant. SAD3.1 consistently has lower expression of *ASCL1* and *DCX* after addition of the NL-conditioned media, raising the possibility that there are either secreted factors from the NL neural progenitors or less depletion of the growth factors in the media that is affecting the expression of neuronal genes in the SAD3.1 neural progenitors. This experiment could be expanded to more lines as well as include the re-addition of exogenous growth factors to further delineate the mechanism and to see if significance could be achieved.

Figure 6.4: Effects of Conditioned Media

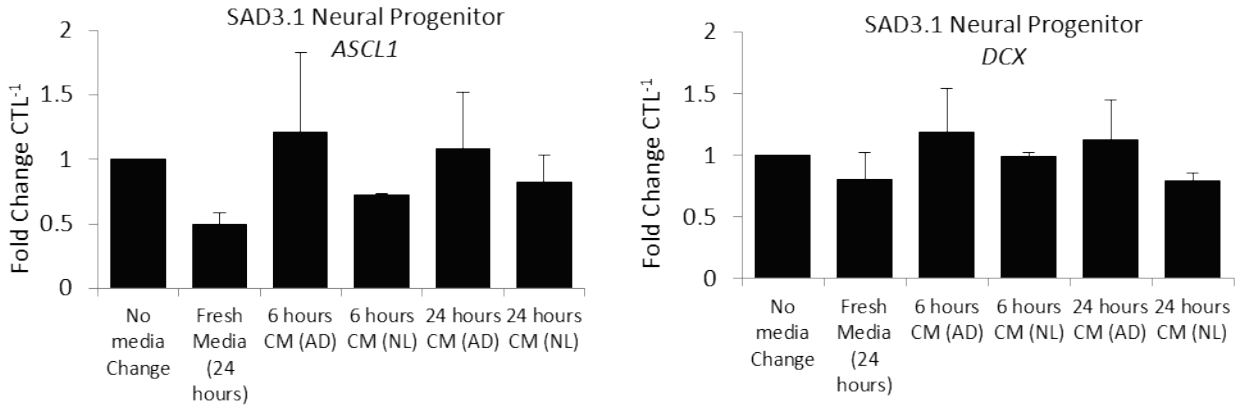

Figure 6.4: Effects of Conditioned Media. mRNA expression of *ASCL1* and *DCX* was averaged over two experiments (4 independent wells per condition per experiment) in SAD3.1 neural progenitors after addition of media cultured for three days with either an SAD (SAD2.1) or NL (NL2.1) neural progenitor line. Non-conditioned media was added as a control at 24 hours. Expression was normalized to GAPDH and converted to fold change over the average gene expression in the wells with no media change in each experiment. There was no significant differences in gene expression in the culture conditions.

Conclusions and Discussion

Investigations into the mechanisms regulating increased expression of neuronal genes in sporadic Alzheimer's disease cells have provided clues, but no definitive answers. Based on the lack of effect from GSK3β inhibition or changes in β-catenin nuclear localization, it is unlikely that differential Wnt signaling is involved. The possible variance in response to media conditioned with SAD or NL neural progenitors provides an intriguing possibility for differences in modulations of the extracellular milieu in SAD neuronal cells, but it needs to be more thoroughly examined before any conclusions can be drawn.

A change in REST activity in the SAD neural progenitors provides another interesting possibility for regulating neuronal differentiation. Although REST expression levels and localization are not different in the SAD and NL lines, REST does have decreased binding to one of its highly up-regulated targets, *DCX*. This difference, along with the functional results showing that increased expression of REST strongly decreases both *DCX* and tau expression in neural progenitors and SY5Y cells respectively, supports the capability of REST to regulate the expression of the SAD neuronal genes.

Furthermore, the pattern of gene expression seen in the prefrontal cortex for the genes up-regulated in the SAD 6-week neurons closely follows the pattern of REST targets in the brain (Lu et al 2014). The REST targets are increased in the young brain, but decrease with advancing age, except in Alzheimer's disease where the targets are again up-regulated. This is the same pattern seen in Figure 5.7 for the SAD neuronal up-regulated genes, suggesting that decreased REST may be a shared mechanism in the SAD neurons and the AD brain. The corresponding loss of neuroprotective effects from REST transcriptional repression may help explain the neurodegeneration seen in the AD brain.

However, since decreased REST expression is not the cause of the decreased activity, another factor must be regulating REST's binding to the RE1-sites. Regulation of REST activity is complicated. In the transition from ES cells to neural progenitors, REST levels are reduced through posttranslational degradation and during the transition to a post-mitotic neuron REST expression is inhibited by the retinoic acid receptor (RARE) (Ballas et al 2005).

REST activity is also modulated by the actions of its cofactors. There are two classes of RE1-containing genes. Class I genes have a binary control where REST recruits cofactors to the RE1 site, including Sin3, $MeCP_2$, HDAC, and CoREST, but when REST dissociates, the entire repressor complex releases and gene expression commences. Class II genes have a more nuanced control in which in addition to the REST complex, there is also a CoREST complex that is bound to a separate methylated site in the gene promoter. REST can dissociate from these genes during neuronal differentiation, but repression will be maintained by the CoREST complex in an activity-dependent mechanism. REST alone is not sufficient for gene silencing (Johnson et al 2008), therefore differential recruitment of the REST cofactors may result in the difference in REST target gene expression seen in the SAD neuronal cells.

Contributions

Tao Lu and Ying Pan performed the ChIP-PCR analysis on the harvested chromatin. Tao Lu created the SY5Y lines that stably overexpress REST and GFP. He also transduced and analyzed the NL2.1 and SAD (SAD2.4 Gs) neural progenitor lines overexpressing REST and GFP.

Chapter 7: Conclusions and discussion

With the discovery of induced pluripotent stem cells and related technology, there is for the first time a method for generating and examining human neurons from patients that develop neurological dysfunction without a known genetic cause. This is an incredible asset for a disease like Alzheimer's disease in which despite the high prevalence, the vast majority of cases have no known cause.

However, it is also surprising that one would see a difference in these cells. Sporadic Alzheimer's disease is typically not diagnosed until after the age of 65 in post-mitotic cells that have been present since development, thus having decades to develop the pathologies that lead to neurodegeneration. Furthermore, it is unclear if all patients that develop Alzheimer's disease share the same disease mechanism, which could make it challenging to find patterns in any differences seen in cellular behavior since it could be pathological or just a difference in that particular line that was unrelated to the development of AD. The idea of recapitulating a disease that takes decades to develop in the human brain in a few weeks in culture dish does not seem entirely feasible.

Therefore, the discovery of a shared phenotype of premature differentiation in the neuronal cells derived from sporadic Alzheimer's disease patients was both surprising and intriguing as well as subject to rigorous confirmation. It suggests there is a genetic or possibly epigenetic predisposition for the development of AD which can be modeled *in vitro*.

A. Generation and characterization of Alzheimer's disease iPS cells

The greatest strength of this study is the large number of individuals studied compared to previous sporadic Alzheimer's disease studies. We derived iPS lines capable of differentiating into neurons from six age-matched control patients (NL), five sporadic Alzheimer's disease

patients (SAD), and one familial AD patient (FAD) with a mutation in *PSEN1* (L286V) using dermal fibroblasts acquired from the Coriell Cell Repository. Both the sporadic and control patients had a variety of *APOE* genotypes, allowing for the analysis of possible effects due to differences in the *APOE4* isoform. One strength of this patient set is the relatively young age of onset for the sporadic AD patients, which may mean that any phenotype resulting in the development of AD would be stronger in these patients than those that develop the disease at an older age.

The fibroblasts were reprogrammed into iPS cells using retroviral transduction of the Yamanaka factors. The iPS cells express the pluripotency markers OCT4, TRA-1-81, SOX2, and NANOG, are capable of forming all three germ layers both *in vitro* and *in vivo*, and have mostly silenced the reprogramming factors. Gene expression differences seen in the fibroblasts between the AD and NL patients in a subset of the SAD and NL fibroblast lines were completely erased through the reprogramming process. Together, these results support that successful reprogramming has occurred and that the iPS cells are appropriate for later differentiation experiments.

We also acquired additional iPS lines derived in other laboratories to both increase our sample size as well as provide evidence that the findings are not specific to cells derived in our laboratory. We obtained two NL lines from the Harvard Stem Cell Institute iPS Cell Repository derived in the Eggan laboratory, as well as iPS lines from two NL and two SAD patients from the Goldstein laboratory (Boulting et al 2011, Israel et al 2012). In all, we analyzed 10 NL lines, 7 SAD lines, and 1 FAD line, the largest cohort of patients yet established for the study of sporadic Alzheimer's disease.

B. Increased markers of neuronal differentiation

Neural progenitors (NPs) were differentiated from iPS cells through an embryoid body intermediate and use of the AMPK inhibitor, dorsomorphin. The NPs expressed the neural stem cells markers of nestin, musashi, and SOX2, however gene expression profiling identified that it is not an entirely homogenous population. The SAD neural progenitor cultures had increased expression of early neuronal markers, including *ASCL1*, *DCX*, and *CD24*. Staining for the neuronal markers TUBB3 and DCX showed that a subset of cells were highly positive for the early neuronal markers and thus had undergone premature neuronal differentiation. Fluorescent-activated cell sorting for the early neuronal cell surface marker CD24 confirmed the increase in early neuronal population in the SAD neural progenitor culture. The differences in gene expression seen in the SAD NPs did not overlap strongly with the differences seen in AD fibroblasts, suggesting that these changes are specific to the neuronal lineage.

Since this result was so novel and surprising, we needed to confirm that stochastic differences in the differentiation process was not the cause of the SAD lines showing higher neuronal markers and that it is specific to the patient. Therefore, we differentiated additional iPS clones from four SAD and four NL patients, including the four lines acquired from the Goldstein laboratory. Although the gene expression at the neural progenitor stage was variable between clones, the overall analysis confirmed a strong up-regulation of the early neuronal genes such as *ASCL1* and *DCX*. Enrichment analysis for both neural progenitor microarray analyses showed the most robust enrichment for genes related to neuronal development and neurogenesis.

The neural progenitors were differentiated into neurons expressing β-tubulin III and MAP2 by the withdrawal of proliferation-inducing bFGF (FGF2) and LIF. After 6 weeks differentiation, the cultures are predominantly glutamatergic with a subset of GABAergic

neurons. There is also a small population of cells which expressed the glial marker GFAP, however it is unclear if these cells are astrocytes or radial glia cells that could differentiate into neurons. The GFAP-positive population is increased in the SAD neuronal cultures. After 6 weeks of differentiation, the cultures are not fully mature neurons with cells still expressing the early neuronal marker doublecortin and the neural progenitor marker nestin, however the morphology is greatly changed from the neural progenitor cultures with all cells showing elongated morphology.

Gene expression profiling of these cells shows that the difference between the SAD and NL neurons is conserved through early maturation. Enrichment analysis still reveals an enhancement of neuronal genes in the SAD lines, but rather than those related to early development, the most significant annotations now relate to synapse formation and vesicle transport, such as the genes used in neurotransmitter release. The neurons also have functional differences in differentiation timeline, with the SAD lines showing more synapsin-1-localized puncta after 6 weeks, signifying increased synaptic formation. Neurons derived from all the lines are capable of forming the action potentials of the electrochemically mature neuron, however SAD lines are able to generate action potentials earlier than any NL line tested. Together, these results support that the differences in neuronal differentiation seen in neural progenitors is conserved during maturation. However, it is unclear if the mature neurons obtain the same level of function from the NL patients as the SAD patients, although the eventual formation of action potentials in all lines supports this possibility.

C. Alzheimer's disease pathologies in the iPS-derived neuronal cells

Increased production of Aβ42 is one of the main hallmarks of FAD, especially in individuals with a *PSEN* mutation (Wolfe 2007). This observation along with the high levels of

Aβ in the human brain led to the amyloid hypothesis of Alzheimer's disease in which the increased production of Aβ and more specifically Aβ42 is thought to cause neurodegeneration (Hardy & Selkoe 2002). However, our results do not support the role of Aβ42 in sporadic Alzheimer's disease. Increased Aβ40 production is seen in the SAD neural progenitors, but in the differentiated neurons this differences is attenuated. Aβ40 and to a lesser degree Aβ42 trend higher in the SAD neurons, but the difference is not significant. Importantly, the ratio of the Aβ42:Aβ40 is significantly decreased in the SAD neurons. Our results do not preclude a model in which Aβ clearance is inhibited and accumulates over time in the SAD brain causing dysfunction, however our results suggests that there is limited difference in Aβ production and strongly refutes any increased production of Aβ42 in the SAD neurons.

The second pathological hallmark of Alzheimer's disease is the formation of intracellular aggregates of hyperphosphorylated tau protein. *MAPT* expression is robustly increased in the SAD neural progenitors and to a lesser degree in the SAD 6-week neurons. This difference is confirmed at the protein levels with SAD neural progenitors showing increased total tau protein and the neurons trending higher, but not reaching statistical significance. Adversely, phosphorylated tau levels are not increased at the neural progenitor stage but are higher in SAD neurons at the Thr231 residue. Together, these results suggest that tau may have an expression profile similar to other neuronal markers in which expression is higher in SAD at the earlier stages of differentiation, but becomes more similar as differentiation progresses. The phosphorylation difference, however, suggests that there are still differences in kinase or phosphatase activity in the SAD neurons which could lead to the tangles seen during Alzheimer's disease. Since the phosphorylation of tau is associated with neuronal differentiation

(Brion et al 1994), this difference could also be a function of the neuronal differentiation variance between the SAD and NL patient lines.

D. A network of SAD genes?

One consistent observation throughout the differentiation process, but especially once the cells become neurons, is how many of the differentially expressed genes have a functional connection to APP and APOE. APP is very much at the center of the Alzheimer's disease puzzle since increased expression of APP alone, such as in APP duplications and Down's Syndrome, is enough to lead to the development of AD (Sleegers et al 2006). However, it is possible that its most important function in the development of AD is not as the Aβ fragment but through another signaling pathway. The physiological role of AD has been the subject of much research, but the strongest evidence supports an important role in axon pruning through binding to DR6/ TNFRSF21, in a newly clarified BACE-independent mechanism (Olsen et al 2014). *DR6* (*TNFRSF21*) is up-regulated in our 6-week neuronal microarray.

Although there was no clear pattern to the differences in the SAD lines due to their *APOE* genotype, APOE remains the most important genetic risk factor for sporadic AD with the different isoforms capable of being both protective and increasing risk for AD. APOE interacts with a family of cell surface receptors with varying affinity called the low density lipoprotein receptor (LDLR) or APOE receptor family. These receptors include the LDLR, very low density lipoprotein receptors (VLDL), the LDLR-related proteins (LRPs), APOE receptor 2 (APOER2), and the sortilin-related receptor, LDLR class (SORL1) (Jiang et al 2014). Several of these receptors also interact with APP, including LRP1 and LRP1B which differentially modulate the production of Aβ (Cam et al 2004, Trommsdorff et al 1998).

APP and APOE both bind SORL1, which is up-regulated in the 6-week SAD neurons and is genetically associated with sporadic Alzheimer's disease development (Rogaeva et al 2007). SORL1 localizes mainly in late endosomal and Golgi compartments and increased expression is thought to reduce Aβ production by localizing APP to the Golgi, while loss of SORL1 is thought to increase Aβ production by leaving APP in Aβ-generating endosomes (Offe et al 2006).

LRP2, LRP3, and LRP4 are all differentially expressed in the 6-week neurons, with LRP2 and LRP4 down-regulated and LRP3 up-regulated. LRP4 has been found to interact with both APP and APOE, but its function is not well studied, although it may affect neuronal survival (Choi et al 2013, Lu et al 2007). LRP3 has not been widely studied. A mutation in the *LRP2* (Megalin) promoter which decreases gene expression increases the risk of developing AD (Vargas et al 2010). LRP2, which is an endocytic receptor, interacts with APP and may play a role in internalizing it (Alvira-Botero et al 2010). This interaction acts as a negative regulator of neurite branching.

Clusterin *(CLU),* which has also been strongly genetically linked to the development of AD, is another ligand of LRP2, APOER2, and VLDLR (Gil et al 2013, Leeb et al 2014). It may act in the SVZ to induce proliferation and increased neurogenesis by the same pathways as reelin (Leeb et al 2014). Reelin interacts with APOER2 and VLDLR and is highly up-regulated in three of the SAD lines. It interacts with APP as well and may help scaffold its interaction with integrin α3β1, increasing APP cell surface levels, decreasing β-cleavage, and promoting neurite outgrowth (Hoe et al 2009). Thrombospondin *(THBS1)* is another ligand for APOER2 and VLDLR and it is down-regulated 6-fold in the SAD neurons. It also activates the same signaling pathway as reelin and may play a role in promoting neuronal migration in the SVZ independent of reelin (Blake et al 2008).

APP also binds f-spondin, which increases its localization to the membrane and provides a scaffold by which it interacts with APOER2, which is also a receptor for APOE (Hoe et al 2005). This interaction both decreases the β-cleavage of APP, but also may affect the downstream signaling from the c-terminal domain of both APP and APOER2. F-spondin (*SPON1*) is one of the strongest up-regulated genes in the 6-week SAD neurons. F-spondin is also regulated by plasmin, which cleaves f-spondin to detach it from the extracellular matrix, possibly disrupting its interaction with APOER2 and APP (Tzarfaty-Majar et al 2001). Plasmin is activated by the tissue plasminogen activator (*PLAT*, tPA, down 5-fold in the SAD neurons) and inhibited by the tissue factor pathway inhibitor 2 (*TFPI2*, down 5.8-fold in SAD neurons) (Liu et al 1999). tPA is also a ligand for the low-density LRP1 in its right and plays a role in long-term potentiation (Zhuo et al 2000).

Clearly, APP and APOE are intrinsically linked to wide range of proteins that are differentially expressed in the 6-week SAD neurons. Other genetic risk factors for sporadic AD, including *SORL1* and *CLU*, are also involved in the same family of interactions. It is difficult to predict the downstream effects from changes in expression data since mRNA levels will not necessarily correlate with protein functioning due to post-translational regulation or response to feedback loops, however this network is an attractive candidate for disruption during Alzheimer's development. Many of these receptor-ligand interactions have been shown to affect not only Aβ processing and clearance, but also neuronal migration, neurite outgrowth, or progenitor proliferation. Therefore, the premature differentiation seen the iPS-derived neuronal cells from SAD patients may be a manifestation of the changes in this network that will leads to neurodegeneration during the progression of Alzheimer's disease.

E. Possible role of REST in regulating the neuronal gene expression

The mechanism for the increased neuronal gene expression in SAD neuronal cells remains a major question for these results. Using bioinformatics, the transcriptional repressor REST/NRSF was identified as the most significant conserved transcription factor affecting differential gene expression in the SAD neural progenitors and neurons. It is especially significant in the up-regulated genes, indicating a reduction in activity. REST is a master coordinator of neuronal gene repression and plays an important role in suppressing neuronal genes in non-neuronal tissues (Schoenherr & Anderson 1995). It also plays an important role in the transition from neural progenitor to neuron, where some of its target genes are fully de-repressed and others retain a residual repression through the maintained binding of a CoREST complex which can be removed in response to activity (Ballas et al 2005). In support of REST's role in regulating the genes that are differentially expressed in the SAD neurons, REST overexpression causes decreased expression of both *DCX* and tau protein.

The primary established method for regulating REST levels is through posttranslational degradation in neural progenitors and transcriptional inhibition by the retinoic acid receptor (RARE) during the transition to a post-mitotic neuron (Ballas et al 2005). In the AD brain, there are reduced levels of both total REST protein and nuclear localized REST (Lu et al 2014). We do not see a difference in REST protein or mRNA levels in the SAD neuronal cells, however we do see decreased binding at the RE1 site of *DCX* in SAD cells. Therefore, there is decreased activity of REST in the SAD neuronal cells, but it may not be regulated through a transcriptional or posttranslational mechanism.

Although baseline REST expression was not changed in the SAD cells, there may be differences in regulations of its cofactors, including Sin3, MeCP2, HDAC, and CoREST, since

REST alone is not sufficient for gene silencing (Johnson et al 2008). Additionally, REST expression is induced in neuronal cells in response to oxidative and Aβ stressors (Lu et al 2014), so even though the baseline expression is the same in the SAD and NL neuronal cells, there may be a difference in ability to respond to stress that could modulate the expression of neuronal genes. A difference in stress-induced expression would be of particular importance in the AD brain where there is excessive amounts of oxidative and other cellular stresses.

F. Speculation on how increased neuronal genes may lead to the development of AD

We were very surprised when we analyzed the first neural progenitor microarray data to see such a strong increase in neuronal genes in the SAD neurons. Since AD is a neurodegenerative disorder, we expected to see decreased capability to form functional neurons. This hypothesis was supported by much of the AD brain microarray data published at that point, which had showed a substantial decrease in genes related to neuronal functions, such as synapses (Berchtold et al 2013, Colangelo et al 2002, Ginsberg et al 2000). The 6-week SAD neurons express many genes in a direction that is the opposite the changes seen in the later AD brain.

One gene that is differentially expressed is *FGF2*. *FGF2* and its receptor, *FGFR*, are down-regulated in our 6-week neurons and predicted to be highly inactivated by Ingenuity Pathway Analysis. However, FGF2 levels have been widely shown to be higher in the AD brain (Gomez-Pinilla et al 1990). Additionally, we see a highly robust increase of *RELN* expression in three of the SAD lines, but reelin protein and mRNA are decreased in AD brains (Herring et al 2012). Many groups have seen an increase of cell cycle genes in the AD brain, whereas we see a decrease in genes that support cell cycle progression, such as *CCND2* (Nagy et al 1997).

Therefore, there is a large dichotomy between what is occurring at the later stages of the disease once neurodegeneration has started and what is occurring in the culture dish in neurons

from AD patients. One strength of our approach is that we are looking specifically at gene expression of neuronal cells, the cells most vulnerable to AD pathology, whereas many studies of the AD brain are complicated by the presence of other cell types, such as astrocytes, microglia, and oligodendrocytes. Furthermore, the later studies are complicated by the stress caused by the neurodegeneration which can greatly affect gene and protein expression due to increases in inflammation and oxidative stress. Thus, by modeling sporadic Alzheimer's disease in developing neurons using the induced pluripotent stem cell technology, we may be gaining insight into the upstream pathologies that lead to AD that can never be visualized in the human brain due to the lack of outward manifestations.

I will explore two hypotheses of how the premature differentiation seen in the SAD cells could be the causative factor for the development of AD: 1) by increasing neuronal activity levels or 2) by affecting adult neurogenesis.

G. How increased neuronal activity could lead to AD

First, I have not fully established that the NL neurons reach the same level of neuronal function as the SAD neurons. At six weeks, the SAD neurons have more synapses and although all lines are able to eventually form action potentials, there may be a difference in the amplitude and frequency of the spike trains with the SAD neurons showing greater activity of ion channels. This is supported by the increased expression of sodium and potassium channel genes in the SAD 6-week neurons. If this increased neuronal excitability was maintained in the adult brain, it could cause later neurodegeneration.

This hypothesis is supported by the gene expression changes seen in mild cognitive impairment, rather than the later stages of AD (Berchtold et al 2014). Berchtold et al found that gene expression changes that increased synaptic excitability and plasticity were associated with a

lower MMSE, while gene changes that inhibited plasticity were associated with a higher MMSE score. They hypothesized that the up-regulation of these neuronal genes could be leading to up-regulated baseline processing and thus an inability to encode new information.

Using fMRI, multiple groups have shown hyperactivity in the hippocampus during mild cognitive impairment, especially in the dentate gyrus (Dickerson et al 2005, Hamalainen et al 2007, Putcha et al 2011). Patients that generate more activity in the hippocampus to perform a task have a faster rate of cognitive decline and tend to develop AD (Vannini et al 2007). Inhibition using an antiepileptic drug that reduces hippocampal activity to a level similar to that seen in unaffected patients improved cognitive function, showing that the increased activation in MCI is dysfunctional (Bakker et al 2012). Some authors speculated whether the increased activity was a compensatory response to the damage already occurring in the brain, but this increase in hippocampal activity is also seen in cognitively normal offspring of sporadic AD patients who may have an increased genetic risk of developing AD (Bassett et al 2006, Yassa et al 2008).

The formation of amyloid plaques and neurofibrillary tangles is a part of normal aging, yet only some individuals go on to develop Alzheimer's disease (Price & Morris 1999). The rate of cognitive decline can be directly correlated to the amount of activation in the hippocampus (Vannini et al 2007), therefore a possible model is that the increased expression of neuronal genes in the SAD patient neurons causes hyperexcitability. Increased activity would results in increased metabolic demands and increased production of oxidative species. Excessive glutamate in the extracellular space could cause excitotoxicity and neuronal cell loss and then the loss of neuronal cells and synapses would set off the vicious cycle of increasing pathology and increasing cellular stress which leads to the neurodegeneration spreading through the brain. In

support of the hypothesis for changes in glutamatergic dynamics, a recent meta-analysis of GWAS studies found that genetic variance of glutamate signaling network genes was overrepresented in AD (Perez-Palma et al 2014)

The difference in excitability in SAD neurons could be a baseline increase or it could also be induced by the pathologies associated with aging, such as Aβ accumulation and neurofibrillary tangles and the resulting stress.

H. How modulations in adult neurogenesis could lead to AD

However, we see the most robust difference in the SAD and NL gene and protein expression at the neural progenitor stage with many of the neuronal genes, such as *MAPT* and *SNAP25* becoming more variable and less significant with differentiation, particularly in the larger cohort including iPSC lines derived in different laboratories. The functional differences are also stronger at the neural progenitor stage with a significant increase in Aβ production and decrease in cell proliferation rates. Therefore, we hypothesize that aberrant transitioning from neural progenitors to neurons could lead to the development of AD.

There is some evidence that AD could have a developmental component. In the Nun study, analysis of autobiographies written by the subjects at the average of 23 years old had an inverse correlation between idea density and Alzheimer's disease pathology, indicating that there are cognitive differences even in the young brain (Snowdon et al 2000). However, most cognitive changes are not diagnosable until many decades later therefore processes that happen in the adult brain are also of utmost importance in the progression of AD.

The neuronal culture system developed in this thesis seems to most closely follow the patterns of neurogenesis seen in the subgranular zone (SGZ) in the dentate gyrus. High levels of ASCL1 expression, such as in the SAD neural progenitors are specific to the maturation of

neurons in the subgranular zone and is not seen during fetal corticogenesis (Hodge et al 2008). The tandem increase of ASCL1 and DCX seen in the SAD neural progenitors is typical of the neurogenesis process that occurs at the subgranular zone in which after the cell leaves a quiescent state expressing GFAP, it transitions into a nestin- and SOX2-expressing progenitor similar to the cells in our neural progenitor culture. As it matures, the progenitor will start to express ASCL1 and DCX and lose its nestin expression. When the cell is only DCX- and not nestin-positive, it is considered a type 3 neuroblast and will migrate out of the SGZ and differentiate into a glutamatergic dentate granule cell, similar to the cells we've generated in culture (Hodge et al 2008, Kempermann et al 2004). Therefore, the differentiation protocol used in this thesis may be the best for modeling adult neurogenesis rather than neurogenesis that occurs in development.

Adult neurogenesis occurs in two regions in the adult brain, the subventricular zone which generates GABAergic neurons and feeds into the olfactory bulb and the SGZ which feeds glutamatergic neurons into the dentate gyrus and hippocampus, the regions most affected during Alzheimer's disease. Using incorporation of ^{14}C due to nuclear bomb tests to measure the rate of new neuron creation, Spalding et al (2013) estimated that one third of hippocampal neurons are subject to exchange and that the annual turnover rate is 1.75%. It is thought to play an important role in learning and memory (Deng et al 2010). Interestingly, in addition to the dentate gyrus and hippocampus, the olfactory bulb is also affected in early stages of Alzheimer's disease, leading to the well-established loss of olfactory ability (Kovacs et al 2001).

It is not clear from our data if the increase in neuronal gene expression would increase or decrease the amount of neurogenesis in the AD brain. In support of increased neurogenesis, the increased expression of neuronal genes might induce more precursors to differentiate into

neurons. However, increased neurogenesis could also exhaust the progenitor pool when the progenitors differentiate into neurons rather than self-renew and produce more progenitors.

In Alzheimer's disease, there are mixed data on changes in neurogenesis. In the human brain, Jin et al (2004) showed increased staining for doublecortin and other early neuronal markers TUC-4 and NCAM and another group showed a more measured increase of DCX expression, significant only in the dentate gyrus granule layer of the AD brain (Perry et al 2012). Results in mouse models of Alzheimer's disease, which model the familial form of Alzheimer's disease, not the sporadic, are more mixed with increased hippocampal neurogenesis shown in an APP/PSEN1 double transgenic mouse model, but impaired neurogenesis in a triple transgenic (APP, PSEN1, and MAPT) model of Alzheimer's disease (Rodriguez et al 2008, Yu et al 2009b). In a APP/PSEN1 mouse, Aβ42 treatment induces the proliferation of neural precursor cells and adult neurogenesis, however after 12-months the progenitors were no longer responsive, possibly due to depletion of the progenitor pool (Sotthibundhu et al 2009).

Therefore, two different models are possible. In the first, an increase in SAD neurogenesis depletes the neural progenitor pool and at advanced age the SAD hippocampus is no longer receiving new neurons, disrupting learning and memory. This loss of incoming cells leads to network disruption, synaptic loss, and the start of Alzheimer's disease neurodegeneration. In the second model, the SAD SGZ has pathologically high levels of neurogenesis, possibly induced by a stress such as the nearby formation of plaques or tangles. This increase of cells in the hippocampus also disrupts the networks, leading to cellular dysfunction and Alzheimer's disease progression. This model is supported by a recent paper from Akers et al (2014) in which high levels of hippocampal neurogenesis was found to induce forgetting.

I. Conclusion

In this thesis, we show a robust and surprising up-regulation of neuronal differentiation genes and resulting neuronal function in neuronal cells derived from SAD patients. Although we cannot definitively suggest a mechanism for the development of sporadic AD, this suggests alternative pathways to the classic amyloid cascade hypothesis in sporadic AD. It also suggests that sporadic AD may develop by a mechanism distinct from FAD, at least from the L286V mutation, since the FAD line recapitulated some, but not all of the SAD phenotypes and the SAD lines showed no relative increase in Aβ42 production. Finally, this thesis supports the use of induced pluripotent stem cells and similar technologies to model sporadic disease since we found a shared phenotype in cells derived from patients who had already developed Alzheimer's disease.

References

Adeosun SO, Hou X, Zheng B, Stockmeier C, Ou X, et al. 2014. Cognitive deficits and disruption of neurogenesis in a mouse model of apolipoprotein E4 domain interaction. *The Journal of biological chemistry* 289: 2946-59

Agostini M, Tucci P, Steinert JR, Shalom-Feuerstein R, Rouleau M, et al. 2011. microRNA-34a regulates neurite outgrowth, spinal morphology, and function. *Proceedings of the National Academy of Sciences of the United States of America* 108: 21099-104

Ahmed RR, Holler CJ, Webb RL, Li F, Beckett TL, Murphy MP. 2010. BACE1 and BACE2 enzymatic activities in Alzheimer's disease. *Journal of neurochemistry* 112: 1045-53

Akers KG, Martinez-Canabal A, Restivo L, Yiu AP, De Cristofaro A, et al. 2014. Hippocampal neurogenesis regulates forgetting during adulthood and infancy. *Science* 344: 598-602

Alvira-Botero X, Perez-Gonzalez R, Spuch C, Vargas T, Antequera D, et al. 2010. Megalin interacts with APP and the intracellular adapter protein FE65 in neurons. *Molecular and cellular neurosciences* 45: 306-15

Arriagada PV, Growdon JH, Hedley-Whyte ET, Hyman BT. 1992. Neurofibrillary tangles but not senile plaques parallel duration and severity of Alzheimer's disease. *Neurology* 42: 631-9

Bae S, Bessho Y, Hojo M, Kageyama R. 2000. The bHLH gene Hes6, an inhibitor of Hes1, promotes neuronal differentiation. *Development* 127: 2933-43

Bakker A, Krauss GL, Albert MS, Speck CL, Jones LR, et al. 2012. Reduction of hippocampal hyperactivity improves cognition in amnestic mild cognitive impairment. *Neuron* 74: 467-74

Baldwin EL, Osheroff N. 2005. Etoposide, topoisomerase II and cancer. *Current medicinal chemistry. Anti-cancer agents* 5: 363-72

Bali J, Gheinani AH, Zurbriggen S, Rajendran L. 2012. Role of genes linked to sporadic Alzheimer's disease risk in the production of beta-amyloid peptides. *Proceedings of the National Academy of Sciences of the United States of America* 109: 15307-11

Ballas N, Grunseich C, Lu DD, Speh JC, Mandel G. 2005. REST and its corepressors mediate plasticity of neuronal gene chromatin throughout neurogenesis. *Cell* 121: 645-57

Bally-Cuif L, Hammerschmidt M. 2003. Induction and patterning of neuronal development, and its connection to cell cycle control. *Current opinion in neurobiology* 13: 16-25

Barry DS, Pakan JM, McDermott KW. 2014. Radial glial cells: key organisers in CNS development. *The international journal of biochemistry & cell biology* 46: 76-9

Barzilai A. 2007. The contribution of the DNA damage response to neuronal viability. *Antioxidants & redox signaling* 9: 211-8

Bassett SS, Yousem DM, Cristinzio C, Kusevic I, Yassa MA, et al. 2006. Familial risk for Alzheimer's disease alters fMRI activation patterns. *Brain : a journal of neurology* 129: 1229-39

Bassus S, Herkert O, Kronemann N, Gorlach A, Bremerich D, et al. 2001. Thrombin causes vascular endothelial growth factor expression in vascular smooth muscle cells: role of reactive oxygen species. *Arteriosclerosis, thrombosis, and vascular biology* 21: 1550-5

Berchtold NC, Coleman PD, Cribbs DH, Rogers J, Gillen DL, Cotman CW. 2013. Synaptic genes are extensively downregulated across multiple brain regions in normal human aging and Alzheimer's disease. *Neurobiology of aging* 34: 1653-61

Berchtold NC, Sabbagh MN, Beach TG, Kim RC, Cribbs DH, Cotman CW. 2014. Brain gene expression patterns differentiate mild cognitive impairment from normal aged and Alzheimer's disease. *Neurobiology of aging*

Bertram L, McQueen MB, Mullin K, Blacker D, Tanzi RE. 2007. Systematic meta-analyses of Alzheimer disease genetic association studies: the AlzGene database. *Nature genetics* 39: 17-23

Blake SM, Strasser V, Andrade N, Duit S, Hofbauer R, et al. 2008. Thrombospondin-1 binds to ApoER2 and VLDL receptor and functions in postnatal neuronal migration. *The EMBO journal* 27: 3069-80

Blalock EM, Geddes JW, Chen KC, Porter NM, Markesbery WR, Landfield PW. 2004. Incipient Alzheimer's disease: microarray correlation analyses reveal major transcriptional and tumor suppressor responses. *Proceedings of the National Academy of Sciences of the United States of America* 101: 2173-8

Bolstad BM, Irizarry RA, Astrand M, Speed TP. 2003. A comparison of normalization methods for high density oligonucleotide array data based on variance and bias. *Bioinformatics* 19: 185-93

Boulting GL, Kiskinis E, Croft GF, Amoroso MW, Oakley DH, et al. 2011. A functionally characterized test set of human induced pluripotent stem cells. *Nature biotechnology* 29: 279-86

Brion JP, Octave JN, Couck AM. 1994. Distribution of the phosphorylated microtubule-associated protein tau in developing cortical neurons. *Neuroscience* 63: 895-909

Brion JP, Smith C, Couck AM, Gallo JM, Anderton BH. 1993. Developmental-Changes in Tau-Phosphorylation - Fetal-Tau Is Transiently Phosphorylated in a Manner Similar to Paired Helical Filament-Tau Characteristic of Alzheimers-Disease. *Journal of neurochemistry* 61: 2071-80

Brown JP, Couillard-Despres S, Cooper-Kuhn CM, Winkler J, Aigner L, Kuhn HG. 2003. Transient expression of doublecortin during adult neurogenesis. *The Journal of comparative neurology* 467: 1-10

Bruce AW, Donaldson IJ, Wood IC, Yerbury SA, Sadowski MI, et al. 2004. Genome-wide analysis of repressor element 1 silencing transcription factor/neuron-restrictive silencing factor (REST/NRSF) target genes. *Proceedings of the National Academy of Sciences of the United States of America* 101: 10458-63

Buee L, Bussiere T, Buee-Scherrer V, Delacourte A, Hof PR. 2000. Tau protein isoforms, phosphorylation and role in neurodegenerative disorders. *Brain research. Brain research reviews* 33: 95-130

Caceres A, Banker GA, Binder L. 1986. Immunocytochemical localization of tubulin and microtubule-associated protein 2 during the development of hippocampal neurons in culture. *The Journal of neuroscience : the official journal of the Society for Neuroscience* 6: 714-22

Calaora V, Chazal G, Nielsen PJ, Rougon G, Moreau H. 1996. mCD24 expression in the developing mouse brain and in zones of secondary neurogenesis in the adult. *Neuroscience* 73: 581-94

Callaway E. 2012. Alzheimer's drugs take a new tack. *Nature* 489: 13-14

Cam JA, Zerbinatti CV, Knisely JM, Hecimovic S, Li YH, Bu GJ. 2004. The low density lipoprotein receptor-related protein 1B retains beta-amyloid precursor protein at the cell surface and reduces amyloid-beta peptide production. *Journal of Biological Chemistry* 279: 29639-46

Castellano JM, Kim J, Stewart FR, Jiang H, DeMattos RB, et al. 2011. Human apoE isoforms differentially regulate brain amyloid-beta peptide clearance. *Science translational medicine* 3: 89ra57

Chandana R, Mythri RB, Mahadevan A, Shankar SK, Bharath MMS. 2009. Biochemical analysis of protein stability in human brain collected at different post-mortem intervals. *Indian J Med Res* 129: 189-99

Chen F, Hu SJ. 2012. Effect of microRNA-34a in cell cycle, differentiation, and apoptosis: a review. *Journal of biochemical and molecular toxicology* 26: 79-86

Chen H, Tung YC, Li B, Iqbal K, Grundke-Iqbal I. 2007. Trophic factors counteract elevated FGF-2-induced inhibition of adult neurogenesis. *Neurobiology of aging* 28: 1148-62

Chen Y, Durakoglugil MS, Xian X, Herz J. 2010. ApoE4 reduces glutamate receptor function and synaptic plasticity by selectively impairing ApoE receptor recycling. *Proceedings of the National Academy of Sciences of the United States of America* 107: 12011-6

Chen ZL, Strickland S. 1997. Neuronal death in the hippocampus is promoted by plasmin-catalyzed degradation of laminin. *Cell* 91: 917-25

Cherry SR, Biniszkiewicz D, van Parijs L, Baltimore D, Jaenisch R. 2000. Retroviral expression in embryonic stem cells and hematopoietic stem cells. *Molecular and cellular biology* 20: 7419-26

Chin MH, Mason MJ, Xie W, Volinia S, Singer M, et al. 2009. Induced pluripotent stem cells and embryonic stem cells are distinguished by gene expression signatures. *Cell stem cell* 5: 111-23

Chitnis AB. 1999. Control of neurogenesis--lessons from frogs, fish and flies. *Current opinion in neurobiology* 9: 18-25

Cho JH, Johnson GV. 2003. Glycogen synthase kinase 3beta phosphorylates tau at both primed and unprimed sites. Differential impact on microtubule binding. *J Biol Chem* 278: 187-93

Choi HY, Liu Y, Tennert C, Sugiura Y, Karakatsani A, et al. 2013. APP interacts with LRP4 and agrin to coordinate the development of the neuromuscular junction in mice. *Elife* 2

Choi J, Ababon MR, Soliman M, Lin Y, Brzustowicz LM, et al. 2014. Autism associated gene, engrailed2, and flanking gene levels are altered in post-mortem cerebellum. *PloS one* 9: e87208

Citron M, Westaway D, Xia W, Carlson G, Diehl T, et al. 1997. Mutant presenilins of Alzheimer's disease increase production of 42-residue amyloid beta-protein in both transfected cells and transgenic mice. *Nature medicine* 3: 67-72

Colangelo V, Schurr J, Ball MJ, Pelaez RP, Bazan NG, Lukiw WJ. 2002. Gene expression profiling of 12633 genes in Alzheimer hippocampal CA1: transcription and neurotrophic factor down-regulation and up-regulation of apoptotic and pro-inflammatory signaling. *Journal of neuroscience research* 70: 462-73

Cole SL, Vassar R. 2008. The role of amyloid precursor protein processing by BACE1, the beta-secretase, in Alzheimer disease pathophysiology. *J Biol Chem* 283: 29621-5

Conti L, De Fraja C, Gulisano M, Migliaccio E, Govoni S, Cattaneo E. 1997. Expression and activation of SH2/PTB-containing ShcA adaptor protein reflects the pattern of neurogenesis in the mammalian brain. *Proceedings of the National Academy of Sciences of the United States of America* 94: 8185-90

Corbin JG, Gaiano N, Juliano SL, Poluch S, Stancik E, Haydar TF. 2008. Regulation of neural progenitor cell development in the nervous system. *Journal of neurochemistry* 106: 2272-87

Corder EH, Saunders AM, Strittmatter WJ, Schmechel DE, Gaskell PC, et al. 1993. Gene dose of apolipoprotein E type 4 allele and the risk of Alzheimer's disease in late onset families. *Science* 261: 921-3

Couillard-Despres S, Winner B, Schaubeck S, Aigner R, Vroemen M, et al. 2005. Doublecortin expression levels in adult brain reflect neurogenesis. *The European journal of neuroscience* 21: 1-14

Dean C, Liu H, Staudt T, Stahlberg MA, Vingill S, et al. 2012. Distinct subsets of Syt-IV/BDNF vesicles are sorted to axons versus dendrites and recruited to synapses by activity. *The Journal of neuroscience : the official journal of the Society for Neuroscience* 32: 5398-413

DeBoer EM, Azevedo R, Vega TA, Brodkin J, Akamatsu W, et al. 2014. Prenatal deletion of the RNA-binding protein HuD disrupts postnatal cortical circuit maturation and behavior. *The Journal of neuroscience : the official journal of the Society for Neuroscience* 34: 3674-86

Deng W, Aimone JB, Gage FH. 2010. New neurons and new memories: how does adult hippocampal neurogenesis affect learning and memory? *Nature Reviews Neuroscience* 11: 339-50

Dickerson BC, Salat DH, Greve DN, Chua EF, Rand-Giovannetti E, et al. 2005. Increased hippocampal activation in mild cognitive impairment compared to normal aging and AD. *Neurology* 65: 404-11

Doody GM, Care MA, Burgoyne NJ, Bradford JR, Bota M, et al. 2010. An extended set of PRDM1/BLIMP1 target genes links binding motif type to dynamic repression. *Nucleic acids research* 38: 5336-50

Dubuissez M, Faiderbe P, Pinte S, Dehennaut V, Rood BR, Leprince D. 2013. The Reelin receptors ApoER2 and VLDLR are direct target genes of HIC1 (Hypermethylated In Cancer 1). *Biochemical and biophysical research communications* 440: 424-30

Duering M, Grimm MOW, Grimm HS, Schroder J, Hartmann T. 2005. Mean age of onset in familial Alzheimer's disease is determined by amyloid beta 42. *Neurobiology of aging* 26: 785-88

Duyckaerts C, Delatour B, Potier MC. 2009. Classification and basic pathology of Alzheimer disease. *Acta Neuropathol* 118: 5-36

Elkabetz Y, Panagiotakos G, Al Shamy G, Socci ND, Tabar V, Studer L. 2008. Human ES cell-derived neural rosettes reveal a functionally distinct early neural stem cell stage. *Genes & development* 22: 152-65

Enarsson M, Erlandsson A, Larsson H, Forsberg-Nilsson K. 2002. Extracellular signal-regulated protein kinase signaling is uncoupled from initial differentiation of central nervous system stem cells to neurons. *Molecular cancer research : MCR* 1: 147-54

Ertekin-Taner N. 2007. Genetics of Alzheimer's disease: a centennial review. *Neurol Clin* 25: 611-67, v

Ertekin-Taner N. 2010. Genetics of Alzheimer disease in the pre- and post-GWAS era. *Alzheimers Res Ther* 2: 3

Faigle R, Song H. 2013. Signaling mechanisms regulating adult neural stem cells and neurogenesis. *Biochimica et biophysica acta* 1830: 2435-48

Fernandez-Chacon R, Konigstorfer A, Gerber SH, Garcia J, Matos MF, et al. 2001. Synaptotagmin I functions as a calcium regulator of release probability. *Nature* 410: 41-9

Franklin JL, Johnson EM, Jr. 1992. Suppression of programmed neuronal death by sustained elevation of cytoplasmic calcium. *Trends in neurosciences* 15: 501-8

Freeman RS, Estus S, Johnson EM, Jr. 1994. Analysis of cell cycle-related gene expression in postmitotic neurons: selective induction of Cyclin D1 during programmed cell death. *Neuron* 12: 343-55

Freude KK, Penjwini M, Davis JL, LaFerla FM, Blurton-Jones M. 2011. Soluble amyloid precursor protein induces rapid neural differentiation of human embryonic stem cells. *The Journal of biological chemistry* 286: 24264-74

Fukuhara S, Sako K, Noda K, Nagao K, Miura K, Mochizuki N. 2009. Tie2 is tied at the cell-cell contacts and to extracellular matrix by angiopoietin-1. *Experimental & molecular medicine* 41: 133-9

Fuster-Matanzo A, de Barreda EG, Dawson HN, Vitek MP, Avila J, Hernandez F. 2009. Function of tau protein in adult newborn neurons. *FEBS letters* 583: 3063-8

Gaulden J, Reiter JF. 2008. Neur-ons and neur-offs: regulators of neural induction in vertebrate embryos and embryonic stem cells. *Human molecular genetics* 17: R60-6

Ghil S, McCoy KL, Hepler JR. 2014. Regulator of G Protein Signaling 2 (RGS2) and RGS4 Form Distinct G Protein-Dependent Complexes with Protease Activated-Receptor 1 (PAR1) in Live Cells. *PloS one* 9: e95355

Giachino C, Taylor V. 2014. Notching up neural stem cell homogeneity in homeostasis and disease. *Frontiers in neuroscience* 8: 32

Gil SY, Youn BS, Byun K, Huang H, Namkoong C, et al. 2013. Clusterin and LRP2 are critical components of the hypothalamic feeding regulatory pathway. *Nature communications* 4: 1862

Ginsberg SD, Hemby SE, Lee VM, Eberwine JH, Trojanowski JQ. 2000. Expression profile of transcripts in Alzheimer's disease tangle-bearing CA1 neurons. *Annals of neurology* 48: 77-87

Gleeson JG, Lin PT, Flanagan LA, Walsh CA. 1999. Doublecortin is a microtubule-associated protein and is expressed widely by migrating neurons. *Neuron* 23: 257-71

Glickstein SB, Monaghan JA, Koeller HB, Jones TK, Ross ME. 2009. Cyclin D2 is critical for intermediate progenitor cell proliferation in the embryonic cortex. *The Journal of neuroscience : the official journal of the Society for Neuroscience* 29: 9614-24

Gobbi P, Castaldo P, Minelli A, Salucci S, Magi S, et al. 2007. Mitochondrial localization of Na+/Ca2+ exchangers NCX1-3 in neurons and astrocytes of adult rat brain in situ. *Pharmacological research : the official journal of the Italian Pharmacological Society* 56: 556-65

Gomez-Isla T, Price JL, McKeel DW, Jr., Morris JC, Growdon JH, Hyman BT. 1996. Profound loss of layer II entorhinal cortex neurons occurs in very mild Alzheimer's disease. *J Neurosci* 16: 4491-500

Gomez-Pinilla F, Cummings BJ, Cotman CW. 1990. Induction of basic fibroblast growth factor in Alzheimer's disease pathology. *Neuroreport* 1: 211-4

Goodison S, Urquidi V, Tarin D. 1999. CD44 cell adhesion molecules. *Molecular pathology : MP* 52: 189-96

Gotz M, Huttner WB. 2005. The cell biology of neurogenesis. *Nature reviews. Molecular cell biology* 6: 777-88

Gould J, Getz G, Monti S, Reich M, Mesirov JP. 2006. Comparative gene marker selection suite. *Bioinformatics* 22: 1924-5

Grundke-Iqbal I, Iqbal K, Tung YC, Quinlan M, Wisniewski HM, Binder LI. 1986. Abnormal phosphorylation of the microtubule-associated protein tau (tau) in Alzheimer cytoskeletal pathology. *Proc Natl Acad Sci U S A* 83: 4913-7

Guillemot F. 2005. Cellular and molecular control of neurogenesis in the mammalian telencephalon. *Current opinion in cell biology* 17: 639-47

Hafez DM, Huang JY, Richardson JC, Masliah E, Peterson DA, Marr RA. 2012. F-spondin gene transfer improves memory performance and reduces amyloid-beta levels in mice. *Neuroscience* 223: 465-72

Hajjar KA, Krishnan S. 1999. Annexin II: a mediator of the plasmin/plasminogen activator system. *Trends in cardiovascular medicine* 9: 128-38

Hamalainen A, Pihlajamaki M, Tanila H, Hanninen T, Niskanen E, et al. 2007. Increased fMRI responses during encoding in mild cognitive impairment. *Neurobiology of aging* 28: 1889-903

Hanger DP, Anderton BH, Noble W. 2009. Tau phosphorylation: the therapeutic challenge for neurodegenerative disease. *Trends Mol Med* 15: 112-9

Haque T, Nakada S, Hamdy RC. 2007. A review of FGF18: Its expression, signaling pathways and possible functions during embryogenesis and post-natal development. *Histology and histopathology* 22: 97-105

Hardy J, Selkoe DJ. 2002. The amyloid hypothesis of Alzheimer's disease: progress and problems on the road to therapeutics. *Science* 297: 353-6

Haubensak W, Attardo A, Denk W, Huttner WB. 2004. Neurons arise in the basal neuroepithelium of the early mammalian telencephalon: a major site of neurogenesis. *Proceedings of the National Academy of Sciences of the United States of America* 101: 3196-201

Hebert LE, Scherr PA, Bienias JL, Bennett DA, Evans DA. 2003. Alzheimer disease in the US population: prevalence estimates using the 2000 census. *Arch Neurol* 60: 1119-22

Helias-Rodzewicz Z, Perot G, Chibon F, Ferreira C, Lagarde P, et al. 2010. YAP1 and VGLL3, encoding two cofactors of TEAD transcription factors, are amplified and overexpressed in a subset of soft tissue sarcomas. *Genes, chromosomes & cancer* 49: 1161-71

Hellstrom-Lindahl E, Viitanen M, Marutle A. 2009. Comparison of Abeta levels in the brain of familial and sporadic Alzheimer's disease. *Neurochemistry international* 55: 243-52

Henke RM, Meredith DM, Borromeo MD, Savage TK, Johnson JE. 2009. Ascl1 and Neurog2 form novel complexes and regulate Delta-like3 (Dll3) expression in the neural tube. *Developmental biology* 328: 529-40

Herring A, Donath A, Steiner KM, Widera MP, Hamzehian S, et al. 2012. Reelin Depletion is an Early Phenomenon of Alzheimer's Pathology. *Journal of Alzheimers Disease* 30: 963-79

Herrup K, Yang Y. 2007. Cell cycle regulation in the postmitotic neuron: oxymoron or new biology? *Nature reviews. Neuroscience* 8: 368-78

Herwig S, Strauss M. 1997. The retinoblastoma protein: a master regulator of cell cycle, differentiation and apoptosis. *European journal of biochemistry / FEBS* 246: 581-601

Hirate Y, Okamoto H. 2006. Canopy1, a novel regulator of FGF signaling around the midbrain-hindbrain boundary in zebrafish. *Current biology : CB* 16: 421-7

Hixson JE, Vernier DT. 1990. Restriction isotyping of human apolipoprotein E by gene amplification and cleavage with HhaI. *Journal of lipid research* 31: 545-8

Hodge RD, Kowalczyk TD, Wolf SA, Encinas JM, Rippey C, et al. 2008. Intermediate progenitors in adult hippocampal neurogenesis: Tbr2 expression and coordinate regulation of neuronal output. *The Journal of neuroscience : the official journal of the Society for Neuroscience* 28: 3707-17

Hoe HS, Lee KJ, Carney RS, Lee J, Markova A, et al. 2009. Interaction of reelin with amyloid precursor protein promotes neurite outgrowth. *The Journal of neuroscience : the official journal of the Society for Neuroscience* 29: 7459-73

Hoe HS, Rebeck GW. 2008. Functional interactions of APP with the apoE receptor family. *Journal of neurochemistry* 106: 2263-71

Hoe HS, Wessner D, Beffert U, Becker AG, Matsuoka Y, Rebeck GW. 2005. F-spondin interaction with the apolipoprotein E receptor ApoEr2 affects processing of amyloid precursor protein. *Molecular and cellular biology* 25: 9259-68

Holtzman DM, Herz J, Bu G. 2012. Apolipoprotein E and apolipoprotein E receptors: normal biology and roles in Alzheimer disease. *Cold Spring Harbor perspectives in medicine* 2: a006312

Hotta A, Ellis J. 2008. Retroviral vector silencing during iPS cell induction: an epigenetic beacon that signals distinct pluripotent states. *Journal of cellular biochemistry* 105: 940-8

Huang da W, Sherman BT, Lempicki RA. 2009a. Bioinformatics enrichment tools: paths toward the comprehensive functional analysis of large gene lists. *Nucleic acids research* 37: 1-13

Huang da W, Sherman BT, Lempicki RA. 2009b. Systematic and integrative analysis of large gene lists using DAVID bioinformatics resources. *Nature protocols* 4: 44-57

Huang DC, O'Reilly LA, Strasser A, Cory S. 1997. The anti-apoptosis function of Bcl-2 can be genetically separated from its inhibitory effect on cell cycle entry. *The EMBO journal* 16: 4628-38

Hurt CM, Bjork S, Ho VK, Gilsbach R, Hein L, Angelotti T. 2014. REEP1 and REEP2 proteins are preferentially expressed in neuronal and neuronal-like exocytotic tissues. *Brain research* 1545: 12-22

Huttner WB, Kosodo Y. 2005. Symmetric versus asymmetric cell division during neurogenesis in the developing vertebrate central nervous system. *Current opinion in cell biology* 17: 648-57

Hyman BT, Van Hoesen GW, Damasio AR, Barnes CL. 1984. Alzheimer's disease: cell-specific pathology isolates the hippocampal formation. *Science* 225: 1168-70

Imayoshi I, Isomura A, Harima Y, Kawaguchi K, Kori H, et al. 2013. Oscillatory control of factors determining multipotency and fate in mouse neural progenitors. *Science* 342: 1203-8

Inestrosa NC, Varela-Nallar L. 2014. Wnt signaling in the nervous system and in Alzheimer's disease. *Journal of molecular cell biology* 6: 64-74

Inoue T, Ota M, Ogawa M, Mikoshiba K, Aruga J. 2007. Zic1 and Zic3 regulate medial forebrain development through expansion of neuronal progenitors. *The Journal of neuroscience : the official journal of the Society for Neuroscience* 27: 5461-73

Irizarry RA, Bolstad BM, Collin F, Cope LM, Hobbs B, Speed TP. 2003a. Summaries of Affymetrix GeneChip probe level data. *Nucleic acids research* 31: e15

Irizarry RA, Hobbs B, Collin F, Beazer-Barclay YD, Antonellis KJ, et al. 2003b. Exploration, normalization, and summaries of high density oligonucleotide array probe level data. *Biostatistics* 4: 249-64

Israel MA, Yuan SH, Bardy C, Reyna SM, Mu Y, et al. 2012. Probing sporadic and familial Alzheimer's disease using induced pluripotent stem cells. *Nature* 482: 216-20

Iwatsubo T, Odaka A, Suzuki N, Mizusawa H, Nukina N, Ihara Y. 1994. Visualization of A beta 42(43) and A beta 40 in senile plaques with end-specific A beta monoclonals: evidence that an initially deposited species is A beta 42(43). *Neuron* 13: 45-53

Jahanshad N, Rajagopalan P, Hua X, Hibar DP, Nir TM, et al. 2013. Genome-wide scan of healthy human connectome discovers SPON1 gene variant influencing dementia severity. *Proceedings of the National Academy of Sciences of the United States of America* 110: 4768-73

Jalink K, Moolenaar WH. 1992. Thrombin receptor activation causes rapid neural cell rounding and neurite retraction independent of classic second messengers. *The Journal of cell biology* 118: 411-9

Jessell TS, JR. 2000. The Development of the Nervous System In *The Principles of Neuroscience*, ed. ES Kandel, JH Jessell, TM. United States: McGraw-Hill

Jhas S, Ciura S, Belanger-Jasmin S, Dong Z, Llamosas E, et al. 2006. Hes6 inhibits astrocyte differentiation and promotes neurogenesis through different mechanisms. *The Journal of neuroscience : the official journal of the Society for Neuroscience* 26: 11061-71

Ji CN, Chen JZ, Xie Y, Wang S, Qian J, et al. 2003. A novel cDNA encodes a putative hRALY-like protein, hRALYL. *Molecular biology reports* 30: 61-7

Jiang S, Li Y, Zhang X, Bu G, Xu H, Zhang YW. 2014. Trafficking regulation of proteins in Alzheimer's disease. *Molecular neurodegeneration* 9: 6

Jin KL, Peel AL, Mao XO, Xie L, Cottrell BA, et al. 2004. Increased hippocampal neurogenesis in Alzheimer's disease. *Proceedings of the National Academy of Sciences of the United States of America* 101: 343-47

Johnson R, Teh CH, Kunarso G, Wong KY, Srinivasan G, et al. 2008. REST regulates distinct transcriptional networks in embryonic and neural stem cells. *PLoS biology* 6: e256

Jones FS, Meech R. 1999. Knockout of REST/NRSF shows that the protein is a potent repressor of neuronally expressed genes in non-neural tissues. *BioEssays : news and reviews in molecular, cellular and developmental biology* 21: 372-6

Jousse C, Deval C, Maurin AC, Parry L, Cherasse Y, et al. 2007. TRB3 inhibits the transcriptional activation of stress-regulated genes by a negative feedback on the ATF4 pathway. *The Journal of biological chemistry* 282: 15851-61

Kaech S, Banker G. 2006. Culturing hippocampal neurons. *Nature protocols* 1: 2406-15

Kageyama R, Ohtsuka T, Shimojo H, Imayoshi I. 2009. Dynamic regulation of Notch signaling in neural progenitor cells. *Current opinion in cell biology* 21: 733-40

Kane CJ, Brown GJ, Phelan KD. 1996. Transforming growth factor-beta 2 both stimulates and inhibits neurogenesis of rat cerebellar granule cells in culture. *Brain research. Developmental brain research* 96: 46-51

Kaspar JW, Niture SK, Jaiswal AK. 2009. Nrf2:INrf2 (Keap1) signaling in oxidative stress. *Free radical biology & medicine* 47: 1304-9

Kempermann G, Jessberger S, Steiner B, Kronenberg G. 2004. Milestones of neuronal development in the adult hippocampus. *Trends in neurosciences* 27: 447-52

Kerchner GA, Hess CP, Hammond-Rosenbluth KE, Xu D, Rabinovici GD, et al. 2010. Hippocampal CA1 apical neuropil atrophy in mild Alzheimer disease visualized with 7-T MRI. *Neurology* 75: 1381-7

Khan UA, Liu L, Provenzano FA, Berman DE, Profaci CP, et al. 2014. Molecular drivers and cortical spread of lateral entorhinal cortex dysfunction in preclinical Alzheimer's disease. *Nature neuroscience* 17: 304-11

Kirkby DL, Higgins GA. 1998. Characterization of perforant path lesions in rodent models of memory and attention. *Eur J Neurosci* 10: 823-38

Kitchens DL, Snyder EY, Gottlieb DI. 1994. FGF and EGF are mitogens for immortalized neural progenitors. *Journal of neurobiology* 25: 797-807

Kondo T, Asai M, Tsukita K, Kutoku Y, Ohsawa Y, et al. 2013. Modeling Alzheimer's disease with iPSCs reveals stress phenotypes associated with intracellular Abeta and differential drug responsiveness. *Cell stem cell* 12: 487-96

Kordower JH, Chu Y, Stebbins GT, DeKosky ST, Cochran EJ, et al. 2001. Loss and atrophy of layer II entorhinal cortex neurons in elderly people with mild cognitive impairment. *Ann Neurol* 49: 202-13

Kovacs T, Cairns NJ, Lantos PL. 2001. Olfactory centres in Alzheimer's disease: olfactory bulb is involved in early Braak's stages. *Neuroreport* 12: 285-88

Kowalczyk T, Pontious A, Englund C, Daza RA, Bedogni F, et al. 2009. Intermediate neuronal progenitors (basal progenitors) produce pyramidal-projection neurons for all layers of cerebral cortex. *Cereb Cortex* 19: 2439-50

Kriegstein A, Noctor S, Martinez-Cerdeno V. 2006. Patterns of neural stem and progenitor cell division may underlie evolutionary cortical expansion. *Nature reviews. Neuroscience* 7: 883-90

Kuehn H, Liberzon A, Reich M, Mesirov JP. 2008. Using GenePattern for gene expression analysis. *Current protocols in bioinformatics / editoral board, Andreas D. Baxevanis ... [et al.]* Chapter 7: Unit 7 12

Lambert JC, Ibrahim-Verbaas CA, Harold D, Naj AC, Sims R, et al. 2013. Meta-analysis of 74,046 individuals identifies 11 new susceptibility loci for Alzheimer's disease. *Nature genetics* 45: 1452-U206

Lau LF. 2011. CCN1/CYR61: the very model of a modern matricellular protein. *Cellular and molecular life sciences : CMLS* 68: 3149-63

Le Belle JE, Orozco NM, Paucar AA, Saxe JP, Mottahedeh J, et al. 2011. Proliferative neural stem cells have high endogenous ROS levels that regulate self-renewal and neurogenesis in a PI3K/Akt-dependant manner. *Cell stem cell* 8: 59-71

Leeb C, Eresheim C, Nimpf J. 2014. Clusterin is a ligand for apolipoprotein E receptor 2 (ApoER2) and very low density lipoprotein receptor (VLDLR) and signals via the Reelin-signaling pathway. *The Journal of biological chemistry* 289: 4161-72

Leipzig ND, Xu C, Zahir T, Shoichet MS. 2010. Functional immobilization of interferon-gamma induces neuronal differentiation of neural stem cells. *Journal of biomedical materials research. Part A* 93: 625-33

Lerou PH, Yabuuchi A, Huo H, Miller JD, Boyer LF, et al. 2008. Derivation and maintenance of human embryonic stem cells from poor-quality in vitro fertilization embryos. *Nature protocols* 3: 923-33

Leroy K, Ando K, Laporte V, Dedecker R, Suain V, et al. 2012. Lack of tau proteins rescues neuronal cell death and decreases amyloidogenic processing of APP in APP/PS1 mice. *The American journal of pathology* 181: 1928-40

Leroy K, Yilmaz Z, Brion JP. 2007. Increased level of active GSK-3beta in Alzheimer's disease and accumulation in argyrophilic grains and in neurones at different stages of neurofibrillary degeneration. *Neuropathology and applied neurobiology* 33: 43-55

Lessard J, Wu JI, Ranish JA, Wan M, Winslow MM, et al. 2007. An essential switch in subunit composition of a chromatin remodeling complex during neural development. *Neuron* 55: 201-15

Li C, Wong WH. 2001. Model-based analysis of oligonucleotide arrays: expression index computation and outlier detection. *Proceedings of the National Academy of Sciences of the United States of America* 98: 31-6

Li G, Bien-Ly N, Andrews-Zwilling Y, Xu Q, Bernardo A, et al. 2009a. GABAergic interneuron dysfunction impairs hippocampal neurogenesis in adult apolipoprotein E4 knockin mice. *Cell stem cell* 5: 634-45

Li H, Liu H, Corrales CE, Risner JR, Forrester J, et al. 2009b. Differentiation of neurons from neural precursors generated in floating spheres from embryonic stem cells. *BMC neuroscience* 10: 122

Li L, Walker TL, Zhang Y, Mackay EW, Bartlett PF. 2010. Endogenous interferon gamma directly regulates neural precursors in the non-inflammatory brain. *The Journal of neuroscience : the official journal of the Society for Neuroscience* 30: 9038-50

Li S, Stys PK. 2000. Mechanisms of ionotropic glutamate receptor-mediated excitotoxicity in isolated spinal cord white matter. *The Journal of neuroscience : the official journal of the Society for Neuroscience* 20: 1190-8

Lim LS, Loh YH, Zhang W, Li Y, Chen X, et al. 2007. Zic3 is required for maintenance of pluripotency in embryonic stem cells. *Molecular biology of the cell* 18: 1348-58

Lim Y, Lim ST, Tomar A, Gardel M, Bernard-Trifilo JA, et al. 2008. PyK2 and FAK connections to p190Rho guanine nucleotide exchange factor regulate RhoA activity, focal adhesion formation, and cell motility. *The Journal of cell biology* 180: 187-203

Lister R, Pelizzola M, Kida YS, Hawkins RD, Nery JR, et al. 2011. Hotspots of aberrant epigenomic reprogramming in human induced pluripotent stem cells. *Nature* 471: 68-73

Liu DX, Greene LA. 2001. Neuronal apoptosis at the G1/S cell cycle checkpoint. *Cell and tissue research* 305: 217-28

Liu Y, Stack SM, Lakka SS, Khan AJ, Woodley DT, et al. 1999. Matrix localization of tissue factor pathway inhibitor-2/matrix-associated serine protease inhibitor (TFPI-2/MSPI) involves arginine-mediated ionic interactions with heparin and dermatan sulfate: heparin accelerates the activity of TFPI-2/MSPI toward plasmin. *Archives of biochemistry and biophysics* 370: 112-8

Lu T, Aron L, Zullo J, Pan Y, Kim H, et al. 2014. REST and stress resistance in ageing and Alzheimer's disease. *Nature* 507: 448-54

Lu Y, Tian QB, Endo S, Suzuki T. 2007. A role for LRP4 in neuronal cell viability is related to apoE-binding. *Brain research* 1177: 19-28

Mandell JW, Banker GA. 1996. A spatial gradient of tau protein phosphorylation in nascent axons. *The Journal of neuroscience : the official journal of the Society for Neuroscience* 16: 5727-40

Marchetto MC, Carromeu C, Acab A, Yu D, Yeo GW, et al. 2010. A model for neural development and treatment of Rett syndrome using human induced pluripotent stem cells. *Cell* 143: 527-39

Martinez-Herrero S, Larrayoz IM, Ochoa-Callejero L, Garcia-Sanmartin J, Martinez A. 2012. Adrenomedullin as a growth and cell fate regulatory factor for adult neural stem cells. *Stem cells international* 2012: 804717

Matyash V, Kettenmann H. 2010. Heterogeneity in astrocyte morphology and physiology. *Brain research reviews* 63: 2-10

McGowan E, Pickford F, Kim J, Onstead L, Eriksen J, et al. 2005. Abeta42 is essential for parenchymal and vascular amyloid deposition in mice. *Neuron* 47: 191-9

McLaughlin JN, Mazzoni MR, Cleator JH, Earls L, Perdigoto AL, et al. 2005. Thrombin modulates the expression of a set of genes including thrombospondin-1 in human microvascular endothelial cells. *The Journal of biological chemistry* 280: 22172-80

Methot N, Rubin J, Guay D, Beaulieu C, Ethier D, et al. 2007. Inhibition of the activation of multiple serine proteases with a cathepsin C inhibitor requires sustained exposure to prevent pro-enzyme processing. *The Journal of biological chemistry* 282: 20836-46

Moon C, Yoo JY, Matarazzo V, Sung YK, Kim EJ, Ronnett GV. 2002. Leukemia inhibitory factor inhibits neuronal terminal differentiation through STAT3 activation. *Proceedings of the National Academy of Sciences of the United States of America* 99: 9015-20

Mulligan P, Westbrook TF, Ottinger M, Pavlova N, Chang B, et al. 2008. CDYL bridges REST and histone methyltransferases for gene repression and suppression of cellular transformation. *Molecular cell* 32: 718-26

Muratore CR, Rice HC, Srikanth P, Callahan DG, Shin T, et al. 2014. The familial Alzheimer's disease APPV717I mutation alters APP processing and Tau expression in iPSC-derived neurons. *Human molecular genetics*

Nagasaka Y, Dillner K, Ebise H, Teramoto R, Nakagawa H, et al. 2005. A unique gene expression signature discriminates familial Alzheimer's disease mutation carriers from their wild-type siblings. *Proceedings of the National Academy of Sciences of the United States of America* 102: 14854-9

Nagy Z, Esiri MM, Cato AM, Smith AD. 1997. Cell cycle markers in the hippocampus in Alzheimer's disease. *Acta neuropathologica* 94: 6-15

Nakamura M, Choe SK, Runko AP, Gardner PD, Sagerstrom CG. 2008. Nlz1/Znf703 acts as a repressor of transcription. *BMC developmental biology* 8: 108

Newman AM, Cooper JB. 2010. Lab-specific gene expression signatures in pluripotent stem cells. *Cell stem cell* 7: 258-62

Nikolaev A, McLaughlin T, O'Leary DD, Tessier-Lavigne M. 2009. APP binds DR6 to trigger axon pruning and neuron death via distinct caspases. *Nature* 457: 981-9

Nikolic M. 2004. The molecular mystery of neuronal migration: FAK and Cdk5. *Trends in cell biology* 14: 1-5

Nishimura N, Araki K, Shinahara W, Nakano Y, Nishimura K, et al. 2008. Interaction of Rab3B with microtubule-binding protein Gas8 in NIH 3T3 cells. *Archives of biochemistry and biophysics* 474: 136-42

Nunan J, Small DH. 2000. Regulation of APP cleavage by alpha-, beta- and gamma-secretases. *FEBS letters* 483: 6-10

Oddo S, Caccamo A, Shepherd JD, Murphy MP, Golde TE, et al. 2003. Triple-transgenic model of Alzheimer's disease with plaques and tangles: intracellular Abeta and synaptic dysfunction. *Neuron* 39: 409-21

Offe K, Dodson SE, Shoemaker JT, Fritz JJ, Gearing M, et al. 2006. The lipoprotein receptor LR11 regulates amyloid beta production and amyloid precursor protein traffic in endosomal compartments. *The Journal of neuroscience : the official journal of the Society for Neuroscience* 26: 1596-603

Olbrich HG, Braak H. 1985. Ratio of pyramidal cells versus non-pyramidal cells in sector CA1 of the human Ammon's horn. *Anatomy and embryology* 173: 105-10

Olsen O, Kallop DY, McLaughlin T, Huntwork-Rodriguez S, Wu Z, et al. 2014. Genetic Analysis Reveals that Amyloid Precursor Protein and Death Receptor 6 Function in the Same Pathway to Control Axonal Pruning Independent of beta-Secretase. *The Journal of neuroscience : the official journal of the Society for Neuroscience* 34: 6438-47

Pang PT, Teng HK, Zaitsev E, Woo NT, Sakata K, et al. 2004. Cleavage of proBDNF by tPA/plasmin is essential for long-term hippocampal plasticity. *Science* 306: 487-91

Pang ZP, Yang N, Vierbuchen T, Ostermeier A, Fuentes DR, et al. 2011. Induction of human neuronal cells by defined transcription factors. *Nature* 476: 220-3

Park IH, Lerou PH, Zhao R, Huo H, Daley GQ. 2008a. Generation of human-induced pluripotent stem cells. *Nature protocols* 3: 1180-6

Park IH, Zhao R, West JA, Yabuuchi A, Huo H, et al. 2008b. Reprogramming of human somatic cells to pluripotency with defined factors. *Nature* 451: 141-6

Perez-Palma E, Bustos BI, Villaman CF, Alarcon MA, Avila ME, et al. 2014. Overrepresentation of glutamate signaling in Alzheimer's disease: network-based pathway enrichment using meta-analysis of genome-wide association studies. *PloS one* 9: e95413

Perry EK, Johnson M, Ekonomou A, Perry RH, Ballard C, Attems J. 2012. Neurogenic abnormalities in Alzheimer's disease differ between stages of neurogenesis and are partly related to cholinergic pathology. *Neurobiology of disease* 47: 155-62

Philips MA, Lillevali K, Heinla I, Luuk H, Hundahl CA, et al. 2014. Lsamp is implicated in the regulation of emotional and social behavior by use of alternative promoters in the brain. *Brain structure & function*

Polager S, Ginsberg D. 2009. p53 and E2f: partners in life and death. *Nature reviews. Cancer* 9: 738-48

Pommier Y. 2006. Topoisomerase I inhibitors: camptothecins and beyond. *Nature reviews. Cancer* 6: 789-802

Price JL, Morris JC. 1999. Tangles and plaques in nondemented aging and "preclinical" Alzheimer's disease. *Annals of neurology* 45: 358-68

Pruszak J, Ludwig W, Blak A, Alavian K, Isacson O. 2009. CD15, CD24, and CD29 define a surface biomarker code for neural lineage differentiation of stem cells. *Stem Cells* 27: 2928-40

Pujadas L, Rossi D, Andres R, Teixeira CM, Serra-Vidal B, et al. 2014. Reelin delays amyloid-beta fibril formation and rescues cognitive deficits in a model of Alzheimer's disease. *Nature communications* 5: 3443

Putcha D, Brickhouse M, O'Keefe K, Sullivan C, Rentz D, et al. 2011. Hippocampal hyperactivation associated with cortical thinning in Alzheimer's disease signature regions in non-demented elderly adults. *The Journal of neuroscience : the official journal of the Society for Neuroscience* 31: 17680-8

Qiang L, Fujita R, Yamashita T, Angulo S, Rhinn H, et al. 2011. Directed conversion of Alzheimer's disease patient skin fibroblasts into functional neurons. *Cell* 146: 359-71

Qiu C, Kivipelto M, von Strauss E. 2009. Epidemiology of Alzheimer's disease: occurrence, determinants, and strategies toward intervention. *Dialogues in clinical neuroscience* 11: 111-28

Rankin CA, Sun Q, Gamblin TC. 2005. Pseudo-phosphorylation of tau at Ser202 and Thr205 affects tau filament formation. *Brain research. Molecular brain research* 138: 84-93

Rengaraj D, Lee BR, Park KJ, Lee SI, Kang KS, et al. 2011. The distribution of neuron-specific gene family member 1 in brain and germ cells: Implications for the regulation of germ-line development by brain. *Developmental dynamics : an official publication of the American Association of Anatomists* 240: 850-61

Rescher U, Ludwig C, Konietzko V, Kharitonenkov A, Gerke V. 2008. Tyrosine phosphorylation of annexin A2 regulates Rho-mediated actin rearrangement and cell adhesion. *Journal of cell science* 121: 2177-85

Resende R, Ferreiro E, Pereira C, Oliveira CR. 2008. ER stress is involved in Abeta-induced GSK-3beta activation and tau phosphorylation. *Journal of neuroscience research* 86: 2091-9

Richards AJ, McNinch A, Martin H, Oakhill K, Rai H, et al. 2010. Stickler syndrome and the vitreous phenotype: mutations in COL2A1 and COL11A1. *Human mutation* 31: E1461-71

Rodriguez-Grande B, Swana M, Nguyen L, Englezou P, Maysami S, et al. 2014. The acute-phase protein PTX3 is an essential mediator of glial scar formation and resolution of brain edema after ischemic injury. *Journal of cerebral blood flow and metabolism : official journal of the International Society of Cerebral Blood Flow and Metabolism* 34: 480-8

Rodriguez JJ, Jones VC, Tabuchi M, Allan SM, Knight EM, et al. 2008. Impaired adult neurogenesis in the dentate gyrus of a triple transgenic mouse model of Alzheimer's disease. *PloS one* 3: e2935

Rogaeva E, Meng Y, Lee JH, Gu Y, Kawarai T, et al. 2007. The neuronal sortilin-related receptor SORL1 is genetically associated with Alzheimer disease. *Nature genetics* 39: 168-77

Rohatgi T, Sedehizade F, Reymann KG, Reiser G. 2004. Protease-activated receptors in neuronal development, neurodegeneration, and neuroprotection: thrombin as signaling molecule in the brain. *The Neuroscientist : a review journal bringing neurobiology, neurology and psychiatry* 10: 501-12

Rosa AI, Goncalves J, Cortes L, Bernardino L, Malva JO, Agasse F. 2010. The angiogenic factor angiopoietin-1 is a proneurogenic peptide on subventricular zone stem/progenitor cells. *The Journal of neuroscience : the official journal of the Society for Neuroscience* 30: 4573-84

Ruiz J, Kouiavskaia D, Migliorini M, Robinson S, Saenko EL, et al. 2005. The apoE isoform binding properties of the VLDL receptor reveal marked differences from LRP and the LDL receptor. *Journal of lipid research* 46: 1721-31

Saitoh O, Kubo Y, Miyatani Y, Asano T, Nakata H. 1997. RGS8 accelerates G-protein-mediated modulation of K+ currents. *Nature* 390: 525-9

Sasaki T, Kitagawa K, Yagita Y, Sugiura S, Omura-Matsuoka E, et al. 2006. Bcl2 enhances survival of newborn neurons in the normal and ischemic hippocampus. *Journal of neuroscience research* 84: 1187-96

Scahill RI, Schott JM, Stevens JM, Rossor MN, Fox NC. 2002. Mapping the evolution of regional atrophy in Alzheimer's disease: unbiased analysis of fluid-registered serial MRI. *Proceedings of the National Academy of Sciences of the United States of America* 99: 4703-7

Schoenherr CJ, Anderson DJ. 1995. The neuron-restrictive silencer factor (NRSF): a coordinate repressor of multiple neuron-specific genes. *Science* 267: 1360-3

Schubert D, Herrera F, Cumming R, Read J, Low W, et al. 2009. Neural cells secrete a unique repertoire of proteins. *Journal of neurochemistry* 109: 427-35

Seki T, Sato T, Toda K, Osumi N, Imura T, Shioda S. 2014. Distinctive population of Gfap-expressing neural progenitors arising around the dentate notch migrate and form the granule cell layer in the developing hippocampus. *The Journal of comparative neurology* 522: 261-83

Sessa A, Mao CA, Colasante G, Nini A, Klein WH, Broccoli V. 2010. Tbr2-positive intermediate (basal) neuronal progenitors safeguard cerebral cortex expansion by controlling amplification of pallial glutamatergic neurons and attraction of subpallial GABAergic interneurons. *Genes & development* 24: 1816-26

Sherrington R, Rogaev EI, Liang Y, Rogaeva EA, Levesque G, et al. 1995. Cloning of a gene bearing missense mutations in early-onset familial Alzheimer's disease. *Nature* 375: 754-60

Shin S, Mitalipova M, Noggle S, Tibbitts D, Venable A, et al. 2006. Long-term proliferation of human embryonic stem cell-derived neuroepithelial cells using defined adherent culture conditions. *Stem Cells* 24: 125-38

Sies H. 2014. Role of Metabolic H2O2 Generation: REDOX SIGNALING AND OXIDATIVE STRESS. *The Journal of biological chemistry* 289: 8735-41

Sleegers K, Brouwers N, Gijselinck I, Theuns J, Goossens D, et al. 2006. APP duplication is sufficient to cause early onset Alzheimer's dementia with cerebral amyloid angiopathy. *Brain : a journal of neurology* 129: 2977-83

Snowdon DA, Greiner LH, Markesbery WR. 2000. Linguistic ability in early life and the neuropathology of Alzheimer's disease and cerebrovascular disease. Findings from the Nun Study. *Annals of the New York Academy of Sciences* 903: 34-8

Sobczak A, Debowska K, Blazejczyk M, Kreutz MR, Kuznicki J, Wojda U. 2011. Calmyrin1 binds to SCG10 protein (stathmin2) to modulate neurite outgrowth. *Biochimica et biophysica acta* 1813: 1025-37

Soleman S, Filippov MA, Dityatev A, Fawcett JW. 2013. Targeting the neural extracellular matrix in neurological disorders. *Neuroscience* 253: 194-213

Sotthibundhu A, Li QX, Thangnipon W, Coulson EJ. 2009. A beta(1-42) stimulates adult SVZ neurogenesis through the p75 neurotrophin receptor. *Neurobiology of aging* 30: 1975-85

Spalding KL, Bergmann O, Alkass K, Bernard S, Salehpour M, et al. 2013. Dynamics of Hippocampal Neurogenesis in Adult Humans. *Cell* 153: 1219-27

Spiliotopoulos D, Goffredo D, Conti L, Di Febo F, Biella G, et al. 2009. An optimized experimental strategy for efficient conversion of embryonic stem (ES)-derived mouse neural stem (NS) cells into a nearly homogeneous mature neuronal population. *Neurobiology of disease* 34: 320-31

Spillantini MG, Murrell JR, Goedert M, Farlow MR, Klug A, Ghetti B. 1998. Mutation in the tau gene in familial multiple system tauopathy with presenile dementia. *Proc Natl Acad Sci U S A* 95: 7737-41

Sproul AA, Jacob S, Pre D, Kim SH, Nestor MW, et al. 2014. Characterization and molecular profiling of PSEN1 familial Alzheimer's disease iPSC-derived neural progenitors. *PloS one* 9: e84547

St George-Hyslop PH, Tanzi RE, Polinsky RJ, Haines JL, Nee L, et al. 1987. The genetic defect causing familial Alzheimer's disease maps on chromosome 21. *Science* 235: 885-90

Storey JD, Tibshirani R. 2003. Statistical significance for genomewide studies. *Proceedings of the National Academy of Sciences of the United States of America* 100: 9440-5

Stouffer GA, Runge MS. 1998. The role of secondary growth factor production in thrombin-induced proliferation of vascular smooth muscle cells. *Seminars in thrombosis and hemostasis* 24: 145-50

Sun J, Li R. 2010. Human negative elongation factor activates transcription and regulates alternative transcription initiation. *The Journal of biological chemistry* 285: 6443-52

Suter DM, Tirefort D, Julien S, Krause KH. 2009. A Sox1 to Pax6 switch drives neuroectoderm to radial glia progression during differentiation of mouse embryonic stem cells. *Stem Cells* 27: 49-58

Suto F, Ito K, Uemura M, Shimizu M, Shinkawa Y, et al. 2005. Plexin-a4 mediates axon-repulsive activities of both secreted and transmembrane semaphorins and plays roles in nerve fiber guidance. *The Journal of neuroscience : the official journal of the Society for Neuroscience* 25: 3628-37

Suzuki N, Numakawa T, Chou J, de Vega S, Mizuniwa C, et al. 2014. Teneurin-4 promotes cellular protrusion formation and neurite outgrowth through focal adhesion kinase signaling. *FASEB journal : official publication of the Federation of American Societies for Experimental Biology* 28: 1386-97

Swistowski A, Peng J, Han Y, Swistowska AM, Rao MS, Zeng X. 2009. Xeno-free defined conditions for culture of human embryonic stem cells, neural stem cells and dopaminergic neurons derived from them. *PloS one* 4: e6233

Takahashi H, Liu FC. 2006. Genetic patterning of the mammalian telencephalon by morphogenetic molecules and transcription factors. *Birth defects research. Part C, Embryo today : reviews* 78: 256-66

Takahashi K, Tanabe K, Ohnuki M, Narita M, Ichisaka T, et al. 2007. Induction of pluripotent stem cells from adult human fibroblasts by defined factors. *Cell* 131: 861-72

Takashima A. 2006. GSK-3 is essential in the pathogenesis of Alzheimer's disease. *Journal of Alzheimer's disease : JAD* 9: 309-17

Takei Y, Laskey R. 2008. Tumor necrosis factor alpha regulates responses to nerve growth factor, promoting neural cell survival but suppressing differentiation of neuroblastoma cells. *Molecular biology of the cell* 19: 855-64

Tanzi RE, Bertram L. 2005. Twenty years of the Alzheimer's disease amyloid hypothesis: a genetic perspective. *Cell* 120: 545-55

Tapia-Gonzalez S, Munoz MD, Cuartero MI, Sanchez-Capelo A. 2013. Smad3 is required for the survival of proliferative intermediate progenitor cells in the dentate gyrus of adult mice. *Cell communication and signaling : CCS* 11: 93

Thies W, Bleiler L, Assoc As. 2013. 2013 Alzheimer's disease facts and figures Alzheimer's Association. *Alzheimers Dement* 9: 208-45

Toivonen S, Ojala M, Hyysalo A, Ilmarinen T, Rajala K, et al. 2013. Comparative analysis of targeted differentiation of human induced pluripotent stem cells (hiPSCs) and human embryonic stem cells reveals variability associated with incomplete transgene silencing in retrovirally derived hiPSC lines. *Stem cells translational medicine* 2: 83-93

Tonjes M, Barbus S, Park YJ, Wang W, Schlotter M, et al. 2013. BCAT1 promotes cell proliferation through amino acid catabolism in gliomas carrying wild-type IDH1. *Nature medicine* 19: 901-8

Tratnjek L, Zivin M, Glavan G. 2013. Up-regulation of Synaptotagmin IV within amyloid plaque-associated dystrophic neurons in Tg2576 mouse model of Alzheimer's disease. *Croatian medical journal* 54: 419-28

Trommsdorff M, Borg JP, Margolis B, Herz J. 1998. Interaction of cytosolic adaptor proteins with neuronal apolipoprotein E receptors and the amyloid precursor protein. *The Journal of biological chemistry* 273: 33556-60

Tsunekawa Y, Britto JM, Takahashi M, Polleux F, Tan SS, Osumi N. 2012. Cyclin D2 in the basal process of neural progenitors is linked to non-equivalent cell fates. *The EMBO journal* 31: 1879-92

Tzarfaty-Majar V, Lopez-Alemany R, Feinstein Y, Gombau L, Goldshmidt O, et al. 2001. Plasmin-mediated release of the guidance molecule F-spondin from the extracellular matrix. *The Journal of biological chemistry* 276: 28233-41

Uemura M, Refaat MM, Shinoyama M, Hayashi H, Hashimoto N, Takahashi J. 2010. Matrigel supports survival and neuronal differentiation of grafted embryonic stem cell-derived neural precursor cells. *Journal of neuroscience research* 88: 542-51

Urban N, Martin-Ibanez R, Herranz C, Esgleas M, Crespo E, et al. 2010. Nolz1 promotes striatal neurogenesis through the regulation of retinoic acid signaling. *Neural development* 5: 21

Vanderluit JL, Wylie CA, McClellan KA, Ghanem N, Fortin A, et al. 2007. The Retinoblastoma family member p107 regulates the rate of progenitor commitment to a neuronal fate. *The Journal of cell biology* 178: 129-39

Vannini P, Almkvist O, Dierks T, Lehmann C, Wahlund LO. 2007. Reduced neuronal efficacy in progressive mild cognitive impairment: a prospective fMRI study on visuospatial processing. *Psychiatry research* 156: 43-57

Varga AC, Wrana JL. 2005. The disparate role of BMP in stem cell biology. *Oncogene* 24: 5713-21

Vargas T, Bullido MJ, Martinez-Garcia A, Antequera D, Clarimon J, et al. 2010. A megalin polymorphism associated with promoter activity and Alzheimer's disease risk. *American journal of medical genetics. Part B, Neuropsychiatric genetics : the official publication of the International Society of Psychiatric Genetics* 153B: 895-902

Vattem KM, Wek RC. 2004. Reinitiation involving upstream ORFs regulates ATF4 mRNA translation in mammalian cells. *Proceedings of the National Academy of Sciences of the United States of America* 101: 11269-74

Vazin T, Ball KA, Lu H, Park H, Ataeijannati Y, et al. 2014. Efficient derivation of cortical glutamatergic neurons from human pluripotent stem cells: a model system to study neurotoxicity in Alzheimer's disease. *Neurobiology of disease* 62: 62-72

Verghese PB, Castellano JM, Garai K, Wang Y, Jiang H, et al. 2013. ApoE influences amyloid-beta (Abeta) clearance despite minimal apoE/Abeta association in physiological conditions. *Proceedings of the National Academy of Sciences of the United States of America* 110: E1807-16

Vierbuchen T, Ostermeier A, Pang ZP, Kokubu Y, Sudhof TC, Wernig M. 2010. Direct conversion of fibroblasts to functional neurons by defined factors. *Nature* 463: 1035-41

Vukicevic S, Kleinman HK, Luyten FP, Roberts AB, Roche NS, Reddi AH. 1992. Identification of multiple active growth factors in basement membrane Matrigel suggests caution in interpretation of cellular activity related to extracellular matrix components. *Experimental cell research* 202: 1-8

Wagner W, Wein F, Roderburg C, Saffrich R, Diehlmann A, et al. 2008. Adhesion of human hematopoietic progenitor cells to mesenchymal stromal cells involves CD44. *Cells, tissues, organs* 188: 160-9

Wang JZ, Grundke-Iqbal I, Iqbal K. 2007a. Kinases and phosphatases and tau sites involved in Alzheimer neurofibrillary degeneration. *The European journal of neuroscience* 25: 59-68

Wang JZ, Xia YY, Grundke-Iqbal I, Iqbal K. 2013. Abnormal hyperphosphorylation of tau: sites, regulation, and molecular mechanism of neurofibrillary degeneration. *Journal of Alzheimer's disease : JAD* 33 Suppl 1: S123-39

Wang X, Fu S, Wang Y, Yu P, Hu J, et al. 2007b. Interleukin-1beta mediates proliferation and differentiation of multipotent neural precursor cells through the activation of SAPK/JNK pathway. *Molecular and cellular neurosciences* 36: 343-54

Wautier F, Wislet-Gendebien S, Chanas G, Rogister B, Leprince P. 2007. Regulation of nestin expression by thrombin and cell density in cultures of bone mesenchymal stem cells and radial glial cells. *BMC neuroscience* 8: 104

Weisgraber KH, Rall SC, Jr., Mahley RW. 1981. Human E apoprotein heterogeneity. Cysteine-arginine interchanges in the amino acid sequence of the apo-E isoforms. *The Journal of biological chemistry* 256: 9077-83

Wen L, Lu YS, Zhu XH, Li XM, Woo RS, et al. 2010. Neuregulin 1 regulates pyramidal neuron activity via ErbB4 in parvalbumin-positive interneurons. *Proceedings of the National Academy of Sciences of the United States of America* 107: 1211-6

West MJ, Gundersen HJ. 1990. Unbiased stereological estimation of the number of neurons in the human hippocampus. *The Journal of comparative neurology* 296: 1-22

Widera D, Mikenberg I, Elvers M, Kaltschmidt C, Kaltschmidt B. 2006. Tumor necrosis factor alpha triggers proliferation of adult neural stem cells via IKK/NF-kappaB signaling. *BMC neuroscience* 7: 64

Wilkinson DG. 2001. Multiple roles of EPH receptors and ephrins in neural development. *Nature reviews. Neuroscience* 2: 155-64

Wilson PG, Stice SS. 2006. Development and differentiation of neural rosettes derived from human embryonic stem cells. *Stem cell reviews* 2: 67-77

Wolfe MS. 2002. APP, Notch, and presenilin: molecular pieces in the puzzle of Alzheimer's disease. *Int Immunopharmacol* 2: 1919-29

Wolfe MS. 2007. When loss is gain: reduced presenilin proteolytic function leads to increased Abeta42/Abeta40. Talking Point on the role of presenilin mutations in Alzheimer disease. *EMBO reports* 8: 136-40

Wolfe MS. 2009. gamma-Secretase in biology and medicine. *Semin Cell Dev Biol* 20: 219-24

Wright LS, Li J, Caldwell MA, Wallace K, Johnson JA, Svendsen CN. 2003. Gene expression in human neural stem cells: effects of leukemia inhibitory factor. *Journal of neurochemistry* 86: 179-95

Xu RH, Peck RM, Li DS, Feng X, Ludwig T, Thomson JA. 2005. Basic FGF and suppression of BMP signaling sustain undifferentiated proliferation of human ES cells. *Nature methods* 2: 185-90

Yagi T, Ito D, Okada Y, Akamatsu W, Nihei Y, et al. 2011. Modeling familial Alzheimer's disease with induced pluripotent stem cells. *Human molecular genetics* 20: 4530-9

Yamada K, Akiyama N, Yamada S, Tanaka H, Saito S, et al. 2008. Taip2 is a novel cell death-related gene expressed in the brain during development. *Biochemical and biophysical research communications* 369: 426-31

Yan Q, Wang J, Matheson CR, Urich JL. 1999. Glial cell line-derived neurotrophic factor (GDNF) promotes the survival of axotomized retinal ganglion cells in adult rats: comparison to and combination with brain-derived neurotrophic factor (BDNF). *Journal of neurobiology* 38: 382-90

Yang CP, Gilley JA, Zhang G, Kernie SG. 2011. ApoE is required for maintenance of the dentate gyrus neural progenitor pool. *Development* 138: 4351-62

Yassa MA, Verduzco G, Cristinzio C, Bassett SS. 2008. Altered fMRI activation during mental rotation in those at genetic risk for Alzheimer disease. *Neurology* 70: 1898-904

Yoshihara M, Adolfsen B, Galle KT, Littleton JT. 2005. Retrograde signaling by Syt 4 induces presynaptic release and synapse-specific growth. *Science* 310: 858-63

Young-Pearse TL, Chen AC, Chang R, Marquez C, Selkoe DJ. 2008. Secreted APP regulates the function of full-length APP in neurite outgrowth through interaction with integrin beta1. *Neural development* 3: 15

Yu Y, Run X, Liang Z, Li Y, Liu F, et al. 2009a. Developmental regulation of tau phosphorylation, tau kinases, and tau phosphatases. *Journal of neurochemistry* 108: 1480-94

Yu YX, He J, Zhang YB, Luo HM, Zhu SH, et al. 2009b. Increased Hippocampal Neurogenesis in the Progressive Stage of Alzheimer's Disease Phenotype in an APP/PS1 Double Transgenic Mouse Model. *Hippocampus* 19: 1247-53

Yuan SH, Martin J, Elia J, Flippin J, Paramban RI, et al. 2011. Cell-surface marker signatures for the isolation of neural stem cells, glia and neurons derived from human pluripotent stem cells. *PloS one* 6: e17540

Zhang J, Ji F, Liu Y, Lei X, Li H, et al. 2014. Ezh2 regulates adult hippocampal neurogenesis and memory. *The Journal of neuroscience : the official journal of the Society for Neuroscience* 34: 5184-99

Zhang K, Xu H, Cao L, Li K, Huang Q. 2013a. Interleukin-1beta inhibits the differentiation of hippocampal neural precursor cells into serotonergic neurons. *Brain research* 1490: 193-201

Zhang L, Wahlin K, Li Y, Masuda T, Yang Z, et al. 2013b. RIT2, a neuron-specific small guanosine triphosphatase, is expressed in retinal neuronal cells and its promoter is modulated by the POU4 transcription factors. *Molecular vision* 19: 1371-86

Zhou J, Su P, Li D, Tsang S, Duan E, Wang F. 2010. High-efficiency induction of neural conversion in human ESCs and human induced pluripotent stem cells with a single chemical inhibitor of transforming growth factor beta superfamily receptors. *Stem Cells* 28: 1741-50

Zhuo M, Holtzman DM, Li Y, Osaka H, DeMaro J, et al. 2000. Role of tissue plasminogen activator receptor LRP in hippocampal long-term potentiation. *The Journal of neuroscience : the official journal of the Society for Neuroscience* 20: 542-9

Zisman S, Marom K, Avraham O, Rinsky-Halivni L, Gai U, et al. 2007. Proteolysis and membrane capture of F-spondin generates combinatorial guidance cues from a single molecule. *The Journal of cell biology* 178: 1237-49